



COGNITIVE 2012

The Fourth International Conference on Advanced Cognitive Technologies and
Applications

ISBN: 978-1-61208-218-9

July 22-27, 2012

Nice, France

COGNITIVE 2012 Editors

Terry Bossomaier, CRiCS/ Charles Sturt University, Australia

Stefano Nolfi, Institute of Cognitive Sciences and Technologies/Consiglio

Nazionale delle Ricerche (CNR-ISTC) - Roma, Italy

COGNITIVE 2012

Foreword

The Fourth International Conference on Advanced Cognitive Technologies and Applications (COGNITIVE 2012), held between July 22 and 27, 2012 in Nice, France, targeted advanced concepts, solutions and applications of artificial intelligence, knowledge processing, agents, as key-players, and autonomy as manifestation of self-organized entities and systems. The advances in applying ontology and semantics concepts, web-oriented agents, ambient intelligence, and coordination between autonomous entities led to different solutions on knowledge discovery, learning, and social solutions.

We take here the opportunity to warmly thank all the members of the COGNITIVE 2012 Technical Program Committee, as well as the numerous reviewers. The creation of such a broad and high quality conference program would not have been possible without their involvement. We also kindly thank all the authors who dedicated much of their time and efforts to contribute to COGNITIVE 2012. We truly believe that, thanks to all these efforts, the final conference program consisted of top quality contributions.

Also, this event could not have been a reality without the support of many individuals, organizations, and sponsors. We are grateful to the members of the COGNITIVE 2012 organizing committee for their help in handling the logistics and for their work to make this professional meeting a success.

We hope that COGNITIVE 2012 was a successful international forum for the exchange of ideas and results between academia and industry and for the promotion of progress in the field of advanced cognitive technologies and applications.

We are convinced that the participants found the event useful and communications very open. We hope Côte d'Azur provided a pleasant environment during the conference and everyone saved some time for exploring the Mediterranean Coast.

COGNITIVE 2012 Chairs:

COGNITIVE Advisory Chairs

Hermann Kaindl, TU-Wien, Austria

Jaime Lloret Mauri, Polytechnic University of Valencia, Spain

Sugata Sanyal, Tata Institute of Fundamental Research - Mumbai, India

Petre Dini, Concordia University - Montreal, Canada / China Space Agency Center - Beijing, China

Po-Hsun Cheng (鄭伯璦), National Kaohsiung Normal University, Taiwan

Narayanan Kulathuramaiyer, UNIMAS, Malaysia

COGNITIVE 2012 IndUstry/Research Chair
Qin Xin, Simula Research Laboratory, Norway

COGNITIVE 2012

Committee

COGNITIVE Advisory Chairs

Hermann Kaindl, TU-Wien, Austria
Jaime Lloret Mauri, Polytechnic University of Valencia, Spain
Sugata Sanyal, Tata Institute of Fundamental Research - Mumbai, India
Petre Dini, Concordia University - Montreal, Canada / China Space Agency Center - Beijing, China
Po-Hsun Cheng (鄭伯堦), National Kaohsiung Normal University, Taiwan
Narayanan Kulathuramaiyer, UNIMAS, Malaysia

COGNITIVE 2012 IndUstry/Research Chair

Qin Xin, Simula Research Laboratory, Norway

COGNITIVE 2012 Technical Program Committee

Siby Abraham, University of Mumbai, India
Witold Abramowicz, Poznan University of Economics, Poland
Rajendra Akerkar, Western Norway Research Institute, Norway
Jesús B. Alonso Hernández, Universidad de Las Palmas de Gran Canaria, Spain
Giner Alor Hernández, Instituto Tecnológico de Orizaba - Veracruz, México
Farah Benamara, IRIT - Toulouse, France
Petr Berka, University of Economics - Prague, Czech Republic
Ateet Bhalla, NRI Institute of Information Science and Technology, Bhopal, India
Mauro Birattari, IRIDIA, Université Libre de Bruxelles, Belgium
Terry Bossomaier, CRiCS/ Charles Sturt University, Australia
Rodrigo Calvo, University of Sao Paulo - São Carlos, Brazil
Yaser Chaaban, Leibniz University of Hanover, Germany
Po-Hsun Cheng, National Kaohsiung Normal University, Taiwan
Sunil Choenni, Ministry of Security & Justice & Rotterdam University of Applied Sciences - Rotterdam, the Netherlands
Yuska Paola Costa Aguiar, UFCG, Campina Grande, Brazil
Aba-Sah Dadzie, The University of Sheffield, UK
Leonardo Dagui de Oliveira, Escola Politécnica da Universidade de São Paulo, Brazil
Stamatia Dasiopoulou, Centre for Research and Technology Hellas, Greece
Darryl N. Davis, University of Hull, UK
Tiansi Dong, University of Hagen, Germany
Juan Luis Fernández Martínez, Universidad de Oviedo, España
Simon Fong, University of Macau, Macau SAR
Tamas (Tom) D. Gedeon, The Australian National University, Australia
Ewa Grabska, Jagiellonian University - Kraków, Poland
Evrin Ursavas Güldoğan, Yasar University-Izmir, Turkey

Maik Günther, SWM Versorgungs GmbH - Munich, Germany
Ioannis Hatzilygeroudis, University of Patras, Greece (Hellas)
Tzung-Pei Hong 洪宗貝, National University of Kaohsiung, Taiwan
Kenneth Hopkinson, Air Force Institute of Technology - Dayton, USA
Abdelr Koukam, Université de Technologie de Belfort Montbéliard (UTBM), France
Narayanan Kulathuramaiyer, Universiti Malaysia Sarawak, Malaysia
Jan Charles Lenk, OFFIS Institute for Information Technology-Oldenburg, Germany
Yakim Mihov, Technical University of Sofia, Bulgaria
Claus Moebus, University of Oldenburg, Germany
Shin-ichi Ohnishi, Hokkai-Gakuen University, Japan
Yiannis Papadopoulos, University of Hull, UK
Srikanta Patnaik, SOA University - Bhubaneswar, India
Dilip K. Prasad, Nanyang Technological University, Singapore
Mengyu Qiao, South Dakota School of Mines and Technology - Rapid City, USA
J. Javier Rainer Granados, Universidad Politécnica de Madrid, Spain
Paolo Remagnino, Kingston University - Surrey, UK
Kenneth Revett, British University in Egypt, Egypt
Andrea Roli, Università di Bologna - Cesena, Italia
Fariba Sadri, Imperial College London, UK
Abdel-Badeeh M. Salem, Ain Shams University-Abbasia, Egypt
David Sánchez, Universitat Rovira i Virgili, Spain
Fermin Segovia, University of Granada, Spain
Paulo Jorge Sequeira Gonçalves, Polytechnic Institute of Castelo Branco, Portugal
Uma Shanker Tiwary, Indian Institute of Information Technology-Allahabad, India
Shunji Shimizu, Tokyo University of Science - Suwa, Japan
Anupam Shukla, ABV-IIITM - Gwalior, India
Tanveer J. Siddiqui, University of Allahabad, India
Sofia Stamou, Ionian University, Greece
Stanimir Stoyanov, Plovdiv University 'Paisii Hilendarski', Bulgaria
Mari Carmen Suárez-Figueroa, Universidad Politécnica de Madrid (UPM), Spain
Kenji Suzuki, The University of Chicago, USA
Antonio J. Tallón-Ballesteros, University of Seville, Spain
Abdel-Rahman Tawil, University of East London, UK
Ingo J. Timm, University of Trier, Germany
Bogdan Trawinski, Wroclaw University of Technology, Poland
Johann Uhrmann, Munich University of the German Armed Forces-Neubiberg, Germany
Blesson Varghese, Dalhousie University, Canada
Shirshu Varma, Indian Institute of Information Technology, India
Mario Verdicchio, Università di Bergamo-Dalmine, Italy
Maria Fatima Q. Vieira, Universidade Federal de Campina Grande (UFCG), Brazil
Michal Wozniak, Wroclaw University of Technology, Poland
Bin Zhou, University of Maryland, Baltimore County (UMBC), USA

Copyright Information

For your reference, this is the text governing the copyright release for material published by IARIA.

The copyright release is a transfer of publication rights, which allows IARIA and its partners to drive the dissemination of the published material. This allows IARIA to give articles increased visibility via distribution, inclusion in libraries, and arrangements for submission to indexes.

I, the undersigned, declare that the article is original, and that I represent the authors of this article in the copyright release matters. If this work has been done as work-for-hire, I have obtained all necessary clearances to execute a copyright release. I hereby irrevocably transfer exclusive copyright for this material to IARIA. I give IARIA permission to reproduce the work in any media format such as, but not limited to, print, digital, or electronic. I give IARIA permission to distribute the materials without restriction to any institutions or individuals. I give IARIA permission to submit the work for inclusion in article repositories as IARIA sees fit.

I, the undersigned, declare that to the best of my knowledge, the article does not contain libelous or otherwise unlawful contents or invading the right of privacy or infringing on a proprietary right.

Following the copyright release, any circulated version of the article must bear the copyright notice and any header and footer information that IARIA applies to the published article.

IARIA grants royalty-free permission to the authors to disseminate the work, under the above provisions, for any academic, commercial, or industrial use. IARIA grants royalty-free permission to any individuals or institutions to make the article available electronically, online, or in print.

IARIA acknowledges that rights to any algorithm, process, procedure, apparatus, or articles of manufacture remain with the authors and their employers.

I, the undersigned, understand that IARIA will not be liable, in contract, tort (including, without limitation, negligence), pre-contract or other representations (other than fraudulent misrepresentations) or otherwise in connection with the publication of my work.

Exception to the above is made for work-for-hire performed while employed by the government. In that case, copyright to the material remains with the said government. The rightful owners (authors and government entity) grant unlimited and unrestricted permission to IARIA, IARIA's contractors, and IARIA's partners to further distribute the work.

Table of Contents

Studying the Impact of Minority Views in a Computational Model of Collective Sensemaking: The Role of Network Structure <i>Paul Smart</i>	1
Enrichment of Cartographic Maps with the Elements of Spatial Cognition <i>Farid Karimipour and Ali Khazravi</i>	9
Energy Saving Accounts for the Suppression of Sensory Detail <i>Terry Bossomaier, Lionel Barnett, Vaenthan Thiruvarudchelvan, and Herbert Jelinek</i>	14
Cyber Forensics: Representing and (Im)Proving the Chain of Custody Using the Semantic Web <i>Tamer Gayed, Hakim Lounis, and Moncef Bari</i>	19
Action Development and Integration in a Humanoid iCub Robot How Language Exposure and Self-Talk Facilitate Action Development <i>Tobias Leugger and Stefano Nolfi</i>	24
Gaining Insights from Symbolic Regression Representations of Class Boundaries <i>Ingo Schwab and Norbert Link</i>	31
Learning Cognitive Human Navigation Behaviors for Indoor Mobile Robot Navigation <i>Luz Abril Torres Mendez and Roberto Cervantes Jacobo</i>	37
Cognitive Information in Business Process - Decision-Making Results <i>Andreia Pereira and Flavia Santoro</i>	46
Vision-based Inspection Algorithm for Identifying the Carbide Phase State in 12CrMoV Steel <i>Alexander Tzokev, Anton Mihaylov, Tzanko Georgiev, and Irina Topalova</i>	53
Indoor User Tracking with Particle Filter <i>Incheol Kim, Eunmi Choi, and Huikyung Oh</i>	59
Speed Up Learning in a Test Feature Classifier Using Overlap Index Lists <i>Yoshikazu Matsuo, Takamichi Kobayashi, Hidenori Takauji, and Shuni'ichi Kaneko</i>	63
Towards Cooperative Cognitive Models in Multi-Agent Systems <i>Jan Charles Lenk, Rainer Droste, Cilli Sobiech, Andreas Ludtke, and Axel Hahn</i>	67
EEG-based Valence Recognition: What do we Know About the influence of Individual Specificity? <i>Timo Schuster, Sascha Gruss, Stefanie Rukavina, Steffen Walter, and Harald C. Traue</i>	71

Impact of Stimulus Configuration on Steady State Visual Evoked Potentials (SSVEP) Response <i>Chi-Hsu Wu and Heba Lakany</i>	77
A Basic Study for Grasping Movement on Cognitive Task <i>Shunji Shimizu, Hiroaki Inoue, and Noboru Takahashi</i>	83
The Relationship between Human Brain Activity and Movement on the Spatial Cognitive Task <i>Shunji Shimizu, Hiroaki Inoue, Hiroyuki Nara, Noboru Takahashi, Fumikazu Miwakeichi, Nobuhide Hirai, Senichiro Kikuchi, Eiju Watanabe, and Satoshi Kato</i>	89
EEG-controlled Table Bike for Neurorehabilitation Based on Sensorimotor-rhythm BCI <i>Jin-Chern Chiou, Sheng-Chuan Liang, Chia-Hung Yen, Chun-Jen Chien, Yung-Jiun Lin, Tien-Fu Chang, Nei-Hsin Meng, Ching-Hung Lin, and Jeng-Ren Duann</i>	95
How Robust the Motor Imagery Induced EEG Sensorimotor Rhythm can be Extracted: A Test from a Cohort of Normal Subjects <i>Jeng-Ren Duann, Tien-Fu Chang, Yung-Jiun Lin, and Jin-Chern Chiou</i>	98
Fundamental Study to New Evaluation Method Based on Physical and Psychological Load in Care <i>Hiroaki Inoue, Shunji Shimizu, Noboru Takahashi, Hiroyuki Nara, Takeshi Tsuruga, Fumikazu Miwakeichi, Nobuhide Hirai, Senichiro Kikuchi, Eiju Watanabe, and Satoshi Kato</i>	101
Geometry of Intentionality in Neurodynamics <i>Germano Resconi and Robert Kozma</i>	107
Co-adaptivity in Unsupervised Adaptive Brain-Computer Interfacing: a Simulation Approach <i>Martin Spuler, Wolfgang Rosenstiel, and Martin Bogdan</i>	115
Handling of Deviations from Desired Behaviour in Hybrid Central/Self-Organising Multi-Agent Systems <i>Yaser Chaaban, Christian Muller-Schloer, and Jorg Hahner</i>	122
Fuzzy Weights Representation of AHP for Inner Dependence among Alternatives <i>Shin-ichi Ohnishi and Takahiro Yamanoi</i>	129
Measuring Robustness in Hybrid Central/Self-Organising Multi-Agent Systems <i>Yaser Chaaban, Christian Muller-Schloer, and Jorg Hahner</i>	133
Some New Concepts in MCS Ontology for Cognitics; Permanence, Change, Speed, Discontinuity, Innate versus Learned Behavior, and More <i>Jean-Daniel Dessimoz, Pierre-Francois Gauthey, and Hayato Omori</i>	139
Experiencing and Processing Time with Neural Networks <i>Michail Maniadakis and Panos Trahanias</i>	145

A Predictive System for Distance Learning Based on Ontologies and Data Mining <i>Evangelia Boufardea and John Garofalakis</i>	151
An Experiment in Students' Acquisition of Problem Solving Skill from Goal-Oriented Instructions <i>Matej Guid, Jana Krivec, and Ivan Bratko</i>	159
Learning Long Sequences in Binary Neural Networks <i>Xiaoran Jiang, Vincent Gripon, and Claude Berrou</i>	165
Extending the World to Sense and Behave: a Supportive System Focusing on the Body Coordination for Neurocognitive Rehabilitation <i>Hiroaki Wagatsuma, Marie Fukudome, Kaori Tachibana, and Kazuhiro Sakamoto</i>	171

Studying the Impact of Minority Views in a Computational Model of Collective Sensemaking: The Role of Network Structure

Paul R. Smart

*School of Electronics and Computer Science,
University of Southampton,*

*Southampton,
SO17 1BJ, UK*

Email: ps02v@ecs.soton.ac.uk

Abstract—A series of experiments were performed in order to explore the effect of communication network structure on collective sensemaking under a variety of informational conditions. A multi-agent computational model of collective sensemaking was used in which each agent was implemented as a constraint satisfaction network. Within the simulations, agents were tasked with the interpretation of information indicating the presence of a particular object, and they were allowed to share information with other agents while performing this task subject to the constraints imposed by the structure of a communication network. In all simulations, a minority of agents (5) received evidence in favor of one interpretation, while a majority of agents (15) received evidence in favor of a conflicting interpretation. Communication networks with four types of topological structure (i.e., disconnected, random, small-world and fully-connected) were used in the experiments. The results suggest that network topology influences the extent to which minority views are able to influence collective cognitive outcomes. In particular, fully-connected networks deliver a performance profile in which minority influence is minimized in situations where both minority and majority groups are exposed to weak evidence. However, the same networks serve to maximize minority influence when minority group members are selectively exposed to strong evidence. These results suggest that fully-connected networks differentially regulate minority influence based on the kinds of evidence presented to both minority and majority group members.

Keywords-sensemaking; distributed cognition; social influence; network science; social information processing.

I. INTRODUCTION

The emergence of network science as a scientific discipline in recent years has focused attention on how the various features of social and communication networks can affect aspects of human thought and action. The study of social networks, for example, has yielded a number of important findings regarding the effect of network structure on the adoption of specific ideas or technological innovations (see [1]), and such findings have important implications for those who seek to influence the spread of specific beliefs, attitudes and behavioral patterns throughout a target community. Other studies within the network science literature have attempted to shed light on how particular features of networks (for example, time-variant changes in network

structure) affect the dynamics of cognitive processing, either at the individual or social (collective) levels [2], [3].

In general, there are two approaches to studying the relationship between cognitive processes and the features of social/communication networks. The first of these involves the use of human subjects who are observed in a specific experimental context. This is the approach typically adopted by members of the cognitive and social psychology communities. A second approach involves the use of multi-agent simulation environments and computational models of cognitive processing. This approach has the advantage of enabling researchers to explore scenarios that would be difficult or impossible to explore with human subjects; however, it is an approach that has been criticized in terms of the psychological plausibility and relevance of the computational methods used to simulate aspects of human cognition [4], [5]. Clearly, any computational model needs to make some simplifying assumptions about the real-world; otherwise it loses the elements of computational tractability and explanatory concision that make it useful as an aid to both analysis and comprehension. However, the problem with many multi-agent simulations is that the agents are too rigid and simplistic to be even approximate simulacra of their real-world human counterparts. In many cases, the agents are represented by single, time-variant numerical values, and they lack any kind of internal cognitive processing capability. This is arguably a crucial limitation, and one that needs to be addressed in the context of future work on multi-agent cognition (see [6]).

The current series of experiments seeks to further our understanding of the relationship between network structure and the dynamics of collective cognition. It relies on the use of multiple, inter-connected constraint satisfaction networks (CSNs) in order to provide a model of what is called collective sensemaking. Collective sensemaking is an extension of sensemaking abilities at the level of individual agents. At the individual level, sensemaking has been defined as “a motivated, continuous effort to understand connections (which can be among people, places, and events) in order to anticipate their trajectories and act effectively” [7]. The

notion of collective sensemaking simply extends this ability to the realm of multiple agents. It refers to the effort of multiple agents to coordinate their individual sensemaking capacities in order to accurately interpret some body of environmental information, which is typically ambiguous, conflicting or uncertain in nature. Collective sensemaking is therefore a specific form of socially-distributed cognition in which cognitive processing can be seen as involving the information processing efforts of multiple, interacting individuals [8].

The use of CSNs to provide a model of sensemaking abilities is justified on the grounds that the ability to interpret (make sense of) information (especially when that information is incomplete, uncertain, ambiguous or conflicting) can be seen as a form of constraint satisfaction in which an agent attempts to establish a consistent set of beliefs subject to the constraints imposed by background knowledge, initial expectations and received information. In addition to this, CSNs have been used to model a wide variety of psychological phenomena, including belief revision, explanation, schema completion, analogical reasoning, causal attribution, discourse comprehension, content-addressable memories, cognitive dissonance and attitude change [9], [10], [11], [12], [13]. This helps to address some of the issues of psychological plausibility and relevance that are often associated with computer simulation studies of collective cognition.

By representing individual agents as CSNs, each engaged in the process of making sense of environmental information, a model of collective sensemaking can be implemented by allowing agents to exchange information with one another via communication links. These links enable agents to share information about their beliefs with other agents, and they support investigations into how factors like network structure might affect collective sensemaking abilities. CSNs have been used in precisely this way to explore the dynamics of collective sensemaking in a couple of previous studies [14], [8]. In one study, Smart and Shadbolt [14] used CSNs to examine the way in which collective sensemaking was affected by manipulations that altered the dynamics of inter-agent communication. The current work extends these initial observations in a number of ways. Firstly, the current work uses a larger number of agents, which are connected together in a greater variety of ways. All of the experiments described by Smart and Shadbolt [14] involved the use of only 4 agents, and these agents were connected together using a fully-connected network topology. The current study uses 20 agents in each simulation, and these agents are connected together using a variety of network topologies. Secondly, the study by Smart and Shadbolt [14] aimed to investigate the effect of a number of communication variables (e.g., communication frequency) on collective sensemaking using a fixed body of environmental information. This contrasts with the current work where the aim is to examine the effect

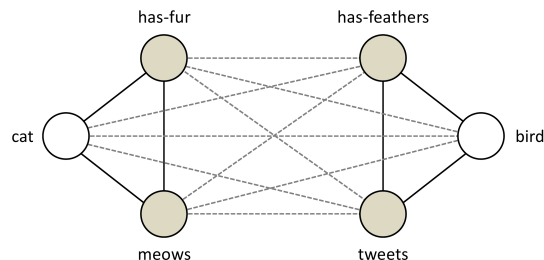


Figure 1. Organization of cognitive units in a single agent. Nodes represent cognitive units, each of which consists of two processing units. Solid lines represent excitatory connections between the units, while broken lines represent inhibitory links. Colored circles represent beliefs about the features of objects (feature beliefs), while white circles represent beliefs about the object type (object beliefs).

of different network structures on agents' ability to make sense of different bodies of environmental information.

The specific aim of the current work is to examine the way in which different communication network structures (i.e., communication networks with different structural topologies) affect collective sensemaking performance under a variety of informational conditions. Three experiments were performed in which a minority of agents were presented with evidence supporting one interpretation and a majority of agents were presented with evidence supporting an alternative, conflicting interpretation. The evidence presented to agents at the outset of the simulation caused agents to adopt different beliefs or views, and these were subsequently subject to modification across successive processing cycles. In the absence of any social influence (i.e., input from other agents), agents developed cognitive states that were consistent with the initial evidence they were provided with. However, in situations where agent communication was enabled, agents were forced to factor in the views of other agents into their emerging belief states. Communication networks with different structural topologies might be expected to differentially influence the dynamics of collective cognitive processing in this situation; however, it is unclear what the nature of this influence is at present. The three experiments reported in this paper aim to shed light on this issue.

II. METHOD

A. Computational Architecture

Details of the computational model used in the current study are described in Smart and Shadbolt [14]. The CSNs used in the current study are based on a model developed by Schultz and Lepper [15], called the consonance model. This model was used by Schultz and Lepper to replicate the findings associated with a number of studies purporting to study the phenomenon of cognitive dissonance [16].

Each agent within the current model is implemented as a CSN based on the design specification outlined by Schultz

and Lepper. The nodes which make up each CSN at the agent level are organized into a number of cognitive units, each of which represents a particular belief or view held by an agent. The agent depicted in Figure 1 shows the internal structure of all the agents used in the current study. As can be seen from Figure 1, each agent consists of 6 cognitive units, and each of these units represents beliefs about two types of animals, namely cats and birds. Four of the units represent beliefs about the features typically associated with objects, while the other two units represent beliefs about the object itself. For convenience, the former are called ‘feature beliefs’, while the latter are referred to as ‘object beliefs’.

The pattern of connectivity between the units in Figure 1 reflects the compatibility or consistency between different types of beliefs. Cognitive units can be connected to other cognitive units via inhibitory or excitatory links, and these reflect the background knowledge or experience that an agent has of a particular domain. Whether the connection between two cognitive units is excitatory or inhibitory in nature depends on the compatibility or consistency of the beliefs represented by the cognitive units. Thus, in our simulations, agents are presented with the task of making a decision about the type of an object (an animal) based on limited information about the presence of its associated features (e.g., whether it has feathers or fur). The result is that cognitive units are always connected together in a way that reflects the association of particular animals with particular features. For example, the ‘cat’ cognitive unit is always positively connected to the ‘meows’ and ‘has-fur’ units because if an agent believes that a cat is present then they will also believe in the presence of cat-related features. Similarly, the ‘bird’ cognitive unit is positively connected to the ‘tweets’ and ‘has-feathers’ units because of the natural association between birds and these features.

Note that it is a feature of these models that mutually reinforcing sets of beliefs will tend to emerge across the course of successive processing cycles. Thus, if the ‘has-feathers’ unit was activated at the beginning of a simulation, then both the ‘bird’ and ‘tweets’ units would also become active at later stages during the simulation. All these units would then reinforce one another’s activation throughout the remainder of the simulation. By the end of the simulation, the agent could be said to believe that the object was both a bird and that it had tweeting features, even though no evidence for these particular beliefs was provided at the outset of the simulation (e.g., in the form of an initial activation vector). The process of forming beliefs in the absence of evidence reflects the inferential capabilities of an agent. These inferences occur against a backdrop of background knowledge, which is encoded in the organizational structure (i.e., pattern of inhibitory and excitatory connections) of the CSN.

In addition to a sign, indicating whether a connection exerts an excitatory or inhibitory influence on its target node,

each connection has a weighting that determines the amount of influence it exerts. Although these weights could assume a variety of values, in the current study we limit all weights to values of either 0.5 (excitatory) or -0.5 (inhibitory).

B. Computational Processing

Computational processing in each CSN proceeds by the activation of particular cognitive units at the beginning of a simulation. This initial activation is deemed to represent an agent’s beliefs or views at the outset of the simulation. In the case of feature beliefs, the activation of each cognitive unit reflects the agent’s beliefs or views in response to information about the features of different types of objects (in our case, either cats or birds). Computational processing then occurs via the spreading of activation between the cognitive units of the CSN following the pattern of excitatory and inhibitory linkages between the units (see Figure 1). At each processing cycle in the simulation, the activation of each node in the CSN is updated according to the following rules:

$$a_i(t+1) = a_i(t) + net_i(ceiling - a_i(t)) \quad (1)$$

when $net_i \geq 0$, and

$$a_i(t+1) = a_i(t) + net_i(a_i(t) - floor) \quad (2)$$

when $net_i < 0$.

In these equations, $a_i(t+1)$ is the activation of node i at time $t+1$, $a_i(t)$ is the activation of node i at time t , $ceiling$ is the maximal level of activation of the node, $floor$ is the minimum activation of the node (zero for all nodes), and net_i is the net input to node i , which is defined as:

$$net_i = resist_i \sum_j w_{ij} a_j \quad (3)$$

where a_j is the activation of node j that is connected to node i , w_{ij} is the weighting associated with the connection between i and j (as mentioned above, w_{ij} assumes values of either 0.5 or -0.5), and $resist_i$ is a measure of the resistance of node i to having its activation changed. In general, the smaller the value of this parameter, the greater the resistance to activation change, and thus the greater the resistance to cognitive change. One possible use of this parameter is to make certain types of beliefs more or less resistant to change than others; in the current simulation, however, we fixed the $resist_i$ parameter at a value of 0.5 for all nodes.

At each point in the simulation, n nodes were randomly selected and updated according to equations 1 and 2, where n corresponds to the number of nodes in the (agent-level) CSN. Agents were then allowed to communicate information to their connected peers (i.e., their immediate neighbors in the communication network). Communication involved each agent contributing activation to connected agents based on the activation levels of their own constituent nodes.

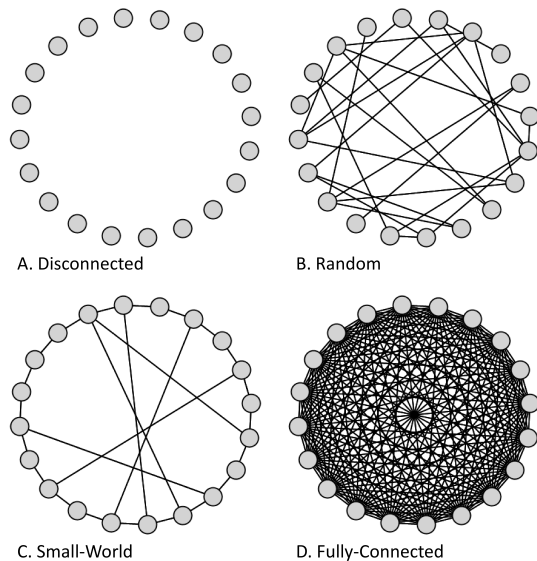


Figure 2. Examples of the different network structures used in the experiments. Nodes represent agents and lines indicate channels of communication.

Each node was associated with a parameter, $comminput_i$, which is the weighted sum of activation received from all talking agents. This parameter was updated according to the following equation:

$$comminput_i = \sum_j W_{ij} A_j \quad (4)$$

where A_j represents the activation value of a node in the talking agent and W_{ij} represents the weight of the connection from node j (in the talking agent) to node i (in the listening agent).

At the next processing cycle, $comminput_i$ was incorporated into the activation equations by extending equation 3 as follows:

$$net_i = resist_i \left(\sum_j w_{ij} a_j + comminput_i \right) \quad (5)$$

Once the communicated activation had been incorporated into the node's current activation level, $comminput_i$ was reset to zero in order to avoid repetitive presentation of the same communicated information across successive processing cycles. Processing continued until the pattern of activation in each of the agent networks had settled down. Typically, in the case of our simulations, 20 processing cycles were sufficient for a stable pattern of activation to be achieved.

C. Communication Networks

In order to examine the effect of network structure on collective performance, agents were organized into communication networks with different structural topologies.

Examples of these network structures are shown in Figure 2. In the case of disconnected networks, no communication links were included between the agents. Experimental conditions involving this type of network structure allowed us to examine the performance of agents when inter-agent communication was effectively disabled and each agent functioned autonomously. The second type of network structure was the random network. Networks of this type were created following the same procedure as that described in Mason et al [3]. Bidirectional links between agents were added at random between the agents until a specific number of bidirectional links (i.e., 1.3 times the number of agents) had been created. Given that all our simulations involved 20 agents, the number of bidirectional links added to random network configurations was $(1.3 \times 20 =) 26$. An additional constraint used in the creation of random networks was that every agent could be reached from every other agent (i.e., the network had a single component). The procedure for generating the small-world network was also the same as that reported by Mason et al [3]. In this case, agents were initially connected into a ring structure. Six agents were then selected at random and each of these randomly selected agents was connected to another randomly selected agent subject to the constraint that connected agents were at least 6 agents apart in the ring topology. Finally, in the case of the fully-connected network, all agents were connected to all other agents.

D. Procedure

Three experiments were performed in order to explore the effect of different networks structures on the processing of minority views. These experiments used the four types of network structure described in Section II-C; the main difference between the experiments was with respect to the initial activation vectors used to activate nodes at the start of each simulation. Table I shows the activation vectors that were used in each experiment.

At the beginning of each simulation, 20 agents were created and configured according to the description in Section II-A. All agents were created with identical cognitive architectures. Agents were then configured into one of four communication network structures using the procedures described in Section II-C.

At the beginning of each simulation 5 agents were selected at random and assigned to a 'Minority' group; the remaining (15) agents were assigned to a 'Majority' group. The agents in each group were then initialized with the activation vectors shown in Table I. In the case of Experiment 1, the minority group were presented with weak evidence that favored a cat interpretation, while the majority group were presented with weak evidence that favored a bird interpretation. The aim of this experiment was to examine the effect of different network structures on sensemaking performance when only weak evidence was available to all

Table I
INITIAL ACTIVATION VECTORS USED IN THE EXPERIMENTS.

Experiment	Agent Group	cat	has-fur	meows	bird	has-feathers	tweets
Experiment 1	Minority Group (5 agents)	0.0	0.1	0.0	0.0	0.0	0.0
	Majority Group (15 agents)	0.0	0.0	0.0	0.0	0.1	0.0
Experiment 2	Minority Group (5 agents)	0.0	0.2	0.0	0.0	0.1	0.0
	Majority Group (15 agents)	0.0	0.1	0.0	0.0	0.2	0.0
Experiment 3	Minority Group (5 agents)	0.0	0.5	0.0	0.0	0.0	0.0
	Majority Group (15 agents)	0.0	0.0	0.0	0.0	0.1	0.0

the agents. In Experiment 2, conflicting information was presented to agents in both the minority and majority groups. The aim of this experiment was to examine the impact of communication network structures under conditions of high uncertainty or ambiguity. The third experiment examined the effect of communication network structures under conditions where a minority of agents received strong evidence in favor of one interpretation, and a majority of agents received weak evidence in favor of a conflicting interpretation.

After the initial activation levels had been established for each agent, the simulation commenced and continued for 20 processing cycles. The activation level of both the 'cat' and 'bird' cognitive units was recorded from each agent throughout each simulation. The activation levels of these units at the end of the simulation (i.e., at the 20th processing cycle) was subjected to statistical analysis.

The design for all three experiments was a two-way (4×2) factorial design with a between subjects factor of Network Structure (with levels reflecting the types of networks tested: Disconnected, Random, Small-World and Fully-Connected) and a within subjects factor of Belief Type (with two levels - Cat and Bird - each corresponding to the activation of the 'cat' and 'bird' cognitive units, respectively). The data were analyzed using Analysis of Variance (ANOVA) procedures. For each experiment, significant two-way interactions were explored by running separate one-way ANOVAs at each level of the Belief Type factor (i.e., separate ANOVAs were performed for both the 'cat' and 'bird' cognitive unit data). Comparisons between the activation levels obtained for cognitive units across the 4 network structure conditions were made using Tukey's HSD test.

Fifty simulations were run for each of the different network structure conditions. This yielded a total of ($50 \times 4 =$) 200 simulations for each experiment. Given that there were 20 agents in each network and we recorded from two cognitive units, each experiment yielded a total of ($20 \times 200 =$) 8000 data points for each experiment.

III. RESULTS

A. Experiment 1: Minority and Majority Views Based on Weak Evidence

The results from Experiment 1 are shown in Figure 3A. ANOVA revealed significant main effects of Network Structure ($F_{(3,3996)} = 11.908$, $P < 0.001$) and Belief Type

($F_{(1,3996)} = 2879.846$, $P < 0.001$), as well as a significant two-way interaction ($F_{(3,3996)} = 73.720$, $P < 0.001$). The interaction was explored by running two reduced one-way ANOVAs at each level of the Belief Type factor. These analyses revealed significant differences between the network structures for both the 'cat' ($F_{(3,3996)} = 73.713$, $P < 0.001$) and 'bird' ($F_{(3,3996)} = 73.726$, $P < 0.001$) cognitive units. Post hoc comparisons using Tukey's HSD test revealed that, in the case of the 'cat' cognitive unit, all the activation levels were the same, except for the fully-connected network in which the level of activation was significantly below that seen with other network types. Similar results were obtained in the case of the 'bird' cognitive unit: activation levels were the same across all network types with the exception of the fully-connected network. In the case of the 'bird' cognitive unit, activation in the fully-connected network was significantly above that seen with other network types.

B. Experiment 2: Minority and Majority Views Based on Conflicting Evidence

The results from Experiment 2 are shown in Figure 3B. As is suggested by Figure 3B, the activation of the 'bird' cognitive unit was, in general, higher than that of the 'cat' cognitive unit (main effect of Belief Type: ($F_{(1,3996)} = 2965.586$, $P < 0.001$)). ANOVA also revealed a significant main effect of Network Structure ($F_{(3,3996)} = 4.820$, $P < 0.01$) and a significant two-way interaction ($F_{(3,3996)} = 4.820$, $P < 0.01$). ANOVAs at each level of the Belief Type factor revealed significant differences across the network conditions for both 'cat' ($F_{(3,3996)} = 4.817$, $P < 0.01$) and 'bird' ($F_{(3,3996)} = 4.824$, $P < 0.01$) cognitive units. Post hoc analyses revealed that the activation of the 'bird' cognitive unit was significantly higher in the fully-connected network versus the disconnected network. The reverse result was seen in the case of the 'cat' cognitive unit (i.e., activation levels in the fully-connected network condition were significantly below that seen in the disconnected network condition). No other differences between the network structure conditions were observed at either level of the Belief Type factor.

C. Experiment 3: Minority Views Based on Strong Evidence versus Majority Views Based on Weak Evidence

Figure 3C shows the results for Experiment 3. As with the other experiments, ANOVA revealed significant main effects of Network Structure ($F_{(3,3996)} = 11.038$, $P < 0.01$), Belief

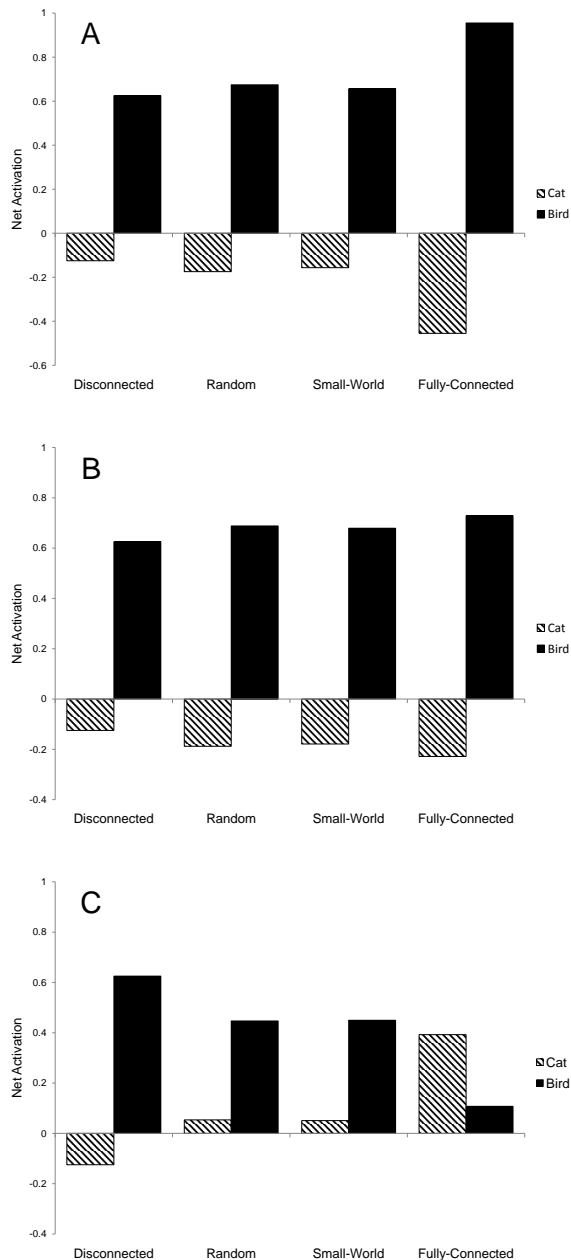


Figure 3. Mean activation levels of ‘cat’ and ‘bird’ cognitive units in each of the four network structure conditions for Experiment 1 (A), Experiment 2 (B) and Experiment 3 (C). Standard error of the mean (SEM) is not shown. In all cases, SEM was less than 0.03.

Type ($F_{(1,3996)} = 196.247, P < 0.001$) and a significant two-way interaction ($F_{(3,3996)} = 93.131, P < 0.001$). Separate one-way ANOVAS at each level of the Belief Type factor revealed significant differences between the network structure conditions for both the ‘cat’ ($F_{(3,3996)} = 93.140, P < 0.001$) and ‘bird’ ($F_{(3,3996)} = 93.121, P < 0.001$) cognitive units. Post hoc analyses revealed significant differences between the activation levels of the ‘cat’ cognitive unit across all the

network conditions with the exception of the small-world and random networks, which did not differ from each other. The same pattern of results was seen in the case of the ‘bird’ cognitive unit (i.e., significant differences were observed across the different network structures with the exception of the small-world and random networks). As is suggested by Figure 3C, in the case of the ‘cat’ cognitive unit, activation was greatest in the fully-connected network and lowest in the disconnected network; activation in the random and small-world networks was at an intermediate level between these two extremes. In the case of the ‘bird’ cognitive unit, the reverse pattern of results was obtained: activation was lowest in the fully-connected network, highest in the disconnected network, and at intermediate levels in the random and small-world networks.

IV. DISCUSSION

The results of this study suggest that communication networks with different structural topologies differentially affect performance in a simulated sensemaking task under a variety of informational conditions. Some of the most interesting results were obtained with fully-connected networks. When minority and majority groups were presented with weak evidence (Experiment 1), a performance profile emerged in which the majority view predominated. This is reflected in the higher average activation of the ‘bird’ cognitive unit in the fully-connected network condition relative to that seen with other network types. It was also the case that the minority view (reflected in activation of the ‘cat’ cognitive unit) had less influence in fully-connected networks relative to other networks (this is reflected in the fact that activation of the ‘cat’ cognitive unit in the fully-connected network condition was below that seen with other types of network). Fully-connected networks therefore seem to result in the discounting of minority views in favor in majority opinions when weak evidence is presented to all agents. In other words, when weak evidence is presented to all agents and agents are configured into communication networks with fully-connected topologies, then the evidence available to minority groups has less influence on final collective judgements compared to other types of communication network structure (i.e., networks with random and small-world topologies). This particular result may be attributable to the greater speed at which information is shared between agents in fully-connected networks. Because all agents receive information from all other agents in fully-connected networks, there is a tendency for minority views to be swamped by the weight of initial majority opinion. Other types of network, such as the small-world and random networks tend to support information propagation rates that are slower than those seen in fully-connected networks, and thus there is greater chance that minority views will have time to become established before majority influence begins to take effect.

Experiment 3 differed from Experiment 1 in that it examined the effect of network structure on performance in cases where minority group members were presented with strong rather than weak evidence. In this situation, fully-connected network topologies yielded a collective outcome in which ‘cat’ beliefs predominated. This contrasted with the results obtained with all other network types in which ‘bird’ beliefs predominated. The results seem to indicate that fully-connected networks are particularly effective at integrating minority views into collective judgements when the evidence in favor of the minority view is high and the evidence in favor of the majority view is weak. Random and small-world networks were not as effective as fully-connected networks in producing this effect, although they were better than the situation observed in the disconnected network condition. These results may be interpreted in terms of the nature of the dynamics of social influence in fully-connected networks. Fully-connected networks enable strong, but uncommon, evidence to quickly influence the beliefs of all agents before weaker, contradictory evidence has had time to contribute to opposing beliefs. In the case of small-world and random networks, weaker evidence has longer to contribute to beliefs that are progressively more resistant to change across successive processing cycles.

The profile of results seen in Experiment 3 is particularly interesting when compared to the results obtained in Experiment 1. In Experiment 1, fully-connected networks were the most effective in terms of attenuating minority influence; the same networks, in Experiment 3, were the most effective in terms of promoting the influence of minority views. The difference between these results stems from the relative differences in the initial strength of minority versus majority opinion.

Experiment 2 studied the effect of conflicting information that was presented to both minority and majority groups. Notwithstanding the significant differences between fully-connected and disconnected networks, the results from this experiment suggest that network topology has little effect on collective sensemaking in this particular informational condition. In all cases, inter-agent communication seemed to result in a performance profile in which majority views predominated.

V. CONCLUSION AND FUTURE WORK

The current work explored the effect of different network structures in a simulated version of a collective sensemaking task. This work extends earlier work that has used CSNs to explore the dynamics of collective cognition [14], [17]. The results suggest that network topology influences the extent to which minority information is able to influence collective cognitive outcomes. In particular, fully-connected networks deliver a performance profile in which minority influence is minimized in situations where both minority and majority groups are exposed to weak evidence. However,

the same networks serve to maximize minority influence when minority group members are selectively exposed to strong evidence. These results suggest that fully-connected networks differentially regulate minority influence based on the kinds of evidence presented to both minority and majority group members.

There are variety of ways in which the current work could be extended. One direction for future research is to explore models in which agents have more complicated belief structures; for example, agents could have a greater number of beliefs arranged in more complex configurations. In the current study, all cognitive units were configured so that positive (excitatory) connections had a weight of 0.5 and negative (inhibitory) connections had a weight of -0.5. One extension of the current work is thus to examine the effect of variable weightings between cognitive units. Since each linkage between cognitive units represents a psychological implication or association between belief states, the weighting associated with inter-cognition linkages may be deemed to reflect the strength of this implication or association. We assume that inter-cognition linkages are acquired as a result of prior learning, experience or training, and that they reflect the background knowledge (including assumptions, stereotypes and prejudices) that an agent brings to bear on a particular problem-solving activity. Inasmuch as this is true, we can see individual variability in the inter-cognition linkages as reflecting differences in the background knowledge that was acquired before the simulation. Such manipulations may have value in terms of shedding light on how individual differences in background knowledge and experience can influence the dynamics of collective cognition in a variety of network-mediated communication contexts.

ACKNOWLEDGMENT

This research was sponsored by the US Army Research laboratory and the UK Ministry of Defence and was accomplished under Agreement Number W911NF-06-3-0001. The views and conclusions contained in this document are those of the authors and should not be interpreted as representing the official policies, either expressed or implied, of the US Army Research Laboratory, the U.S. Government, the UK Ministry of Defence, or the UK Government. The US and UK Governments are authorized to reproduce and distribute reprints for Government purposes notwithstanding any copyright notation hereon.

REFERENCES

- [1] D. J. Watts, *Six Degrees: The Science of a Connected Age*. London, UK: William Heinemann, 2003.
- [2] P. R. Smart, T. D. Huynh, D. Braines, and N. R. Shadbolt, “Dynamic networks and distributed problem-solving,” in *Knowledge Systems for Coalition Operations*, Vancouver, British Columbia, Canada, 2010.

- [3] W. A. Mason, A. Jones, and R. L. Goldstone, "Propagation of innovations in networked groups," in *27th Annual Conference of the Cognitive Science Society*, Stresa, Italy, 2005.
- [4] P. R. Smart, W. R. Sieck, D. Braines, T. D. Huynh, K. Sycara, and N. R. Shadbolt, "Modelling the dynamics of collective cognition: A network-based approach to socially-mediated cognitive change," in *4th Annual Conference of the International Technology Alliance (ACITA'10)*, London, UK, 2010.
- [5] P. R. Smart, T. D. Huynh, D. Braines, K. Sycara, and N. R. Shadbolt, "Collective cognition: Exploring the dynamics of belief propagation and collective problem solving in multi-agent systems," in *1st ITA Workshop on Network-Enabled Cognition: The Contribution of Social and Technological Networks to Human Cognition*, Maryland, USA, 2010.
- [6] R. Sun, "Cognitive science meets multi-agent systems: A prolegomenon," *Philosophical Psychology*, vol. 14, no. 1, pp. 5–28, 2001.
- [7] G. Klein, B. Moon, and R. R. Hoffman, "Making sense of sensemaking 1: Alternative perspectives," *Intelligent Systems*, vol. 21, no. 4, pp. 70–73, 2006.
- [8] E. Hutchins, *Cognition in the Wild*. Cambridge, Massachusetts, USA: MIT Press, 1995.
- [9] K. Holyoak and P. Thagard, "Analogical mapping by constraint satisfaction," *Cognitive Science*, vol. 13, no. 3, pp. 295–355, 1989.
- [10] W. Kintsch, "The role of knowledge in discourse comprehension: A construction-integration model," *Psychological Review*, vol. 95, pp. 163–182, 1988.
- [11] B. Spellman, J. Ullman, and K. Holyoak, "A coherence model of cognitive consistency: Dynamics of attitude change during the persian gulf war," *Journal of Social Issues*, vol. 49, no. 4, pp. 147–165, 1993.
- [12] P. Thagard, "Explanatory coherence," *Behavioral and Brain Sciences*, vol. 12, no. 3, pp. 435–502, 1989.
- [13] D. Rumelhart, P. Smolensky, J. McClelland, and G. Hinton, "Schemata and sequential thought processes in pdp models," in *Parallel Distributed Processing: Explorations in the Microstructure of Cognition, Volume 2*, D. Rumelhart and J. McClelland, Eds. Cambridge, Massachusetts: MIT Press, 1986, pp. 7–58.
- [14] P. R. Smart and N. R. Shadbolt, "Modelling the dynamics of team sensemaking: A constraint satisfaction approach," in *Knowledge Systems for Coalition Operations*, Pensacola, Florida, USA, 2012.
- [15] T. R. Schultz and M. R. Lepper, "Cognitive dissonance reduction as constraint satisfaction," *Psychological Review*, vol. 103, no. 2, pp. 219–240, 1996.
- [16] L. Festinger, *A Theory of Cognitive Dissonance*. Stanford, USA: Stanford University Press, 1957.
- [17] E. Hutchins, "The social organization of distributed cognition," in *Perspectives on Socially Shared Cognition*, L. Resnick, J. Levine, and S. Teasley, Eds. Washington DC, USA: The American Psychological Association, 1991.

Enrichment of Cartographic Maps with the Elements of Spatial Cognition

Farid Karimipour, Ali Khazravi

Department of Surveying and Geomatics Engineering, College of Engineering, University of Tehran
Tehran, Iran

e-mail: {fkarimipr, khazravi}@ut.ac.ir

Abstract—Human activities are embedded in the space. People need to know where they are and how they can arrive to their destination. They may use their spatial cognition in familiar space, or navigation aids (e.g., cartographic maps and satellite navigation systems) in unfamiliar areas for positioning and wayfinding purposes. Today, satellite navigation systems are widely used by even non-expert users. Dealing with cartographic maps, however, need prior knowledge and experience on map reading as well as enough spatial cognition. Enriching cartographic maps with the elements of spatial cognition could help to navigate more easily in unfamiliar environments. This paper represents the result of a research to enrich cartographic maps with features used by pedestrians for navigation in urban areas.

Keywords—Spatial cognition; Cartographic maps; Cognitive map; Urban navigation; Pedestrian navigation

I. INTRODUCTION

Human activities are embedded in the space. People need to know where they are and how they can arrive to their destination. This so-called *wayfinding* is a directed process to move from a source to a given destination through intermediate path(s) [1]. People may use their spatial cognition in familiar space, or navigation aids (e.g., cartographic maps and satellite navigation systems) in unfamiliar areas for positioning and wayfinding purposes. Today, satellite navigation systems are widely used by even non-expert users. Dealing with cartographic maps, however, need prior knowledge and experience on map reading as well as enough spatial cognition.

Suppose you are navigating in a familiar environment (for example, you are walking from your home to the university). In this case, you will navigate through the path without paying attentions to the name of the streets, roundabouts, etc.; instead your spatial cognition is used to get oriented in the environment based on existing familiar features in the way (e.g., landmarks). On the other hand, suppose you are in an unfamiliar city for a conference and you are walking from hotel to the conference venue. In this case, you use a cartographic map and the only connection between the environment and the map is the name of the streets, roundabouts, etc. as well as their relations. However, there are different distinguished features in the way that could have helped you for an easier navigation. More clearly, your map shows that you have to walk straight until you reach the street “A”. Then, you walk and look at the name of the streets until finding the street “A”. However, a big blue

building located at the corner of the street “A” could have been a better indicator for you to find the street even before you reach the street and see the street name plate.

A shortcoming of cartographic maps is that they are limited to a top view representation of the space [2]. Therefore, they only provide metric information and topological relations, but do not contain any spatial categorical knowledge (e.g., landmarks), which is the basis of human spatial cognition.

Spatial cognition has been extensively studied in psychological and geographical research. Kevin Lynch investigate the spatial cognition and its relation with urban design [3]. He studied behavior of people in wayfinding and environment recognition in three cities with different textures. The elements of cognitive maps introduced in his book are the main elements for cartographic map enrichment proposed in this paper.

A recent research in the field of pedestrian navigation was done by Giasbauer and Frank [2], who modeled a pedestrian navigation system for urban areas. There are many studies on spatial cognition in psychology including [1, 4, 5, 6, 7].

This paper suggests enrichment of cartographic maps with the elements of spatial cognition to improve their value for navigation in unfamiliar environments. Especially, we concentrate on enrichment of cartographic maps with features used by pedestrians for navigation in urban areas. Section 2 reviews spatial cognition and spatial knowledge in more details. In Section 3, the elements of spatial cognition are introduced from geographic point of view. Section 4 contains the results of enriching a cartographic map with the elements of spatial cognition introduced in Sections 2 and 3. Finally, Section 5 concludes the paper and represents ideas for future work.

II. SPATIAL COGNITION AND SPATIAL KNOWLEDGE

Cognition encompasses acquiring, storing, retrieving and manipulation of information used by human, animals or intelligence machines. Especially, *spatial cognition* is acquiring, organizing, updating and usage of spatial knowledge about the environment [8]. A cognitive system may consist of sensing and imagery, learning, reasoning, decision making, and problem solving sub-systems [9].

A. Cognitive map

A *cognitive map* is a mental model of the environment. It may contain spatial elements (e.g., path, landmarks, direction

and distance) and sensual attributes (e.g., odor, sounds, images, and sensations). Cognitive maps do not have an integrated structure, but they consist of five distinct spatial elements: *paths, edges, districts, nodes* and *landmarks* [3].

B. Types of spatial knowledge

Spatial knowledge is divided into *metric* and *categorical knowledge*. Metric parameters are quantitative and comparable. While, categorical parameters are qualitative terms (e.g., left, right, near, far, etc.). Categorical parameters are better understood by people. In some cases, however, they could be ambiguous.

In terms of types of the elements and comprehensiveness, spatial knowledge is divided into *landmark knowledge, route knowledge, and survey knowledge*.

1) Landmark knowledge

In the first step of understanding the environment, people pay attention to specific objects or features, called landmarks (Fig. 1). Landmark knowledge is an egocentric knowledge and is the first element of spatial knowledge [1].



Figure 1. Landmark knowledge: distinct landmarks

2) Route knowledge

Route knowledge is a sequence of familiar or known paths, junctions, and landmarks. This kind of spatial knowledge is gained gradually, and makes a sequential structure by its elements (Fig. 2). This knowledge is used to move in routes and paths based on a sequence of landmarks, features, junctions, and nodes. Route knowledge is based on egocentric view, too [1].



Figure 2. Route knowledge: sequence of features

3) Survey knowledge

Survey (also called configurational) knowledge is more comprehensive comparing to the landmark and route knowledge. It is built up by integrating all the landmarks, routes, and paths as well as the relations among these elements into a unified complex network. Survey knowledge could be thought of as the view of a bird that flies over a city and see everything and their relations at once (Fig. 3).



Figure 3. Survey knowledge

III. ELEMENTS OF COGNITIVE MAP

As mentioned, Lynch defines five spatial elements for a cognitive map: *paths, edges, districts, nodes* and *landmarks* [3].

A. Path

A path is a linear channel through which the navigators move. Streets, sidewalks, railways, and channels are examples of paths (Fig. 4). For many people, paths are the main elements of their cognitive map, along which other spatial elements are organized [3]. Slope is an attribute of a path that can be easily reminded and recognized by people, but is neglected in current cartographic maps.



Figure 4. Different paths for different navigators: Buses (left); cars,(middle) and pedestrians (right)

B. Edge

Edges are linear features that are not considered as a path, but are located between two areas. A wall is an example of an edge [3]. Hard edges are continuous visible features that are passable or impassable. Note that the difference between paths and edges depends on the navigator, i.e., an object considered a path for a navigator could be an edge for others. For instance, a road is a path for a car, railway is a path for a train, and both are hard edges for a pedestrian. The same applies to passable or impassable

edges. For example, in Fig. 5, the left edge is an impassable hard edge for a car, but passable for a pedestrian.



Figure 5. Examples of edges: (a) An impassable hard edge for a car, but passable for a pedestrian; (b) An impassable hard edge for both cars and pedestrians

C. District

Districts are medium to large scale 2D areas of a city. A navigator enters mentally into a district. Each district is recognized and identified by some features [3], including the building structure, air quality, traffic, inhabitants' appearance, topography, vegetation cover, etc. Some districts have a hard core (visible object), and features around which are homogeneous.

D. Node

Nodes are strategic and reference points in the city into which a navigator mentally enters. A node can be a junction, the start or end of a path, the intersection of two paths, or the centric points or the core of a district.

Lynch considers nodes as decision points [3]. The number of relations to a node is a key factor to assign an importance value to a node: The more relations to a node, the more importance value is assigned to it. Furthermore, prominence of a node depends on selected paths and destination of the navigator.

E. Landmark

Landmarks are special type of reference points that navigators do not enter into it, but see it in their path (e.g., buildings, mountains, etc.). Different disciplines represent different definitions for landmarks, but they all agree on visibility, contrast and usability for navigation. Landmarks may be used for:

- Selecting a path based on familiar landmarks
- Selecting a path by excluding unfamiliar landmarks
- Approving or denying a selected path
- Orientation

1) Global vs. local landmarks

Regarding the scale and distance to the viewer, landmarks are divided into local and global [10]:

- *Local landmarks* are only visible from near distances and are used for selecting a proper path. These landmarks are relatively small and conspicuous. Examples are signs and buildings.

- *Global Landmark* are visible from far distances and are used to create an allocentric reference system. A global landmark can determine a cardinal direction for the reference system. The sun, mountains, and sky scraper are instances of global landmarks. Global landmarks can be useful on nodes where the navigator has to choose a path considering the direction to a global landmark.

2) Objective vs. subjective features

Landmarks may have two types of features; *objective* and *subjective* features.

a) Objective features

Objective features are unequivocal features which do not need any interpretation. They are physical attributes of a landmark and people with different individual perception have the same understanding of them. Objective features are so critical for a landmark that an object with no objective features cannot be considered as a landmark [1].

One of the most important objective feature is contrast (Fig. 6). It is the key to recognize and to identify a landmark. Objects with high contrast in the environment are naturally considered as a landmark [1]. Such contrast could be visual (e.g., a red house in a block where other buildings are white), or defined based on other senses (e.g., odor, sounds, etc.).



Figure 6. Examples of contrast in the environment

b) Subjective features

Subjective features rely on individual knowledge or memory [1]. Subjective feature are less equivocal, namely they mostly depend on the individual perception, which is different from a person to another.

Table 1 illustrates the characteristics of objective and subjective features of landmarks.

TABLE 1. CHARACTERISTICS OF OBJECTIVE AND SUBJECTIVE FEATURES OF LANDMARKS [1]

Objective features	Subjective features
Contrast	Point of reference
Creation	Usage
Visibility	Remembrance
Location	Legend
Stationary	Distinguishability

IV. IMPLEMENTATION

This section represents the result of enriching a cartographic map with the elements of spatial cognition to improve its value for pedestrian navigation purpose. For

landmarks, we only concentrate on objective features discussed in Section 4.

The study area is a cartographic map of the Sohrevardi area located in the North of Tehran. The transportation network of the area was extracted from a digital map (Fig. 7). Then, the following elements of spatial cognition were selected to be added to the map:

- The study area will be highlighted on the map as a district.
- The nodes of the area will be added to the map.
- The local and global landmarks that could be used for navigation in the area will be added to the map.
- All the streets and highways will be considered as edges for pedestrians.
- The sidewalks will be added to the map as paths for pedestrians.
- The crosswalks, where pedestrians can cross the streets, will be added to the map.

The data needed for the above enrichment were collected on the field. As mentioned, we concentrated on objective features and unequivocal features of the landmarks, which need a little description. The collected data are as follow:

- The objective features of local landmarks, along some unequivocal description about their appearance
- Slope of the paths
- The crosswalks and other paths where a pedestrian can cross an edge
- Identifying junctions, which have heavy usage, as nodes
- Identifying features that are repeated along the district

In the enrichment process, landmarks were identified and highlighted on the map by a symbol. This information is used for a categorical addressing or address matching systems. In order to assign descriptive (textual) information about the objective features of the landmarks, a distinct number were added to the symbols used for each landmark, and the related descriptions were provided on the side of the map.

To help the user to find the cardinal direction, a global landmark was used. In case of Tehran, the mountain chain located in the top north of the city (called Damavand) was used.

Finally, the street slopes were classified into low, medium, and high, which were illustrated by different symbols and colors (Fig. 8). Furthermore, a symbol was used to represent abrupt changes in slope of a path. Then, each path on the map was equipped with such slope symbols.

The final cartographic map enriched with these unequivocal elements of spatial cognition is illustrated in Fig. 9.

V. CONCLUSION AND FUTURE WORK

Cartographic maps are one of the most important navigation aids. They are mostly a top view representation of the space, which provide metric information and topological

relations. However, maps do not contain any spatial categorical knowledge (e.g., landmarks), which is the basis of human spatial cognition. In this paper we suggested that cartographic maps are enriched with the elements of spatial cognition to improve their value for navigation in unfamiliar environments.



Figure 7. GIS-Ready Road-Network of studied area

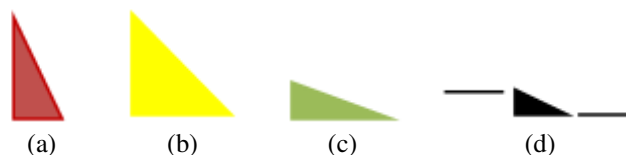


Figure 8. slopes (a): high, (b): medium, (c): low, (d): change in slope

The result of this study is a cartographic map that is enriched with the unequivocal elements of spatial cognition. Deploying this map will increase the performance of navigation in unfamiliar places. However, the output was presented on a paper map, which results in limitations and complexities for adding attribute information. The same process could be applied on digital maps, which are dynamic. It will enable us to provide the user with more attributes through filtering the presented information, changing the map scale and usage of other media (e.g.,

voice). Such map will support a spatial information system for navigation purposes.

In order to evaluate the validity and usability of the produced map, we are developing an agent-based model that deploys the enriched map for navigation. The results will be compared with another agent that performs the task using a plain cartographic map.

Adding visibility constraints to landmarks is considered as a future work. It helps the user to know where to expect a landmark to be seen. Furthermore, by investigating other districts, it is possible to compare the results and find more specific features to be added to the map. Finally, we are working on an automatic cognitive map enrichment system, which uses cadastral and land-use data.

REFERENCES

[1] E. Platzer, "Spatial cognition research: The human navigation process and its comparability in complex real and virtual environments", PhD. Dissertation, University of Munich, 2005.
 [2] C. Gaisbauer and A.U. Frank. "Wayfinding Model For Pedestrian Navigation". The 11th AGILE International Conference on Geographic Information Science, University of Girona, Spain, pp. 21-29, May 2008.

[3] K. Lynch, "The Image of the City", p194, MIT Press, 1960.
 [4] C. Presson and D. Montello, "Points of reference in spatial cognition: Stalking the elusive landmark", British Journal of Developmental psychology, Vol. 6, pp. 378-381.
 [5] K. Schweizer and T. Herrmann, "Sprachliches Lokalisieren und seine kognitiven Grundlagen", Hans Huber, 1998.
 [6] H. Stumpf and J. Eliot, "Gender-related differences in spatial ability and the k factor of general spatial ability in a population of academically talented students", Personality and Individual Differences, Vol. 19, Issue 1, pp. 33-45, 1995.
 [7] J. Xia, D. Packer and C. Dong, "Individual differences and tourist wayfinding behaviours". Proceedings of 18th World IMACS Congress and MODSIM09 International Congress on Modelling and Simulation, Cairns, Australia, pp. 1272-1278, 2009.
 [8] S. Werner, B.K. Brückner, H.A. Mallot, K. Schweizer and C. Freksa, "Spatial cognition: The role of landmark, route, and survey knowledge in human and robot navigation", Ph.D. in Computer Science, Springer, Vol. 27, pp. 41-50, 1997.
 [9] N.J. Smelser, J. Wright and P.B. Baltes [ed.], "International encyclopedia of social & behavioral sciences", Elsevier, pp. 14771-14775, 2001.
 [10] S.D. Steck and H.A. Mallot, "The role of global and local Landmarks in virtual environment navigation", Journal of Teleoperators and Virtual Environments archive, Vol. 9, Issue 1, pp. 69-83, 2000.

Enriched map of Sohrevardi District

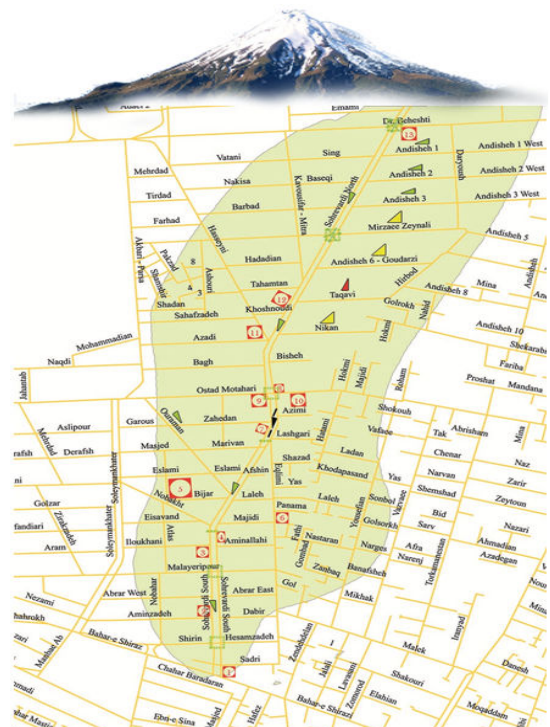
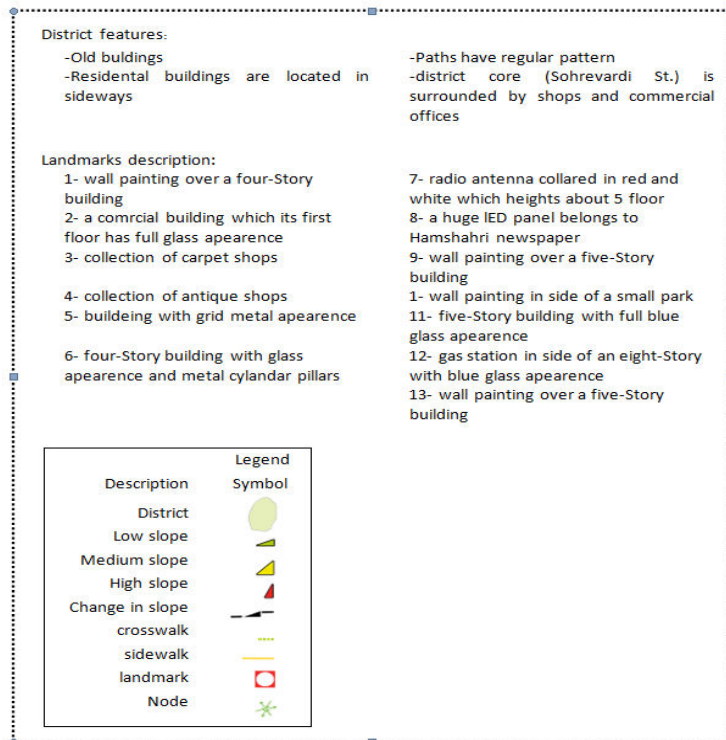


Figure 9. The final enriched cartographic map with the elements of spatial cognition

Energy Saving Accounts for the Suppression of Sensory Detail

Terry Bossomaier*, Lionel Barnett†, Vaenthan Thiruvarduchelvan* and Herbert Jelinek*

*Centre for Research in Complex Systems

Charles Sturt University

Bathurst, Australia

e-mail: {tbossomaier,vthiru,hjelinek}@csu.edu.au

†Sackler Centre for Consciousness Science

University of Sussex

Brighton, United Kingdom

e-mail: lionelb@sussex.ac.uk

Abstract—High functioning autistic people can exhibit exceptional skills with numbers, eidetic imagery and recall of concrete detail, as brought to popular attention in the film *Rain Man*. However, it now transpires that these skills are to some extent latent within all of us. We do not have access under normal circumstances to this concrete detail, yet brain stimulation experiments show that it exists in all of us. This paper proposes that one of the reasons for this lies in the brain's need to conserve energy. Computer simulations using a spiking neural network support this hypothesis. A spiking neural network was set up with a number of feature detectors feeding an output unit, which in turn generates inhibition of the input neurons. This reduces the spike activity of the input, and thus overall energy usage.

Keywords—energy saving; computer simulation; spiking neural network; Bayesian prior; detail suppression

I. INTRODUCTION

The evidence from high functioning autistic individuals shows the overwhelming advantage of concept formation in the human brain. Such individuals tend to have weak concept formation but can have very powerful perception and memory for detail. The evolutionary significance is abundantly clear. What is less clear is *why the raw detail to which these people have access is not available to everybody else*. The surprising thing, revealed by direct brain stimulation, is that this detail is *not* destroyed on the way to conscious awareness, but is somehow *blocked from access*. This paper provides a novel solution to this conundrum.

Early indicators that some of this low-level detail might be accessible came from studies on victims of stroke and brain injury, where, for example, a person might discover the ability to draw realistically. Snyder and Mitchell [1] predicted that such access might be obtained using brain stimulation techniques in which the conceptual part of the brain was blocked, because concepts inhibit lower level detail [2].

It transpired that this was indeed the case. The direct brain stimulation techniques, *Transcranial Magnetic Stimulation* (TMS) and the more recent technique, *Transcranial Direct-Current Stimulation* (TDCS) can be used to “switch off” part

of the brain. By targeting the anterior temporal lobe in the left hemisphere—a brain area highly involved in concept formation and storage—it is possible to block access to concepts and thus release access to lower-level detail. In the first such study, now nearly a decade old, drawing and proof-reading [3] were found to be enhanced by TMS. So, for example, it is hard for many people to see the word “the” when it is repeated on a following line. The ability to spot the error is enhanced when the meaning of the sentence is blocked by brain stimulation. Likewise, numerosity [4] (rapidly estimating the number of objects in the field of view, inspired by an incident in the film *Rain Man*) also goes up with TMS to the left anterior temporal lobe. Over the subsequent decade, a diverse range of higher-level cognitive phenomena have been shown to be enhanced through dis-inhibition with brain stimulation. False memory, where like objects may get mixed up in memory tests (e.g., chair instead of stool), can be reduced in this way [5]. Even the ability to solve visual puzzles can be enhanced [6].

There are numerous arguments for why this might be the case, such as the possibility of computational overload, discussed further in Section IV. In this era of information overload, such an explanation is at first sight appealing, but is hard to quantify with our existing knowledge of the brain.

Closely linked to computational overload is the energy cost of neural computation. The human brain uses about 20% of the body's energy [7] and various evolutionary changes, such as the appearance of meat in the diet, may have allowed the brain's energy consumption to grow. Navarette et al. [8] show that in over 100 species of mammal, adipose deposits correlate negatively with encephalisation. This suggests that fat storage and increased brain size are alternative evolutionary strategies for avoiding starvation.

Laughlin and Sejnowski [9] show that the brain's overarching network structure is consistent with preserving energy. The energy required for the transmission of nerve impulses, or spikes, and synaptic transmission are very tightly optimized, approaching the thermodynamic limits within cellular constraints [10]. Neuronal spikes account for a significant fraction

of neuronal energy usage [11].

The idea that the number of spikes might be kept to a minimum to save energy began with the idea of *sparse coding* in sensory systems [12][13]. More recently, cells have been observed which fire strongly when the subject is exposed to stimuli corresponding to a particular person, say Bill Clinton, and to very little else [14][15]. They respond to the *concept*, and can be activated by pictures, voice or unique events. Obviously, for most people such a cell would fire very infrequently. The alternative distributed representation might have many cells coding for all US presidents. All of these cells would be active for any president, thus making their average activity much higher.

However, sparse coding is not the only way to reduce energy consumption by neurons using action potentials (APs). Changing the kinetics of the ion channels involved in generating the spike can reduce the energy requirements of the APs. Sengupta et al. [16] show that considerable differences in the relative cost of spike transmission versus the energy of synaptic transmission may be found, depending upon the exact ion channel kinetics, for example between giant squid neurons and those in mouse cortex.

The strong need to conserve energy suggests a possible explanation for why raw sensory input is not accessible to us, excluding external means like TMS. *It is turned off to save energy.* Snyder et al. [2] and Bossomaier and Snyder [17] propose a *concept model* for how inhibition mechanisms might generate the observed effects of TMS. The effect is to turn off the inhibitory mechanisms, dis-inhibiting their targets.

Inhibition is of course widespread in the brain, and the prefrontal cortex—the area with most development over other primates—abounds in inhibitory effects. But, evidence is now emerging that even sensory perception in early areas such as primary visual area V1 depends upon top-down modulation, of which a large part is inhibitory [18][19].

Feedback mechanisms are a common way of modulating input from lower processing areas of the cortex to higher processing areas. Visual processing streams provide a good example, where higher-order visual areas display an inhibitory top-down activity to lower visual processing areas like V1 [18][19]. However these models only consider connectivity patterns in the cortex related to visual processing. Jelinek and Elston [20] have shown that on a cellular level, processing complexity increases from V1 to prefrontal cortex, with layer-III pyramidal cell dendritic branching patterns becoming more complex and larger, thus requiring more energy. Higher visual processing areas deal more with conceptual phenomena by integrating simple bits of information from lower processing areas.

Such top-down effects reduce activity at lower levels. Zhang et al. [21] show that in inferotemporal cortex, activity corresponding to a particular object is vastly different depending upon whether attention is focussed on that object.

In this paper, we show that spiking neural networks, even when using the most basic approximation to the established Hodgkin-Huxley spike-dynamic equations [22], can exhibit

significant energy savings within such inhibition models. We note that the energy cost of neural computation is split between the generation of spikes and synaptic activity, the relative proportion varying across species [16]. This article focusses on the spike activity component.

We consider two cases. The first implements a concept model outlined by the previous paragraphs. The second uses a Bayesian or attention approach to reduce energy costs even further. The essential feature of both models is the inhibition of inputs as soon as a concept has been activated.

II. SIMULATION MODELS

The simplest approximation to the Hodgkin-Huxley equations is the Leaky Integrate and Fire model. Izhikevich [23] points out that this neuron is capable of only a few of the 20 or so behaviors of which the full Hodgkin-Huxley model is capable. However, it is used here because *if a very simple model can generate the behavior we observe, then so can any of the more complex models.* This assures that the model is reasonably robust to parameter variations. Since more powerful neural models, such as the Izhikevich [23] model, can imitate the behaviour of simpler models (such as integrate and fire) then these more powerful models will have the same behaviour.

Equation 1 shows the model for one neuron, where R is resistance, I the input current, u the membrane voltage and τ the time constant:

$$\frac{du}{dt} = -\frac{u}{\tau} + \frac{IR}{\tau} \quad (1)$$

Synaptic activation is represented by an alpha function with another time constant τ_s :

$$\varepsilon(t) = \frac{1}{\tau_s} e^{1-t/\tau_s} \quad (2)$$

The two simulation models use the same type of neuron, although the time constants are not the same.

A. Model 1: Basic Concept and Inhibition

In Model 1 we use a local inhibitory circuit, shown in Figure 1. Since an eye fixation takes around 200msec [24], we assume this represents the minimum time for which a concept would remain active. The inhibitory circuit requires around 20msec. It does not matter if input spikes come in as a single volley or as some Poisson process; if the maximum spike rate is around 100 spikes per second, the concept cell can see about 2 spikes in 20msec, and should it see a spike from every cell, then it takes 40msec to turn the input cells off. This would represent an spike-saving factor of around five.

B. Model 2: Prior Knowledge and Intention

There is abundant evidence of the use of Bayesian information processing throughout sensory and cognitive processing. For the purposes of this paper, the implication is that only a small subset of feature detectors need to fire to recognize something, given the assumption that something is going to appear.

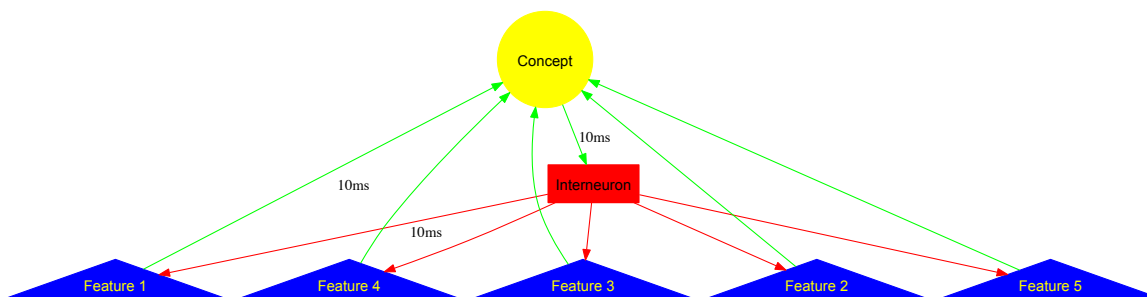


Figure 1. The basic model. Sensory signals are the features in blue, of which there may be many more than 5. Green connections are excitatory (from features to concept and to interneuron). Red connections from the interneuron to the features are inhibitory.

For instance, sometimes just a single cue, like hair colour, might be enough to distinguish between two people. So if we know that the person coming up the driveway is one of two similar-looking people, then hair colour might be enough to identify them. In this case, it is not necessary to wait for all feature cells to fire. Just a few cells may suffice, in which case inhibition can start sooner. This is the essence of Model 2, illustrated in Figure 2. The *prior* neuron represents the assumption of what will appear: as soon as it has its minimal set of features, it activates the output neuron, in turn suppressing the input activity early.

Now, assume that we have attentional control or a mindset that one is going to see objects K5 or K7, represented by the cell labelled *prior* in Figure 2. The facilitating cell is activated from higher up, but is agnostic as to whether K5 or K7 appears. It fires slowly with a long recovery time and brings a small subset of features closer to threshold. This only costs a small number of spikes and synaptic events, since on average only one cell will fire, facilitating a particular hypothesis. Now, only this small number of features needs to be activated for the concept to trigger. But, since these features lead over the remainder, only they will be allowed to fire.

All simulations were carried out in Matlab using the Biological Neural Network Toolbox [25]. The toolbox uses Matlab’s integration routines for solving differential equations.

III. RESULTS

Figure 3 shows the spiking patterns for Model 1. The features are suppressed for the duration of activation of the concept, representing at least a substantial decrease in energy usage. Whereas the activity of the concept and inhibitory neurons are maintained throughout the 200msec simulation, activity of the feature neurons rapidly dies away. Without the inhibition, their firing would also be maintained. Figure 4 shows the average number of spikes in each neuron over 100 runs.

The prior or attention neuron of Model 2 pre-activates some of the features, as shown in Figure 5. Figure 6 shows the average number of spikes over 100 runs of this simulation.

In this paper, only one concept neuron is ultimately activated, but a single prior could pre-activate any number of feature neurons, in turn subserving more than one concept.

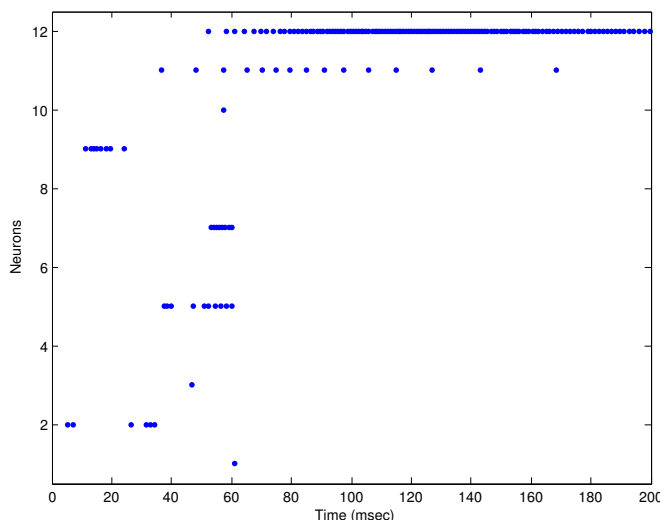


Figure 3. Spike activity of the network of Model 1. Cells are laid out along the y-axis. The top cell is the inhibitory interneuron, the next cell down is the concept and the remainder are the features. Each dot represents a spike event. The inhibition in neuron 12 sets in after the concept neuron has started to fire.

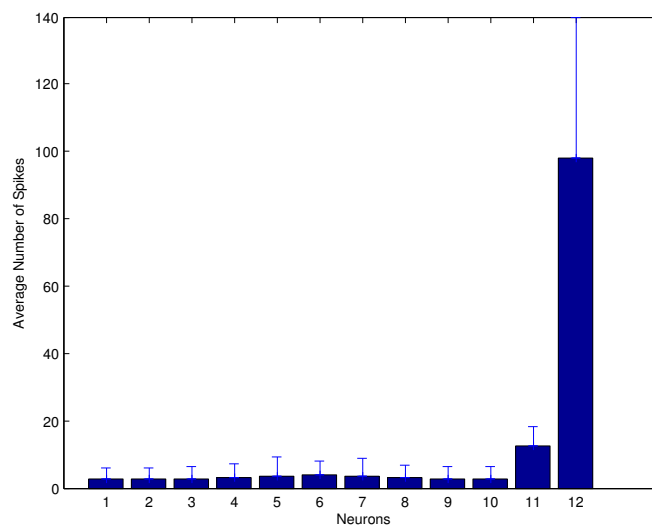


Figure 4. The average number of spikes for each neuron in Model 1. Neurons 1–10 are the input features, neuron 11 the concept and neuron 12 the inhibitory interneuron.

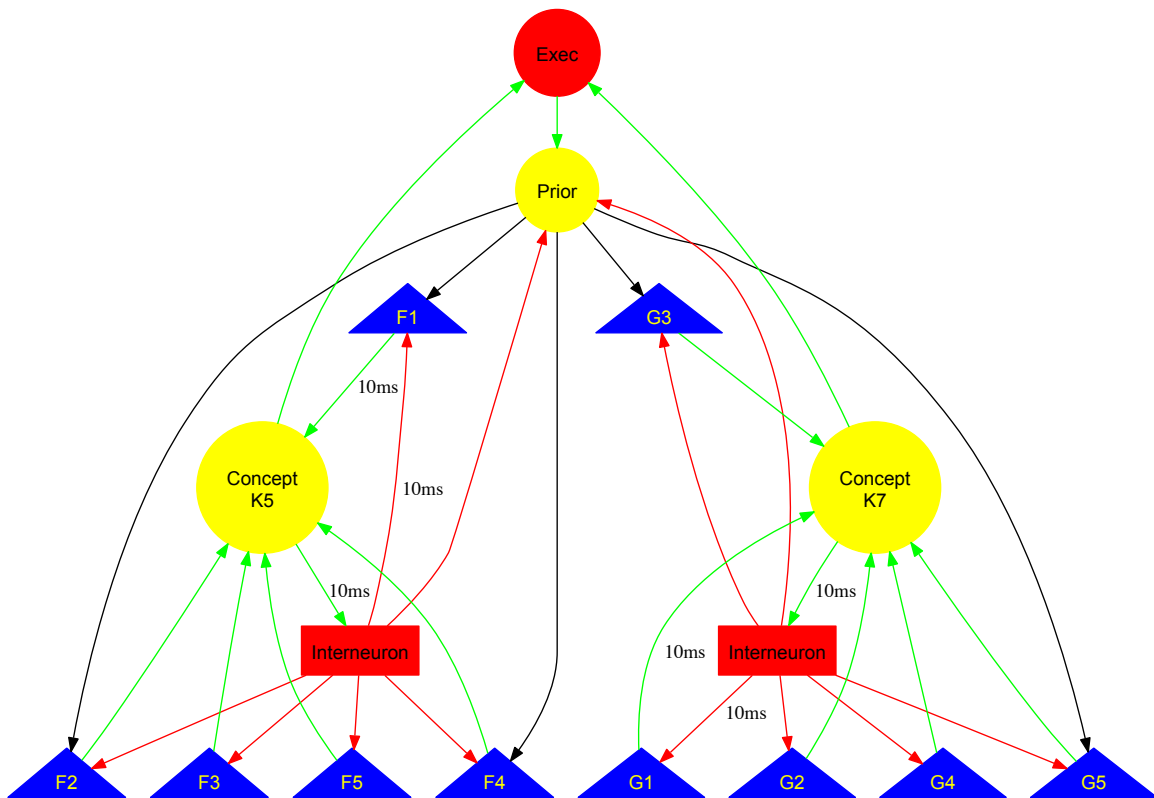


Figure 2. The prior/attention model. Features, concepts and inhibitory interneurons are similar to Figure 1. Here we have two concepts and a single prior/attention neuron selecting them. The latter has excitatory connections to a small subset of feature detectors (black).

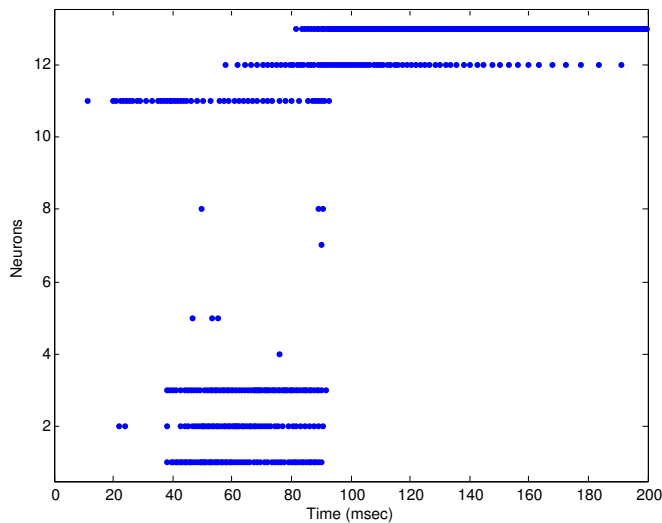


Figure 5. The effect of attention bias or prior assumption (Model 2). The prior neuron (number 11) is already active and the three sensitized neurons fire first (1–3). Firing in the other feature detectors is suppressed.

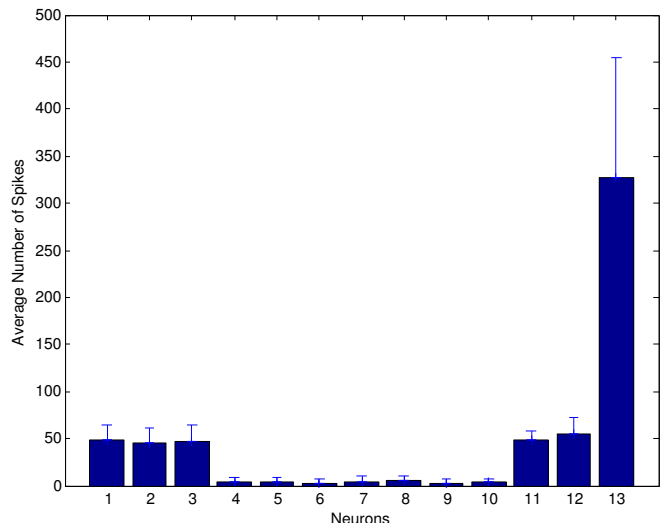


Figure 6. Mean number of spikes in Model 2. The prior neuron is number 11, the concept, 12 and the inhibitory interneuron, 13.

Thus, the prior biases the outcome to some subset of possible concepts in a given context.

IV. DISCUSSION

The conjecture that it is possible to reduce the spikes generated by a feature might seem surprising. There is, however, substantial work demonstrating that a single spike per neuron may be enough for pattern recognition. Thorpe et al. [26] discovered that people can make *very* rapid decisions on

whether pictures contain animals – so rapid that they are likely to be able to use only a single spike along the path from retina to associative cortex. Subsequent computational models have demonstrated the feasibility of the single-spike model.

The information overload argument for detail suppression suffers from a lack of understanding of what the brain can actually do on a large scale. We know something about the capacity of simple neural networks, such as the number of patterns storable in a Hopfield network or the Vapnik-Chervonenkis Dimension of feedforward networks. But on the scale of the cortex, we have only the most rudimentary of measures.

Darwin [27] famously remarked: *to suppose that the eye [...] could have been formed by natural selection, seems, I freely confess, absurd in the highest degree.* A century later, Nillson and Pelger [28] showed that evolving an eye was actually relatively easy. By the same token, without a very good model of the computational limits of the brain, the information-overload argument is hard to substantiate.

On the other hand, people are good at blocking out stimuli. The noise of a busy road, the drone of the engines in an aircraft cabin, the buzz of other speakers in a cocktail party – all demonstrate our remarkable capacity to shut out interference when we so desire. But this blocking is reversible and we can turn our attention to the distractions themselves. Koechlin [29] has shown that the pre-frontal cortex can select one context and block others when choosing an action.

The blocking of sensory detail seems to be hardwired and is *not* switchable. To turn off this inhibition would require additional circuits to turn off conceptual information. In general, such circuits do not seem to have evolved, and external techniques such as TMS are required for their inhibition. This would make sense: strategies to save energy would be likely to have evolved much earlier than the expansion of the cortex and its sophisticated filters and control mechanisms.

REFERENCES

- [1] A. Snyder and D. Mitchell, "Is integer arithmetic fundamental to mental processing?: The mind's secret arithmetic," *Proc. Royal Soc. London B*, vol. 266, pp. 587–592, 1999.
- [2] A. Snyder, T. Bossomaier, and D. Mitchell, "Concept formation: object attributes dynamically inhibited from conscious awareness," *Journal of Integrative Neuroscience*, vol. 3, pp. 31–46, 2004.
- [3] A. Snyder, E. Mulcahy, J. Taylor, D. Mitchell, P. Sachdev, and S. Gandevis, "Savant-like skills exposed in normal people by suppressing the left fronto-temporal lobe," *Journal of Integrative Neuroscience*, vol. 2, no. 2, 2003.
- [4] A. Snyder, H. Bahramali, T. Hawker, and D. Mitchell, "Savant-like numerosity skills revealed in normal people by magnetic pulses," *Perception*, vol. 35, no. 6, pp. 837–845, 2006.
- [5] P. Boggio, F. Fregni, C. Valasek, S. Ellwood, R. Chi, J. Gallate, A. Pascual-Leone, and A. Snyder, "Temporal lobe cortical electrical stimulation during the encoding and retrieval phase reduces false memories," *PLoS One*, vol. 4, no. 3, p. e4959, 2009.
- [6] R. P. Chi and A. Snyder, "Facilitate insight by non-invasive brain stimulation," *PLoS ONE*, vol. 6, no. 2, p. e16655, 02 2011.
- [7] M. Raichle and D. Gusnard, "Appraising the brain's energy budget," *PNAS*, vol. 99, no. 16, pp. 10237–10239, 2002.
- [8] A. Navarette, C. v. Schaik, and K. Isler, "Energetics and the evolution of human brain size," *Nature*, vol. 480, pp. 91–94, 2011.
- [9] S. Laughlin and T. Sejnowski, "Communication in neural networks," *Science*, vol. 301, no. 5641, pp. 1870–1874, 2003.
- [10] S. Laughlin, R. d. Ruyter van Steveninck, and J. Anderson, "The metabolic cost of neural computation," *Nature Neuroscience*, vol. 1, no. 1, pp. 36–41, 1998.
- [11] D. Attwell and S. Laughlin, "An energy budget for signaling in the grey matter of the brain," *J. Cereb. Blood Flow Metab.*, vol. 21, pp. 1133–1145, 2001.
- [12] E. Simoncelli and B. Olshausen, "Natural images statistics and neural representation," *Annual Rev. Neurosci.*, vol. 24, pp. 1193–1216, 2001.
- [13] B. Olshausen and D. Field, "Sparse coding with an overcomplete basis set: A strategy by V1?" *Vision Research*, vol. 37, no. 3, pp. 3311–3325, 1997.
- [14] K. Gaschler, "One person, one neuron?" *Scientific American*, vol. 17, pp. 77–82, 2006.
- [15] R. Quiroga, L. Reddy, G. Kreiman, C. Koch, and L. Fried, "Invariant visual representation by single neurons in the human brain," *Nature*, vol. 435, pp. 1102–1107, 2005.
- [16] B. Sengupta, M. Stemmler, S. Laughlin, and J. Niven, "Action potential energy efficiency varies among neuron types in vertebrates and invertebrates," *PLoS Comput Biol*, vol. 6, no. 7, p. e1000840, 07 2010.
- [17] T. Bossomaier and A. Snyder, "Absolute pitch accessible to everyone by turning off part of the brain?" *Organised Sound*, vol. 9, pp. 181–189, 2004.
- [18] C. Gilbert, M. Ito, M. Kapadia, and G. Westheimer, "Interactions between attention, context and learning in primary visual cortex," *Vision Research*, vol. 40, pp. 1217–1226, 2000.
- [19] R. Schäfer, E. Vasilaki, and W. Senn, "Perceptual learning via modification of cortical top-down signals," *PLoS Computational Biology*, vol. 3, no. 8, p. e165, 2007.
- [20] G. Jelinek, H. and Elston, "Dendritic branching of pyramidal cells in the visual cortex of the nocturnal owl monkey: A fractal analysis," *Fractals*, vol. 11, no. 4, pp. 391–396, 2003.
- [21] Y. Zhang, E. Meyers, N. Bichot, T. Serre, T. Poggio, and R. Desimone, "Object decoding with attention in inferior temporal cortex," *PNAS*, vol. 108, pp. 8850–8855, 2011.
- [22] A. L. Hodgkin and A. F. Huxley, "A quantitative description of membrane current and its application to conduction and excitation in nerve," *Journal of Physiology*, vol. 117, pp. 500–544, 1952.
- [23] E. Izhikevich, "Which model to use for cortical spiking neurons," *IEEE Trans. Neural Networks*, vol. 15, pp. 1063–1070, 2004.
- [24] M. Land and B. Tatler, *Looking and Acting: Vision and Eye Movements during Natural Behaviour*. Oxford University Press, 2009.
- [25] A. Saffari, "Biological Neural Network Toolbox for Matlab." [Online]. Available: <http://www.ymer.org/amir/software/biological-neural-networks-toolbox>
- [26] S. Thorpe, A. Delorme, and R. v. Rullen, "Spike-based strategies for rapid processing," *Neural Networks*, vol. 14, pp. 715–725, 2001.
- [27] C. Darwin, *On the Origin of the Species*. John Murray, 1859.
- [28] D.-E. Nillson and C. Pelger, "A pessimistic estimate of the time required for an eye to evolve," *Proc. Royal Soc. Lond. B*, vol. 256, pp. 53–58, 1994.
- [29] E. Koechlin, C. Ody, and F. Kouneiher, "The architecture of cognitive control in the human prefrontal cortex," *Science*, vol. 302, no. 5648, pp. 1181–1185, 2003.

Cyber Forensics: Representing and (Im)Proving the Chain of Custody Using the Semantic web

Tamer Fares Gayed, Hakim Lounis

Dépt. d'Informatique
 Université du Québec à Montréal
 Case postale 8888, succursale Centre-ville, Montréal
 QC H3C 3P8, Montréal, Canada
gayed.tamer@courrier.uqam.ca
lounis.hakim@uqam.ca

Moncef Bari

Dépt. d'Éducation et Pédagogie
 Université du Québec à Montréal
 Case postale 8888, succursale Centre-ville, Montréal
 QC H3C 3P8, Montréal, Canada
bari.moncef@uqam.ca

Abstract - Computer/Digital forensic is still in its infancy, but it is a very growing field. It involves extracting evidences from digital device in order to analyze and present them in a court of law to prosecute it. Digital evidences can be easily altered if proper precautions are not taken. A chain of custody (CoC) document is used to demonstrate the road map of how evidences have been copied, transported, and stored throughout the investigation process. With the advent of the digital age, the tangible CoC document needs to undergo a radical transformation from paper to electronic data (*e-CoC*), readable and consumed by machines, and applications. Semantic web is a flexible solution to represent different information, because it provides semantic markup languages for knowledge representation, supported by different vocabularies for provenance information. These features can be exploited to represent the tangible COC document to ensure its trustworthiness and its integrity. Moreover, querying mechanisms can be also incorporated over this represented knowledge to answer different forensic and provenance questions asked by juries concerning the case in hand. Thus, this paper proposes the construction of a framework solution based on the semantic web to represent and consume the forensic and provenance knowledge related to the tangible COC document.

Keywords - Knowledge Representation; Chain of Custody; Provenance Vocabularies; Semantic Web; Resource Description Framework.

I. INTRODUCTION

Computer/Digital forensic is a growing field. It combines computer science concepts including computer architecture, operating systems, file systems, software engineering, and computer networking, as well as legal procedures. At the most basic level, the digital forensic process has three major phases; Extraction, Analysis, and Presentation. Extraction (acquisition) phase saves the state of the digital source (ex: laptop and desktop, computers, mobile phones) and creates an image by saving all digital values so it can be later analyzed. Analysis phase takes the acquired data (ex: file and directory contents and recovering deleted contents) and examines it to identify pieces of evidence, and draws conclusions based on the evidences that were found. During presentation phase, the audience is typically the judges; in

this phase, the conclusion and corresponding evidence from the investigation analysis are presented to them [1].

Nevertheless, there exists others forensic process models, each of them relies upon reaching a consensus about how to describe digital forensics and evidences [2][17].

Like any physical evidence, digital evidence needs to be validated for the legal aspects (admissibility) in the court of law. In order for the evidence to be accepted by the court as valid; chain of custody for digital evidence must be kept, or it must be known who exactly, when, and where came into contact with the evidence at each stage of the investigation [3].

The role of players (first responders, investigators, expert witnesses, prosecutors, police officers) concerning CoC is to (im)prove that the evidence has not been altered through all phases of the forensic process. CoC must include documentation containing answers to these questions:

- Who came into contact, handled, and discovered the digital evidence?
- What procedures were performed on the evidence?
- When the digital evidence is discovered, accessed, examined, or transferred?
- Where was digital evidence discovered, collected, handled, stored, and examined?
- Why the evidence was collected?
- How was the digital evidence collected, used, and stored?

Once such questions ("i.e., known as 5Ws and the 1H") are answered for each phase in the forensic process, and players will have a reliable CoC which can be then admitted by the judges' court.

This paper proposes the creation of electronic chain of custody (*e-CoC*) using a semantic web based framework that represent and (im)prove the classical/traditional paper-based CoC during the cyber forensics investigation.

The Knowledge representation concept has been persistent at the centre of the field of Artificial Intelligence (AI) since its founding conference in the mid 50's. This concept described by Davis & al. by five distinct roles [28]. The most important is the definition of knowledge representation as a surrogate for things. This paper suggests the construction of electronic chain of custody (*e-CoC*) using semantic web as a surrogate of the tangible one.

Semantic web will be a flexible solution for this task because it provides semantic markup languages such as Resource Description Framework (RDF), RDF Scheme (RDFS), and Web Ontology Language (OWL) that are used to represent different knowledge.

In addition, the semantic web is rich with different provenance vocabularies [10], such as Dublin Core (DC), Friend of a Friend (FOAF), and Proof Markup Language (PML) that can be used to (im)prove the CoC by answering the 5Ws and the 1H questions.

The remainder of this document is organized as follows: section 2 presents the problem statement encounters the tangible CoC, the related works is presented in section 3, section 4 provides a brief background about the semantic web, the proposed solution is presented in section 5, and finally, conclusion in the last section.

II. PROBLEM STATEMENT

The continuous growing of devices and software in the field of computing and information technology creates challenges for the cyber forensics science in the volume of data (“i.e., evidences”) being investigated. It also increases the need to manage process and present the CoC in order to minimize and facilitate its documentation.

The second issue is related to the interoperability between digital evidence and its CoC documentation. Last works concentrated mainly on the representation and correlation of the digital evidences [24][25] and as an indirect consequence, the improving of the CoC by attempting to replicate the key features of physical evidence bags into Digital Evidence Bags (DEB) [5]. However, the documentation of CoC for digital evidences remains an exhausted task. Knowledge communication between the digital evidence and the information documentation about the evidence, apart from natural language, can create some automation and minimize human’s intervention.

The third issue concerns the CoC documents. They must be affixed securely when they are transported from one place to another. This is achieved using a very classical way: seal them in plastic bags (“i.e., together with physical evidence if it exists, such as hard disk, USB, cables, etc.”), label them, and sign them into a locked evidence room with the evidences themselves to ensure their integrity.

The fourth issue is about the judges’ awareness and understandings are not enough to evaluate, understand, and take the proper decision on the digital evidences related to the case in hand. One solution is to organize a training program to educate the juries the field of Information and Communication Technology (ICT) [6]. From the point of view of the authors, this will not be an easy task to teach juries the ICT concepts. The other solution is to provide a descriptive *e*-CoC using forensic and provenance metadata that the juries can query to find the answers to their questions through these metadata.

The last issue is that the problem is not only to represent the knowledge of the tangible CoC in order to solve the issues mentioned above, but also to express information about where the CoC information came from. Juries can find the answers to their questions on the CoC, but they need also

to know the provenance and origins of those answers. Provenance of information is crucial to guarantee the trustworthiness and confidence of the information provided. This paper distinguishes between forensic information and provenance information. Forensic information is responsible to answer the 5Ws and 1H questions related to the case in hand, while provenance information is responsible to answer questions about the origin of answers (“i.e., what information sources were used, when they were updated, how reliable the source was”).

III. RELATED WORK

Works related to this paper can be summarized over three dimensions.

The first dimension is the works on improving the CoC. In [22], a conceptual Digital Evidence Management Framework (DEMF) was proposed to implement secure and reliable digital evidence CoC. This framework answered the who, what, why, when, where, and how questions. The ‘what’ is answered using a fingerprint of evidences. The ‘how’ is answered using the hash similarity to changes control. The ‘who’ is answered using the biometric identification and authentication for digital signing. The ‘when’ is answered using the automatic and trusted time stamping. Finally, the ‘where’ is answered using the GPS and RFID for geo location.

Another work in [23], discusses the integrity of CoC through the adaptation of hashing algorithm for signing digital evidence put into consideration identity, date, and time of access of digital evidence. The authors provided a valid time stamping provided by a secure third party to sign digital evidence in all stages of the investigation process.

Other published work to improve the CoC is based on a hardware solution. SYPRUS Company provides the Hydra PC solution. It is a PC device that provides an entire securely protected, self contained, and portable device (“i.e., connected to the USB Port”) that provides high-assurance cryptographic products to protect the confidentiality, integrity, and non-repudiation of digital evidence with highest-strength cryptographic technology [15]. This solution is considered as an indirect improving of the CoC as it preserves the digital evidences from modification and violation.

Recently, a work for managing and understanding CoC has been provided using an ontological approach. This approach can be used to share common understanding of the structure of the digital forensic domain among different players, among software agents, and between players and software. This approach can also be used to enable the reuse of knowledge in digital investigation process [29].

The second dimension concerns knowledge representation. An attempt was performed to represent the knowledge discovered during the identification and analysis phase of the investigation process [26]. This attempt uses the Universal Modeling Language (UML) for representing knowledge. It is extended to a unified modeling methodology framework (UMMF) to describe and think about planning, performing, and documenting forensics tasks.

The third dimension is about the forensic formats. Over the last few years, different forensic formats were provided.

In 2006, Digital Forensics Research Workshop (DRWS) formed a working group called Common Digital Evidence Storage Format (CDEF) working group for storing digital evidence and associated metadata [12]. CDEF surveyed the following disk image main formats: Advanced Forensics Format (AFF), Encase Expert Witness Format (EWF), Digital Evidence Bag (DEB), gzip, ProDiscover, and SMART.

Most of these formats can store limited number of metadata, like case name, evidence name, examiner name, date, place, and hash code to assure data integrity [12]. The most commonly used formats are described here.

AFF is defined by Garfinkel et al. in [27] as a disk image container which supports storing arbitrary metadata in single archive, like sector size or device serial number. The EWF format is produced by EnCase's imaging tools. It contains checksums, a hash for verifying the integrity of the contained image, and error information describing bad sectors on the source media.

Later, Tuner's digital evidence bags (DEB) proposed a container for digital crime scene artifacts, metadata, information integrity, access, and usage audit records [5]. However, such format is limited to name/value pairs and makes no provision for attaching semantics to the name. It attempts to replicate key features of physical evidence bags, which are used for traditional evidence capture.

In 2009, Cohen et al. in [4] have observed problems to be corrected in the first version of AFF. They released the AFF4 user specific metadata functionalities. They described the use of distributed evidence management systems AFF4 based on an imaginary company that have offices in two different countries. AFF4 extends the AFF to support multiple data sources, logical evidence, and several others improvements such the support of forensic workflow and the storing of arbitrary metadata. Such work explained that the Resource Description Framework (RDF) [7] resources can be exploited with AFF4 in order to (im)prove the forensics process model.

IV. SEMANTIC WEB

Semantic web is an extension of the current web, designed to represent information in a machine readable format by introducing knowledge representation languages based in XML. The semantic markup language such as Resource Description Framework (RDF), RDF Schema (RDFS) and the web ontology language (OWL) are the languages of the semantic web that are used for knowledge representation.

According to the W3C recommendation [7], RDF is a foundation for encoding, exchange, and reuse of structured metadata. RDF supports the use of standards mechanisms to facilitate the interoperability by integrating separate metadata elements (vocabularies) defined by different resource description communities ("e.g., Dublin Core").

RDF consists of three slots: resource, property, and object. Resources are entities retrieved from the web ("e.g., persons, places, web documents, picture, abstract concepts,

etc."). RDF, resources are represented by uniform resource identifier (URI) of which URLs are a subset. Resources have properties (attributes) that admit a certain range of value or attached to be another resource. The object can be literal value or resources.

The main aim of the semantic web is to publish data on the web in a standard structure and manageable format [8]. Tim Berners Lee outlined the principles of publishing data on the web. These principles known as Linked Data Principles ("i.e., LD principles"):

- Use URI as names for things.
- Use HTTP URIs so that people can look up those names.
- When someone looks up a URI, provide useful information using the standards (RDF, SPARQL).
- Include RDF statements that link to other URIs so that they can discover related things.

The Linking Open Data (LOD) project is the most visible project using this technology stack (URLs, HTTP, and RDF) and converting existing open license data on the web, into RDF according to the LOD principles [9]. The LOD project created a shift in the semantic web community. Instead of being concentrated on the ontologies for their own sake and their semantic (languages to represent them, logics for reasoning with them, methods and tools to construct them), it becomes on the web aspects ("i.e., how data is published and consumed on the web").

Semantic web provides provenance vocabularies that enable providers of web data to publish provenance related metadata about their data. Provenance information about a data item is information about the history of the item, starting from its creation, and including information about its origins. Provenance information about the data on the web must comprise the aspects of publishing and accessing the data on the Web. Providing provenance information as linked data requires vocabularies that can be used to describe the different aspects of provenance [11][10][13][14].

V. SOLUTION FRAMEWORK

The solution framework is about the use of the semantic web to represent the CoC using RDF and improve its integrity through different built in provenance vocabularies. Thus, the CoC forensic information and its provenance metadata will be published and consumed on the web.

There exist various vocabularies to describe provenance information with RDF data. The popular standard metadata that can be used in different contexts is the Dublin core metadata terms defined in the RDFS schema [19]. The main goal of consuming this provenance metadata is to assess the trustworthiness and quality of the represented knowledge.

The W3C Provenance Incubator Group detected the needs for provenance in different context. Provenance Interchange Language (PIL) has been considered by the Provenance Interchange Working Group (PIWG) to publish and access provenance using that language. Heterogeneous systems and agents can export and import their provenance information into such a core language and reason over it [30].

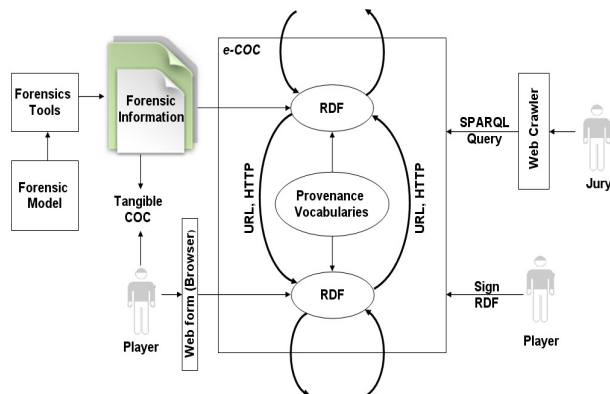


Figure1. Framework for representing and improving CoC using semantic web

As mentioned in Section 2, digital evidence can be stored in open or proprietary formats (“e.g., CDEF, AFF, EWF, DEB, gzip, ProDiscover, and SMART”). These formats store forensic metadata (“e.g., the sector size and device serial number”). The most advanced format for representing the digital evidence is the AFF4 which is an extension of the AFF to accommodate multiple data sources, logical evidence, arbitrary information, and forensic workflow [16].

The framework proposed in Figure-1 shows that the tangible CoC can be created manually from the output of forensic tools (“e.g., AFF4 or any other format”). AFF4 can be modeled into RDF. Human creates the CoC according to a predefined form determined by the governmental/commercial institution and fill the forms from the forensic information synthesized from the forensic tools. Experience can be used, if necessary, to prune or add some forensic metadata not provided on the current output format.

This framework is generalized to all phases of the forensic investigation. As we have different forensic models with different phases, the framework can be adapted for different phases of different models. A summary of different process models can be found in [2][17]. Each phase for specific forensic process model has its own information: forensic metadata, forensic algorithm, player who came into contact, etc.

The AFF4 can be directly represented using the RDF. Researchers have proposed several solutions on the use of AFF4 and RDF resources to improve digital forensics process model or software. The tangible CoC associated to each phase/digital evidences can be also represented in RDF. Players of each phase can enter the necessary information through a web form interface which is then transformed to RDF triple using web service tool (“e.g., triplify”) [18]. The RDF data are supported by different build in provenance vocabularies like DC [19], FOAF [20], and Proof Markup Language (PML) [21]. For example, the provenance terms used by the DC are: `dcterms:contributor`, `dcterms:creator`, `dcterms:created`, `dcterms:modified`, `dcterms:provenance`, which can give the juries information about who contributed, created, modified, the information provided to the court.

FOAF provides classes and properties to describe entities such as persons, organizations, groups, and software agents. The Proof Markup Language describes justifications for results of an answering engine or an inference process.

CoC representation for each phase in RDF data can be linked with another, using the same principle of the LOD project (“i.e., RDF graph/statement can be linked and be navigated using the semantic technology stack: URLs, HTTP, and RDF”). Digital evidence may be also integrated with its CoC information. After representing all information related to the digital evidence and its associated CoC, the player who comes into work in this phase can finally sign his RDF data. Finally, we will have an interlinked RDF based on the LOD principle which represents the whole *e-CoC* of the case in hand.

Juries can use application based on the same idea of the web crawler; they can not only navigate over the interlinked RDF graph/statement, but also, run query through a web application over the represented knowledge using SPARQL query language, and find the necessary semantic answers about their forensic and provenance questions.

The proposed framework can provide solutions to the issues mentioned in Section 2. Representation of the tangible CoC knowledge to RDF facilitates the management and processing because it is a machine readable form (first issue). It is also interoperable; digital evidence representation and its CoC description can be unified together under the same framework (“i.e., RDF”). Also, each player comes into role can secure (“i.e., using cryptographic approaches”) and sign his RDF data (“i.e., using digital signature”) to ensure the integrity and identity, respectively (second issue and third issue). On the other hand, juries can consume and navigate over the interlinked RDF data which present the whole and detailed information about the history of evidence from its collection to its presentation in the court (fourth issue). Provenance vocabularies can also be used to provide extra and descriptive metadata beyond the forensic metadata provided by the forensic tools (last issue).

VI. CONCLUSION

This paper proposes the construction of a semantic web based framework to represent and (im)prove tangible chain of custody using RDF and provenance vocabularies. After the definition and analysis of all related information (metadata) for each phase in a selected forensic process (“i.e., source will be the human experience and forensic tools output”), we will focus on the conversion and representation of tangible COCs information into interlinked RDF (*e-COCs*). This representation will contain forensic and provenance metadata (built-in/custom) related to the case in hand. The last phase will be the construction of a web interface that let the juries consume and query these interlinked RDF data in order to answer all questions related to the COCs of evidences and their provenances.

REFERENCES

- [1] Erin Kenneally. Gatekeeping Out Of The Box: Open Source Software As A Mechanism To Assess Reliability For Digital Evidence. Virginia Journal of Law and Technology. Vol 6, Issue 3, Fall 2001.
- [2] Michael W. Andrew "Defining a Process Model for Forensic Analysis of Digital Devices and Storage Media" Proceedings of the 2nd International Workshop on Systematic Approaches to Digital Forensic Engineering SADFE 2007
- [3] Ćosić, J., Bača, M. Do we have a full control over integrity in digital evidence life cycle, Proceedings of ITI 2010, 32nd International Conference on Information Technology Interfaces, Dubrovnik/Cavtat, pp. 429-434, 2010
- [4] Cohen, M.; Garfinkel, S.; Schatz, B. Extending the advanced forensic format to accommodate multiple data sources, logical evidence, arbitrary information and forensic workflow. Digital Investigation, 2009. S57-S.
- [5] Turner, P. Unification of Digital Evidence from Disparate Sources (Digital Evidence Bags). In 5th DFRW. 2004. New Orleans
- [6] Judges' Awareness, Understanding and Application of Digital Evidence, Phd Thesis in computer technology in Education, Graduate school of computer and information sciences, Nova Southeastern University, 2010
- [7] RDF: Model and Syntax Specification. W3C recommendation, 22 February 1999, www.w3.org/TR/REC-rdf-syntax-19990222/1999
- [8] The semantic web, Linked and Open Data, A Briefing paper By Lorna M. Campbell and Sheila MacNeill, June 2010, JISC CETIS
- [9] Christian Bizer, Tom Heath, Tim Berners-Lee: Linked Data - The Story So Far. Int. J. Semantic Web Inf. Syst. 5(3): 1-22 (2009)
- [10] Olaf Hartig: Provenance Information in the Web of Data. In Proceedings of the Linked Data on the Web (LDOW) Workshop at the World Wide Web Conference (WWW), Madrid, Spain, Apr. 2009
- [11] Olaf Hartig and Jun Zhao: Publishing and Consuming Provenance Metadata on the Web of Linked Data. In Proceedings of the 3rd International Provenance and Annotation Workshop (IPAW), Troy, New York, USA, June 2010
- [12] CDESf. Common Digital Evidence Format. 2004 [Viewed 21 December 2005]; Available from: <http://www.dfrws.org/CDESf/index.html>
- [13] [Olaf Hartig and Jun Zhao: Using Web Data Provenance for Quality Assessment. In Proceedings of the 1st Int. Workshop on the Role of Semantic Web in Provenance Management (SWPM) at ISWC, Washington, DC, USA, October 2009 Download PDF
- [14] Olaf Hartig, Jun Zhao, and Hannes Mühleisen: Automatic Integration of Metadata into the Web of Linked Data (Demonstration Proposal). In Proceedings of the 2nd Workshop on Trust and Privacy on the Social and Semantic Web (SPOT) at ESWC, Heraklion, Greece, May 2010
- [15] Solving the digital Chain of Custody Problem, SPYRUS, Trusted Mobility Solutions, © Copyright 2010
- [16] M. I. Cohen, Simson Garfinkel and Bradley Schatz, Extending the Advanced Forensic Format to accommodate Multiple Data Sources, Logical Evidence, Arbitrary Information and Forensic Workflow, DFRWS 2009, Montreal, Canada
- [17] MD Köhn, JHP Eloff and MS Olivier, "UML Modeling of Digital Forensic Process Models (DFPMs)," in HS Venter, MM Eloff, JHP Eloff and L Labuschagne (eds), Proceedings of the ISSA 2008 Innovative Minds Conference, Johannesburg, South Africa, July 2008 (Published electronically)
- [18] <http://triplify.org/Overview>
- [19] <http://dublincore.org/>
- [20] <http://www.foaf-project.org/>
- [21] P. P. da Silva, D. L. McGuinness, and R. Fikes. A Proof Markup Language for Semantic Web Services. Information Systems, 31(4-5):381-395, June 2006
- [22] Ćosić, J., Bača, M. (2010) A Framework to (Im)Prove Chain of Custody in Digital Investigation Process, Proceedings of the 21st Central European Conference on Information and Intelligent Systems, pp. 435-438, Varaždin, Croatia
- [23] Ćosić, J., Bača, M. (2010) (Im)proving chain of custody and digital evidence integrity with timestamp, MIPRO, 33. međunarodni skup za informacijsku i komunikacijsku tehnologiju, elektroniku i mikroelektroniku, Opatija, 171-175
- [24] Schatz, B., Mohay, G. And Clark, A. (2004) 'Rich Event Representation for computer Forensics', Proceedings of the 2004 Asia Pacific Industrial Engineering and Management System
- [25] Schatz, B., Mohay, G. and Clark, A. (2004) 'Generalising Event Forensics Across Multiple domains' Proceedings of the 2004 Australian Computer Network and Information Forensics Conference (ACNIFC 2004), Perth, Australia.
- [26] Bogen, A. and D.Dampier. Knowledge discovery and experience modeling in computer forensics media analysis. In international Symposium on Information and Communication Technologies. 2004: Trinity College Dublin
- [27] Garfinkel, S.L., D.J. Malan, K.-A. Dubec, C.C. Stevens, and C. Pham, Disk Imaging with the Advanced Forensics Format, library and Tools. Advances in Digital Forensics (2nd Annual IFIP WG 11.9 International Conference on Digital Forensics), 2006
- [28] Davis, R., H. Shrobe, and P. Szolovits. What is a knowledge representation? AI Magazine, 1993. 14(1): p.17-3
- [29] Jasmin Ćosić, Zoran Ćosić, Miroslav Bača, An Ontological Approach to Study and Manage Digital Chain of Custody of Digital Evidence, Journal of Information and Organizational Sciences (JIOS) e-ISSN: 1846-9418, Vol. 35, No.1 (2011), PP.1-13
- [30] Provenance Interchange Working group <http://www.w3.org/2011/01/prov-wg-charter>

Action Development and Integration in a Humanoid iCub Robot

How Language Exposure and Self-Talk Facilitate Action Development

Tobias Leugger

Laboratory of Intelligent Systems
École Polytechnique Fédérale de Lausanne
EPFL-STI-IMT-LIS, Station 11
CH-1015, Lausanne, Switzerland
tobias.leugger@epfl.ch

Stefano Nolfi

Institute of Cognitive Science and Technologies,
National Research Council (CNR-ISTC)
Via S. Martino della Battaglia, 44
00185, Roma, Italy
stefano.nolfi@istc.cnr.it

Abstract— One major challenge in evolutionary/developmental robotics is constituted by the need to identify design principles that allow robots to acquire progressively more complex action skills by integrating them into their existing behavioral repertoire. In this paper, we present a novel method that address this objective, the theoretical background behind the proposed methodology, and the results obtained in a series of experiments in which a simulated iCub robot develops lower-level and then integrated higher-level action skills. Moreover, we illustrate how the development of integrated action skill is facilitated by language exposure and self-talk.

Keywords— *developmental robotics; action integration; language and action; self-talk.*

I. INTRODUCTION

The acquisition of new behavioral skills and the ability to progressively expand our behavioral repertoire represents one key aspect of human intelligence and a fundamental capacity for robots companion, i.e., robots that should cooperate with humans in everyday environments [1]. Unfortunately the issue of how robots can acquire new action skills by integrating them into their existing behavioral repertoire still represent an open challenge for evolutionary/developmental robotics [1-3].

In this paper we provide a model validated through a series of experiments that demonstrates how a simulated humanoid robot can be trained incrementally for the ability to develop lower-level and then higher-level goal directed action skills (i.e., action capabilities that enable the robot to achieve a given desired goal in varying environmental conditions).

The first assumption behind our approach is that behavioral and cognitive processes in embodied agents should be conceived as dynamical processes with a multi-level and multi-scale organization [4]. This means that behavior (and cognitive skills) are: (i) dynamical processes originating from the continuous interaction between the robot and the physical and social environment, and (ii) display a multi-level and multi-scale organization in which the combination and interaction between lower-level behaviors, lasting for limited time duration, give rise to higher-level behaviors, extending over longer time scale and in which higher-level behaviors later affect lower-level

behaviors and the robot/environmental interaction from which they arise. This assumption implies that a behavioral unit does not necessarily correspond to a dedicated control unit or modules of the robot's neural controller. Moreover, it implies that the development of additional and higher-level behavior can occur through the recombination and re-use of pre-existing motor skills even when these skills do not correspond to separated physical entities but rather to processes that ultimately emerge from the robot/environmental interactions.

The second theoretical assumption behind our approach is that the concurrent development of cognitive and social skills (with particular reference to early language comprehension skills and language mediated interactions skills) might represent an important prerequisite for the development of action skills and vice versa [5]. Indeed, as originally hypothesized by Vygotsky [6-7], we believe that human language does not only play a communicative function but also constitutes a cognitive tool that facilitate/enable the development of other capabilities, including action capabilities. A comprehensive discussion of this hypothesis and of the implications of this idea for developmental robotics is provided by Mirolli and Parisi [8] that constitutes one of the main source of inspiration of the work described in this paper.

On the basis of these theoretical assumptions we studied how a robot provided with a non-modular neural controller can be trained for the ability to produce a series of lower-level elementary actions through a form of trial and error learning. Moreover we studied how such robot can later be trained for the ability to perform high-level integrated actions by re-using and re-combing previously learned skills. Such training process can potentially be extended to the acquisition of still higher-level action capabilities generated through the combination and re-use of previously acquired higher-level skills.

The acquisition of action skills at all level of organization is realized by enriching the robots' sensory state with symbolic linguistic inputs that allow the robot to more easily learn the affordance of different categorical contexts as well as to disambiguate between contexts affording multiple actions (for a related approach see [9]).

The acquisition of action skills at higher (non-elementary) level of organization is realized by also

enriching the robot's sensory state with a linguistic description of the elementary actions that can be re-used to generate new integrated behavior capabilities (for a related approach see [10]). Moreover, the acquisition of higher-level skills is realized by providing the robot with a neural architecture that allows it to develop and exploit a form of self-talk. By talking to ourselves or self-talk we refer to the ability to self-generate the linguistic stimulation produced by other agents, as both children and adult human beings do both externally (as in private speech) and internally (as in inner speech [7,11]).

In section II, we describe the experimental scenario and in section III, the obtained results. Finally, in section IV, we draw our conclusions.

II. EXPERIMENTAL SCENARIO

A simulated humanoid iCub robot has been trained for the ability to display low-level (elementary) behaviors and higher-level behaviors by combining and integrating the previously acquired low-level behaviors.

A. The robot and the environment

The iCub is a humanoid robot developed at IIT as part of the EU project RobotCub [12]. It has 53 motors that move the head, arms and hands, waist, and legs. From the sensory point of view, the iCub is equipped with digital cameras, gyroscopes and accelerometers, microphones, force/torque sensors, tactile sensors. In the experiment reported in this paper, the sensors and actuators located on the head, the right arm and on the legs have not been used. The experiments have been carried out by using the simulator developed at our lab by Gianluca Massera, Tomassino Ferrauto and others. The simulator reproduces as accurately as possible the physics and the dynamics of the robot and robot/environment interaction, and is based on the Newton Game Dynamics open-source physics engine.

The robot is located in front of a table containing a red object (Figure 1). The object is a sphere with a mass of 200 grams and a diameter of 7 cm with a flattened base to prevent it from rolling away. A green spot indicates the target location in which the object should be moved. At the beginning of each trial the target object is placed in one of four possible areas (10 cm to the front, back, left, and right respectively to a point 30 cm in front and 10 cm to the left of the robot). To increase robustness the position of the object is randomly moved between $[-2, 2]$ cm from the four points indicated above. The target spot is randomly placed within two areas located 10cm left or right with respect to the front of the robot at a height of 25cm above the table and at a distance of 25 cm from the robot.

B. The robot's neural controller

The controller of the robot is constituted by an artificial neural network (Figure 2) that receives proprioceptive input from torso and from the left-arm/hand and exteroceptive input from the visual system, the tactile sensors, and from the linguistic input units that encode the labels provided by a caretaker (see below). The network produces as output the desired states of the joints of the torso and of the right

arm/hand and an output that determines the focus of attention.

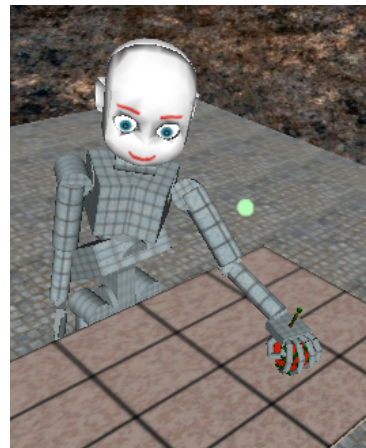


Figure 1. The simulated robot and the environment.

More specifically, the focus output unit binarily encodes whether the visual system of the robot is paying attention to the red object or to the green target, the 2 torso motor neurons encode the desired angular position of the rotation and extension/flexion Degree of Freedoms (DOFs) of the torso, the 7 arm motor neurons encode the desired angular position of the 7 DOFs of the left-arm and of the wrist, and the 3 fingers motor neurons indicate the extension/flexion of thumb, the opposition of the thumb with respect to the other fingers, and the extension/flexion of all other fingers (i.e. to simplify the model all fingers joints are actuated through only 3 motor neurons).

All the arm and hand joints are allowed to move in the full range of motion possible on the physical iCub. The yaw and pitch torso joints are both limited to a range of $[-10,40]$ degrees to eliminate un-desirable postures.

The 3 position sensors indicate the relative position of the red ball or of the green target (depending on what the robot is paying attention to) with respect to the left-hand along the three orthogonal axis, the 12 proprioceptors encode the current position of the torso, left-arm, and fingers joints, the 6 tactile sensors encode the activation state of the tactile sensors located on the left-hand palm and on the tips of the 5 fingers, finally the 4 linguistic inputs locally encode whether the caretaker produced the "reach", "grasp", "open", or "move" linguistic label.

The state of the robots' sensors, the state of the neural controller, the desired state of the robots actuators, and the state of the robot and of the environment are updated every step, i.e., every 50 milliseconds.

C. The training algorithm

The architecture of the neural controller is fixed. The connection weights, biases, and time constants are encoded as free parameters and trained thorough an evolutionary robotics method [13]. This method has been chosen since it is one of the most simple yet effective way to train a robot on the basis of a distal reward (i.e., for the ability to display behaviors producing a desired outcome without specifying

how such behaviors should be realized) and since it does not put constraints on the architecture of the robots' controller and/or on the type of parameters that can be subjected to the training process.

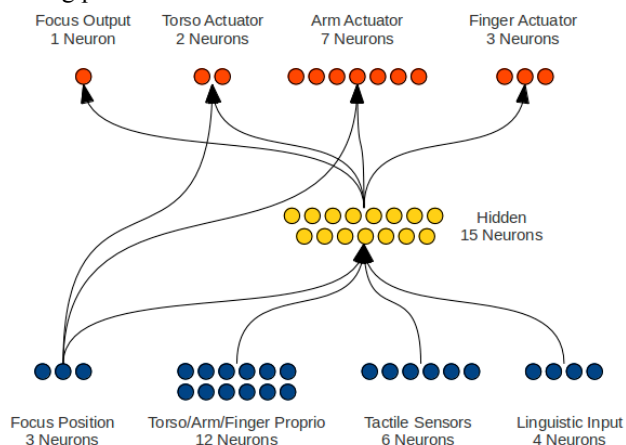


Figure 2. The architecture of the robot's neural controller during the first training phase. The neurons are grouped in clusters. Arrows between two clusters indicate full connectivity between the two corresponding groups of neurons.

The initial population consists of 100 randomly generated genotypes that encode the connection weights and the biases of 100 corresponding neural controllers. Each parameter is encoded by 16 bits, and normalized in the range [-1.0, 1.0] in the case of connection weights and biases, and in the range [0.0, 1.0] in the case of time constants. Each genotype is translated into a corresponding neural controller and evaluated as described below. The top 20 genotypes are allowed to reproduce by generating 5 offspring (1 unvaried and 4 varied copies). Variations are introduced by randomly flipping 0.005% and 0.04% of the bits, during the first and second training phase respectively. The selection of the top genotypes is realized on the overall performance of the robot, i.e., the sum of the rewards obtained by the robot during its entire lifetime.

The training is realized incrementally. During the first training phase, the robot is trained for the ability to display four lower-levels actions: REACH (i.e., bring the hand over an object), OPEN (i.e., open the fingers and align the palm to face downward), GRASP (i.e., close the fingers around the object), MOVE (i.e., move the object toward a target destination). The evaluation of candidate solutions is realized during 16 trials --- 4 trials for each of the four actions with the object placed in four different areas. At the beginning of each trial the posture of the robot is initialized in a position that enable the robot to potentially display the desired action also without possessing the other related skills (e.g., far from the object in the case of REACH, with the fingers closed in the case of OPEN, near and over the object in the case of GRASP, with the object in the hand in the case of MOVE). To force the robot to develop robust solutions the initial posture of the robot at the beginning of each trial is varied within 16 different alternatives. During each trial the robot is rewarded for the ability to achieve the goal of the current

elementary action. The robot receives a small reward every time step on the basis of extent to which its current state approximate the desired state and a significant reward when the goal has been accomplished. In the case of REACH actions, the goal consists in bringing the palm of the left hand within 6cm from the top part of the object. The goal of the OPEN actions consists in stretching out all the fingers while aligning the palm downward and while keeping the palm within a distance of 6 cm from the top part of the object. In the case of GRASP actions, the goal consists in closing the fingers around the object (i.e., reducing the distance between the barycenter of the object and the centroid of the tip of the thumb, the tip of the pinky, and the center of the palm below a threshold). The goal of MOVE actions consists of moving the object within 6cm from the target location. The overall performance (fitness) of each individual robot is computed by calculating the harmonic mean of the scores obtained during trials involving the execution of different actions.

During the second training phase, the robot is trained for the ability to perform integrated actions, such as MOVE-TO-TARGET (i.e., moving a distant object from its location to a target location), by combining and integrating over time the previously acquired elementary action skills. During this second phase each robot is evaluated for 8 trials. At the beginning of each trial the object and the target spot are randomly initialized within the areas described above. The posture of the robot is initialized so that the position of the left-hand is far from the object and from the target location.

The goal of this integrated action is the same of the MOVE elementary action: moving the object to within 6cm of the target location. Due to the different initial conditions, however, the realization of this goal requires the execution of an integrated sequence of actions. The robot receives a significant reward when this goal is accomplished and smaller rewards when the object has been lifted and when the robot correctly focuses its attention on the object and on the target location before and after the object is lifted, respectively.

To study the role of language exposure and self-talk four series of experiments have been carried out in four experimental conditions described in the following section. For more details see [14].

III. RESULTS

In this section, we describe the results obtained during the a training phase, in which the robot is trained for the ability to display the low-level (elementary) behaviors (Section A), and during a second training phase in which the robot is trained for the ability to display the higher-level integrated behavior (Section B-D). For the second phase we report the results obtained in: (i) a control experimental condition (C), (ii) a language exposure condition (LE) in which the robot receives from the caretaker the label that indicates the elementary action that is appropriate in the current context during part of the trials, (iii) a self-talk condition (ST) in which the robot is allowed to self-generate the labels of the elementary actions to be executed, and (iv) a learning to self-talk condition (LST) in which the robot is allowed to self-

generate the labels during part of the trials and to anticipate the labels produced by the caretaker during the remaining trials. The first and second training phases have been replicated 10 times for each experimental condition.

A. Acquisition of elementary action skills

The training of the elementary behaviors reached optimal performance within 1500 generations in 9 out of 10 replications of the experiment. By optimal performance we mean robots displaying successful behavior in 16 out of 16 trials. The fastest and the slowest successful replications reached optimal performance at generation 246 and 711. The best individual of the worst replication (the only one that did not achieved optimal performance) was successful in 15 out of 16 trials.

B. Acquisition of integrated action skills

In the second phase, the robot was trained for the ability to display the MOVE-TO-TARGET high-level behavior that consists in moving a distant object from its current location to a target location indicated by a green spot. Since the initial posture of the robot’s arm/hand is far from the object, the production of this higher-level behavior can be realized by re-using, combining, and integrating the REACH, OPEN, GRASP, and MOVE behaviors acquired previously.

To provide the robots with the computational resources necessary for combining and integrating the elementary action skills we provided their neural controller with four additional continuous time internal neurons receiving and projecting connections from and to the block of 15 internal neurons and from themselves (Figure 3). Moreover, the new block of internal neurons receives connections from high-level linguistic input neurons (only “move-to-target” in the case of the experiment reported in this paper).

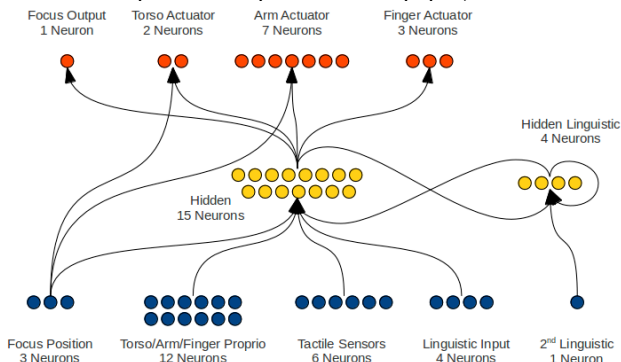


Figure 3. The architecture of the robot’s neural controller during the second training phase (C and LE conditions).

The initial population of candidate solutions is generated by using the genome of the best 10 individuals of the 10 replications of the experiment described above in which the robot were trained for the ability to display the lower-level actions. The values corresponding to the newly added connection weights, biases, and time-constant were randomly generated and subjected to the training process. The values corresponding to the pre-existing connection

weights were kept constant during the second training phase. The training process is continued for 100 generations.

The state of the high-level linguistic input is activated, the state of the four lower-level linguistic inputs is set to a null value.

By post-evaluating the best robots of each generation of each replication for 40 trials we observed that the average performance are rather low and no individual successfully produce the integrated behavior in all trials (see Figure 4, condition C). The best individual successfully displays the integrated behavior in 30 out of 40 trials.

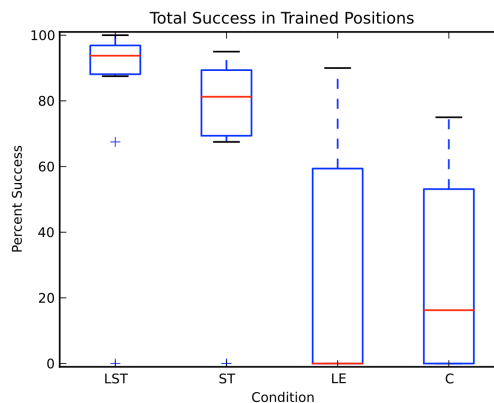


Figure 4. Percentage of successful trials for the best robots trained in the four experimental conditions (see text). Each robot has been post-evaluated for 40 trials during which it did not received any linguistic input from the caretaker. Each boxplot shows the percentage of successful trials displayed by the best 10 robots obtained in the 10 corresponding replications of the experiment. Whiskers expand to the minimum and maximum with outliers marked as +.

C. How language exposure facilitates action development

In a second experimental condition we studied whether the availability of linguistic inputs produced by a caretaker, that specify the label of the elementary behavior that is appropriate in any given circumstance, facilitates the acquisition of the integrated behavior. Given the nature of the integrated behavior, the following sequence of labels is provided: REACH, OPEN, GRASP, and MOVE. For practical reasons, the caretaker has been simulated through a software routine that analyzes the state of the robot and of the environment and determines the point over time in which the current label has to be substituted with the next label. More specifically, caretakers start to produce the “reach” label and switch to the next label as soon as the distance between the top part of the object and the left-palm of the robot decrease below 6 cm. Then, the “open” label is produced until all the fingers are extended sufficiently, the palm is horizontally oriented over the object, and the distance between the palm and the top-part of the object is below 6cm. Then, the “grasp” label is produced until 3 of the tactile sensors are in contact with the object. Finally, the “move” label is produced until the end of the trial.

To force the robot to develop an ability to produce the integrated behavior also autonomously, i.e., without the

support of the caretaker, the artificial caretaker produced the linguistic input only during even trials (i.e., the state of the four linguistic inputs is always null during odd trials).

The linguistic inputs provided by the caretaker thus enrich the robots' sensory information during half of the trials. The way in which the performance of the robot is evaluated, as well as all other parameters, is the same of the experiments described in the previous sub-section.

The analysis of the trained robots indicates that optimal performance are obtained in 4 out of 10 replications of the experiment. The performance obtained by post-evaluating the best trained individuals for 40 trials without linguistic labels and the comparison with the performance obtained in the control (C) condition (Figure 4, condition LE) shows how the exposure to linguistic inputs enables the robot to achieve better performance, although only in few replications.

D. How self-talk facilitates action development

In the third and fourth experimental conditions, we investigated whether the possibility to self-talk, i.e. the possibility to self-generate over time the linguistic labels associated to the elementary actions, can facilitate the development of the integrated behavior.

To enable the robots to develop a form of inner-speech we extended the neural architecture used for the acquisition of the elementary actions in a different manner (Figure 5). More specifically, we added a layer of four neurons that receive and project connections from and to the layer of 15 internal neurons, and receive connections from themselves and from the higher-level linguistic input units (only the "move-to-target" unit in the case of the experiments reported in this paper). These four neurons are used to self-generate linguistic labels (i.e. vector of binary values encoding the labels "reach", "open", "grasp", and "move") that are then used to set the activation of the four lower-level linguistic inputs. This is realized by activating the linguistic input corresponding to the most activated linguistic output and by setting to a null value the activation states of the other linguistic inputs. All other parameters are kept the same as in previous experimental conditions.

As in the case of the experiments performed in the two conditions illustrated above, the value of the additional connection weights and biases are initialized to a random value and subjected to the training process. All other parameters are identical to those used in the experiments described in the other conditions.

More specifically, we studied two self-talk conditions. In the ST condition, the robots never received linguistic labels from the caretaker and always rely on the self-generated labels.

The analysis of the results obtained in this condition indicates that robots displaying successful behaviors in all trials are obtained in 8 out of 10 replications of the experiment. The performance obtained in the post-evaluation test (Figure 4, ST condition) are significantly better than the performance obtained in the language exposure (LE) and control condition (C). Overall the obtained results thus

indicates that the possibility to self-talk strongly facilitates the development of the integrated behavior.

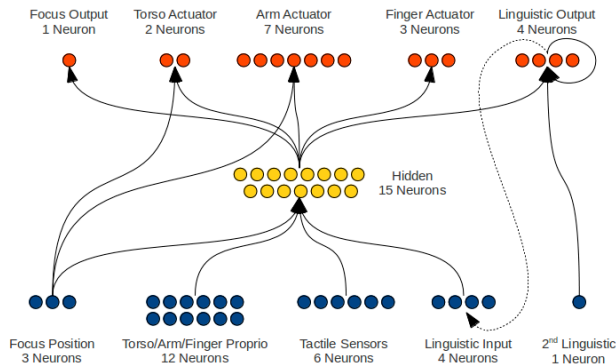


Figure 5. The architecture of the robot's neural controller during the second training phase (ST and LST conditions).

In the ST conditions the robots are not rewarded directly for the ability to self-talk but only for the ability to produce the integrated behavior. In the fourth and last condition (LST) we rewarded the robot for the ability to self-generate and to predict the linguistic labels produced by the caretaker during even trial and for the ability to produce the integrated behavior by self-generating the linguistic labels during odd trials. The aim of the experimental condition was that to verify whether an explicit training to self-talk, realized through the attempt to anticipate the caretaker linguistic behavior, can facilitate the acquisition of the integrated behavior.

To enable the development of an ability to anticipate the caretaker behavior we reward the robot with a big score every time it self-generates the new label 1-5 steps earlier than the caretaker and a smaller reward every time it self-generate the new label 6-20 steps earlier than the caretaker.

The analysis of the performance of individuals during the training process indicate that the best individuals achieve optimal performance in 9 out of 10 replications. Moreover, the analysis of the results obtained by post-evaluating the best individuals for 40 trials without linguistic inputs (see Figure 4, LST condition) indicates that the possibility to self-talk combined with an explicit training to self-talk produce better result with respect to the ST condition.

E. Generalization and integration strategies

To verify the generalization capabilities of trained robots and to compare generalization performance for agents trained in the four experimental conditions we post-evaluated the performance of trained robots by placing the object in 7x7 different positions uniformly distributed over a 35x35 cm² area and by varying the initial position of the arm for each object position within four different alternative postures. As can be seen in Figure 6, overall, the robots display rather good generalization capabilities. That is performance decrease only slightly with respect to the case in which the robots have been post-evaluated in the same condition experienced during the training process. A two-

tailed Mann-Whitney U Test indicate that the LST condition is significantly better than the other three conditions and that the ST condition is significantly better than the C condition.

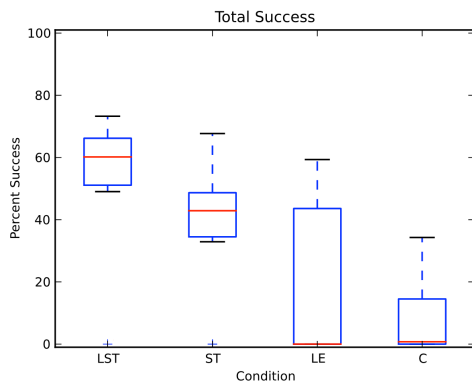


Figure 6. Percentage of successful trials for the best robots of the four experimental conditions post-evaluated for 49 different object positions.

The comparison of the behavior produced during even and odd trials in the LST conditions (in which the robot receives and does not receive the linguistic labels from the caretaker, respectively) indicates that 6 of the 10 robots of the LST condition that have a better generalized performance when they operate autonomously than when they receive the linguistic inputs from the caretaker. Moreover, during self-talk all the 6 robots are also faster in performing the integrated behavior. The significance of the difference has been evaluated on the basis of a two-tailed Mann-Whitney U Test. This result indicates that robots are capable of developing better strategies than those conveyed by the caretaker.

IV. DISCUSSION AND CONCLUSION

In this paper, we demonstrated how a simulated iCub robot can acquire multiple goal-oriented action skills through an incremental training process in which it first develop lower-level (elementary) actions and then higher-level integrated behaviors by combining and integrating previously acquired lower-level action skills. Overall, the obtained results represent one of the first demonstrations of how a relatively complex robot can acquire and display multiple behavioral skills and can expand its behavioral repertoire (for a related work see [15]).

The behavioral skills developed by our robots are not simply elements or objects but rather dynamical processes that originate from the robot/environmental interaction (and in some cases also from the interaction with the social environment constituted by the caretaker). They are flexible entities that are able to achieve the appropriate goal in varying robot/environmental circumstances. Similarly, the way in which these processes are combined to generate higher-level action skill is realized in a manner that is fluid and flexible enough to achieve the appropriate goal in varying environmental circumstances.

One important aspect that characterizes the model presented is that it relies on a non-modular controller, i.e., it does not require a control system divided into modules (as

for example in [16]) and does not assume a one-to-one correspondence between modules and behaviors. This aspect is particularly important from a developmental point of view, since it allows the development of behaviors that emerge from the interaction between the robot and the environment and from the interaction between previously developed control mechanisms that are responsible for the generation of other action labels. Moreover, this aspect facilitates the development of behavioral capabilities that are more suitable to be recombined and integrated. To appreciate this point we should consider that the development of low-level action capabilities (such as “REACH” and “GRASP”) through the use of different control modules will likely end up with the exhibition of behaviors based on different equivalent postures that are hard to combine to produce integrated behavior. The realization of the lower-level behaviors through the same neural controller, instead, leads to the production of more similar behaviors that are more ready to be integrated.

A second important aspect that characterizes the model proposed is constituted by the key role played by language mediated social interactions with particular reference to language exposure and self-talk.

For what concern language exposure, the availability of linguistic labels such as “grasp” and “move” during the acquisition of low-level actions facilitate the acquisition of an ability to discriminate the categorical contexts affording specific actions. Moreover, as previously demonstrated by [17] in a study conducted on a similar experimental scenario, the availability of linguistic inputs indicating the current appropriate action allows the robot to overcome the problem caused by the need to handle robot/environmental contexts affording multiple actions. Finally, the availability of linguistic inputs indicating the sequence and the timing with which lower-level actions should be concatenated to generate new high-level behaviors facilitates the acquisition of an ability to produce integrated actions also autonomously, i.e. without linguistic inputs.

For what concerns self-talk, the possibility to self-generate internal states analogous to the linguistic inputs produced by the caretaker strongly facilitates the development of integrated behaviors and leads to robust solutions that generalize well also in new environmental circumstances. This can be explained by considering that the combination of language exposure and self-talk facilitates the re-use of previously developed action skills. An additional facilitation effect can be gathered by explicitly training the robot to anticipate the linguistic inputs provided by the caretaker.

The model proposed also allows the robot to develop more effective strategies with respect to those demonstrated by the caretaker. Indeed, the training method proposed constitutes a form of socially assisted individual learning that on one hand allows the robot to exploit the social feedback to facilitate the discovery of effective solutions, but that on the other hand, leaves the robot free to improve its current solution also with respect to the strategy illustrated by the caretaker.

ACKNOWLEDGMENT

This research work was supported by the ITALK project (EU, ICT, Cognitive Systems and Robotics Integrated Project, grant n. 214668).

REFERENCES

- [1] Schaal S. (2007). The new robotics: towards human-centered machines," *HFSP Journal*, vol. 1, no. 2, pp. 115-126.
- [2] Weng J.J., McClelland J., Pentland A., Sporns O., Stockman I., Sur M. and Thelen E. (2001). Autonomous mental development by robots and animals. *Science*, 291:599–600.
- [3] Bongard J. (2008) *Behavior Chaining: Incremental Behavior Integration for Evolutionary Robotics*, Artificial Life XI, MIT Press, Cambridge, MA.
- [4] Nolfi S. (2006). Behaviour as a complex adaptive system: on the role of self-organization in the development of individual and collective behaviour. *ComplexUs*, 2 (3-4): 195-203.
- [5] Cangelosi A., Metta G., Sagerer G., Nolfi S., Nehaniv C, Fischer K., Tani J., Belpaeme T., Sandini G., Fadiga L., Wrede B., Rohlfing K., Tuci E., Dautenhahn K., Saunders J. and Zeschel A. (2010). Integration of action and language knowledge: A roadmap for developmental robotics. *IEEE Transactions on Autonomous Mental Development*, (2) 3: 167-195
- [6] Vygotsky L.S. (1962). *Thought and language*, MIT Press, Cambridge, MA.
- [7] Vygotsky L.S. (1978). *Mind in society*. Cambridge, MA: Harvard University Press.
- [8] Mirolli M. and Parisi D. (2011). Towards a Vygotskian Cognitive Robotics: The Role of Language as a Cognitive Tool, *New Ideas in Psychology*, vol. 9, pp. 298-311.
- [9] Yamashita Y. and Tani J. (2008). Emergence of functional hierarchy in a multiple timescale neural network model: a humanoid robot experiment. *PLoS Computational Biology*, Vol.4, Issue.11, e1000220.
- [10] Zhang Y. and Weng J. (2007). Task transfer by a developmental robot. *IEEE Transactions on Evolutionary Computation*, (11) 2: 226-248.
- [11] Diaz R. and Berk L.E., ed. (1992), *Private speech: From social interaction to self regulation*, Erlbaum, New Jersey, NJ
- [12] Sandini G., Metta G., and Vernon D. (2004). *Robotcub: An open framework for research in embodied cognition*. *International Journal of Humanoid Robotics*, 8(2), 18-31.
- [13] Nolfi S. and Floreano D. (2000). (2000). *Evolutionary Robotics: The Biology, Intelligence, and Technology of Self-Organizing Machines*. Cambridge, MA: MIT Press/Bradford Books.
- [14] Leugger T. (2012). *Development of Integrated Behaviour in a Simulated Humanoid Robot: Exploiting Language Assisted Training and Self Talk*. Masters Thesis. School of Computer and Communication Sciences. Ecole Polytechnique Federale de Lausanne, Switzerland.
- [15] Tani J., Nishimoto R. and Paine R.W. (2008). Achieving 'organic compositionality' through self-organization: Reviews on 'brain-inspired robotics experiments', *Neural Networks*, 21:584-603.
- [16] Brooks R. (1986). A robust layered control system for a mobile robot. *IEEE J of Robotics and Automation*, 2(1):14–23.
- [17] Massera G., Tuci E., Ferrauto T. and Nolfi S. (2010). The facilitatory role of linguistic instructions on developing manipulation skills, *IEEE Computational Intelligence Magazine*, (5) 3: 33-42.

Gaining Insights from Symbolic Regression Representations of Class Boundaries

Ingo Schwab

Karlsruhe University of Applied Sciences
Karlsruhe, Germany
Ingo.Schwab@hs-karlsruhe.de

Norbert Link

Karlsruhe University of Applied Sciences
Karlsruhe, Germany
Norbert.Link@hs-karlsruhe.de

Abstract- In this paper, we propose a generalization of the well-known regression analysis to fulfill supervised classification aiming to produce a learning model which best separates the class members of a labeled training set. The class boundaries are given by a separation surface which is represented by the level set of a model function. The separation boundary is defined by the respective equation. The model is represented by mathematical formulas and composed of an optimum set of expressions of a given superset. We show that this property gives human experts additional insight in the application domain. Furthermore, the representation in terms of mathematical formulas (e.g., the analytical model and its first and second derivative) adds additional value to the classifier and enables to answer questions, which other classifier approaches cannot. The symbolic representation of the models enables an interpretation by human experts.

Keywords- Classification; Symbolic Regression; Knowledge Management; Data Mining; Pattern Recognition.

I. INTRODUCTION

Supervised classification algorithms aim at assigning a class label for each input example. Given a training dataset of the form (x_i, y_i) , where $x_i \in \mathbb{R}^n$ is the i th example and $y_i \in \{-1, +1\}$ is the i th class label in a binary classification task. A model φ is learned, so that $\varphi(x_i) = y_i$ for new unseen examples. In fact, it is an optimization task and the learning process is mainly data driven. It results in an adaptation of the model to reproduce the data with as few errors as possible. Several algorithms have been proposed to solve this task and the result of the learning process is an internal knowledge model φ .

There are basically two ways to represent the knowledge of model φ . The first approach includes algorithms like Naïve Bayes Classifiers, Hidden Markov Models or Belief Networks [1]. The main idea is to represent it as probability distribution. The classification boundary is the intersection of the posterior probabilities in Bayes decision theory.

The other approach for representing the knowledge is to determine a surface in the feature space which separates the different classes of the training data as good as possible. The decision surface is represented by parameterized functions which can be the sum of weighted base functions of one function class. Examples include the logistic functions and

radial basis functions, which can be used in Neural Networks and Support Vector Machines [1].

It is important to point out that the base functions are closely linked to the used classifiers. Our approach further refines this idea (see Sections II and III). Again, the decision surface is determined by a level surface of a model function. But, in this case, the function is composed of arbitrary mathematical symbols, forming a valid expression of a parameterized function. This approach allows the human users of the system to control the structure and complexity of the solutions.

Following this idea, we try to find solutions which are as short (and understandable) as possible. Additionally, the selected solutions should model the dataset as good as possible. Clearly, this is a contradiction and of the nature of multiobjective decision making. Therefore, we select all good compromises of the pareto front [4] and sort them by complexity. This approach extends the concept presented in [11] and helps human experts to choose the best compromise. Standard classification approaches (e.g., Neural Networks) in which the structure of the base functions is predefined are not able to reduce their structural complexity. In most nontrivial applications they are not understandable to the human expert and the represented knowledge can therefore not be refined and reused for other purposes [2].

There are many different ways to further subdivide this class of learning algorithms (e.g., greedy and lazy, inductive and deductive [5]). In this paper we focus on the symbolic and subsymbolic paradigm (see [2][3] for more details) and its consequences for the reusability of the model φ and the inherent learned knowledge. This subdivision separates the approaches with symbolic representations in which the knowledge of model φ is characterized by explicit symbols, whereas subsymbolic are associated with continuous representations. One of the main disadvantages of subsymbolic classifiers (e.g., Neural Network or SVM) is that the class of classifiers includes rather the properties of a black box and the learned model cannot be interpreted or reformulated.

The main advantages of our approach (see Table I) are determined by the inherent nature of mathematical formulas and there are many rules to reformulate, simplify and derive additional information from them (e.g., first and second derivative). In fact, reformulating mathematical formulas is one of the most important areas of mathematics. For the

black box character of the subsymbolic learning algorithms such rules simply do not exist.

The remaining part of this paper is arranged as follows. In Section II, the proposed Symbolic Regression Algorithm is presented. Section III summarizes our approach and shows how to generalize the regression task to classification. Furthermore, the main advantages of the approach are briefly shown. Section IV explains some of our experiments and Section V concludes.

II. BACKGROUND AND RELATED WORK

A. Symbolic vs. Subsymbolic Representation

As Smolensky [3] noted, the term subsymbolic paradigm is intended to suggest symbolic representations that are built out of many smaller constituents: “Entities that are typically represented in the symbolic paradigm by symbols are typically represented in the subsymbolic paradigm by a large number of subsymbols” (p.3). From this point of view the syntactic role of subsymbols can be described that subsymbols participate in numerical computation. In contrast operations in the symbolic paradigm that consist of a single discrete operation are often achieved in the subsymbolic paradigm as the result of a large number of much finer-grained numerical operations. One well known problem with subsymbolic networks which have undergone training is that they are extremely difficult to interpret and analyze. In [2], it is argued that it is the inexplicable nature of mature networks.

B. Pareto Front

In this subsection we discuss the Pareto Front or Pareto Set in multiobjective decision making [4]. This area of research has a strong impact on machine learning and data mining algorithms.

Many problems in the design of complex systems are formulated as optimization problems, where design choices are encoded as valuations of decision variables and the relative merits of each choice are expressed via a utility or cost function over the decision variables.

In most real-life optimization situations, however, the cost function is multidimensional. For example, a car can be evaluated according to its cost, size, fuel consumption, storage room, and a configuration s which is better than s' according to one criteria, can be worse according to another. Consequently, there is no unique optimal solution but rather a set of efficient solutions, also known as pareto solutions, characterized by the fact that their cost cannot be improved in one dimension without being worsened in another. In machine learning algorithms the competing criteria are the prediction accuracy and the size of the learning model.

The set of all Pareto solutions, the Pareto front, represents the problem trade-offs, and being able to sample this set in a representative manner is a very useful aid in decision making.

In other words the solutions are ordered by complexity. Through the symbolic representation the human expert is able to interpret the solutions of the pareto front (see section IV c).

C. Classical Regression Analysis and Symbolic Regression

Regression analysis [7] is one of the basic tools of scientific investigation enabling identification of functional relationship between independent and dependent variables. The general task of regression analysis is defined as identification of a functional relationship between the independent variables $\mathbf{x} = [x_1, x_2, \dots, x_n]$ and dependent variables $\mathbf{y} = [y_1, y_2, \dots, y_m]$, where n is a number of independent variables in each observation and m is a number of dependent variables.

The task is often reduced from an identification of a functional relationship f to an identification of the parameter values of a predefined (e.g., linear) function. That means that the structure of the function is predefined by a human expert and only the free parameters are adjusted. From this point of view Symbolic Regression goes much further.

Like other statistical and machine learning regression techniques Symbolic Regression also tries to fit observed experimental data. But unlike the well-known regression techniques in statistics and machine learning, Symbolic Regression is used to identify an analytical mathematical description and it has more degrees of freedom in building it. A set of predefined (basic) operators is defined (e.g., add, multiply, sin, cos) and the algorithm is mostly free in concatenating them. In contrast to the classical regression approaches which optimize the parameters of a predefined structure, here also the structure of the function is free and the algorithm both optimizes the parameters and the structure of the base functions.

There are different ways to represent the solutions in Symbolic Regression. For example, informal and formal grammars have been used in Genetic Programming to enhance the representation and the efficiency of a number of applications including Symbolic Regression [8].

Since Symbolic Regression operates on discrete representations of mathematical formulas, non-standard optimization methods are needed to fit the data. The main idea of the algorithm is to focus the search on promising areas of the target space while abandoning unpromising solutions (see [4][9] for more details). In order to achieve this, the Symbolic Regression algorithm uses the main mechanisms of Genetic and Evolutionary Algorithms. In particular, these are mutation, crossover and selection [9] which are applied to an algebraic mathematical representation.

The representation is encoded in a tree [9] (see Figure 1). Both the parameters and the form of the equation are subject to search in the target space of all possible mathematical expressions of the tree. The operations are nodes in the tree (Figure 1 represents the formula $6x+2$) and can be mathematical operations such as additions (add), multiplications (mul), abs, exp and others. The terminal

values of the tree consist of the function's input variables and real numbers. The input variables are replaced by the values of the training dataset.

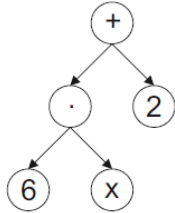


Figure 1. Tree representation of the equation 6x+2.

In Symbolic Regression, many initially random symbolic equations compete to model experimental data in the most promising way. Promising are those solutions which are a good compromise between correct prediction quality of the experimental data and the length of the symbolic complexity.

Mutation in a symbolic expression can change the mathematical type of formula in different ways. For example, a div is changed to an add, the arguments of an operation are replaced (e.g., change 2*x to 3*x), an operation is deleted (e.g., change 2*x+1 to 2*x), or an operation is added (e.g., change 2*x to 2*x+1).

The fitness objective in Symbolic Regression, like in other machine learning and data mining mechanisms, is to minimize the regression error on the training set. After an equation reaches a desired quality level of accuracy, the algorithm returns the best equation or a set of good solutions (the pareto front). In many cases the solution reflects the underlying principles of the observed system.

III. PROPOSED METHOD

This section explains our knowledge acquisition workflow (see Figure 2). The core of the workflow is structured in 4 steps.

1. The human expert defines the set of base functions. The functions should be adapted to the domain problem. For example many geometrical problems are much easier to solve with trigonometric base functions.
2. The second step in the workflow is the main optimization process (see [12], section II c. and III a. of this paper for more details). Symbolic Regression is used to solve this task. It should be noted, however, that other optimization algorithms which can handle discrete black-box optimization can be used for this task.
3. A human expert can interpret and reformulate the solutions of the pareto front (see section IV b.).
4. The knowledge can be transferred to other domains.

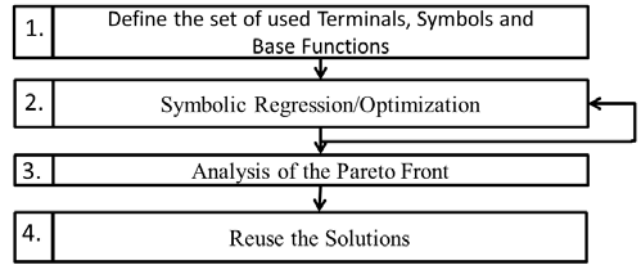


Figure 2. The knowledge acquisition workflow.

A. From Regression to Classification

In this subsection the symbolic regression algorithm is generalized to a symbolic regression classification.

First, an activation function is defined. In our approach it is a step function which is defined as $\Phi(z) = \begin{cases} 1 & \text{iff } z \geq 0 \\ 0 & \text{iff } z < 0 \end{cases}$.

Given is a training set of N feature vectors $\{\vec{x}_i\}_{i=1}^N$ and assigned class label $\{y_i\}_{i=1}^N, y_i \in [0,1]$. The main challenge and computer time consuming task is to find a function f which transforms the input space in the way that $\Phi(f(\vec{x})) = \vec{y}$ with as few errors as possible. In other words, a function $f(\vec{x})$ is sought with $f(\vec{x}) = 0$ separating the areas of the feature space, where the vectors of the different classes are located. The zero-crossing $f(\vec{x}) = 0$ therefore defines the decision surface. So far, the approach is Perceptron-like [6]. Instead of replacing the step-functions by continuous and differentiable base functions to allow cost function optimization, Symbolic Regression is used to optimize the cost function $J = \sum_{i=1}^N (\Phi[f(\vec{x}_i)] - y_i)^2$ and therefore to find $f(\vec{x})$.

The main advantage of this approach is due to the fact that complexity and interpretability of the solution can be controlled by the user by the set of allowed operations and by selecting the appropriate complexity by means of the pareto front. Further approach advantages (see the next subsection) are consequences of this property.

B. Advantages

In this subsection we summarize the additional advantages of the proposed approach. It should be noted that all mathematical reformulations of the classifier do not change its behavior in classification.

To be understandable to human experts our approach tries to find solutions which are as simple as possible. The pareto front [4] sorts the solutions by complexity and prediction quality.

One of the main advantages is that this approach enables to calculate the first derivative of the classifier. One

scenario could be in engineering technologies or medical systems.

TABLE I. ADVANTAGES

Can be interpreted by human experts
Can be reused in other domains
Knowledge Base
Rules to simplify and reformulate. The reformulations do not change its behaviour.
Analytical Boundary Detection
Analytical Gradient Calculation
Blocks of analytical expert knowledge can be used

For example it could be the task to learn when a workpiece is damaged or when there is a risk of an illness. The general learning approaches enable only to predict the class (e.g., defect or no defect). With the first derivative which can be analytically calculated by our approach we can also say which attributes of the classifier should be changed (and in which direction) to leave the undesired class as soon as possible.

IV. EXPERIMENTS AND RESULTS

This section discusses and demonstrates some of the conducted experiments. First we show two experiments based on artificial datasets while the third described experiment is based on a real-world dataset.

A. First Experiment

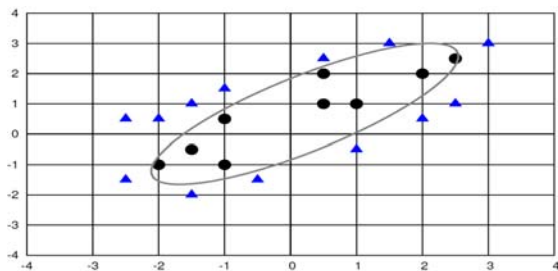


Figure 3. First dataset.

Figure 3 shows the data of a two class learning task in a two-dimensional plot. The first class is represented by the circles and the second by the triangles. The zero-crossing $f(\vec{x}) = 0$ decision boundary of the different classes of formula 1 (calculated by our Symbolic Regression algorithm) is displayed in Figures 3 and 4 by the parabola. In order to find interpretable formulas we restricted the search on using add, sub, mul and all real numbers as operators.

$$f(x, y) = 1.54516 + y + 1.63312 xy - x^2 - y^2 - 0.672694 x \quad (1)$$

As discussed in Section III, it is easy for a human expert to interpret this solution. It is a representation of an ellipse. With this knowledge the user can conclude much more about the domain. The additional knowledge includes conclusions about the decision area. Based on their high complexity black box machine learning algorithms usually give no additional insight into its behavior.

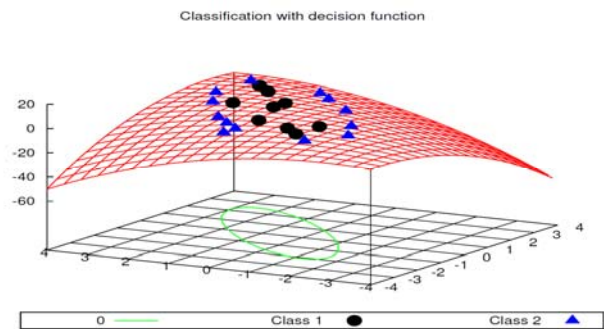


Figure 4. The transformation of the feature space.

As a result of the interpretable analytical solution (formula 1) we know that there is only one decision boundary (the zero-crossing). This knowledge is essential for some domains (application scenarios can include medical or other critical domains) which require robust classifiers. This robustness includes predictable behaviour to unknown datasets which include so far uncovered areas of the feature space.

B. Second Experiment

The second experiment is based on the well-known spiral dataset [10][12]. The problem to distinguishing two intertwined spirals is a non-trivial one. Figure 5 depicts the 970 patterns that form the two intertwined spirals. These patterns were provided in [10].

This experiment is an example of the way in which additional human expert knowledge can improve the quality of the found solutions (see section III). For a human expert it is obvious that the problem is periodic. To find good and short models it is therefore essential to add periodic and trigonometric base functions. Therefore, we allowed the algorithm to use additions (add), subtractions (sub), divisions (div), multiplications (mul), sin, cos and all real numbers. Several correct problem solving solutions had been found by our system for this classification problem. One of them is formula (2) (the numbers in the formula are rounded using 3 fractional digits) which is able to classify the spiral dataset without an error and figure 6 shows the three-dimensional plot of the function. To the best of our knowledge it is one of the shortest known solutions to solve this classification tasks.

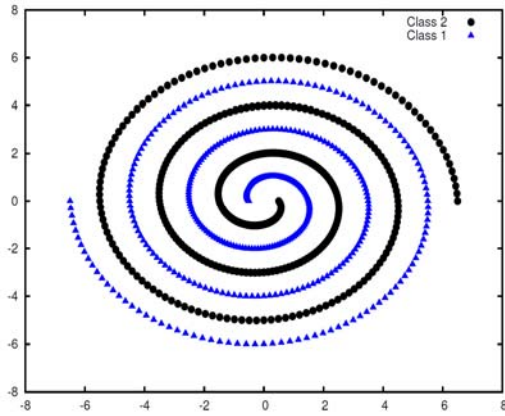


Figure 5. The spiral dataset.

$$f(x, y) = \sin\left(3,35x + \frac{y}{0,042} + \frac{x}{y} - 0,0356\right) \left(\frac{x}{y} + 0,005 * \frac{y}{x}\right) \quad (2)$$

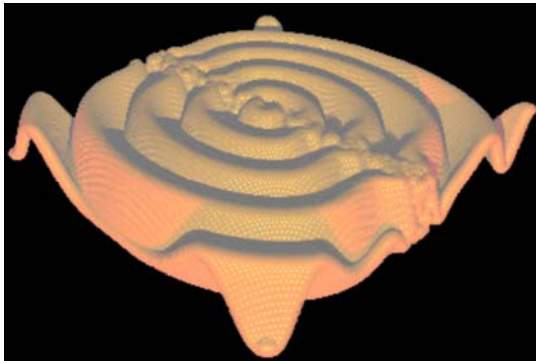


Figure 6. The three-dimensional plot of function 3.

C. Real Life Dataset – Haberman’s Survival Data Set

The Haberman’s Survival Dataset dataset contains cases from a medical study that was conducted between 1958 and 1970 at the University of Chicago’s Billings Hospital on the survival of patients who had undergone breast cancer surgery [13][14][15][16].

It consists of 4 attributes:

1. Age of patient at time of operation (age).
2. Patient’s year of operation (the year of the operation).
3. Number of positive axillary nodes detected (nodes).
4. The survival status (class attribute) .

Table II summarizes the rules of the pareto front of one run found by our Symbolic Regression system [12]. The formulas are ordered by complexity. It should be mentioned that repeating this procedure can result in different solutions.

complexity	accuracy	formula
13	0.478355	$f(\text{age,operation,nodes}) = \text{operation}/(2.05368*\text{age}*nodes - 83.8188*nodes - 154.58)$
9	0.493074	$f(\text{age,operation,nodes}) = \text{nodes}*nodes/(\text{age} - 43.7473) - 6.15$
7	0.493074	$f(\text{age,operation,nodes}) = \text{age} - 71/nodes - 41.35$
5	0.52987	$f(\text{age,operation,nodes}) = \text{nodes} - 469.83/\text{age}$
3	0.544589	$f(\text{age,operation,nodes}) = \text{nodes} - 8.69$
1	0.596104	$f(\text{age,operation,nodes}) = 0$

TABLE II. RULES.

As a simple showcase to show how additional insights in a domain can be gained we consider the formula $f(\text{age,operation,nodes}) = \text{age} - 71/nodes - 41.35$ (complexity 7) in Table II. It can be reformulated by $\text{age} = 71/nodes + 41.35$. A human user knows that the number of axillary nodes cannot have negative values. This implies that if the age of the patient is less than 41.35 the survival status is greater than 50 percent. This simple example shows, that reformulating and adding additional domain knowledge adds further insight. New knowledge is derived and it can be used in another context. This procedure is however, only possible on the basis of the symbolic and interpretable representation of the formulas (see section II).

V. CONCLUSIONS AND FUTURE WORK

In this paper, we showed a generalization of the well-known regression task to classification problems. Furthermore, the focus was set on understandable solutions achieved via Symbolic Regression which enable human experts to redefine and reuse the knowledge. Very important is that mathematically correct reformulations of the classifier formulas do not change its properties. Additional knowledge can be derived by reformulation the formulas. The power of our approach has been shown in experiments. Future work will focus on how the developed techniques can be transferred to other domains. Additionally, we will cooperate with our industrial partners to put the approaches into practice.

REFERENCES

[1] R. O. Duda, P. E. Hart, and D. G. Stork, "Pattern Classification", 2nd ed., Wiley Interscience, 2000.

- [2] D. Robinson, "Implications of Neural Networks for How We Think about Brain Function", in *Behavioral and Brain Science*, 15, pp. 644-655, 1992.
- [3] P. Smolensky, "On the Proper Treatment of Connectionism", in *Behavioral and Brain Sciences*, 11, pp. 1-74, 1988.
- [4] R. E. Steuer, "Multiple Criteria Optimization: Theory, Computations, and Application". New York: John Wiley & Sons, 1986.
- [5] J. H. Holland, K. J. Holyoak, R. E. Nisbett, and P. R. Thagard, "Induction: Processes of Inference, Learning, and Discovery". Cambridge, MA, USA, 1989.
- [6] W. McCulloch and W. Pitts, "A logical calculus of the ideas immanent in nervous activity". *Bulletin of Mathematical Biophysics*, pp. 115-133, 1943.
- [7] D. A. Freedman, "Statistical Models: Theory and Practice, Cambridge University Press, 2005.
- [8] M. O'Neill and C. Ryan, "Grammatical Evolution: Evolutionary Automatic Programming in an Arbitrary Language"; Kluwer Academic Publishers, Dordrecht Netherlands, 2003.
- [9] J. R. Koza, "Genetic Programming: On the Programming of Computers by Means of Natural Selection. Cambridge, MA, USA: MIT Press, 1992.
- [10] K. Lang and M. Witbrock, "Learning to tell two spirals apart". *Proceedings of 1988 Connectionists Models Summer School*. Morgan Kaufmann, San Mateo CA, pp. 52-59, 1989.
- [11] J. K. Kishore, L. M. Patnaik, V. Mani, and V. K. Agrawal "Application of Genetic Programming for Multicategory Pattern Classification". *IEEE Transactions on Evolutionary Computation*, 4 (3). pp. 242-258, 2000.
- [12] I. Schwab and N. Link, "Reusable Knowledge from Symbolic Regression Classification", *Genetic and Evolutionary Computing (ICGEC 2011)*, 2011.
- [13] S. J. Haberman. *Generalized Residuals for Log-Linear Models*, *Proceedings of the 9th International Biometrics Conference*, Boston, pp. 104-122, 1976.
- [14] J. M. Landwehr, D. Pregibon, and A. C. Shoemaker, *Graphical Models for Assessing Logistic Regression Models (with discussion)*, *Journal of the American Statistical Association* 79: pp. 61-83, 1984.
- [15] W.-D., Lo. "Logistic Regression Trees", PhD thesis, Department of Statistics, University of Wisconsin, Madison, WI, 1993.
- [16] A. Frank, A. Asuncion. *UCI Machine Learning Repository* [<http://archive.ics.uci.edu/ml>]. Irvine, CA: University of California, School of Information and Computer Science, 2010.

Learning Cognitive Human Navigation Behaviors for Indoor Mobile Robot Navigation

Luz Abril Torres-Méndez and Roberto Cervantes-Jacobo
Robotics and Advanced Manufacturing Group, Cinvestav Saltillo
Carr. Saltillo-Monterrey Km. 13, Ramos Arizpe, Coah, 25900, Mexico
E-mails: abril.torres@cinvestav.edu.mx; bortreo@gmail.com

Abstract—We present a framework to transfer cognitive human navigation behaviors to an artificial agent so it can generate route directions similar to those created by humans. Our method is based on a spatial conceptual map that attempts to emulate the cognitive process carried on by living beings during the navigation process. This conceptual map is modeled as a three-level of interconnected graphs to simulate human spatial reasoning. We based some of our ideas of spatial reasoning on qualitative definitions of neighborhood, distance and orientation. The first level of the conceptual model contains the approximated metric of the environment and the physical obstacles that influence the navigation trajectory. In the second level, we define the abstract characteristics that give information about the ambient, such as the areas of influence and key features. Finally, in the third level, the navigation route obtained from the first two levels is stored. The visual and cognitive skills of each person in the experiments are captured in terms of the space-time perception while navigating. Our experimental results demonstrate that the inference of the route directions can be easily obtained and transferred to an agent from this spatial conceptual map.

Keywords-human navigation; cognitive conceptual maps.

I. INTRODUCTION

Navigation is generally defined as the process of monitoring and controlling the movement of an agent (i.e., a vehicle, person or animal) from one place to another towards a goal. To be able to navigate, the agent has to have the capability of moving in the space and determine if the goal has been reached or not. The study of navigation of living beings has a long history in neuroscience [1], [2], [3], [4], [5]. The discoveries found in the last fifty years have provided a physiological grounding related to the type of representation of spatial locations in our brain. In order to efficiently achieve the navigation task, some information about the environment is required. In robotics, particularly in indoor robotic navigation, this knowledge is commonly represented by a metric map containing distances between walls, doors, objects, corners, etc. However, to obtain precise metric information may result in a cumbersome task. Moreover, for the particular case of human navigation, a metric map seems not to be a natural way to navigate as humans are not good on measuring exact distances from one point to another nor in memorizing them to build an internal map of that kind.

In other words, the notion of navigation does not imply that the current position of the agent must be exactly known. Thus, for human navigation, the cognitive process carried on does not require a precise metric. This cognitive process is mainly based on the relationships we build between the information captured from the environment through our senses (i.e., visual and geometric information) and the conceptual information based on previous knowledge about the functional characteristics of the environment. The last is obtained according to the experience of having navigated before that environment or similar ones.

When walking through an environment, we all have experienced the need to perceive our *spatial* sense, also known as spatial awareness or proximity sense, that is, to know the dimensions our body occupies with respect to the empty space of the environment in which we can walk in. Because of this spatial sense, we are able to get a clearer perception of how much we have moved forward, related to where we were, and associate it to what we see next. This type of perception could be represented in a topological map, which is another representation that is commonly used in robotics. A topological map is a graph of connected landmarks that exist in the environment. However, as we will see in this research work, the whole process of navigation is so complex, that having just a topological or a metric map is not enough to achieve the task efficiently.

In our daily life, humans efficiently achieve a variety of skill-motor tasks. Yet today, it is not well understood the learning processes carried on in our brains that allow us to navigate a familiar environment. More intriguing is to understand how we manage to navigate unfamiliar or even not-seen-before environments – of course, those not-seen-before environments need to fulfill some requirements regarding its geometric structure and physical laws in order to be able to navigate them. However, from research done in behavior and neural sciences [7], [9], [10], [11], we know that the learning process in navigation involves storage of the learned skills for future reference. For the case of human navigation, we store in our memory navigation skills to which our brain automatically assigns weights according to how well or bad the task were carried on. Then, our

brain and memory connections are updated accordingly, so that both types of skills (“good” and “bad” ones) are kept as experiences in order to generate flexible behavioral responses when similar situations are encountered.

In nature, one of the most ubiquitous form of learning skills is by imitation. In general, imitation involves the interaction of perception, memory, and motor control. There is an inherent transference of knowledge as the brain is capable of building networks to recreate actions that have even never executed before. It has been demonstrated that humans build mental images to facilitate the execution of tasks. For the case of navigation, humans build navigation blocks from the mental representation of the environment, generating what it is known as *cognitive maps*.

We have managed to transfer those skills, behaviors or even experiences, to other humans to facilitate their learning process. However, we still have some difficulties on teaching or transferring those skills to artificial agents. The reasons for this are not simple but they could be posited as being primarily twofold. One is because we do not completely understand how our brain builds its own reasoning and type of representations. And two, because we are trying to teach a task that can be developed by complex systems to a simple one. In other words, the computer on a robotic system would need to entirely have the functionality that a human’s brain has in order to truly understand a concept that is being taught. This is still an open problem in artificial intelligence, although big advances has been made.

The research question we are interested to answer in this work is: how do we transfer navigation skills to a mobile robot such that it can generate route directions similar to those created by humans? To answer that question, we need to construct a model capable of emulating the human perception over a navigable environment. This model must have a good understanding of the functional properties of the space that can be used while the robot is navigating. We based our method on a spatial conceptual map to simulate human spatial reasoning. A spatial conceptual map is a computerized analogy of the mental maps generated by humans. There is not a standardized way to build a conceptual map of a given environment. However, some information such as the objects and its area of influence, the notion of neighborhood, orientation and distance, can be used as they are part of the process of spatial reasoning. Then, this spatial conceptual map can be used by the mobile robot to navigate the environment.

The outline of this paper is as follows. Section II describes the human behaviours in the navigation process. In Section III, we mention the relevant aspects in robotic navigation. Section IV presents in detail the components for creating the spatial conceptual map we propose. Some simulation results are shown in Section V. Finally, we give some conclusions and future work in Section VI.

II. HUMAN BASIC NAVIGATION BEHAVIORS

It has been proved that mental imagery is critical for human navigation. However, it remains unclear how this mental representation of the environment, namely a cognitive map, is built related to specific orientation strategies [12], [13]. We gather information by using our sensorial organs and then we build a mental image of the external world. The unconscious conception of our bodies in the space that helps us to interact with our surroundings is called *proprioception*. We need to coordinate our movements in order to know where our body is and what it is doing. This skill has been refined through our lives thanks to a system of constant feedback which has been developed since we were inside our mother’s womb. The sensors give us constant feedback so the movements can be refined until reaching perfection. Each person may adopt alternative strategies while moving along the same well-known route, but it is widely accepted that cognitive maps are a key element for orientation since any target can be reached from any place in the environment. Thus the ability to create a cognitive map is related to the particular ability of performing mental rotations of simple geometric shapes, and the ability to visualizing how we move on a map. In order to navigate successfully in both known and unknown environments, individuals need the ability to become familiar and orient in the environment, this is known as *topographical orientation* [14]. This complex task requires many cognitive skills such as visual perception, memory, attention, and decision-making techniques [15], [16], being mental imagery skills one of the most important for orienting within the environment [15], [3].

When navigating through an indoor environment, humans, contrary to animals, have the understanding of functional and spatial properties of the environment, while interacting safely with it. We make use of labels to share common concepts like the existence of corridors, corners, specific furniture, areas, etc. These concepts are not only labels but semantic expressions that are related to a complete object or to an objective situation. For example, the label “living room” generally is related to a place that has a particular structure and contains objects (furniture) such as couch, center table, tv, etc. Thus, representing the space as “seeing” by humans requires to take into account the way in which we make reference to entities in the space through language.

In general, an artificial agent can use different type of strategies to go from one place to another. However, if these strategies are to be used every time without storing them in a map, it has to learn everything again and again, even if some distances have been previously covered. To this end, the topological information and the navigation based on searching use spatial memory that does not depend of the goal and can be used for route planning independently of the final goal. The memory that does not depend of the final goal is called cognitive map [10] in which the knowledge about

the routes is a form of preprocessed memory. From the field of cognitive psychology and the experimental results in [17], the notion of object’s influence area was born. This notion consists on the idea that people mentally build an “subjective influence area” that surrounds the objects in the environment to be navigated in order to talk about their relative position, distance and orientation. According to this, the influence area is an abstraction of the way objects influence in the vision and perception of people. It allows to reason in a context, evaluate quantitative measures and qualify positions and distances between objects. It also allows to reason in a qualitative manner about space.

III. ROBOTIC NAVIGATION

In order to build internal representations of the environment, robots use its sensors. The sensors can capture information of the objects in the environment that can be used to position the robot in it or to integrate the path the robot has navigated. For a robot, to use an internal representation of the space distribution for navigation, can result in a complex task. As today, there exist several localization systems in robotics that use metric and/or topological maps as internal representations. A metric map considers the space in two dimensions in which the objects are localized with precise coordinates. Metric maps can be created independently to the robot, with a high level of precision according to the type of sensors used. A metric map facilitates the operation of robots. However, to create a metric map to be used by a robot can be a cumbersome task. The time for the acquisition and processing of information could be very high as the robot needs to take measurements constantly of the environment while navigating. A topological map considers the relationships between places and objects. The map is represented as a graph in which the nodes correspond to places/objects and the edges could represent directions or path convenience. Contrary to the metric maps, a topological map does not require models based on precise range measurements, and this is an important advantage upon localizing the robot. However, the precision of using a topological map is not high. A common solution is to use both, a metric and a topological map, in order to get better robot’s pose estimates [18], [19].

There exist a vast amount of research work related to navigation systems for indoor and outdoor robots (for a survey that highlights the more interesting works see DeSouza and Avinash [20]). It is clear that in order to navigate we need perceptual and metrical information from the environment. In robotics, the most common sensors are cameras and laser range finders to obtain visual and geometric information, respectively. However, to incorporate conceptual and cognitive knowledge about the environment into an internal map for navigation purposes is not a trivial task. This knowledge, in terms of geometry of space, perceptual and other metrical information transmitted by the human-like perception of the

world needs a better understanding of the inherent spatial and functional properties, while still being able to safely navigate in it. As such, there has been proposed in the literature a variety of ways to represent this knowledge into maps (metric, topological and conceptual maps) to be used by a mobile robot for self-localization and navigation tasks. Alternatives to map-based navigation strategies are biologically inspired navigation methods (behavior-based) that imitate navigational cues observed in animals. In this research work we adopt a hybrid approach that combines the two approaches, that is, we construct a map based on cognitive-behavioral knowledge as well as conceptual knowledge obtained directly from human while navigating an indoor environment.

IV. CREATING THE SPATIAL CONCEPTUAL MAP

Humans generate mental images that represent the spatial knowledge of the area they are navigating. These mental images are then processed and analyzed in order to generate a cognitive map. Figure 1 shows the navigation process as a comparison between humans and artificial systems and the components involved in the construction of a spatial conceptual map as an analogy of the human cognitive map.

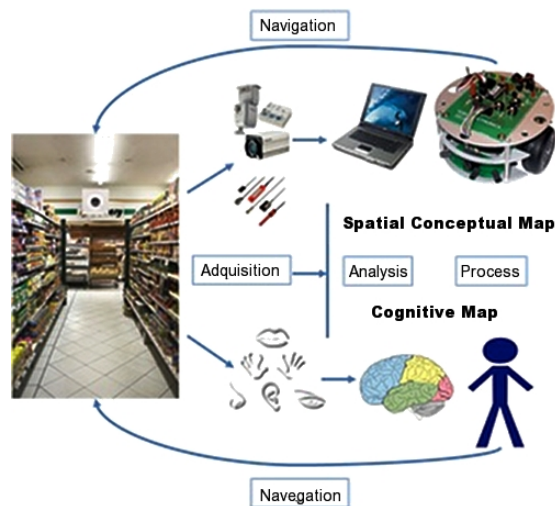


Figure 1. A comparison of the navigation process carried on by humans and artificial agents. The arrows indicate the flow of information.

A cognitive map can function as a navigation problem solver to find routes, relative positions, as well as to describe the location of the subject in a given moment. Thus, the cognitive map is a non-observable physical structure of information that represents the spatial knowledge. The learning process is based on the assimilation of what was captured by our senses into a cognitive map, and the problem solution is a process that extracts the answers to particular questions from the cognitive map. The need of analyzing, processing

route navigated by the five participants. All gathered information was used in the spatial conceptual map construction.

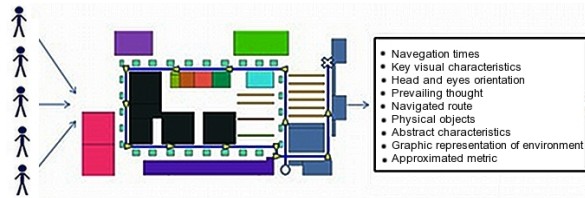


Figure 3. Diagram of the experiment. Five people participate in the navigation tests. The information gathered was used for building the Spatial Conceptual Map.

B. Representing the spatial conceptual map

From the information obtained by the five people through the navigation tests we can conform two types of maps: a metric map containing information about distances that define the location of objects; and a topological map containing the existing relationships (mainly vicinity and connectivity) between the present entities in the space to navigate, such as objects, areas or free space units. As mentioned before, the metric information is obtained in an approximately as people indicate roughly the distances between visualized objects and the traveled length in each segment of the route navigated. This information makes possible to colocate objects in a map and locate from a common referential frame. However, this information only allows knowing the approximated position of the object within the environment, thus, to make the navigation possible for a robotic system, is necessary to consider an average intrinsic referential of the routes navigated by the five subjects that, together with the average extrinsic referential (which is fixed and common among objects) in the environment, allows a continuous update of the robot pose, thus making possible the process of route integration, which, as it was mentioned is one of the main elements in the navigation process.

The metric and topological maps that conform the spatial conceptual map (SCM) are shown in Figure 4. These maps are integrated in order to define the navigation routes, in which the identification of the relevant objects is crucial. An important characteristic of the SCM is that all information in it comes from the participants in the navigation tests. Therefore, it will totally depend on the way the participants perceive the environment, regarding the key features in the navigation process, the salient objects used as reference, or the abstract areas conformed by physical objects (also used as reference) together with the concepts of area of influence, orientation, and neighborhood.

In the SCM, each relevant object has a set of properties, one is its *neighborhood* (see Figure 5). We define the neighborhood of an object in terms of orientation and approximated distance between its neighbors. In the SCM, each physical object must have at least one neighboring

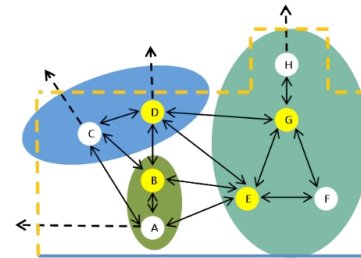
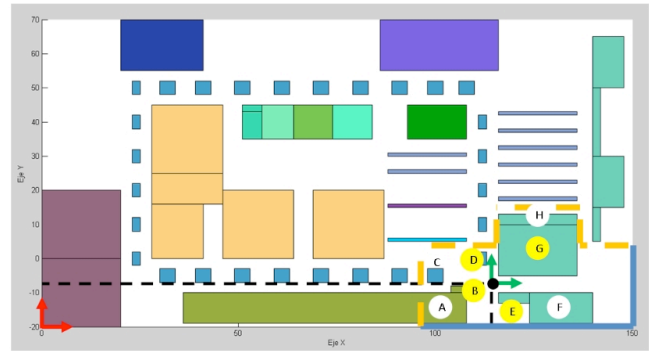


Figure 4. Graphic representation of the integration of metric and topological information. The shaded nodes represent key characteristics in the environment identified by the participants in the navigation tests. It shows how a locality can be defined as a function of nearby objects.

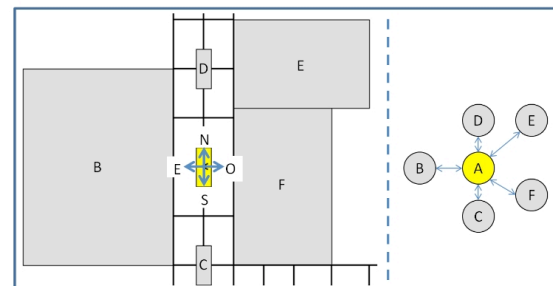


Figure 5. The neighborhood property. The right side shows the topological relationship that a physical object has with its neighbors. The left side shows a metric map generated from the neighborhood information defined in distances and relative orientations between an object and its neighbors.

object (either physical or abstract). This generates in the SCM a strong interrelated structure that complement the approximated metric with the local blocks of qualitative relative information between each of the objects. Thus allowing, by identifying one or more objects in a locality, the inference of an approximate relative robot position to the local objects, and an absolute robot position to the common extrinsic referential for each of the entities in the environment. The knowledge of the relative and absolute robot position together with the real-time identification of key features in the environment, makes possible the navigation process and to correct any errors present in the estimation due to the approximated metric and/or the robot's odometry.

Another important property of the SCM, which allows the existence of one of the three levels in the map, is the area to which an object belongs. We call this the *membership* property, and consists in wrapping all objects with common characteristics (see Figure 6).

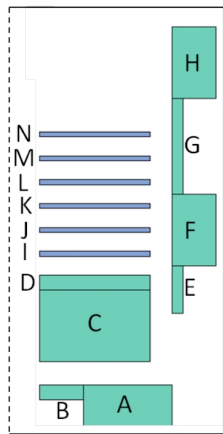


Figure 6. The membership property. The figure shows a portion of the graphical representation of the SCM. It can be identified two set of objects (labeled nodes from A to H and from I to N, in alphabetical order) which have similar characteristics and therefore form part of the same area.

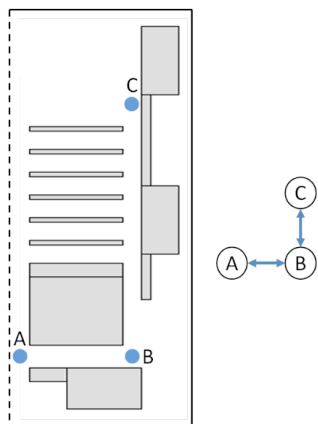


Figure 7. The connectivity property. The left side of the figure shows a portion of the SCM. It can be identified three nodes of free space. The right side shows the topological relationship of the connectivity among the nodes. It can be seen that it is possible to go from node “A” to node “C” going through “B”.

By encapsulating common objects in areas, we strengthen the existing neighborhood interrelations among them by facilitating the manipulation of information in the SCM. Additionally, the recognition process is simpler because we only need to recognize only one or two objects and then know in which area is the robot. Thus, the robot, similar to humans, is navigating using complete areas as reference.

The last property is the *connectivity* property and is used

to manipulate the free space in the SCM. The free space is considered as a set of points in the space, and it is free of obstacles, thus is navigable. This property allows that the free space can be represented as a graph, where each of the nodes represents a point in the free space. The connectivity property dictates if it is possible to go from node “A” to node “C” (see Figure 7). Thus, by knowing the individual connections of each of the nodes conforming the free space, it is possible to generate a network that englobes all nodes and to know if a given route is possible or not. Each of the properties mentioned above facilitate the access and manipulation of the information in the SCM. Moreover, as these properties allow that the elements in different SCMs of the same environment can be related among them, we can identify another property, which integrates all information in one SCM. We call this the *interrelation* property. This property allows the existence of the multilevel structure in the SCM, in which there can be a direct or indirect interrelation between each of the elements in the same level or in different levels. We explain in detail the interrelation between three levels conforming our SCM in the next section.

C. The multi-level structure of our SCM

The three levels of the SCM are structured to follow a hierarchy. The physical objects conform the basic (bottom) level. Once the objects are classified according to their characteristics the next (middle) level is generated, that is, each area is defined exclusively by their objects in it, giving origin to the first interrelation: physical objects with areas. Then, the main (top) level contains all the nodes of free space. These nodes are referenced to nearby physical objects such that the definition of the location of each free space unit is dictated directly by the referenced physical object, and indirectly by the area that object belongs to; thus giving origin to a direct interrelation of physical objects with free space and an indirect one of free space with areas. These interrelations allow to integrate the whole information in only one SCM (see Figure 8).

It is important to note that each level in the SCM is conforming by a set of individual and unrepeatable elements of similar hierarchy. Moreover, each node’s structure has all the necessary information to establish the existing interrelations with the nodes of the same or different levels of the SCM.

The level of *physical objects* is integrated by the existing objects in the navigation space indicated as key elements. These objects can be obstacles or those considered as reference to facilitate the navigation process. Each node representing a physical object contains information such as an identification label, nominal label, area, dimensions, neighbors and its orientation w.r.t. to the object.

The *area* level has the objective of complementing the level of physical objects. The elements that conform this level are of abstract nature and are based on the membership

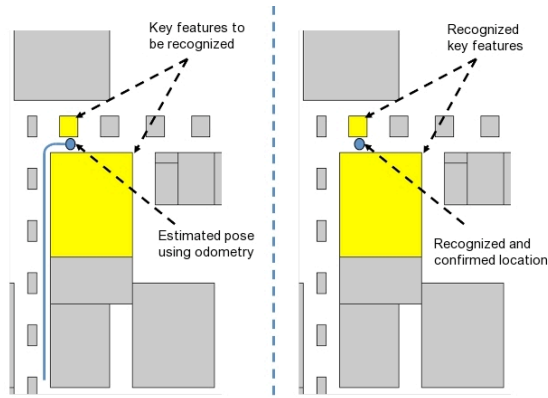


Figure 10. The recognition stage of the environment.

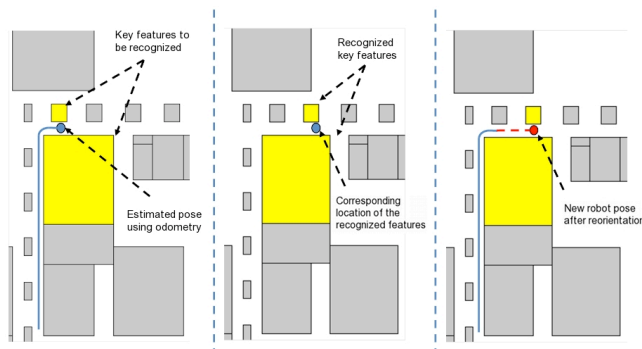


Figure 11. Reorientation.

consistent between the six people since the proportion at each section with respect to the complete route, for the three navigation trials, is similar and with low standard deviation. Therefore, it can be considered that the approximated metric is good enough since it is also congruent with the data obtained during the navigation trials. Table I shows the average steps for each section for the three navigation trials.

Table I
THE AVERAGE STEPS AS THE APPROXIMATED METRIC FOR EACH SECTION IN THE ROUTE NAVIGATION.

	Average of steps
Section 1	64.00
Section 2	85.00
Section 3	49.67
Section 4	112.00
Section 5	56.00
Total in route	366.00

V. SIMULATION RESULTS

At this point, from any physical man-made indoor environment, our model is validated through simulation. We use the final graphical representation, which englobes the gathered information of the 15 navigation tests carried on in

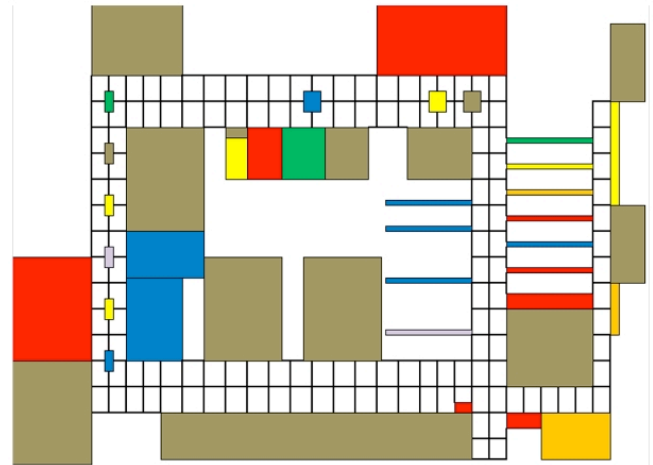


Figure 12. Final graphical representation of the navigation trials. The color of objects (boxes) indicate if they were seen only by 1 person (yellow), 2 (blue), 3 (red), 4 (green), or all subjects (brown).

the shopping centre. We simulate the cinematics of a point robot in a bidimensional space, without considering changes in orientation. This in order to simplify the robot's cinematic model. Thus, the robot pose in the space is defined by:

$$q(t) = (x(t), y(t)), \quad (1)$$

where $q(t)$ is the robot pose at time t , $x(t)$ and $y(t)$ are the coordinates of the robot in the axis X and Y , respectively. The robot's pose at time i is given by:

$$q_i = (x_i, y_i). \quad (2)$$

The change of the robot's pose in a time interval Δt_i , can be calculated as:

$$\Delta t_i = t_i - t_{i-1}, \Delta q_i = q_i - q_{i-1}. \quad (3)$$

From the above equations, we can compute the velocity of the point robot for the time interval Δt_i by:

$$v_i = \frac{\Delta q_i}{\Delta t_i}, \quad (4)$$

For the simulation, the physical objects considered in the map (Figure 13) are colored according to their corresponding area. The free space is defined by the route established in the navigation tests. As it is assumed that the visual recognition of the relevant characteristics in the environment is always correct, the integration of the route navigated in our simulation is free of errors. However, what it is relevant to note here is the fact that the model works by using as a reference only an approximated metric of the environment and the topological information of the spatial conceptual map. Moreover, in a real application, following the route indicated would strongly depend on the correct recognition of the key characteristics in the environment described in the spatial conceptual map.

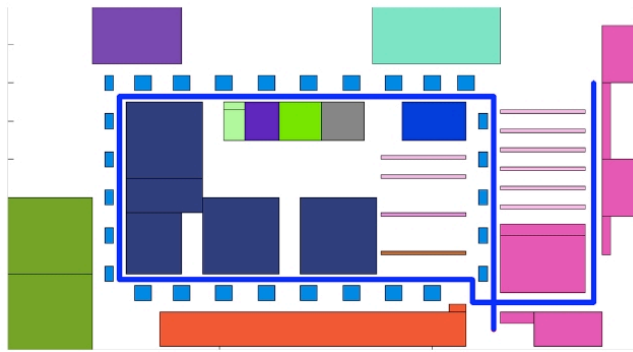


Figure 13. Graphical representation of the route navigation for the simulation. The blue line on the free space is the route.

VI. CONCLUSION AND FUTURE WORK

Mobile robot navigation is generally based only on the information acquired by the robot’s sensors. However, we have observed that sensors have great limitations in terms of coverage capabilities, quality in the measurements and also factors such as elevated acquisition times and costs. Current research trends are being focused on the study of the cognitive behaviors of humans navigation and how conceptual maps are created.

In general, humans do not have exact knowledge of the metric of the environment they navigate. They navigate by constructing a topological hierarchy of the free space according to specific characteristics observed in the environment that are more relevant than others.

In this work, we have created a model based in a conceptual map that considers human navigation behaviors in close indoor environments. Our preliminary results have shown that this map can be used by a mobile robot to facilitate its navigation and eliminate the need of using sensors for capturing exact metric information of the environment. The information contained in the conceptual map is enough to estimate the robot pose and orientation if visual landmarks are correctly matched.

Future work involves the implementation of our spatial conceptual model in a real robotic platform. For this, it is necessary to integrate a robust recognition model of the key visual features.

VII. ACKNOWLEDGEMENTS

The authors gratefully acknowledge to CONACYT for funding this project.

REFERENCES

[1] R.G. Golledge and G. Zannaras, “Cognitive Approaches to the Analysis of Human Spatial Behaviour”, *Environmental Cognition*, pp. 59–94, 1973.

[2] M. J. Farah, “The Handbook of Neuropsychology”, Disorders of visual behavior. F. Boller, J. Grafman, eds., Elsevier, Amsterdam, pp. 395–413, 1989.

[3] M. Riddoch, G. Humphreys, “Neuropsychology of visual perception”. Hillsdale: Lawrence Erlbaum Associates, pp. 79–103, 1989.

[4] R.G. Golledge, “Do People Understand Spatial Concepts: The Case of First-Order Primitives”, *Theories of Spatio-Temporal Reasoning in Geographic Space*, pp. 1–21, 1992.

[5] A. D. Redish and D. S. Touretzky, “Cognitive Maps Beyond the Hippocampus”, *Hippocampus* 7, pp. 15–35, 1997.

[6] M. Denis, “Image et Cognition”, 1989.

[7] S. Gopal, R. L. Klatzky, T. R. Smith, “Navigator: A Psychologically Based Model of Environmental Learning Through Navigation”, *Journal of Environmental Psychology* 9, pp. 309-331, 1989.

[8] P. Gould and R. White, “Mental Maps”, 1974.

[9] D. Hernández, “Qualitative Representation of Spatial Knowledge”, 1994.

[10] J. O’Keefe, L. Nadel, “The hippocampus as a cognitive map”, Oxford: Clarendon, 1978.

[11] B. J. Kuipers, “Modeling Spatial Knowledge”, *Cognitive Science* 2, pp. 129-153, 1978.

[12] L. Palermo, G. Iaria and C. Guariglia, “Mental Imagery Skills and Topographical Orientation in Humans: A Correlation Study”, *Behavioral Brain Research* 192, pp. 248-253, 2008.

[13] A. D. Ekstrom, et al., “Cellular Networks underlying Human Spatial Navigation”, *Nature* 425, pp. 184-188, 2003.

[14] E. A. Maguire, T. Burke, J. Phillips, H. Staunton. “Topographical Disorientation following Unilateral Temporal Lobe Lesions in Humans”. *Neuropsychology* 34, pp. 993-1001, 1996.

[15] R. Brunson, L. Nickels, M. Coltheart, “Topographical Disorientation: Towards an Integrated Framework for Assessment”, *Neuropsychology Rehabilitation* 17, pp. 3452, 2007.

[16] A. D. Reddish, “Beyond the Cognitive Map from Place Cells to Episodic Memory”, London: MIT Press, 1999.

[17] B. Moulin and D. Keitani, “Route Generation and Description using the Notions of Object’s Influence Area and Spatial Conceptual Map”, *Spatial Cognition and Computation* 1, pp. 227-259, 1999.

[18] V. Vanessa Hafner, *Learning Places in Newly Explored Environments*, 2000.

[19] H. Zender, O. Martínez Mozos, P. Jenselt, G.-J.M. Kruijff, W. Burgard, “Conceptual Spatial Representations for Indoor Mobile Robots”, *Robotics and Autonomous Systems* 56, pp. 493-502, 2008.

[20] G. N. DeSouza and A. C. Kak, “Vision for Mobile Robot Navigation: A Survey”, *IEEE Trans. on PAMI* 24(2), pp. 237-267, 2002.

Cognitive Information in Business Process - Decision-Making Results

Andreia C. T. D. Pereira

NP2Tec -PPGI - Departamento de Informática Aplicada
Universidade Federal do Rio de Janeiro (UNIRIO)
Rio de Janeiro, Brasil
andrea.pereira@uniriotec.br

Flávia M. Santoro

NP2Tec -PPGI - Departamento de Informática Aplicada
Universidade Federal do Rio de Janeiro (UNIRIO)
Rio de Janeiro, Brasil
flavia.santoro@uniriotec.br

Abstract — The performed work in business processes in organizations can be defined as situated activity, fundamentally, surrounded by a context. Contextual knowledge resides not only in the activities, conditions, facts and situations, which occur during a task performance. Contextual knowledge also resides in people's mental activities of thinking, reasoning and judging. In other words, contextual knowledge also resides in people's cognitive processes. We argue that the cognitive process of decision-making can be considered a contextual element, since it could explain how a decision was made and how its outcomes were reached. We presented an approach for capturing and representing individual cognitive decision-making process as contextual knowledge in decisions activities of business process. This paper presents an approach for using decision results as contextual information for new decisions within business process.

Keywords - *Decision-making result; Context; Business Process; Knowledge Management; Organisational Learning*

I. INTRODUCTION

The work performed by people can be defined as situated activity, fundamentally, surrounded by a context [2]. Business processes, which represent the way organizations work, consist of sets of activities through which information and knowledge are generated, transferred and converted. In this sense, for business process actions and events total understanding, all relevant contextual information involved in particular situations should be available. Besides, learning with past tasks and how to deal with changes that arise might create opportunities for reusing content produced in previous circumstances [7][20].

A formal definition for context is provided by [1]: context is a set of circumstances which surrounds an event or subject and the structures of mental models which represent knowledge. Contextual elements may refer to group members, task planning, interactions which led to a conclusion and the environment where a task was carried out. Thus, the contextual knowledge resides not only in the activities' conditions, but also in people's cognitive processes as thinking, reasoning and judging, for instance.

We argue that decision-making cognitive process can be considered a contextual element, since it could explain how

an activity was performed as well as the outcomes reached. We presented [13][15] a meta-model and a set of guidelines to support meta-model instances creation. This proposal goal was to capture and to represent individual cognitive decision-making process as contextual knowledge in business process activities.

This paper proposes to extend [13] meta-model including other important information related to the decision consequences and moreover about the process goals achievement. The goal of this paper is to discuss the approach of using decision results records as contextual information. Besides, we also discuss how retrieving registered decisions results would help making new decisions.

The paper is organized as follows: Section 2 describes the concept of cognitive information and context in business process and how decision results could be argued as part of contextual information. Section 3 presents related work. Section 4 describes the improved model proposed. Section 5 discusses new results obtained. Section 6 concludes the paper.

II. COGNITIVE INFORMATION AS CONTEXT IN BUSINESS PROCESS

According to Rowlands [19], cognitive processes are those essential to performing information acquisition and usage. Lima and Borém [8] affirm that cognitive processes include the mental activities of thinking, imagining, remembering, problem-solving, perceiving, recognizing, conceiving, judging, reasoning, etc., occurring differently for each individual, depending on his skills. Thus, the outcome of each process is different, depending on experiences, abilities and knowledge of whoever carries it out.

This emphasizes the relevance of describing cognitive processes information and making them available. For Lima and Borém [8] and Maximiano [9], mental activities recognition is important for understanding a situation, since each person has a particular perception about a problem.

Contextual knowledge is the experience of each worker, device, as well as activities, conditions, events and situations which occur during a job performance [1]. So, we regard cognitive processes as contextual information. Besides that, context cannot be disjointed from its use (business

processes). The information about the context of past activities performed by an individual can help other people to understand current situation. So, we aim to promote OL (Organizational Learning) by completing knowledge spiral model [14] alternating between tacit and explicit knowledge.

Our research focuses on problem-solving cognitive process description, i.e., decision-making. We emphasize the decision-making cognitive process, because we believe that making this information explicit allows people to learn from it, helping them making new decisions.

According to Brézillon [1], context only exists in a given focus, for instance, when someone performs a task or any problem solving activity. At this moment, three types of knowledge related to context [18] emerge: proceduralized context, context knowledge and external knowledge. Proceduralized context is directly related to the focus and is used to carry a task out. Contextual knowledge is not directly used but it covers all available information that remains. External knowledge covers all other knowledge that is not relevant to the current focus. Since context is directly related to focus, in our case, business process activities, it changes dynamically through time.

For example, context identification of a task performance or an artifact generation can answer questions like: “Why did we do that?”, “What would happen if we stopped doing this and that?”, “Has this problem been solved before?”, “Did anyone considered using a different approach?”. These are questions that make people deal with subjects that have been already addressed before. The analysis of social, cultural and organizational issues should be done, since they are all related to the context and provides greater meaning to the action taken, increasing learning chances. We include cognitive processes, such as decision-making, among those issues, which can answer questions like: “Which belief or feeling influenced the decision?”, “Any past experience influenced the decision?”.

In the decision-making process, for instance, we evaluate every alternative and the weight of each criterion carefully when we are not used to making such decision. On the other hand, we carry out this process automatically, upon this situation becoming commonplace, without stopping to think how we have reached a conclusion, or why we have started from a premise [16]. In spite of how automation of these processes happens, it is important to identify decision components, in order to understand its result and the cognitive process used to achieve it.

In previous papers [13][15], we described a model to represent the cognitive decision process. We extended this model including decision consequences. We argue that it would improve its characterization as process contextual information.

III. RELATED WORK

Some proposals aim to make explicit the decision-making process [5]. Others focus on helping people making better decisions by defining criteria [18]. Others try to help people by applying methods [12] or providing Computer-based systems [11][3].

Montibeller et al. [5] propose to explain decision-making process by using Causal maps. McMurray [12] proposes some methods to expand people decision-making skills. The proposed methods are brainstorming, nominal group technique and the Delphi technique. These techniques are pointed out because they provide a structured format that helps increasing the quantity and quality of participant responses. The author believes that these methods can be important resources for tasks such as developing courses, setting departmental goals and forecasting trends for planning purposes. This proposal was applied for nursing staff development educators.

According to Roy [18], multiple criteria decision-making proposals aim to enable people to enhance conformity degree and coherence between the decision-making process evolution and the value systems and objectives of those involved in this process. The author states that the purpose of decision-aid is, therefore, to help people make their way even with ambiguity, uncertainty and bifurcations. Multiple criteria decision-making proposals aim to help people to make better decisions. However it focuses on objectivity, neglecting subjective factors.

As stated by Menzel et al. [11], it's necessary to identify the most appropriate IT solutions for Cloud Computing. So, their proposal comprises a generic, multi-criteria-based decision framework and an application for Cloud Computing, the Multi-Criteria Comparison Method for Cloud Computing ((MC2)2). Their framework and method allow organizations to determine what infrastructure best suits their needs by evaluating and ranking infrastructure alternatives using multiple criteria. Their proposal includes a way to distinguish infrastructures not only by costs, but also in terms of benefits, opportunities and risks.

Yigitcanlar [3] affirms that the computing tools and technologies are designed to enhance the planners' capability to deal with complex environments and to plan for prosperous and livable communities. So, he examines the role of IT (Information Technologies) and particularly Internet GIS (Internet Based Geographic Information Systems) as spatial decision support systems to aid community based local decision-making. The paper also covers the advantages and challenges of these internet based mapping applications and tools for collaborative decision-making on the environment.

According to Steiger and Steiger [17], the decision-maker first determines values for key factors and then applies his/her mental model to evaluate the alternatives based on them, estimate potential output and make the best decision. They propose a mining architecture based on cognitive instances (ICM - Instance-based Cognitive Mining), which integrates several technologies to capture and express decision maker mental model. However, Steiger and Steiger [17] do not investigate the decision in the person's mind and do not try to find what causes or influences it.

To maximize the total reward people receive over a fixed number of trials, Steyvers et al. [4] argue that they must choose between a set of alternatives, each with different unknown reward rates. So, with the aim of helping people maximize the number of rewards, Steyvers et al. [4] use a

Bayesian model of optimal decision-making on the task, in which the way people balance exploration with exploitation depends on their assumptions about the distribution of reward rates. They do not consider the individual’s way of thinking.

Some researches on systems are already customized for a specific domain while others are too generic and difficult to customize. There are researches focusing on supporting decision-making. However, they do not care about past decisions neither decision’s context.

Other important aspects to be considered are the decision-making components. Some elements of decision-making that should be informed are indicated by Montibeller et al. [5], but they do not set up how each piece of information is related to each other. Similarly, Steiger and Steiger [17] ask only for the key factors in decision-making and their respective weight, they do not even describe what they are. Steiger and Steiger [17] are interested in representing the decision-making process, however, they do not discuss which individual’s values are considered. They do not care about cognitive processes.

IV. REVISED DECISION-MAKING META-MODEL

A. Meta-Model Source and Goal

Nunes’s knowledge management (KM) model [10] proposes four macro steps, as following: 1) capture context information; 2) associate this information with activities in a business process; 3) store this information in a repository - Organizational Memory (OM); and 4) retrieve information anytime, filtering by similar contexts. They argue that it is possible to make inferences from a model, identifying new information and supporting the understanding of process activities instances.

Pereira and Santoro [13][15] approach extended [10] KM model considering executor context, highlighting the decision-making cognitive process [5]. Pereira and Santoro [13][15] proposal focus on steps one and two: information capture and association with business process. It did not cover storage nor retrieve in OM (steps three and four).

Pereira and Santoro [13][15] proposal was a meta-model for capturing and representing individual cognitive decision-making process as contextual knowledge in business process activities. The meta-model proposed was structured by the development of an ontology, which provides structure for the OM [21]. Pereira and Santoro [13][15] also proposed a set of guidelines to support meta-model instances creation.

The meta-model goal is to explicit how a work process activity executor thought while making a decision. This can be done by instantiating [13][15] context meta-model. This provides a basis for a work process activity executor to describe how his own decision was made; thus the meta-model should draw together all relevant cognitive decision-making process elements and their relationships, which are stored in the OM. The benefits to the decision making process occurs every time someone has to make a new decision, because he will be able to retrieve past decisions with similar context information. This retrieve is done by a reasoner, but is not scope of this research.

B. Meta-Model New Classes

We analyzed Pereira and Santoro’s survey results on decision reuse [13], which was carried out among people of managerial level who are used to make decisions. All interviewees stated that what happens after a decision is very important and makes difference when he wants to retrieve decisions recorded, with the purpose of helping him to make new decisions. We realized that it was not possible to register what happened after the decision by creating an instance of [13] meta-model because it didn’t cover decision consequence as context information.

In order to make it possible to record decision result and to make it available for new decisions, we identified new classes and we extended [13] decision-making meta-model underlining decision consequences, aiming make explicit what happened after that decision. We added the classes Result and Consequence, as pointed out by a rectangle in Fig. 1.

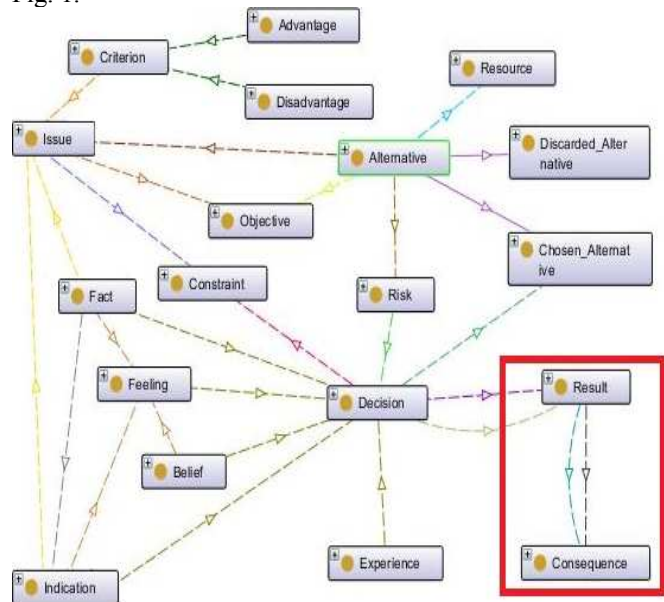


Figure 1. Extended Cognitive Decision-Making Meta-Model – Highlighting Decision Results

The Result class represents how the decision results were regarded by those who made the decision, for example: an executive director decided to reward some employees by giving them a car. He believes that it was a successful decision because it brought more comfort on employees’ way to work. It was above his expectation and he is really satisfied, because those employees had better performance, since they were not so tired because of the traffic jam.

There is also a relationship called Results_ between the Decision class and the Result class. This new relationship represents what the decision made resulted. Result class properties are: Rating, Reason_Rating, Expectation, Satisfaction_Degree and Reason_Satisfaction.

The Rating property indicates how successful the decision was. It may take the following values: Successful, Neutral or Unsuccessful. The Reason_Rating property describes the cause for that success or lack of it.

The Expectation property reports how decision result met what the decision maker looked forward while making the decision. It may assume the following values: Above, Met, Below; representing if decision result exceeded all expectations, if it met expectations or if it was below expectations, respectively.

The property Satisfaction_Degree indicates how pleased the decision maker was with decision result. It may take the following values: Satisfied, Neutral or Dissatisfied. The Reason_Satisfaction describes the cause for this feeling.

Decision result brings consequences, which led to Consequence class creation and to the relationship Brings between them, which represents what happened due to the decision results. The Consequence class represents what happened after the decision. There may have an instance for each consequence identified, continuing the example above: the decision of giving a car had a positive impact of saving employees' time in traffic jam, however it had a negative impact of wasting more money with reward. Consequence class properties are: Impact and Description.

The Impact property reports if the consequence was Positive or Negative. The Description property explains the benefits achieved or the undesired effects. There is also a new relationship between Result and Consequence classes. It is called *Brings*. There is no new relationship between Consequence class and others.

Table 1 shows a brief description of new classes and Table 2 shows new classes summary presenting their properties and the range of some properties can assume.

TABLE I. NEW CLASSES' DESCRIPTION

Class Name	Description
Result	What results from decision
Consequence	Good or bad effects obtained with the decision

TABLE II. NEW CLASSES' SUMMARY

Class Name	Properties	Range
Result	Rating	Successful / Neutral / Unsuccessful
	Reason_Rating	-
	Expectation	Above / Met / Below
	Satisfaction_Degree	Satisfied / Neutral / Dissatisfied
	Reason_Satisfaction	-
Consequence	Impact	Positive / Negative
	Description	-

V. TOWARDS RE-USING THE DECISION-MAKING

We performed 4 cases studies to assess whether new classes, their properties and relationships were enough to explain decision-making consequences details. All participants occupied a leadership position.

The case study focused on identifying what happened after a decision and identifying decision result relevance for making new decisions. Besides we applied a survey that aimed at identifying decisions context similarities comparing them.

These cases studies were based on cases studies results performed by [15]. We asked participants to report decision result reported in the previous case study, which led to the creation of an instance of the cognitive decision-making process meta-model. The decision result was recorded, in order to complement the meta-model instance.

Besides that we carried out a survey recording other context information needs. Moreover, this survey also assessed new decisions of the same context made by that person, in order to identify context similarities and to discuss the approach of using recorded decision results as contextual information for new decisions within business process.

A. Ontology New Instances

In this subsection we describe and assess new instances obtained from participants' responses. To better convey our explanation, we refer to participants as A, B and C.

Participant A reported that the decision recorded in the previous study case happened again. He pointed out that the following classes were presented in both decision instances: Experience, Feeling and Consequence.

Participant A said that decision's context is very important because it makes the difference while identifying alternatives. However, in his opinion, context is never the same. Only some pieces of information are repeated from one decision to another. He informed that there are some things that would lead the decision to a different way. Some of these things are related to his mood. Depending on how he feels, his decision may be different.

Participant A also stated that he could learn from other decisions things that should not be done, because they led to an unsuccessful situation or did not achieve the goal. He reported that having access to his previous recorded decision would change just a little bit his new decision. He also reported that having access to recorded decision of similar context would help him just a little bit to make new decision.

Participant B decision result is shown in Fig. 2. He reported that the decision recorded in the previous study case is recurrent. He pointed out that the following classes were present in both instances: Advantage, Consequence, Feeling, Objective and Risk. He states that accessing his registered decision would not change the new one, because his judgment criteria have been refined through experience.

He believes the context in which he makes decision is essential, despite his wide expertise on making decisions or his judgment criteria. He also believes that those criteria are usually permanent, because they come from people ethical and moral values. However, he stated that having access to recorded decisions of similar contexts would help him to make new decision. He highlighted that these records would help him only because they have similar context to the one he is experiencing.

Participant C reported that the issue of the decision recorded in the previous study case is recurrent, as well as the following classes: Experience, Consequence, Criterion, Objective, Result and Risk. He believes that accessing his recorded decision or any other recorded decision with similar context would change just a little bit his new decision.

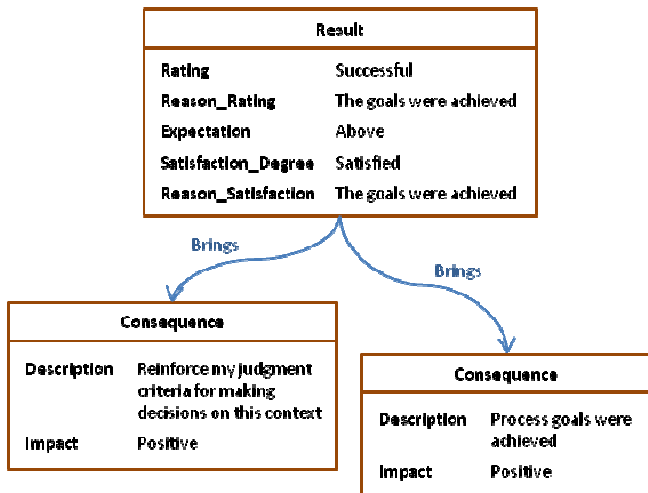


Figure 2. Detailed Recording Activity (focusing on decision's results)

Analyzing those answers we could realize that being aware about other people failure may avoid our own failure, because we can learn by observing someone else experience or by our own experience. This kind of information is provided by Result and Consequence classes. Participants also highlighted the importance of context information. They stated that a historic decision is only valuable if it is contextualized, otherwise it would be useless.

B. Recording Activity

This proposal should be applied at companies that seek to improve their practices in decision-making, sharing information and knowledge. Our research suggests an approach that enables companies to accomplish it through the analysis of historic decisions that were recorded during the process perform.

According to Pereira and Santoro [15], process manager should identify in which work process important decisions activities are made. Once these activities are identified, process manager reviews work process where these activities are, in order to add a further step related to reflection activity and another to decision-making cognitive process recording, for example, the executive manager of the example above is also "Recognition and reward" process manager. Revising this process he realized that rewarding is a very important activity for the company. As he would like to have past decisions registered to learn with them and to help him at the present time to make his own decision, he believes it's a good idea to register his own decision about it to help next "Recognition and reward" manager process to make decisions about it, when he leaves office. So, he reviews "Recognition and reward" process adding the step "Reflect about award" before the activity "Select an award" and after it he adds the step "Register decision about award".

Pereira and Santoro [15] argued to add the activity in the work process focused only on the decision's record. Regarding the scenario above, we extended the concept of this new activity by splitting it into 4 tasks, as shown in Fig. 3.



Figure 3. Detailed Recording Activity

The first task is to search for decisions in the OM which context is similar to the one he is experiencing at that moment. To support this task there should be a recovery mechanism able to identify actual context, to mine similar recorded contexts and to compare them, in order to bring out similar context decisions. Contextual information about decision's consequences may also be recovered.

The second task is to make the decision. This task is going to be performed based on similar context decisions recovered in the previous step.

Then, the third task is to record the cognitive process that occurred while making the decision. Record it means to store context information, associated with the business process activities, in OM, in order to be available for future research.

The fourth and last task occurs some time later because it records decision's result. As decision consequences are also context information, they will be stored in OM, so it might be recovered later.

C. Application Scenario

A model was built with some classes focusing on decision's result, as shown in Fig. 4. These classes came from responses from a case study participant, in order to illustrate how recording activity steps must be performed.

Whenever the worker carries out a decision-making activity, a reasoner (search engine) would compare recorded scenarios (in OM) with the one the worker is reporting or he is living at that time. The worker could choose from which context information the search engine would mine data. Regarding the example shown in Fig. 4, he could choose to retrieve information from OM using criterion "lowest price" or issues related to suppliers' selection and hiring. However, as decision result he reported was unsuccessful and he was dissatisfied with it, he would prefer to recover decisions which result was successful or even where Expectation was "Above" or Satisfaction_Degree was "Satisfied". Then, the reasoner would recover decisions records where the scenario matches.

Then, based on the information about past decisions recovered, the worker would carry out the second task of this activity. By recovering the OM, the worker would be able to analyze recorded events which context information is similar to the one he lives or he reported. It is going to support him to make his own decision. He would analyze these events and realize that the criterion chosen was not good. The research result would indicate that the selection and contracting of suppliers must be based on technical, professional and ethical criteria, but not only on price. However, in this case, he would not be able to use another criterion because this one was a legal requirement. Even so he could look for decisions that have used this same criterion to learn how they avoided or even eliminated the risk of getting a poor quality service or product. He could realize that some people bypassed this risk by specifying a technical

requirement. Afterwards finishing his analysis he would finally make the decision.

Immediately after, he would accomplish the third task registering how he thought to make that decision. He would provide information about the issue to be decided, such as its goal, the fact or indication that led to the need to make that decision and the constraint imposed to its resolution. Next, he would report the alternative selected, as well as the advantages and disadvantages of performing such an option and the risk of carrying this option out. He would also report how this alternative influenced on the decision, the resources used and its goal. Afterwards, he would report each one considered, but rejected alternatives, reporting the same type of information reported in the alternative chosen. Afterwards these pieces of information would be stored in OM.

After a while the worker could report context information about the result of his decision. He could classify if the result was successful or not, how it met his expectations and how pleased he was with it. He could also report its consequences and indicate if it was positive or negative. These are important information because there could be cases where only good results matter. Or even, there could be a working group interested in unsuccessful events results, in order to identify their reasons to avoid their recurrence. The model shown in Fig. 4 illustrates an example of unsuccessful decision. By analyzing its decision's result, we could realize that legal requirement hindered suppliers' selection and hiring process.

VI. CONCLUSIONS AND FUTURE WORK

In our research, we have discussed that decision-making process description can be considered an important context information to support future decision-making, and consequently to improve business process. We proposed a meta-model to represent cognitive decision-making process and a set of guidelines to support workers creating instances of it.

This paper presents an extension of this model that improves the results obtained before, after the instantiated decisions. The goal was to show how this information could be used in practice. In this sense, new case studies have provided information about decision consequences within the process. This result worked as basis to build a scenario that described contextual information possible usage.

We concluded that ontology instances associated with the business process activities might allow the identification of correlation between a decision made and a process outcome. This is a first step towards the effective use of this information as context to promote learning among participants and process improvement. However, the decision-making cognitive meta-model as a whole is quite complex and in many cases reflects subjectivity and individuality. This is an important issue to be deepened, so that it can be addressed in our proposal more effectively.

This paper contribution is the possibility to concentrate all related information about decision-making cognitive process at a unique meta-model, which can be instantiated anytime to register decisions, transforming tacit into explicit knowledge, exteriorization. Once meta-model's instances

were created it can also be used to promote OL by transforming explicit into tacit knowledge, internalization. Knowledge spiral model [14] can be completed even if there is no computational support to automatize recording and retrieving.

We can also observe that a clear limitation of this proposal is the computational support requirement to help identifying similarities among the ontology instances. This feature would make possible to deal with processes that have a big number of cases to be analyzed.

In our future work, we are going perform more case studies at companies where the most relevant decisions-making processes are mapped, and evaluate the models generated in real situations where we presume people will learn with them.

REFERENCES

- [1] Brézillon, P., Context in problem solving: a survey Source, *The Knowledge Engineering Review*, vol. 14, no. 1 (1999), pp. 47-80.
- [2] Suchman, L.A., *Plans and Situated Actions: The Problems of Human Machine Interaction*. Cambridge: Cambridge University Press, 1987.
- [3] Yigitcanlar, T., *Research Monograph: Constructing online collaborative environmental decision making systems*. QUT Digital Repository: <http://eprints.qut.edu.au/26262/>. [retrieved: June, 2012].
- [4] Steyvers, M., Lee, M.D. and Wagenmakers, E., A Bayesian analysis of human decision-making in bandit problems, *Journal of Mathematical Psychology*, vol. 53, Issue 3 (2009), pp. 168-179.
- [5] Montibeller, G.N., Belton, V., Ackermann, F. and Ensslin, L., Reasoning maps for decision aid: an integrated approach for problem-structuring and multi-criteria evaluation, *Journal of the Operational Research Society*, vol. 59, no. 5 (2007) , pp. 575-589.
- [6] Kingston, R., Carver, S., Evans, A. and Turton, I., Web-Based Public Participation Geographical Information Systems: An Aid To Local Environmental Decision-Making. *Computers, Environment and Urban Systems*. vol. 24, no.2 (2000), pp. 109-125.
- [7] Kwan, M. and Balasubramanian, P., Knowledge Scope: managing knowledge in context. *Decision Support Systems*, vol.35 no.4 (2003), pp.467-486.
- [8] Lima G., and Borém A., Interfaces between information science and cognitive science. *Ci. Inf.* vol.32, no.1 (2003), pp.77-87.
- [9] Maximiano A.C.A., *Introduction to administration - Introdução à administração* (in Portuguese), Atlas, São Paulo, 1995.
- [10] Nunes V.T., Santoro F.M. and Borges R.B., A Context-based Model for Knowledge Management embodied in Work Processes. *Information Sciences* vol.179, no. 15 (2009), pp. 2538-2554.
- [11] Menzel, M., Schönherr, M., Nimis, J., and Tai, St., (MC²): A Generic Decision-Making Framework and its Application to Cloud Computing, In *Proceedings of the International Conference on Cloud Computing and Virtualization (CCV 2010)*, Singapore, vol. 1, pp. 287-296, 2010.
- [12] McMurray, A.R., *Three Decision-making Aids: Brainstorming, Nominal Group, and Delphi Technique*. *Jr of Nursing Staff Development*, 1994. vol. 10, no.2, pp. 62-65.

- [13] Pereira A.C.T.D. and Santoro F.M., Cognitive Decision-Making Process as Context Information, *In Proceedings of the 2010 Conference on Bridging the Socio-technical Gap in Decision Support Systems: Challenges for the Next Decade*, Ana Respício, Frédéric Adam, Gloria Phillips-Wren, Carlos Teixeira, and João Telhada (Eds.). IOS Press, Amsterdam, The Netherlands, The Netherlands, pp 346-357 (2010a).
- [14] Nonaka, I. and Takeuchi, H., *The knowledge-creating company*, New York: Oxford University Press, 1995.
- [15] Pereira, A.C.T.D. and Santoro, F.M., A Case Study on the Representation of Cognitive Decision-Making within Business Process, *In Proceedings of the EWG-DSS Workshop on Decision Systems*, F.Dargam, B.Delibasic, J.E.Hernández, S.Liu, R.Ribeiro, P.Zarató (editors), pp. 25, London, 2011.
- [16] Sternberg, R.J., *Cognitive psychology*, 6th Edition, Belmont: Cengage Learning, 2011.
- [17] Steiger, D.M. and, Steiger, N.M., Discovering a Decision Maker’s Mental Model with Instance-Based Cognitive Mining: A Theoretical Justification and Implementation, *Interdisciplinary Journal of Information, Knowledge, and Management*, vol. 4, no.5 (2009), pp-1-22.
- [18] Roy, B., Decision science or decision-aid science?, *European Journal of Operational Research*, vol. 64, no. 66 (1993), pp. 184-203.
- [19] Rowlands, M.. *The body in mind: understanding cognitive processes*, Cambridge University Press, Cambridge, 1999.
- [20] Santoro, F.M., Brézillon, P. and Araujo, R.M., Management of shared context dynamics in software design. *Proceedings of 9th International Conference on CSCW in Design (CSCWD-2005)*, Coventry University, IEEE, vol. 1, pp. 134-139, 2005.
- [21] Simon, H.A. and Newell, A., *Human Problem Solving*, Englewood Cliffs, NJ., Prentice Hall, 1972.

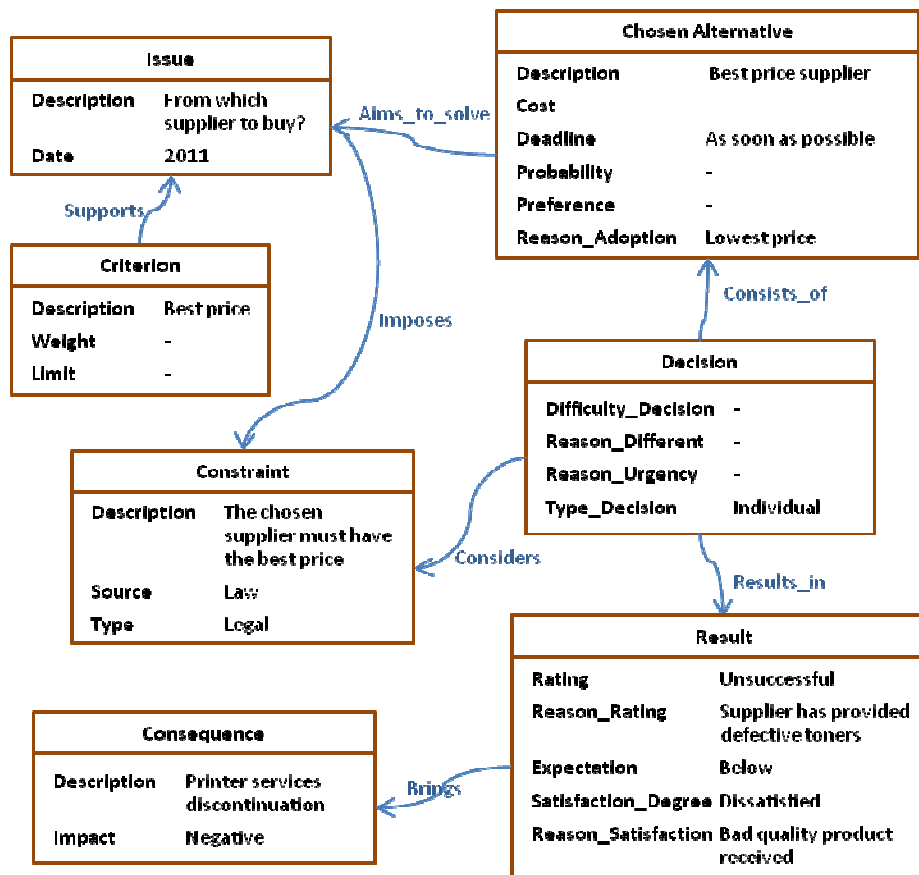


Figure 4. Instance Cognitive Meta-Model Decision-Making Result

Vision-based Inspection Algorithm for Identifying the Carbide Phase State in 12CrMoV Steel

Alexander Tzokev

Theory of Mechanisms and Machines
Technical University of Sofia
Sofia, Bulgaria
alexzt@tu-sofia.bg

Irina Topalova

Automation of Discrete Production Engineering
Technical University of Sofia
Sofia, Bulgaria
itopalova@tu-sofia.bg

Anton Mihaylov

Materials Science and Technology
Technical University of Sofia
Sofia, Bulgaria
amm@tu-sofia.bg

Tzanko Georgiev

Industrial Automation
Technical University of Sofia
Sofia, Bulgaria
tzg@tu-sofia.bg

Abstract—The paper presents a vision-based inspection algorithm for identifying the carbide phase state in 12CrMoV steel microstructures. The algorithm uses image preprocessing, anisotropic segmentation, discriminant analysis and mathematical model for calculating the residual life of the material. Based on the state of the carbide phase, the residual life can be precisely calculated. By implementing automated vision inspection, the subjective evaluation of microstructures by experts will be avoided.

Keywords—vision inspection; discriminant analysis; steel microstructures; carbide phase; 12CrMoV steel

I. INTRODUCTION

The properties and the residual life of many types of steels (heat-resistant steels, tool steels, high strength steels, etc.) depend on the carbide phase, the quantity and the type of carbides, their shape and distribution. The state of the carbide phase is defined by heat treatment and can be altered by the working conditions [1,2].

The 12CrMoV steel pipes are used in thermal power plants for building superheaters with working temperature of up to 580°C. The microstructure of the metal alters (the properties of the material degrade) during exploitation based on the working temperature and the applied pressure. Visual analysis by experts shows that the carbide state in the microstructure is modified during the exploitation of the metal. This alteration is the main assessment factor for the structural state of the material and standard scales are used. The analysis is performed mainly by experts and consists in comparing the analyzed and standard scale images. This evaluation is subjective, uses a qualitative rather than a quantitative method and the results depend on the expert's qualification level, competence and experience [1,3,4].

At the moment, there are no integrated systems for performing this assessment. Some companies offer partial software and hardware solutions.

The microstructure state and the level of spheroidization (carbide phase) are used for calculating the time remaining until metal destruction - the residual life of the material. An automated carbide phase vision-based inspection algorithm (CPVBIA) will minimize the subjective evaluation and will help the experts in making their final decision for the residual life of the material. The CPVBIA applies quantitative assessment methods for achieving a qualitative result.

Fig. 1 shows the structural alterations of the 12CrMoV steel and the corresponding level of the spheroidization based on the adopted standards [1,3].

The photos in Fig. 1 show a metal structure with ferrite (bright zones) and carbide phases (dark zones and grains). Level 1 corresponds to new material and level 5 corresponds to a material with exhausted residual life which must be replaced.

The presented CPVBIA is based only on computer vision algorithms without implementing any adaptive technologies such as neural networks, genetic algorithms or fuzzy logic. The presented approach has 4 general stages, as shown in Fig. 2.

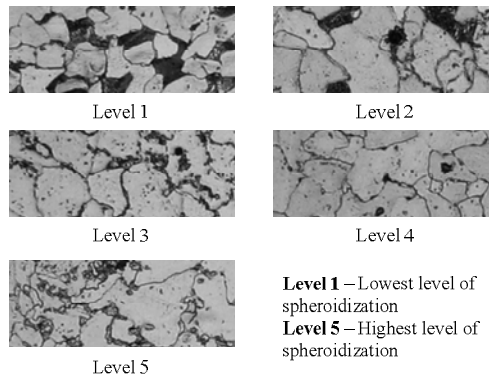


Figure 1. Level of spheroidization in 12CrMoV steel microstructures.

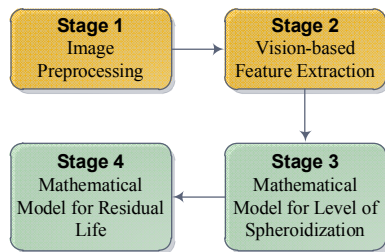


Figure 2. General stages of the CPVBIA

The first stage contains the entire image preprocessing - image resizing, converting to grayscale, filtration, etc. In stage 2, vision algorithms are applied for extracting crystallite borders and for identifying interesting zones that may contain the carbide phase. The result from the second stage is an array of 5 different morphological parameters for the carbide phase. In stage 3, a mathematical model based on morphological parameters is used to define the level of spheroidization. The final fourth stage calculates the residual life of the material based on external variables (working pressure and working time), the calculated carbide phase level and mathematical model of linear approximation, derived from CTO 1723082.100.005-2008 [1].

100 sample images (20 for each level of spheroidization) were used in the study. All of these images were analyzed and classified by experts.

II. IMAGE PREPROCESSING (STAGE 1)

In this study, all input images are acquired by digital microscope camera with 2Mpix resolution. If the input image is not a grayscale one, then color to grayscale conversion is applied.

The time needed for anisotropic segmentation (cf. III. Vision-based feature extraction) depends on the size of the input images. Therefore, in order to achieve higher performance, the algorithms in stage 1 resize the input image to 800x600 pixels if the original image is larger than that. To determine the relation between the size of the input image and the achieved recognition accuracy, a separate study can be conducted. An empirical analysis shows that 800x600 pixels are sufficient for fast and reliable feature extraction.

In general, stage 1 has only two steps:

1. Grayscale conversion
2. Image resizing

III. VISION-BASED FEATURE EXTRACTION (STAGE 2)

The second stage of CPVBIA extracts features from the image for further analysis and calculation of the spheroidization level. The extracted set of features must identify the carbide phase precisely and provide numerical data for stage 3. Two general types of features are extracted:

1. Crystallite borders
2. Interesting zones possibly containing carbide phase blobs

Fig. 3 shows the analyzed image, the interesting zones and the extracted borders of the grains.

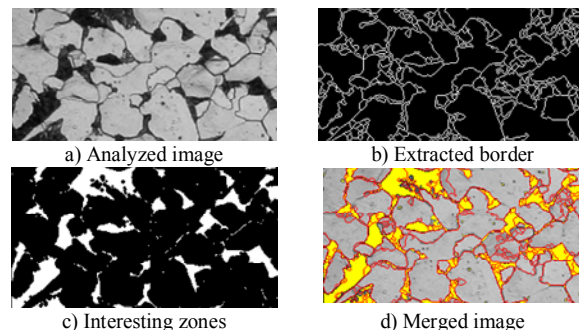


Figure 3. General stages of the CPVBIA

A. Extracting borders of the crystallites

To extract the borders of the grains after the image preprocessing, an anisotropic segmentation algorithm is applied. This segmentation algorithm is based on the method proposed by Malik [5]. This algorithm can segment grayscale images in disjoint regions of coherent brightness and contrast. Contours are treated in the intervening contour framework, while texture is analyzed using textons. Each of these cues has a domain of applicability, so to facilitate cue combination the authors introduce a gating operator based on the texturedness of the neighborhood of a pixel. Having obtained a local measure of how likely two nearby pixels are to belong to the same region, the algorithm uses the spectral graph theoretic framework of normalized cuts to find partitions of the image into regions of coherent texture and brightness [5].

Two parameters are used for the anisotropic filtration - the threshold K and the number of iteration (I). Fig. 4 shows blob extraction with different values for K and I . Experiments show that the best border extraction is achieved when $K=2$ and $I=500$.

After the anisotropic segmentation, a connected component labeling is applied for blob detection. The majority of the borders are connected so the biggest blob is extracted.

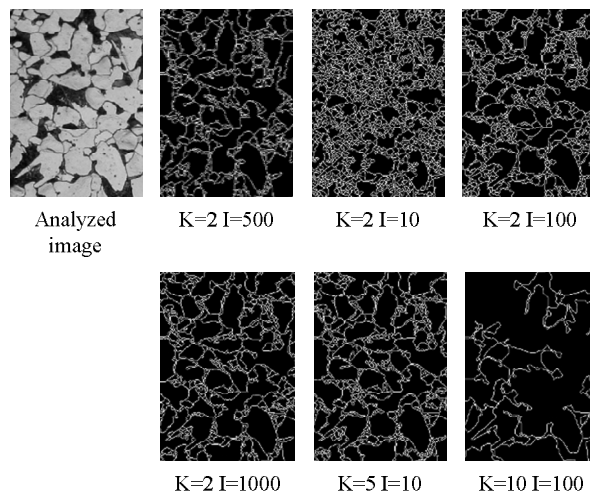


Figure 4. Border extraction with different values for K and I

B. Extracting interesting zones

To define the interesting zones that may contain the carbide phase, a Bradley local threshold algorithm [6] is applied to the analyzed image. This algorithm is a simple extension of Wellner’s method [6] in which each pixel is compared to an average of the surrounding pixels and an approximate moving average of the last N pixels seen is calculated while traversing the image. If the value of the current pixel is T percent lower than the average, then it is set to black, otherwise it is set to white [6].

In the Bradley’s algorithm, by using the integral image (also known as a summed-area table) instead of computing a running average of the last S pixels seen, the average of an SxS window of pixels centered on each pixel is calculated. This is a better average for comparison since it considers neighboring pixels on all sides. The average computation is accomplished in linear time by using the integral image [7].

A previous study shows that this algorithm is suitable for extracting the sigma phase and non-metal inclusions in austenitic stainless-steel microstructures [8]. The sigma phase has similar image features as the carbide phase for 12CrMoV steel. After the local threshold is applied, the resulting image is inverted and hit and miss filter is applied. The result is image containing the interesting zones.

A connected component labeling is used for blob detection. These blobs contain the carbide phase, noise in the image and other detected particles. To extract the sigma phase blobs from the noise, a simple filtration is applied – all blobs with height and width of the bounding rectangular less than 3 pixels are removed.

C. Morphological parameters

The result from stage 2 of the CPVBIA must be a numerical set of data describing the carbide phase. This data contains the following information for each blob:

1. Total number of blobs in the image.
2. Total area of the blobs in the image, measured in pixels.
3. Number of blobs inside the grains and on the borders.
4. Number of blobs on borders.
5. Average height of the bounding rectangular for all blobs, measured in pixels.
6. Average width of the bounding rectangular for all blobs, measured in pixels.
7. Average area of the blobs in the image.
8. Average fullness (area of the blob divided by the surface of the bounding rectangle) for all blobs in the image.
9. Average aspect (maximum of the height or width of the bounding rectangular, divided by the minimum of the height or width) for all blobs.

The numbers of blobs inside the grains and on the borders are used for final decision by the expert and are not used in stage 3. Fig. 5 shows subset analysis of the morphological parameters based on the sample images.

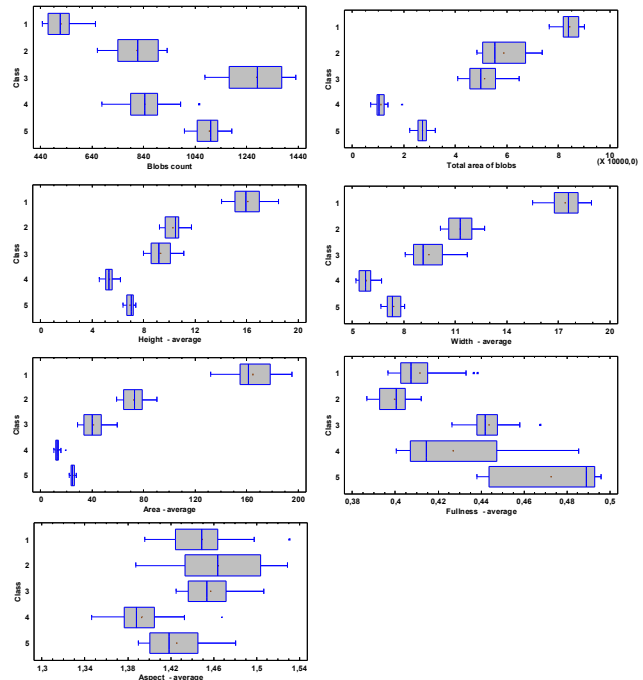


Figure 5. Subset analysis of the morphological parameters

The subset analysis shows that there is no only one morphological parameter that can classify the blobs. Each of the morphological parameters has some overlapping between the classes and a combination of two or more parameters should be used to correctly distinguish all 5 classes.

The summary statistics for the analyzed data is shown in Table I.

TABLE I. SUMMARY STATISTICS FOR THE MORPHOLOGICAL PARAMETERS

Class	Count	Average	Standard Deviation	Coefficient of variation	Minimum	Maximum
1	20	517,6	59,5752	11,5099%	445,0	654,0
2	20	815,1	84,2514	10,3363%	661,0	932,0
3	20	1278,2	110,928	8,67849%	1079,0	1431,0
4	20	844,4	87,631	10,3779%	676,0	1056,0
5	20	1095,5	53,7181	4,90352%	998,0	1182,0
Total	100	910,16	273,071	30,0025%	445,0	1431,0

Class	Range	Standardized Skewness	Standardized Kurtosis
1	209,0	1,5628	0,374479
2	271,0	-0,583478	-0,914204
3	352,0	-0,170449	-1,11532
4	380,0	0,821561	0,695647
5	184,0	0,0152641	-0,919001
Total	986,0	0,0752718	-1,80172

IV. CALCULATING THE LEVEL OF SPHEROIDIZATION (STAGE 3)

A discriminant analysis based on the morphological data from 100 images was used to calculate the parameters for classification functions. Table II contains the classification function coefficients.

TABLE II. CLASSIFICATION FUNCTION COEFFICIENTS

	1	2	3	4	5
C_{Blobs}	0,0280909	0,00172282	0,0926188	-0,020431	0,0405502
C_{Area}	-9,09884	-9,65378	-11,0216	-10,1958	-11,0222
C_{Height}	125,935	128,924	144,078	130,624	139,747
C_{Width}	112,696	95,9607	111,781	101,348	116,161
$C_{Fullness}$	5471,58	5255,23	5589,67	5561,88	5876,29
C_{Aspect}	2508,6	2701,41	2721,89	2861,86	2831,37
$C_{TotalArea}$	-0,0192403	-0,0185858	-0,0205796	-0,0208617	-0,0218383
CONST	-3382,34	-3338,62	-3729,97	-3632,74	-3909,51

$$y_{(i)} = CONST + C_{Blobs_i} \cdot Blob\ Count + C_{Area_i} \cdot Average\ area + C_{Height_i} \cdot Average\ height + C_{Width_i} \cdot Average\ width + C_{Fullness_i} \cdot Average\ fullness + C_{Aspect_i} \cdot Average\ aspect + C_{TotalArea_i} \cdot Total\ area \quad (1)$$

where $i = 1..5$ and the level of the spheroidization is calculated by (2).

$$Level\ of\ spheroidization = MAX(y_{(i)}) \quad (2)$$

The classification with prior probability of 0,2 for all levels is shown in Table III.

TABLE III. CLASSIFICATION TABLE FOR DISCRIMINANT ANALYSIS

Actual Class	Group Size	Predicted Class				
		1	2	3	4	5
1	20	20	0	0	0	0
		(100,00%)	(0,00%)	(0,00%)	(0,00%)	(0,00%)
2	20	0	20	0	0	0
		(0,00%)	(100,00%)	(0,00%)	(0,00%)	(0,00%)
3	20	0	0	20	0	0
		(0,00%)	(0,00%)	(100,00%)	(0,00%)	(0,00%)
4	20	0	0	0	19	1
		(0,00%)	(0,00%)	(0,00%)	(95,00%)	(5,00%)
5	20	0	0	0	0	20
		(0,00%)	(0,00%)	(0,00%)	(0,00%)	(100,00%)

The summary statistics by each group is shown in Table IV.

TABLE IV. SUMMARY STATISTICS BY GROUP

Class	1	2	3	4	5	TOTAL
COUNTS	20	20	20	20	20	100
MEANS						
Blobs count	517,6	815,1	1278,2	844,4	1095,5	910,16
Area average	164,978	72,2296	40,8611	13,0502	24,8825	63,2003
Height average	16,0838	10,282	9,30539	5,32764	6,94183	9,58813
Width average	17,3916	11,2668	9,46961	5,7954	7,3866	10,262
Fullness average	0,411401	0,3996	0,4436	0,427	0,4725	0,430824
Aspect average	1,44945	1,46447	1,45718	1,39305	1,42559	1,43795
Total area of blobs	84434,6	58818,1	51339,6	11120,6	27269,2	46596,4
STD. DEVIATIONS						
Blobs count	59,5752	84,2514	110,928	87,631	53,7181	273,071
Area average	18,5875	8,4545	8,95146	2,00407	1,61811	55,7795
Height average	1,20869	0,630084	0,90664	0,38898	0,2901	3,77871
Width average	1,04933	0,790887	1,04796	0,43678	0,43977	4,11296
Fullness average	0,012544	0,00770	0,00952	0,02654	0,02439	0,0311191
Aspect average	0,035857	0,042157	0,02393	0,02766	0,0278	0,0409149
Total area of blobs	3647,13	8959,74	7020,1	2638,28	2343,12	26143,4

Fig. 6 shows sample plots for some of the discriminant functions.

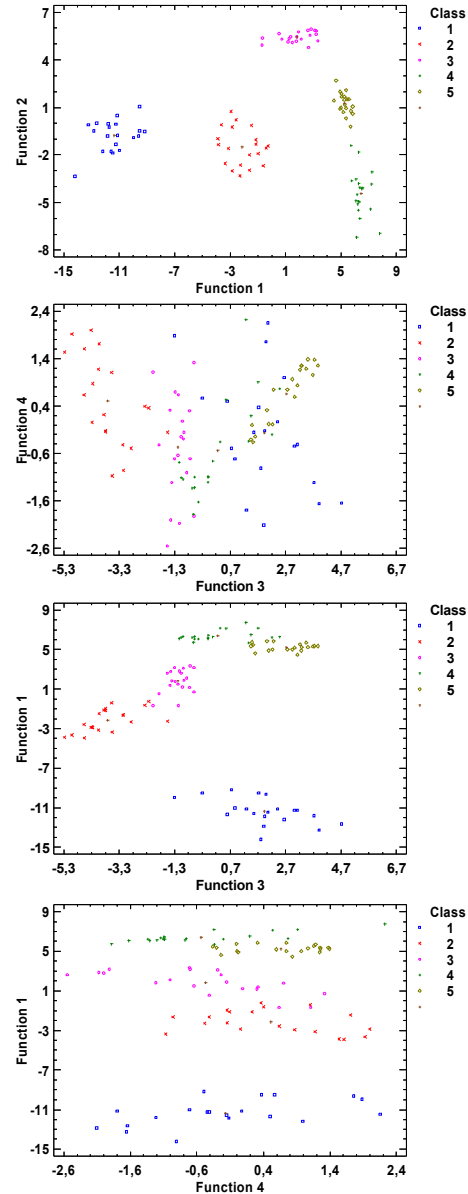


Figure 6. Classification functions

V. CALCULATING THE RESIDUAL LIFE (STAGE 4)

The residual life is defined by the standard curves published in [1] and according to the same metallography standard several parameters are used to calculate this value:

1. Working hours
2. Nominal pressure
3. Level of spheroidization

As it was already defined, this analysis is subjective and highly dependent on the proficiency level of the expert. One of the main advantages of CPVBA is removing the human factor.

From stage 3 the level of spheroidization is calculated. By using linear approximation and the exponential equations from the nomograms the residual life can be precisely calculated avoiding the subjective factor.

VI. CPVBIA COMPLETE STRUCTURE

The complete structure of the CPVBIA algorithm is shown in Fig. 7.

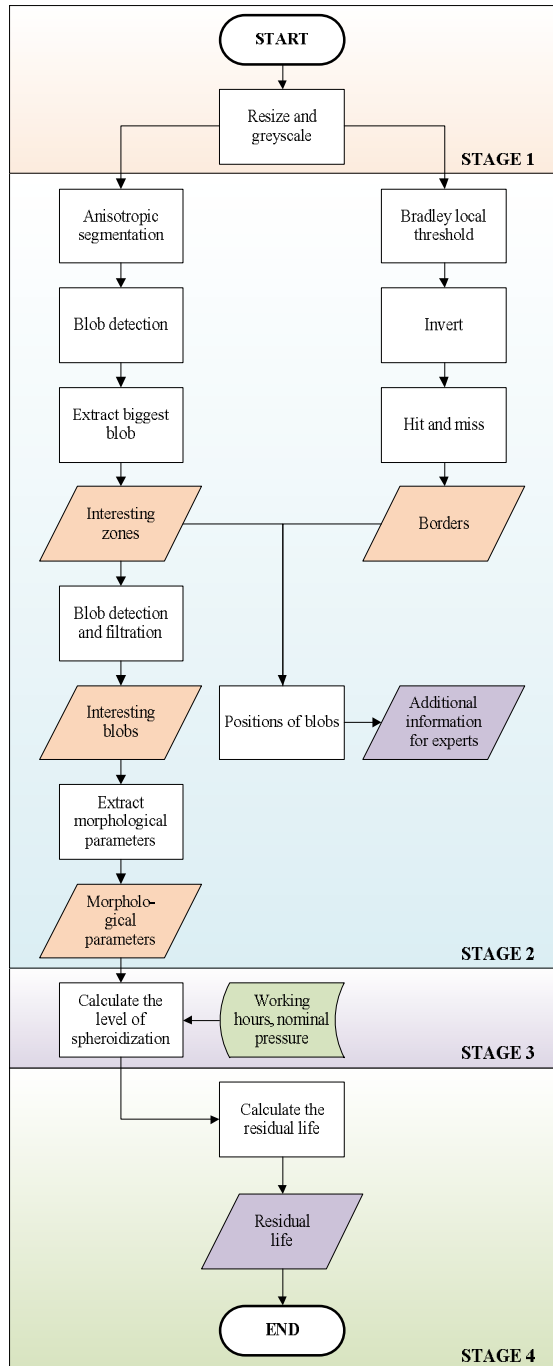


Figure 7. Complete structure of CPVBIA algorithm

VII. EXPERIMENTS AND RESULTS

To test and to validate the proposed algorithm, two groups of images were used. Group A contains images of steel microstructures of 12CrMoV steel for levels 1 to level 5. Group B contains images with varying contrast, microstructures of different steel type, larger optical magnification or insufficient preparation of the steel specimen. The results expected by experts are high classification accuracy within group A and high number of wrong classifications in group B.

All of the images in group A and group B were not used in the preliminary discriminant analysis.

Table V shows the results from the analysis.

TABLE V. EXPERIMENTAL DATA

Test Group	Description	Count	Correctly classified	Wrong classification
Group A	Level 1	8	8	0
	Level 2	13	10	3
	Level 3	6	5	1
	Level 4	18	18	0
	Level 5	11	10	1
Group B	Modified Contrast	4	0	4
	Different steel type	1	0	1
	Bigger optical magnification	8	0	8
	Not well developed borders	2	0	2
	Wrong amount of ferrite	1	0	1

Fig. 8 shows graphical representation for the classification accuracy in group A.

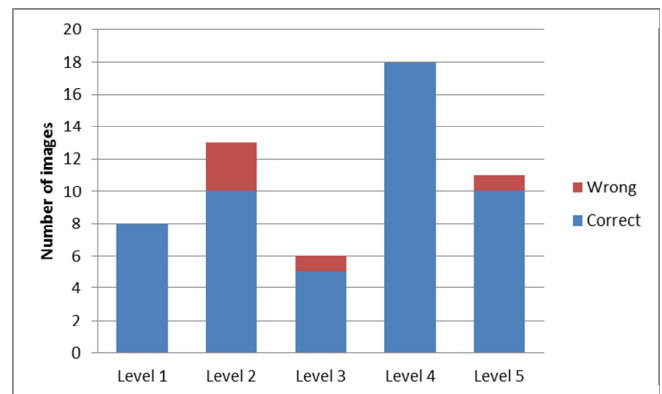


Figure 8. Recognition accuracy for group A

The classification accuracy for group A is 91.07% and 0.00% for group B, and these results confirm the expectations of experts. According to CTO 1723082.100.005-2008, the calculation of the carbide phase should be made on multiple microstructure images from the same steel exemplar [1].

Further analysis shows that two of the wrongly classified images in group A contain high amount of non-metal inclusion in the material, and one image has blurred zones. To improve the recognition accuracy, some images with small amount of non-metal inclusions can be added to the discriminant analysis for each level.

A detailed analysis of the algorithm parameters for group B shows that the error percentage between the correct level (classified by an expert) and the wrong level (classified by the CPVBIA) varies depending on the image type. Table VI contains the average of the classification functions and Δy (see (3)).

$$\Delta y = y_{Correct} - y_{Wrong} \quad (3)$$

TABLE VI. EXPERIMENTAL DATA FOR GROUP B

Description	Classification function - average					Avg ΔY
	y1	y1	y2	y4	y5	
Modified contrast	817.23	845.71	855.76	857.18	857.73	-1.41
Different steel type	1025.8	1025.4	1028.1	1035.5	1041.5	-15.70
Bigger optical magnification	896.90	916.76	919.90	928.95	929.74	-7.32
Poorly developed borders	903.46	919.47	921.56	928.56	931.1	-4.24
Wrong amount of ferrite	1109.8	1104.4	1110.4	1117.4	1126.3	-16.50

If the algorithm is used in an application, two of the most common problems with the input images will be the different contrast and the borders development. The contrast may vary due to different light conditions and the camera – Fig. 9a. Improper preliminary preparation and polishing of the steel specimen can lead to blurred or missing borders of the crystallites (see Fig. 9b).

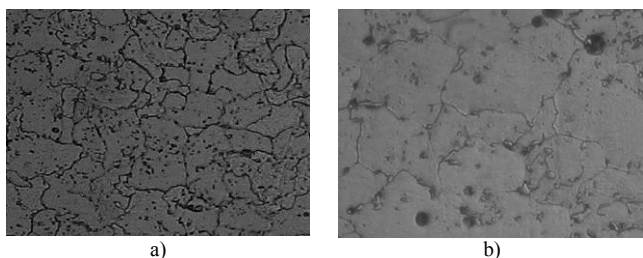


Figure 9. Input images with dissimilar contrast (a) and with poorly developed borders (b)

The Δy for these two types of images is low. If the images used in the discriminant analysis contain samples with varying contrast and poorly developed borders, the overall classification accuracy of the algorithm can be increased.

The analysis time for a single test image with the proposed algorithm parameters is around 170 seconds and depends on the hardware used. The slowest function is the anisotropic segmentation. By modifying the K and decrementing the number of iterations (cf. III, part A) the algorithm will be faster. In this type of analysis the overall inspection time is not important, but faster execution will allow the usage of the CPVBIA in more complex systems.

If a faster execution time is required (for application in real-time systems), an adaptive approach can be adopted. In this case the CPVBIA can be used in parallel for later validation or comparison of the results.

VIII. CONCLUSIONS

A vision-based inspection algorithm for identifying the carbide phase and calculating the level of spheroidization in 12CrMoV is developed.

The algorithm is stable and the calculation accuracy for the carbide phase is very high – 91.07% (based on experiments).

The algorithm can be used in automated applications for carbide phase identification and calculation of the residual life of the material.

The overall execution time is slow due to the large number of iterations in the anisotropic segmentation function.

The CPVBIA can be used in parallel with adaptive approach (neural network) for result comparison.

Future studies can be performed with high resolution images and the algorithm can be tested for real-time application.

REFERENCES

- [1] CTO 1723082.100.005-2008, Russia, 2008.
- [2] I. Savova, N. Petrov, “Vacuum Heat Treatment of Tool Steels and Its Impact on the Operational Qualities of the Tools”, Academic Open Internet Journal, Vol. 8, 2002.
- [3] DL/T 773-2001, Spheroidization evaluation standard of 12Cr1MoV steel used in power plants, 2002.
- [4] “ASM Handbook – Metallography and Microstructures”, Volume 9, ASM, USA, 2004.
- [5] J. Malik, S. Belongie, T. Leung and J. Shi, “Contour and Texture Analysis for Image Segmentation”, International Journal of Computer Vision 43(1), Kluwer, Academic Publishers, Netherlands, pp. 7-27.
- [6] A. Wellner, “Adaptive thresholding for the digitaldesk”, Tech. Rep. EPC-93-110, EuroPARC, 1993.
- [7] D. Bradely and G. Roth, “Adaptive Thresholding Using the Integral Image”, Journal of Graphics Tools, A K Peters Ltd, Vol 12, USA, pp. 13-22.
- [8] A. Tzokev, I. Topalova, and A. Mihaylov, “Adaptive Approach for Filtering the Sigma Phase in Austenitic Stainless Steel Metallographic Microstructures”, Mediterranean Conference on Control and Automation, Greece, 2011, pp. 1259-1264.

Indoor User Tracking with Particle Filter

Incheol Kim

Department of Computer Science
Kyonggi University
Suwon, Korea
kic@kyonggi.ac.kr

Eunmi Choi, Huikyung Oh

Department of Computer Science
Kyonggi University
Suwon, Korea
{allychoi, ohkv770}@kyonggi.ac.kr

Abstract—Recently there have been developed a number of mobile personal assistants, which can provide their users with useful location-based services. In this paper, we propose a WiFi fingerprint-based localization algorithm for tracking the accurate position of a smartphone user in indoor environment. To meet high complexity of localization in a large continuous environment, our algorithm incorporates a graph-based space representation, a linear interpolation-based observation model, and three component motion models into the particle filter framework. In experimental evaluation, our WiFi localization algorithm showed high accuracy and robustness in indoor tracking.

Keywords-WiFi fingerprint; indoor tracking; particle filter; probabilistic model

I. INTRODUCTION

The location information of a user plays a key role in various mobile services. In outdoor environment, GPS is a common solution for obtaining location information, but it does not work well in indoor environments. WiFi fingerprint-based indoor positioning systems [1,2] are currently attracting interest, since they can reduce installation costs. WiFi network modules are readily embedded in a variety of mobile devices, and WiFi APs are commonly installed in modern buildings. However, indoor localization using WiFi signal strength has the problem of unpredictable signal propagation through indoor environments. To meet this uncertainty problem of WiFi fingerprint-based localization, many probabilistic/statistic approaches have been proposed [2,3]. The best known of them is the particle filter, in which the posterior probability distribution of the current position of a user is represented and propagated using the set of weight samples. For the particle filter localization to be successfully used in a large continuous indoor environment, however, decisions should be made on the following important factors: a space and/or state representation to reduce the size of the state space, an observation model to generate likelihoods at locations for which no calibration data is available, and a motion model to predict the accurate position of a pedestrian.

In this paper, we propose a WiFi fingerprint-based localization algorithm for tracking the position of a smartphone user in indoor environment. To meet high complexity of localization in a large continuous environment, our algorithm incorporates a graph-based space representation, an effective observation model, and three

component motion models into the particle filter framework. In experimental evaluation, our WiFi localization algorithm showed high accuracy and robustness in indoor tracking.

The next section presents the representation of an indoor environment and the state of a pedestrian roaming within the environment. Section III describes the WiFi fingerprint map and the observation model built up from the calibration data set. Section IV details the motion model for tracking a pedestrian's motion in an effective manner. Section V describes precisely the particle filter algorithm for tracking the WiFi-enabled smartphone user's position in real-time settings. Section VI explains the experiments for evaluating the performance of our WiFi-based localization algorithm. Section VII concludes and discusses future work.

II. REPRESENTATION OF ENVIRONMENT

We represent an indoor environment as a graph $G=(V, E)$, where V is a set of vertices indicating pre-determined locations in the environment, and E is a set of edges connecting two adjacent vertices. Figure 1 shows an example, representing one floor in a research building.

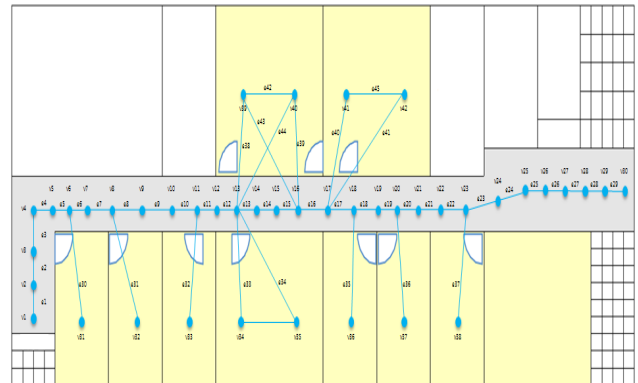


Figure 1. Graph representation of an indoor environment.

Considering important environmental factors such as the layout of corridors and rooms, the position of WiFi APs (WiFi Access Points), the typical motion pattern of residents, the number and the position of vertices are usually decided. We assume a WiFi-equipped smartphone user moves only along the edges of the graph. Hence, an instant position of the user can be viewed as a point on an edge e_t , and the state x_t of the user is represented as a tuple $\langle e_t, s_t, d_t, m_t \rangle$, as illustrated in Figure 2.

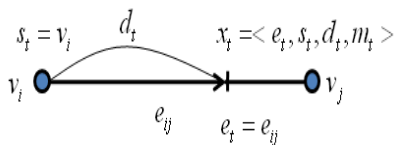


Figure 2. The state of a user roaming in an indoor environment at time t .

e_t represents the edge the user currently walks along, and s_t indicates the starting vertex the user entered the edge through. d_t represents the distance from the position of the starting vertex to the current position of the user, and m_t expresses the motion state indicating whether the user is *moving* or *stopped*.

III. WiFi FINGERPRINT MAP AND OBSERVATION MODEL

To enable online tracking with the particle filter, we need an observation model to tell the likelihood of observing the specific WiFi signal strength at a certain location in the environment. In fingerprint-based localization systems, this observation model and so-called WiFi fingerprint map are obtained from the calibration data. To collect the calibration data over the environment, we scanned WiFi signal strength vectors at the locations indicated by the vertices $v \in V$ on the graph. Each entry of the calibration data consists of the WiFi signal strength vector and the location label, that, a pair of $\langle \text{WiFi RSS vector, location} \rangle$. We assume the likelihood of observing the specific signal strength at a certain location is a Gaussian distribution. Assume there exist $|A|$ number of APs (Access Points) discovered in the indoor environment. In practice, the WiFi fingerprint map includes $|V| \times |A|$ number of Gaussian distributions, each of them represented by two parameters: the mean μ_p and the variance σ_p^2 of WiFi signal strength of each AP as measured from each vertex p . Based on these two parameters μ_p and σ_p^2 of the WiFi distribution at the location x_p , we can compute the likelihood $p(z|x_p)$ of observing the specific signal strength z at the location x_p , as formulated in the equations (1) and (2).

$$p(z | x_p) = \frac{1}{\sqrt{2\pi\sigma_p^2}} \exp\left(-\frac{(z - \mu_p)^2}{2\sigma_p^2}\right) \quad (1)$$

$$p(\bar{z} | x_p) = \prod_{i=1}^k \frac{1}{\sqrt{2\pi\sigma_p^2}} \exp\left(-\frac{(z - \mu_p)^2}{2\sigma_p^2}\right) \quad (2)$$

To obtain a full observation model covering over an entire large continuous state space, we should be able to compute likelihoods at locations for which no calibration data is available. As illustrated in Figure 3, we can estimate (μ_p, σ_p^2) , the likelihood distribution parameters at an arbitrary location x_p on an edge by linearly interpolating (μ_i, σ_i^2) and (μ_j, σ_j^2) , the WiFi distribution parameters of its two end

vertices x_i and x_j . This means that if we know the likelihood distributions of any two vertices, the distribution at every location on the edge connecting these vertices can be also estimated by using the linear interpolation.

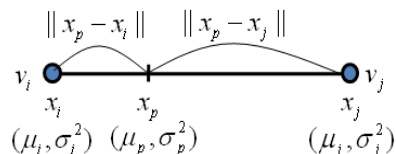


Figure 3. Linear interpolation to compute the likelihood distribution.

The linearly interpolated mean signal strength μ_p and the variance σ_p^2 can be computed by:

$$\mu_p = \frac{\|x_p - x_j\| \cdot \mu_i + \|x_p - x_i\| \cdot \mu_j}{\|x_i - x_j\|} \quad (3)$$

$$\sigma_p^2 = \frac{\|x_p - x_j\| \cdot \sigma_i^2 + \|x_p - x_i\| \cdot \sigma_j^2}{\|x_i - x_j\|} \quad (4)$$

Therefore, by building the WiFi fingerprint map in the form of the annotated graph $G=(V, E)$, where each vertex is annotated with the mean and the variance of the WiFi signal strength distribution at the corresponding location, we can obtain a complete observation model covering over the entire space.

IV. THREE COMPONENT MOTION MODELS

In order to track effectively a WiFi-equipped smartphone user with the particle filter, we need a well-defined motion model of the user as well as a precise observation model. In this paper, we define the motion model $p(x_t|x_{t-1})$ by integrating three component models: motion state transition model $p(m_t|m_{t-1})$, edge transition model $p(e_t|e_{t-1})$, and motion distance model $p(d_t)$.

A. Motion State Transition Model

Motion state transitions $p(m_t|m_{t-1})$ represent the probability of motion state m_t being *moving* or *stopped* given the previous state. Table 1 shows an example of the motion state transition model.

TABLE I. AN EXAMPLE OF THE MOTION STATE TRANSITION MODEL

$p(m_t m_{t-1})$		m_t	
		stopped	moving
m_{t-1}	stopped	0.55	0.45
	moving	0.25	0.75

B. Edge Transition Model

Edge transitions $p(e_t|e_{t-1})$ represent the probability of choosing the next edge when reaching a vertex. They are

stored at each vertex of the graph. An example of the edge transition model is illustrated in Figure 4.

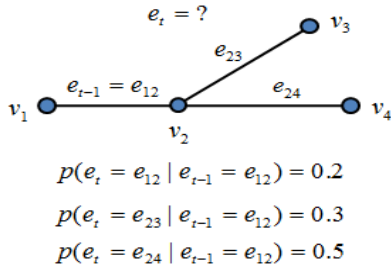


Figure 4. An example of the edge transition model $p(e_t|e_{t-1})$.

C. Motion Distance Model

Motion distance model $p(d)$ represents the probability of going away at distance d from the previous position. The distance d is sampled according to the Gaussian distribution with the mean μ_d and the variance σ_d^2 : $p(d) \sim N(\mu_d, \sigma_d^2)$. The mean μ_d and the variance σ_d^2 are manually set based on typical motion patterns of pedestrians, or learned from a specific user group's training data.

Sampling from the resulting motion model is done as follows. When $x_{t-1} = \langle e_{t-1}, s_{t-1}, d_{t-1}, m_{t-1} \rangle$ is on an edge in the graph, we first sample the motion state m_t with probability proportional to $p(m_t|m_{t-1})$. If $m_t = \text{stopped}$, then x_t is set to be x_{t-1} . Otherwise, if $m_t = \text{moving}$, then we randomly draw a moving distance d according to the Gaussian distribution $N(\mu_d, \sigma_d^2)$. For this distance d , we determine whether the motion along the edge results in a transition over the end vertex of e_{t-1} . If not, then $d_t = d_{t-1} + d$ and $e_t = e_{t-1}$, $s_t = s_{t-1}$. Otherwise, we set $d_t = d_{t-1} + d + |e_{t-1}|$ and the next edge e_t is sampled with probability $p(e_t|e_{t-1})$, and then s_t is set to the starting vertex of the edge e_t .

As a summary, we define the motion model $p(x_t|x_{t-1})$ as follows.

$$\tilde{p}(x_t | x_{t-1}) = p(m_t = \text{moving} | m_{t-1}) \cdot N(d_t; \mu_d, \sigma_d^2) + p(m_t = \text{stopped} | m_{t-1}) \cdot \delta(x_t, x_{t-1}),$$

$$\text{where } \delta(x_t, x_{t-1}) = \begin{cases} 1 & \text{if } x_t = x_{t-1} \\ 0 & \text{if } x_t \neq x_{t-1} \end{cases} \quad (5)$$

$$p(x_t | x_{t-1}) = \begin{cases} p(x_t | x_{t-1}) & \text{if } e_t = e_{t-1} \\ p(e_t | e_{t-1}) \tilde{p}(x_t | x_{t-1}) & \text{if } e_t \neq e_{t-1} \end{cases} \quad (6)$$

V. PARTICLE FILTER FOR INDOOR TRACKING

Particle filters provide a sample-based implementation of general Bayes filters [4,5]. The key idea of particle filters is to represent posterior over the state x_t by sets X_t of M weighted samples: $X_t = \{ \langle x_t^{[m]}, w_t^{[m]} \rangle | m = 1, \dots, M \}$. Here each $x_t^{[m]}$ is a sample state, represented by the tuple $\langle e_t^{[m]},$

$s_t^{[m]}, d_t^{[m]}, m_t^{[m]} \rangle$ in our work, and $w_t^{[m]}$ is an importance weight of the state. Particle filters apply the recursive Bayes filter update to estimate posteriors over the state space. The basic form of the particle filter updates the posterior of the smartphone user's state according to the algorithm summarized in Figure 5. In this algorithm, the probability $p(x_t|x_{t-1})$ is the same one defined as motion model in the Section IV, while the probability $p(z_t|x_t)$ is the same one defined as observation model in the Section III. The input of this algorithm is the particle set X_{t-1} , along with the most recent measurement z_t . The algorithm then first constructs a temporary particle set \hat{X}_t by systematically processing each particle $x_{t-1}^{[m]}$ in the input particle set X_{t-1} . Subsequently, it transforms these particles into the set X_t , which approximates the posterior distribution of the smartphone user's state x_t . Line 4 generates a hypothetical state $x_t^{[m]}$ for time t based on the particle $x_{t-1}^{[m]}$, and this step involves sampling from the distribution $p(x_t|x_{t-1})$. Line 7 calculates for each particle $x_{t-1}^{[m]}$ the so-called importance factor, denoted by $w_t^{[m]}$. The importance is the probability of the measurement z_t under the particle $x_{t-1}^{[m]}$. Line 11 through 15 implemented resampling by drawing with replacement M particles from the temporary set \hat{X}_t .

VI. EXPERIMENTAL EVALUATION

To evaluate the performance of our WiFi localization algorithm, we conduct experiments with a WiFi-equipped Android smartphone in the same indoor environment as shown in Figure 1. The size of the environment is about 52 m x 18 m, and the average length of edges on the graph is about 2.5 m.

1	Algorithm Particle_filter (X_{t-1}, z_t)
2	$\hat{X}_t = X_t = \{ \}$
3	for $m=1$ to M do
4	// Prediction Step
5	Sample $x_t^{[m]}$ with probability $p(x_t x_{t-1})$
6	// Update Step
7	$w_t^{[m]} = p(z_t x_t^{[m]})$
8	$\hat{X}_t = \hat{X}_t + \langle x_t^{[m]}, w_t^{[m]} \rangle$
9	endfor
10	
11	for $m=1$ to M do
12	// Resample Step
13	Draw i with probability $\propto w_t^{[m]}$
14	Add $x_t^{[i]}$ to X_t
15	endfor
16	return X_t

Figure 5. The particle filter algorithm.

A. Accuracy

In this test, we evaluate the accuracy of our localization algorithm by measuring the average error distances during 5 repeated traverses on along 3 different paths in the environment. Additionally, we investigate how the localization accuracy changes as the number of particles increases. Figure 6 shows the result of experiments. We find out that neither there are remarkable differences in error distance among different paths, nor among different particle numbers (200 ~ 400). The average error distance for individual paths is just about 0.94 m ~ 1.2 m. This result makes sure the high accuracy of our WiFi localization algorithm. In our experiments, when the number of particles is 250, we get the best performance.

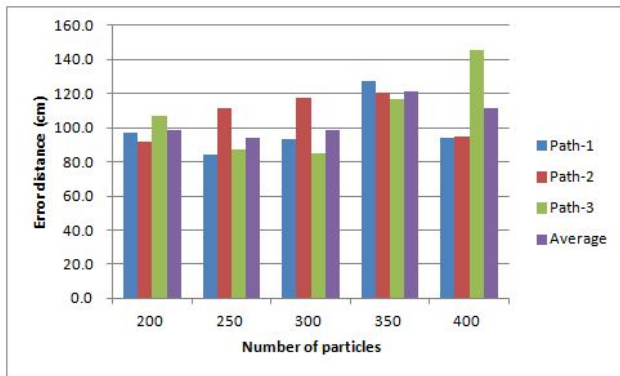


Figure 6. Number of particles vs. localization error.

B. Robustness

In this test, we evaluate the robustness of our WiFi localization algorithm by investigating how the localization accuracy changes as the number of WiFi access points(APs) decreases. Figure 7 shows the result of experiments.

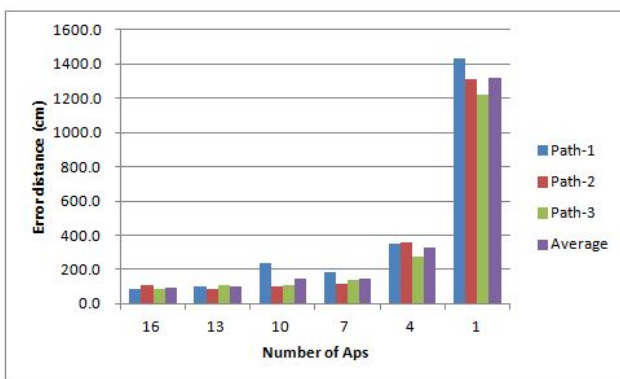


Figure 7. Number of APs vs. localization error.

We find out that until the number of APs decreases from 16 to 7, the average error distance for individual paths remains shorter than 1.5 m. That is, while the number of APs decreases to a certain degree, the localization accuracy does not decrease remarkably. This result makes sure the high robustness of our localization algorithm to meet possible changes of the WiFi environment.

VII. CONCLUSIONS

We proposed a WiFi fingerprint-based localization algorithm for indoor user tracking. To track the position of a smartphone user in a large continuous environment, our algorithm incorporates a graph-based space representation, a linear interpolation-based observation model covering over the entire space, three component motion models into the particle filter framework. Through experiments, we proved the high accuracy and robustness of our localization algorithm. Our WiFi fingerprint-based localization algorithm has the limitation that it needs a large pre-built WiFi fingerprint map of the environment. A lot of effort and time is necessary to construct such a large WiFi fingerprint map. To overcome this limitation, we are now extending our algorithm to adopt some techniques [6,7] from SLAM research communities.

ACKNOWLEDGMENT

This work was supported by the GRR program of Gyeonggi province.

REFERENCES

- [1] J. Biswas and M. Veloso, "WiFi Localization and Navigation for Autonomous Indoor Mobile Robots", Proc. of IEEE International Conference on Robotics and Automation (ICRA), 2010. [retrieved: June, 2012]
- [2] F. Duvallet and A. D. Tews, "WiFi Position Estimation in Industrial Environments Using Gaussian Processes", Proc. of IEEE/RSJ Int. Conf. on Intelligent Robots and Systems (IROS), 2008. [retrieved: June, 2012]
- [3] B. Ferris, D. Hahnel, and D. Fox, "Gaussian Processes for Signal Strength-Based Location Estimation", Proc. of Robotics Science and Systems, 2006. [retrieved: June, 2012]
- [4] F. Gustafsson, F. Gunnarsson, N. Bergman, and U. Forsell, "Particle Filters for Positioning, Navigation, and Tracking", IEEE Transactions on Signal Processing, Vol.50, No.2, pp. 425-437, 2002. [retrieved: June, 2012]
- [5] S. Thrun, W. Burgard, and D. Fox, Probabilistic Robotics, MIT Press, 2005. [retrieved: June, 2012]
- [6] B. Ferris, D. Fox, and N. Lawrence, "WiFi-SLAM Using Gaussian Process Latent Variable Models", Proc. of Int. Joint Conf. on Artificial Intelligence (IJCAI), 2007. [retrieved: June, 2012]
- [7] J. Huang, D. Millman, M. Quigley, D. Stavens, S. Thrun, and A. Aggarwal, "Efficient, Generalized Indoor WiFi GraphSLAM", Proc. of IEEE Int. Conf. on Robotics and Automation (ICRA), 2011. [retrieved: June, 2012]

Speed Up Learning in a Test Feature Classifier Using Overlap Index Lists

Yoshikazu Matsuo
Hokkaido University
Information Science and Technology
Sapporo, Japan
matsuo@ssc.ssi.ist.hokudai.ac.jp

Hidenori Takauji
Muroran Institute of Technology
Robot Arena
Muroran, Japan
uji@mmm.muroran-it.ac.jp

Takamichi Kobayashi
Nippon Steel Corporation
Futtsu, Japan
kobayashi.takamichi@nsc.co.jp

Shun'ichi Kaneko
Hokkaido University
Information Science and Technology
Sapporo, Japan
kaneko@ssi.ist.hokudai.ac.jp

Abstract—This paper presents a novel low cost learning algorithm for a Test Feature Classifier using Overlap Index Lists (OILs). In general, pattern classifiers require a large amount of training data to attain high performance, which is expensive in terms of computation time. Our proposed algorithm uses OILs to efficiently find and check combinations of features starting with lower dimensions and working up-to higher ones. Our algorithm can solve classification problems in real industrial inspection lines with large reductions in computation time.

Keywords-Test Feature Classifier; Overlap Index List; Speed Up Learning; Curse of Dimensionality.

I. INTRODUCTION

Recently, automatic tools for inspecting products have become increasingly important for develop flexible manufacturing lines. Examples can be found in visual inspection in production and precision work that is necessary for quality management. Classification is one of the most important techniques employed in automatic inspection systems. In general, classifiers require a large set of training samples for learning in order to attain a high level of performance. However, the labelling of samples, which makes supervised learning possible for a classifier, is typically, a very time-consuming task.

A current research subject in pattern recognition is reducing the cost of learning. for which several approaches have been proposed. One approach aims at reducing the size of the training data set [1] [2]. Another approach involves streamlining the learning algorithm [3] [4]. In this study, we discuss the latter approach and propose a high speed learning algorithm for a Test Feature Classifier (TFC), which is a pattern classifier. Real inspections of manufacturing-line quality have several problems including the following: 1) some results of labelling for single data are not matched, 2) the reliability of the labels must be validated, and 3) data with low reliability are not useful for learning. Research into

efficient learning methods would contributes to solve these problems.

TFC's learning process involves finding and recording PTFs which are basic sub-features, beginning with a search in lower dimensions. In this paper, we propose the method for efficient learning that exploits the fact that class overlaps in a high dimensional feature space require overlaps in lower dimensions. In addition, we propose an efficient learning technique for adding new features or dimensions. The detail of these methods shows in section 3 and 4. The verification experiments shows in section 5.

II. TEST FEATURE CLASSIFIER

Because the mathematical formalization of TFC has already been provided in [5], we briefly introduce classifiers through qualitative and semantic explanations. TFC consists of learning and discrimination procedures. In the learning procedure, a nonparametric and specific investigation divides the overall feature space into local subspaces of combinatorial features in which class overlap. Combination of features are called "test features", (TFs) or "prime test features", (PTFs), which are irreducible test features. In the discrimination procedure, an unclassified candidate input pattern is checked in each subspace using the corresponding PTF, and then, the pattern is classified according to the average voting scores in sub-spaces. Thus, the classifier aims to achieve high performance with a small training dataset by the partial discriminations contained in sub-spaces. Given a training dataset in which classes do not overlap, a TF is defined as any combination of features that does not classify every pattern with the selected features alone, that is, it satisfies the condition of having non-overlapping classes. In general, smaller combinations of features may allow class overlaps, but they are advantageous form the perspective of low-cost computing. Because it is provable that any combination of features that includes a TF is itself a TF,

Table I
EXAMPLE OF TWO CLASSES PROBLEM.

		f_1	f_2	f_3	f_4
C_1	$1x_1$	2	5	9	7
	$1x_2$	5	6	10	5
	$1x_3$	4	7	7	6
	$1x_4$	5	8	8	9
	$1x_5$	3	9	7	6
C_2	$2x_1$	5	8	6	1
	$2x_2$	7	9	2	2
	$2x_3$	3	10	4	5
	$2x_4$	6	7	2	6
	$2x_5$	5	4	1	5

we should choose irreducible TFs, or PTFs, for discrimination. In [6], an efficient and effective learning method for successively adding training data by using weights for PTFs was proposed.

III. HIGH-SPEED LEARNING ALGORITHM USING OVERLAP INDEX LISTS

TFC's learning procedure involves identifying enough TFs so that the non-overlap condition is satisfied. In our proposed algorithm, the learning procedure finds NTFs, which are sub-spaces that have data with overlapping classes. The learning procedure begins by searching for TFs in low dimensional sub-spaces and adding feature dimensions. Data with overlapping classes in higher-dimensional sub-spaces will be overlapped in each lower dimensional subspace that is contained in a higher dimensional subspace. Therefore, we use Overlap Index Lists (OILs) to record classification overlaps in order to circumvent checking data that are already known to satisfy the non-overlap condition. In this algorithm, additional checking is necessary in lower dimensional sub-spaces where few data overlaps occur, and this checking provides additional overhead for the algorithm. We will briefly discuss the computational complexity of our high-speed learning algorithm using OILs.

A. Creating OILs for Single Feature Dimensions

Table I shows an example of a two class problem. It has a dataset with five data elements $1x_1, 1x_2, \dots, 2x_5$ in each class and four independent features f_1, f_2, f_3 and f_4 . The left subscripted letters indicate the class the elements belong to, whereas the right subscripted letters are indices. We will describe our high-speed learning algorithm by tracing the procedures that search PTFs. The first step of the algorithm is create OILs for one-dimensional features. In the case of f_1 , $1x_2, 1x_4, 2x_1$ and $2x_5$ as well as $1x_5$ and $2x_3$ constitute an interclass overlap. Thus, feature f_1 is an NTF, and the index information below is added to the OIL $L(f_1)$.

$$\begin{aligned} L(f_1) &= \{i_1, i_2\} \\ i_1 &= \{\{2, 4\}, \{1, 5\}\} \\ i_2 &= \{\{5\}, \{3\}\} \end{aligned}$$

The set i_1 shows the interclass overlap consisting of $1x_2, 1x_4, 2x_1$, and $2x_5$. The set $\{2, 4\}$ represents the indices of $1x_2$ and $1x_4$ in class 1, and the set $\{1, 5\}$ represents the indices of $2x_1$ and $2x_5$ in class 2. The set i_2 shows the overlap involving $1x_5$ and $2x_3$, 5 and 3 represent the indices of $1x_5$ in class 1 and $2x_3$ in class 2, respectively. We create OILs for f_2, f_3 and f_4 in a similar manner, obtaining.

$$\begin{aligned} L(f_2) &= \{i_1, i_2, i_3\} \\ i_1 &= \{\{3\}, \{4\}\} \\ i_2 &= \{\{4\}, \{1\}\} \\ i_3 &= \{\{5\}, \{2\}\} \end{aligned}$$

$$\begin{aligned} L(f_4) &= \{i_1, i_2\} \\ i_1 &= \{\{2\}, \{3, 5\}\} \\ i_2 &= \{\{3, 5\}, \{4\}\} \end{aligned}$$

There is no interclass overlap with respect to f_3 . Thus, f_3 is a TF, for which an OIL is not needed.

B. Updating OILs for Higher Feature Dimensions

In the next step, we search TFs and update the OILs for two dimensions using the OILs for single dimensions. Searching all data for interclass overlaps is necessary while checking for TFs in higher dimensions. Thus, the result of checking for TFs does not depend on the order in which features are added. In the sub-feature f_1f_2 , we must decide whether to add information about features f_1 to the OIL for f_2 or vice versa. To perform a more efficient check, we use the OIL with the smallest number of overlapping combination. The number of data elements that must be searched while checking for a TF is $n_1 \times n_2$, where n_1 and n_2 are the number of data elements in class 1 and class 2, respectively. Assume $s(f_1)$ is the number of data elements that must be searched. It is calculated by multiplying the number of $L(f_1)$'s i_1 and i_2 elements of class 1 by the number of elements of class 2:

$$\begin{aligned} s(f_1) &= (2 \times 2) + (1 \times 1) \\ &= 5 \end{aligned}$$

Similarly, $s(f_2) = (1 \times 1) + (1 \times 1) + (1 \times 1) = 3$. Thus, we choose to update L_2 because $s(f_2) < s(f_1)$. In the case of the feature f_1f_2 , the three pair of data $(1x_3, 2x_4)$, $(1x_4, 2x_1)$, and $(1x_5, 2x_2)$. Table I shows that there is a class overlap with respect to these features in the case of $1x_4$ and $2x_1$. Thus, f_1f_2 is not a TF and the OIL is updated:

$$\begin{aligned} L(f_1f_2) &= \{i_1\} \\ i_1 &= \{\{4\}, \{1\}\} \end{aligned}$$

We then check for TFs among the five sets of features $f_1f_3, f_1f_4, f_2f_3, f_2f_4$, and f_3f_4 . Features f_1f_3, f_2f_3 , and

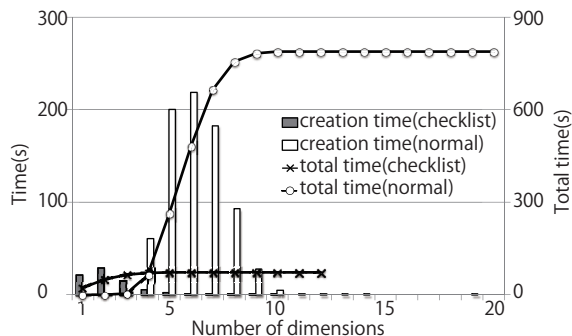


Figure 1. Comparison of time costs for searching PTFs (Inspection Dataset).

f_3f_4 are TFs because f_3 is a TF. Thus, we only need to check the two sets of features f_1f_4 and f_2f_4 . For f_1f_4 , we use f_4 's OIL because $s(f_1) = 5 > s(f_4) = 4$. Checking the data $(1x_2, 2x_3)$, $(1x_2, 2x_5)$, $(1x_3, 2x_4)$ and $(1x_5, 2x_4)$ from the list $L(f_4)$ revealed that there is a class overlap in the case of $1x_2$ and $2x_3$. Thus, f_1f_4 is an NTF and the OIL is updated with $L(f_1f_4) = \{\{2\}, \{5\}\}$. For f_2f_4 , we use f_2 's list because $s(f_2) < s(f_4)$. Similarly, f_2f_4 is an NTF because there is an overlap involving $1x_3$ and $2x_4$. This completes the process of checking for TFs in two dimensions.

Our next step is to check for TFs in three dimensions. The process is almost the same as that for two dimensions. The only feature combination that we need to check is $f_1f_2f_4$. We can use any of the lists $L(f_1f_2)$, $L(f_1f_4)$, or $L(f_2f_4)$ because $s(f_1f_2) = s(f_1f_4) = s(f_2f_4)$. In this case, we will use $L(f_1f_2)$. Based on this list, we only need to check the set $(1x_4, 2x_1)$, where there is no overlap. Thus, the combination $f_1f_2f_4$ is a TF. The process of creating TFC is complete because there are no NTFs in the three dimensional case.

IV. EFFICIENT LEARNING FOR ADDING DIMENSIONS

After defining a set of PTFs, i.e., training the initial TFC with a specified data for which feature dimensions are provided, TFC must be able to up-date or modify itself for augmented feature spaces. We propose an algorithm for modifying a set of PTFs on the basis of new features. When a new feature is presented and new subspaces are added, the original sub-spaces are included in the new set of sub-spaces, but bit vice versa. Thus, the modification procedure will only check for TFs in the new sub-spaces that are not known to be TFs on the basis of previously identified PTFs.

V. EXPERIMENTAL RESULTS

A. High Speed Learning Algorithm using OILs

We used three data sets for our experiments. The first data set is used in a real industrial inspection line (Inspection Dataset). It has two classes and 20 dimensions. Class 1 and

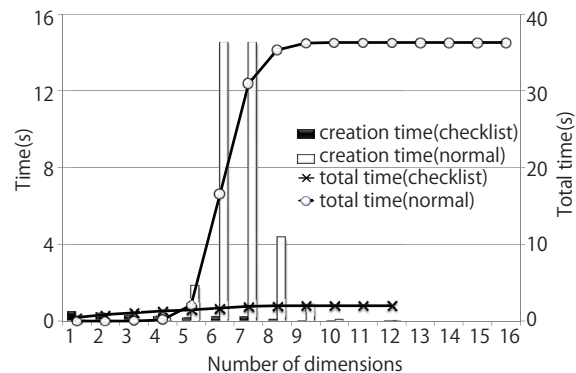


Figure 2. Comparison of time costs for searching for PTFs (Letter Dataset).

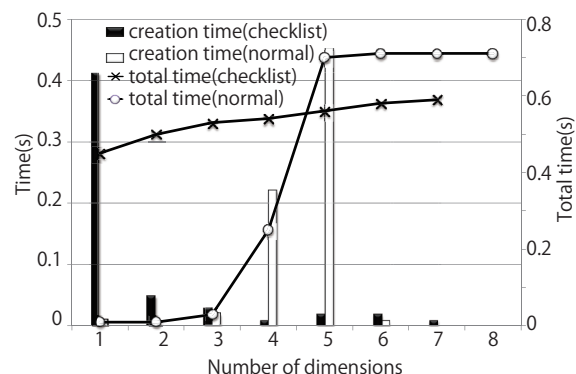


Figure 3. Comparison of time costs for searching for PTFs (Abalone Dataset).

2 contain 2033 and 3799 data elements, respectively. The second dataset is the Letter Data-set from UCI database [7]; it has two classes, class D and class P, and 16 features. Class D and P contain 805 and 803 data elements, respectively. The third dataset is the Abalone Data-set from UCI database [7] that is used for distinguishing between male and female abalones. The male and female classes contain 1528 and 1307, respectively, and there are 8 features. We used these three data sets as training data. The respective times for checking for TFs in each dimension for the three datasets are shown in Fig. 1, 2, and 3. The bar graphs show the time needed for checking for TFs in each dimension, and the line graphs show the total time for each case. These results demonstrate the efficiency of the algorithm for the Inspection and Letter Datasets. However, the method dose not show a clear advantage in the case of the Abalone Dataset because of the overhead for lower dimensions. We believe that one factor may be that the total amount of time needed to create the initial TFC was too small to allow a significant change.

A PTF is defined as a prime TF that dose not include other TFs. In TFC and sTFC, the learning procedure involves searching and recording PTFs. As an example, Fig. 4 shows the number of PTFs and TFs for the Inspection Data-set.

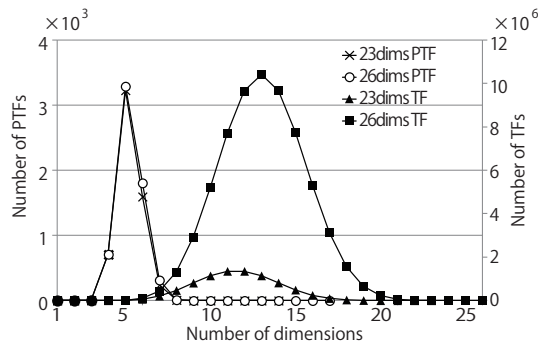


Figure 4. Number of PTFs with increasing number of feature dimensions.

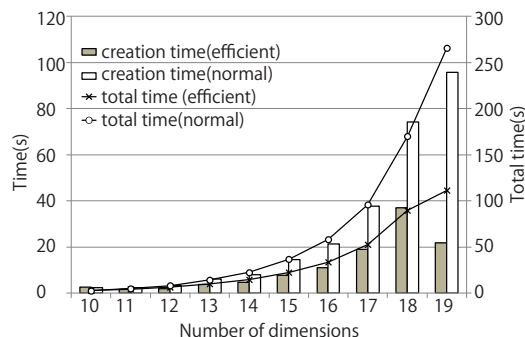


Figure 5. Comparison of time costs for adding feature dimensions (Inspection Dataset).

The figure 4 shows two cases: 23 and 26 features. The highest numbers of dimensions of PTFs in two cases are 8 and 9. We observed similar characteristics for the other two datasets, and we assume that this is a n instance of the curse of dimensionality [8] [9]. In general, higher-dimensional features need sufficient amount of data. Features with very high dimensions can negatively impact training performance. Thus, it is necessary to maintain a certain density when adding features. The highest dimensions that PTFs can have depend on the data set. If we can determine the highest dimensions in advance, TFC can learn more quickly. This will be one of our future research projects.

B. Efficient Learning for Adding Feature Dimensions

In this section, we present the result of an experiment that examined the efficiency of our learning procedure for adding feature dimensions. In the experiment, we used the Inspection Data set with 10 features as training data for the initial learning and up to 19 features were successively added. Fig. 5 shows the times needed for creating TFCs for each dimension. The bar graph shows the time needed for checking for TFs in each dimension, and the line graph shows the total time for creating TFCs in each dimension. The average time reduction for each dimension was approximately 50%.

VI. CONCLUSION AND FUTURE WORK

We have proposed a new method for efficient learning using OILs that can eliminate unnecessary checks and efficient learning method for adding feature dimensions using preliminary information. We compared the performance of our proposed methods with that of conventional TFC methods. Our proposed methods can greatly reduce the time needed for creating TFCs.

We found that the highest number of dimensions in the created PTFs was stable, although the highest number of dimensions depends on the dataset. One topic for our future research will be determining the highest number of dimensions.

ACKNOWLEDGMENTS

We are deeply indebted to associate Professor Tanaka, whose comments and suggestions were invaluable for this research.

REFERENCES

- [1] U. Bhattacharya, S. Vajda, A. Mallick, B.B. Chaudhuri, and A. Belaid.: "On the choice of training set, architecture and combination rule of multiple mlp classifiers for multiresolution recognition of handwritten characters" In IWFHR, pp. 419-424, 2004
- [2] J. Wang, P. Neskovic and L.N. Cooper : "Training Data Selection for Support Vector Machines" LNCS, vol.3610, pp. 554-564, 2005
- [3] D. Thanh-Nghi, N. Van-Hoa and P. Francois: "Speed Up SVM Algorithm for Massive Classification Tasks" Advanced Data Mining and Applications, vol.5139, pp. 147-157, 2008
- [4] J.X. Dong, A. Krzyzak, and C.Y. Suen: "Fast SVM training algorithm with decomposition on very large datasets" IEEE Transaction Pattern Analysis and Machine Intelligence, vol.27, pp. 603-618, 2005.
- [5] V. Lashkia, S. Kaneko and S. Aleshin : "Distance-based Test Feature Classifiers and its Applications" IEICE Trans. Inf. and Syst., vol.E83-D, no.4, pp. 904-913, 2000.
- [6] Y. Sakata, S. Kaneko, Y. Takagi, H. Okuda : "Successive pattern classification based on test feature classifier and its application to defect image classification" Pattern Recognition, vol.38, no.11, pp. 1847-1856, 2005
- [7] P.M. Murphy and D.W. Aha: "UCI Repository of Machine Learning Databases" University of California-Irvine, 1994(anonymous <http://archive.ics.uci.edu/ml/machine-learning-databases/letter-recognition/>) [retrieved: May, 2012].
- [8] Bellman R.E.: "Adaptive Control Processes" Princeton University Press, Princeton, NJ. 1961
- [9] Brown. M, Bossley.K.M, Mills.D.J, Harris.C.J: "High dimensional neurofuzzy systems: overcoming the curse of dimensionality" International Joint Conference of the Fourth IEEE International Conference on Fuzzy Systems, vol.4, pp. 2139 - 2146, 1995

Towards Cooperative Cognitive Models in Multi-Agent Systems

Jan Charles Lenk^{*}, Rainer Droste[†], Cilli Sobiech[‡], Andreas Lüdtkke[§] and Axel Hahn[¶]

^{*‡§}*Transport Research Division*

OFFIS Institute for Information Technology

Escherweg 2, 26121 Oldenburg, Germany

Email: {lenk, cilli.sobiech, andreas.luedtke}@offis.de

^{†¶}*Department of Computing Science*

University of Oldenburg

26111 Oldenburg, Germany

Email: {rainer.droste, axel.hahn}@uni-oldenburg.de

Abstract—Cognitive models capture the behavior of human agents and allow the assessment of risks by prediction of human performance in simulated hazardous environments. In this paper, a combined approach of bottom-up cognitive modeling and top-down operation process modeling is proposed to facilitate the psychologically plausible modeling of complex operations involving multiple human agents. Hereby, we aim at using process and cognitive models productively in the planning and a priori simulation of concrete scenarios to improve safety in offshore operations. We demonstrate our modeling approach with an exemplary multi agent scenario from the maritime domain and discuss its possible application in an operation planning tool aimed at domain experts.

Keywords-Cognitive Modeling; Multi-Agent System; Simulation of human behavior

I. INTRODUCTION

Cognitive modeling aims at creating models of cognitive processes of individual human agents. A common approach is to define a cognitive model as a set of production rules, which implement human behavioral procedures, enabling it to react on changes and manipulate states in its environment. Among the prime benefits of cognitive modeling are executable models which capture the behavior of a human agent interacting with a simulation environment. For instance, cognitive models hereby allow risk assessment by prediction of human performance in concrete simulated hazardous situations.

Many real-life situations demand complex interaction between multiple human actors. Accordingly, also the simulation of such situations requires an integration of multiple simulated human agents and their cognitive processes. Whereas the interaction between agents can be represented as Multi-Agent Systems (MASs), cognitive modeling is so far limited to MAS scenarios from domains where interaction is carried out in a highly compulsory manner, e.g., aeronautics, where aircraft crews have to follow precise procedures prescribed by international aviation laws. This is not the case in other domains such as the offshore wind industry, where personnel also follow procedures, but cooperate in a less formalized way and rely on generic guidelines. In

this paper, we combine bottom-up cognitive modeling with top-down operation process modeling. Dynamic properties of MAS scenarios may be described conveniently with operation process models. While these can specify activities and inter-agent communication for a successful cooperative solution of the scenario, they do not state how the individual human agent solves its tasks and thus cannot be employed within simulations in the same ways as executable cognitive models.

Using operation process models for the specification of inter-agent cooperation and Hierarchical Task Analysis for normative individual behavior, we introduce a modeling paradigm as a combination of high-level modeling languages for cooperative cognitive models embedded in multi-agent scenarios. The process information is derived from expert knowledge, while human behavior is extracted from training manuals and experiments. The exemplary scenario from the maritime domain in this paper demonstrates the combination of the two different modeling languages and their future implementation in a human factors tool for domain experts.

We shall first provide an introduction to cognitive architectures in Section II, then to our scenario and modeling languages in Section III, and finally, present the mappings between these languages and exemplary conforming cognitive models in Section IV.

II. RELATED WORK

A cognitive architecture is itself a model of the human mind, as well as its sensors and actuators. It provides a framework which imposes constraints on the modeler to prevent unrealistic models of human cognitive processes [1]. The most prominent of the cognitive architectures is ACT-R (Adaptive Control of Thought-Rational) [2], yet other more specialized architectures are built upon the same principles, for instance CASCaS (Cognitive Architecture for Safety Critical Task Simulation), which has been applied for pilot and driver modeling [3]. Even if they differ in their purpose and some other aspects, the symbolic elements

of a production system are common to both ACT-R and CASCaS.

Task execution is guided by *goals* and *subgoals* eventually. *Declarative knowledge* is encoded in the form of *memory variables* or *chunks*, whereas *procedural knowledge* is encoded in the form of *production rules*. These consist of a *conditional part* or *left-hand side* (LHS), which includes conditions on goals and other variables and triggers the execution or *firing* of a rule. The *action part* or *right-hand side* (RHS) of a rule is executed and may add new goals to the agenda or manipulate external states.

The environment is represented by *environment variables*, which provide an abstract view on world entities, e.g., concrete human machine interfaces. Thus, the cognitive model is able to perceive and manipulate external world states via the environment variables. The cognitive model is employed within simulations to predict human performance, such as response times and error rates, or cognitive workload and bottlenecks for specific tasks. It also may be used to evaluate interface design with a model-based approach [4].

A. High-Level Languages for Cognitive Modeling

For more complex tasks, cognitive models may easily contain several hundred rules. Maintenance and extension of a complex model is a tedious process. The need for high-level languages and tooling for cognitive modeling is evident, especially if task modeling is carried out by practitioners either in cooperation with an experienced modeler or alone. Several criteria for such a modeling language have been formulated [5]. Examples of high-level languages include the textual Herbal [6] and HTAmap [7], as well as a graphical language and prototypical editor [8].

III. METHODS

In this section, we shall describe the scenario and our modeling languages.

A. Experimental Scenario

As domain for the scenario in this paper serves the offshore construction domain. A 940-ton quadpod has to be moved from the construction vessel to its future location with a heavy lift crane as foundation for a wind turbine. Apart from the banksmen who perform the actual rigging of the load, two further agents also participate in the scenario: the crane operator and the lift supervisor.

A simulation (Fig. 1) of the scenario in a quasi-experimental setting with experienced participants took place in the heavy lift simulator at the MariKom (Maritimes Kompetenzzentrum Wesermarsch) at Elsfleth, Germany. Processes and procedures were derived from the observations made during the simulation.

During the simulation, operator and supervisor communicated over the wireless. First, the crane operator had to exert a gentle pull of just about over 800 tons on the load as

instructed by the lift supervisor. The supervisor stopped the lifting to check the rigging of the load, and gave order to slowly lift the load until the target height was reached. The crane operator had to follow the supervisor’s instructions, as well as to monitor and report the weight of the load as tons on the hook, which were displayed in a mimic diagram in the crane’s cabin. This critical information was hidden from the supervisor and had to be communicated by the operator.

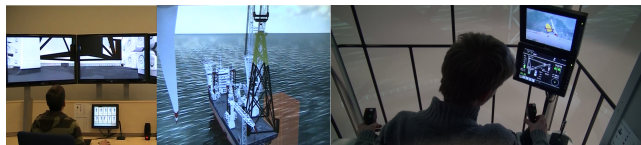


Figure 1. Heavy Lifting simulator scenario. From left to right: Lift Supervisor, Crane and Load, Crane Operator

B. Top-Down Operation Process Modeling

In the business community, suitable concepts and tools for business process specification provide an easily accessible way to identify, systematically describe, and measure processes. For the MAS process model, we have derived the main concepts from the Business Process Modeling Notation (BPMN) language [9]. Thus, we were able to describe and structure the respective processes in order to map different participants representing different interacting agents and their tasks. Fig. 2 shows the cooperative activities of the process step *Load Lifting* involving two **Participants** represented by two **Swimlanes**. The process step starts and ends with **Events**; **Sequence Flows** facilitate a scheduling of the different **Activities** performed by the Participants. Different types of Activities can be further distinguished: Send and Receive Tasks for e.g., reporting weight indicate communication and interaction between different Participants. **Message Flows** describe origin and destination of messages, e.g., reports or commands, in order to synchronize the **Activities** within the process. Resources (e.g., load) are associated to an **Activity** as **Data Objects**.

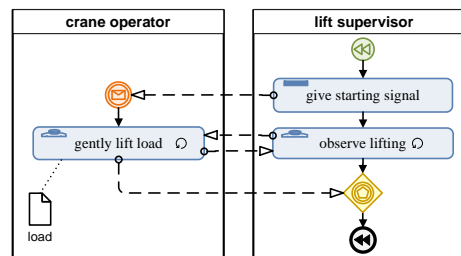


Figure 2. Cooperative activities of the operation process step *Load Lifting*

C. Bottom-Up Procedure Modeling

The Procedure Editor (PED) enables rapid prototyping of cognitive models with a high-level modeling language.

Based on Hierarchical Task Analysis, behavioral models for normative procedures may be defined using a simple graphical notation. Several procedures may be composed to an integrated cognitive model of a human agent.

PED is intended to be a tool to the experienced modeler, as well as to the domain expert with little experience in cognitive modeling. The graphical task definition language provides a high-level abstract view from the concrete procedural and declarative structures needed otherwise for a particular production system. Models may be simulated directly in PED, which shortens the evaluation cycle for the inexperienced modeler. Furthermore, models are validated constantly during the editing process to ensure formal constraints. PED has been used already to model tasks from the automotive and aeronautic domains. The PED language is a subset of CASCaS, although procedures created with PED could also be translated into models for other cognitive architectures. The main elements of the PED language are:

- **Goals:** The control structure of a model consists of goal hierarchy. Goals are executed by being instantiated and expanded onto the goal agenda, a stack-like structure. The last goal on the goal agenda becomes the active goal. Usually, a procedure has an entry goal which starts procedure execution.
- **Rules:** Each regular rule is fired if its top goal is active goal on the goal agenda and if the conditions in its LHS evaluate to true. The conditions are made on **Memory Variables**, which often serve as internal representation of **Environment Variables**. Thus, memory retrievals are necessary to check the condition on the rule.
 - **Percept rules** are also triggered by their top goal, but only if an environment variable is not encoded in a memory variable needed for one of the regular rules below the same top goal.
 - **Reactive rules** can fire at any time if their conditions match, thus they have no top goal. Rather, they listen to changes in the environment variables which are referenced in their LHS.
 - **LHS elements** consist of **Memory Read** items, to retrieve memory variables, and **Conditions** on the variables.
 - **RHS elements** are actions executed when the rule itself is executed. These are **Memory Store**, **Motor**, and **Voice** actions. The first assigns new values to memory variables, the latter two enable direct manipulation of environment variables.

IV. IMPLEMENTATION

The results of our combined top-down and bottom-up modeling approach are the mappings between both languages and their application in the cognitive models for the heavy lift scenario from Section III-A.

A. Mappings between Process and Procedure Languages

Elements from the process language (Section III-B) are mapped onto elements and structure patterns of the PED procedure language (Section III-C). Thus, if a process is specified first, procedures may be validated against the interface defined by the process, i.e., whether control and

message flow, event handling, and activity allocation is implemented in the low-level procedures. The mappings are not yet complete and shall be subject to further modifications and extensions.

- **Activity** \mapsto **Procedure**
Procedures are allocated to Agent Activities according to Swimlane
- **Signal** \mapsto **Environment Variable**
The variable shall represent a concrete property of the system, e.g., an indicator light.
- **Error** \mapsto **Environment Variable**
The variable shall represent an abstract faulty state of the environment.
- **Message** \mapsto **Environment Variable**
The variable shall represent a communication channel, e.g., a wireless channel.
- **Intermediate Catch Event preceding Activity** \mapsto **Reactive Rule in Procedure**
The Reactive Rule is the top most element of the Procedure. Intermediate Catch Events may be used with Messages, Signals, and Errors.
- **Sequence Flow between Activities** \mapsto **Top goal present in second Procedure**
Upon termination of the first, the top goal of the second Procedure is put on the goal agenda.
- **Sequence Flow to Gateway** \mapsto **Top goal in succeeding Procedures**
Control Flow to succeeding Procedures is constrained by conditions.
- **Incoming Message Flow in Activity** \mapsto **Listening Rule Sequence inside Procedure**
The procedure has to listen for a message on an environment variable representing the communication channel.
- **Outgoing Message Flow from Activity** \mapsto **Motor or Voice action in procedure**
There has to be a corresponding action in the procedure.

B. Example Bottom-Up Procedure Models

From the top-down process in Fig. 2, two procedures were selected and modeled bottom-up in PED, applying the mappings in Section IV-A and according to observations made during the simulation: *Gently Lift Load*, executed by the crane operator, and *Observe Lifting* (Fig. 3) for the lift supervisor. The process itself states that the two agents exchange messages and information, but not how and when. This is specified in the structure of the procedures. *Gently Lift Load* is initiated by a message event. For PED elements, this maps to a reactive rule which listens on the wireless channel for the starting command. In the *Observe Lifting* procedure, the supervisor listens in the first loop structure to the weight on the hook in tons as announced by the crane operator and issues a halt command when the load is barely lifted.

If the rigging holds firmly, the supervisor commands the operator to continue lifting until the desired altitude is reached. Here, both procedures terminate for this part of the scenario. Both procedures are executable and may be validated against the process, but also within the simulation when connected directly to the heavy lift simulator.

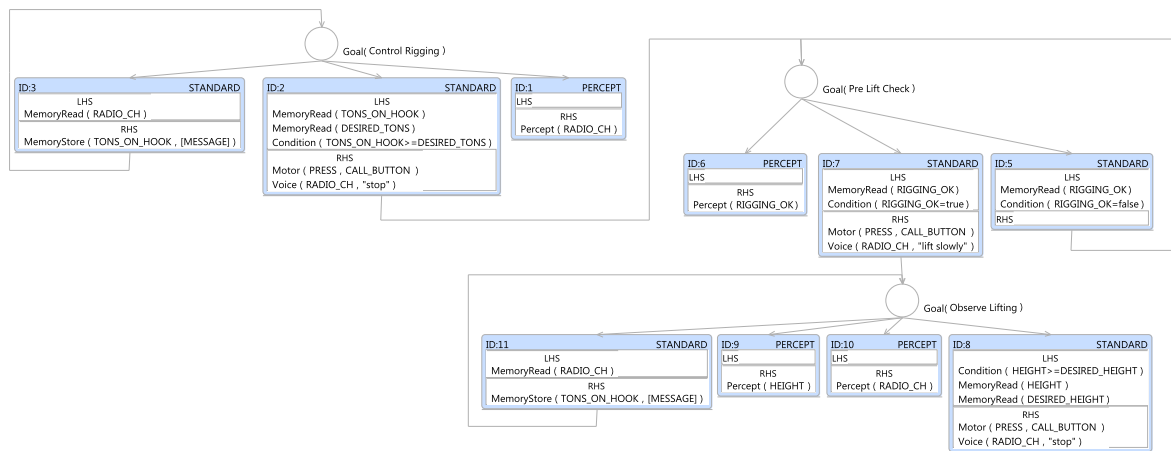


Figure 3. Observe Lifting procedure for the lift supervisor

V. OUTLOOK

Our combined top-down and bottom-up modeling approach enables the fast prototyping of executable cognitive models for complex scenarios involving multiple agents. These can be used to assess cognitive workload for specific, highly cooperative, tasks. Process and procedure models may be transformed into state automata as input for formal model checking with the goal of safety analysis.

We aim at using process and cognitive models productively in the planning and a priori simulation of concrete scenarios to improve safety in offshore operations. For this, we will enhance the Procedure Editor with a process-based MAS editing component. Future domain-specific adaptations of the process language shall also consider physical aspects, such as constraints on perceptual and manipulative capabilities due to agent location. We also consider automatic generation of procedures from processes for our tooling. The domain expert thus shall be enabled to prototype and eventually simulate complex operations in advance for increased efficiency. PED procedures are easily transformed into executable cognitive models for the CASCAs architecture. Thus, safety critical states in an operation may be identified, either by formal analysis, or by prior simulation of the process and its associated procedures within a simulation environment.

ACKNOWLEDGMENT

This modeling approach has been developed within the SOOP (Safe Offshore Operations) project funded by ERDF. The authors would like to thank Prof.-Ing. H. Korte, B. Zerhusen, J. Richter, and I. Ihmels for their assistance during the simulator experiments. We would like to thank MariKom, Elsflath, Germany for project support.

REFERENCES

[1] W. D. Gray, *Integrated Models of Cognitive Systems*. Oxford: Oxford University Press, 2007.

[2] J. R. Anderson, D. Bothell, M. D. Byrne, S. Douglass, C. Lebiere, and Y. Qin, "An integrated theory of the mind," *Psychological Review*, vol. 111, pp. 1036–1060, 2004.

[3] A. Lüdtke, L. Weber, J.-P. Osterloh, and B. Wortelen, "Modeling pilot and driver behavior for human error simulation," in *Digital Human Modeling. Second International Conference, ICDHM 2009, Held as Part of HCI International 2009*, ser. Lecture Notes in Computer Science, V. G. Duffy, Ed., vol. 5620/2009. Springer, 10 2009, pp. 403–412.

[4] F. Ritter and R. Young, "Embodied models as simulated users: Introduction to this special issue on using cognitive models to improve interface design," *International Journal of Human-Computer Studies*, vol. 55, pp. 1–14, 2001.

[5] F. E. Ritter, S. R. Haynes, M. A. Cohen, A. Howes, B. John, B. Best, C. Lebiere, R. M. Jones, J. Crossman, R. L. Lewis, R. St. Amant, S. P. McBride, L. Urbas, S. Leuchter, and A. Vera, "High-level behavior representation languages revisited," in *Proceedings of ICCM - 2006- Seventh International Conference on Cognitive Modeling*, 2006.

[6] M. Cohen, F. E. Ritter, and S. Haynes, "Herbal: A high-level language and development environment for cognitive models in soar," in *Proceedings of the 14th Conference on Behavior Representation in Modeling and Simulation*, 2005.

[7] M. Heinath, "High-level ACT-R modeling based on SGT task models," in *Proceedings of the 9th International Conference of Cognitive Modeling*, 2009.

[8] J. C. Lenk and C. Möbus, "An MDA high-level language implementation for ACT-R," in *Proceedings of KogWis 2010: 10th Biannual Meeting of the German Society for Cognitive Science*, J. Haack, H. Wiese, A. Abraham, and C. Chiarcos, Eds. Universitätsverlag Potsdam, 2010, p. 137.

[9] "Business process model and notation (BPMN)," Object Management Group, 2011, [retrieved: 05, 2012]. [Online]. Available: <http://www.omg.org/spec/BPMN/2.0/>

EEG-based Valence Recognition: What do we Know About the influence of Individual Specificity?

Timo Schuster, Sascha Gruss, Stefanie Rukavina, Steffen Walter & Harald C. Traue

Department for Medical Psychology

University of Ulm

D - 89075 Ulm, Germany

Timo.schuster@uni-ulm.de, Sascha.gruss@uni-ulm.de, Stefanie.rukavina@uni-ulm.de, Steffen.walter@uni-ulm.de, Harald.traue@uni-ulm.de

Abstract — The fact that training classification algorithms in a within-subject design is inferior to training on between subject data is discussed for an electrophysiological data set. Event-related potentials were recorded from 18 subjects, emotionally stimulated by a series of 18 negative, 18 positive and 18 neutral pictures of the International Affective Picture System. In addition to traditional averaging and group comparison of event related potentials, electroencephalographical data have been intra- and inter-individually classified using a Support Vector Machine for emotional conditions. Support vector machine classifications based upon intraindividual data showed significantly higher classification rates [$F(19.498), p < .001$] than global ones. An effect size was calculated ($d = 1.47$) and the origin of this effect is discussed within the context of individual response specificities. This study clearly shows that classification accuracy can be boosted by using individual specific settings.

Keywords - Human-Computer Interaction; Emotion recognition; Affective Computing; EEG; classification;

I. INTRODUCTION

Human life is increasingly influenced by complex information technology. Some years ago it was clear for a given user whether and how he interacted with a technical system. Today and in the future people will interact with various elements of this information technology to a far greater extent and in very heterogeneous ways. Ambient Intelligence for example, will be able to assist users smartly while preserving security and privacy [1]. Also, systems must automatically adapt to different communication modalities and the cognitive, emotional and motivational needs of users. Conceptualization of user-friendly features (usability) must go beyond traditional improvement of dialogs and develop empathic machines [2]. Particularly, methods are required, which allow one to use features and expressions of a user's emotional behavior for functional features and interaction design. Psychobiological parameters of the peripheral (PNS) and central nervous systems (CNS)

are a continuously available source of emotion indicators. Using psychobiological measurements, predictions are more reliable as they show a decreased amount of reactance compared to the assessment via questionnaire or rating.

A. Individual data analysis

The concept of individuality and the associated specificities is nothing new in psychological research. Dealing with these circumstances in technical context means that one can calculate formulas or train classifiers and achieve very good results, but if the application on a single person is tried, classification rates are not ideal. This is especially problematic in an affective context, where things are quite fuzzy. Therefore, we tried to address this phenomenon and discuss the effect.

B. Individual psychobiological classifications

The question is whether there are specific psychobiological emotion patterns that can be assigned to certain emotional states? In past decades, several studies have been done searching for corresponding emotion patterns by means of regression analysis and analysis of variance, and demonstrated differences between subjects (interindividually) [3] [4]. In these psychobiological studies, patterns can be found that differentiate along emotional states: heart-rate variability (HRV) [5], skin conductance level (SCL) [5] or the late positive potential (LPP) [6] [7] for example. The present study shows, when interindividual and within subjects (intraindividually) determined psychobiological patterns are compared, the intraindividual approach shows superior results in classifying emotional states compared to the interindividual (global) one. We statistically tested (by using the effect size) the hypothesis that classification based upon intraindividual variance of the psychobiological reaction [4] shows more accurate results of emotion classification compared to classification based on interindividual variance. The influence of individuality on emotional experience is well known [8] [9], but so far, does

not have a big impact on computer based emotion recognition.

Kim and Andre [5], for instance, argue that emotional experience is a construct of cognitive processes, physiological arousal, motivational tendencies, behavioral reactions and subjective feelings. They further report that physiological activity is not an independent variable, but rather reflects experienced emotional states with consistent correlates. We support this view and additionally believe that variance caused by the subjective character of the emotional experience can be used to achieve a more precise classification. To demonstrate this effect, we used very reliable stimulus material - the International Affective Picture System (IAPS) [10]. This stimulation material is described very well in its ability to induce emotions as well as to evoke CNS activity. Visual stimuli are often used in emotional psychobiology. Many studies have proven the IAPS-stimuli [3] [6] [7] to be a valid tool for controlled induction of emotion.

C. Analyzing central nervous responses

Apart from imaging methods, the electroencephalogram (EEG) is designed for the operationalization of the activity of the central nervous system. EEG is the method of choice for processing emotional stimuli, particularly when processing of emotional information takes place in a rapid temporal state on a scale of seconds [6]. As Schupp and colleagues showed, the time window between 350-750 ms after stimulus onset is profoundly relevant for processing of emotional pleasure. This CNS activity is called late positive potential (LPP) due to its relatively positive change in potential and it's delayed (as far as EEGs go) onset [11]. LPP differentiates CNS processing of negative, neutral and positive visual emotional stimuli in a characteristic manner [6] [7].

D. Aims of this study

The aim of the present study is to determine the affective state post hoc via EEG-analysis by means of mathematical classification algorithms. The influence of individual variances on classification rates is quantified giving their effect size. Support Vector Machines (SVM) are used as classification method. SVMs transform the underlying data set into a higher dimensional space, in which a complex geometric separation plane is then drawn. This separation remains even after the subsequent transformation back to "normal" space [12]. Furthermore, this study intends to demonstrate statistically – with p-level and effect size [12] - that a classification approach, in which the SVM is trained with all data sets of all available subjects is inferior to training with individual data.

E. Article structure

In the following subsections, experimental conditions are described, followed by an overview of the classification procedure. Afterwards, results are presented for a) statistical analysis of preprocessed EEG data and b) comparison of

two classification approaches, optimized using individual- and global fitted parameter settings. Finally, in the discussion part, individual specific influences on classification rates are discussed.

II. METHODS

In this subsection, data assessment and the experimental setup will be described.

A. Subjects

18 (9 female) subjects (age range 18-30) were involved in the study. All subjects were right-handed, healthy, with no psychiatric history and had normal or corrected vision. The study participants received 15 euro remuneration. Subjects were informed about the content and procedure of the study. Following the respective briefing, which was conducted according to the criteria of the Ethics Committee of the Medical Faculty of the University of Ulm, the individual participants signed a written consent form concerning their participation in the study. The present study was classified as ethically unobjectionable (sfb ethics vote no. 245/08).

B. Experimental conditions

The subjects were instructed by the experimenter, about the course of events during the experiment, relevant tasks and the rating procedure using the Self-Assessment Manikin (SAM) [13]. The experiment took place in a darkened room within the Emotion Lab at the University of Ulm (Germany).

Psychobiological parameters were measured using sensors with a MindMedia NeXus-32 amplifier (<http://www.mindmedia.nl>) on 19 EEG and two EOG (horizontal, vertical) channels. EEG was recorded from 19 sites according to the 10/20 system [14] using an Easycap. Ag/AgCl electrodes were placed at FP1, FP2, AFz, F3, F5, F7, F6, Fz, C3, C5, Cz, FCz, P3, P5, Pz, O1, O2, T7 and T8. The linked mastoid (A1, A2) served as a reference. Data were digitized at a sampling rate of 256 Hz. Subjects were instructed to autonomously start the experiment with a mouse click as soon as the researcher left the room. After completing the experiment, subjects were asked to fill out some questionnaires about their personal constitution (NEO-FFI, 16 PF-R).

C. Experimental design

During the experiment, a set of selected images from the International Affective Picture System [10] was presented on a 21" CRT display at a distance of approximately 50 cm from the subject. Eighteen negative, eighteen positive and eighteen neutral pictures (54 in total) were presented in random order. Each image was presented for 6 seconds, followed by a variable jitter between 6 and 12 seconds. This served to prevent expectations. The individual impression of the subject was captured directly after each picture using the SAM [13]. Stimuli were presented using custom written

software [15]. The same software was used for data acquisition.

D. EEG Preprocessing

Because of typical characteristics of an electrophysiological channel, the EEG signal recorded at the skull must be significantly amplified. This makes the analysis of the overall signal more difficult. The amplifier not only amplifies the desired psychobiological signals but also the background noise (mains hum, etc.). EEG signals can easily be corrupted and biased by applying inappropriate preprocessing, which has to be performed carefully for this reason. Therefore, we used the EEGLAB toolbox [16] developed for MATLAB.

First, the recorded data were imported and visualized by EEGLAB. The EEG signal was visually screened for artifacts. Whenever there was an artifact of more than 100mV in amplitude, the entire trial was excluded from further analyses. Subsequently, the EEG-signal was corrected for vertical and horizontal eye movement artifacts as described previously [17]. Only artifact-free trials with congruent subjective and normative categorizations of the pictures were included. Overall, 6.4% of all data were excluded from further investigation due to artifacts. To extract the EEG frequency range relevant for this study, data were band-pass filtered. The lower threshold of the filter was set to 0.1 Hz (high-pass) to eliminate linear trends in signal recording, while an upper threshold of 20 Hz (low-pass) cut off high-frequency noise. Preprocessed data were epoched in a further step – this means, separated by the stimulus category and edited to represent a time window of one second pre-stimulus to 6 seconds post-stimulus. In an averaging procedure data of the individual images of the respective categories were averaged across all subjects. Results of the averaging procedure are shown in Fig. 2. Statistical analysis of EEG data was carried out with SPSS 13. A t-test was used to compare the conditions of positive, negative and neutral conditions. The mean value of 350-750 ms after stimulus onset was used as a basis for statistical analysis.

E. Classification procedure

For classification of different psychobiological affective states we chose SVMs, as they have been proven to be very effective before [18] [19] [20], and to maintain enough flexibility with regard to their main parameter optimization (as discussed below) [21]. The goal of a SVM is to develop a predictive model from a given training data set x , so that respective training sets x_i and their associated labels y_i can be applied to an unlabeled test set in order to assign the test set to a particular class. In this case the SVM [22] aims to find an optimal solution for the following problem: minimize with respect to:

$$w, b, \xi: \frac{1}{2} w^T w + C \sum_{i=1}^m \xi_i \quad (1)$$

So that the following constraint applies:

$$y_i(w^T \phi(x_i) + b) \geq 1 - \xi_i, \forall 1 \leq i \leq m, \xi_i \geq 0 \quad (2)$$

By means of a kernel function :

$$K(x_i, x_j) = \phi(x_i)^T \phi(x_j) \quad (3)$$

the training sets x_i are transformed to a higher dimensional space, in which the SVM finds a separating hyperplane with maximum width. In the present case the Gaussian kernel was used

$$K(x_i, x_j) = \exp(-\gamma \|x_i - x_j\|^2), \gamma > 0 \quad (4)$$

because it is able to handle non-linear dependencies between class labels and input attributes. Furthermore, the Gaussian kernel has the advantage that the complexity of the model is not influenced by too many parameters, but is only limited to two main parameters ($C; \gamma, C > 0$), which enter into the above equation as a penalty parameter for the error term in (1).

For more details, the reader may refer to [12]. In the present study the classification was applied on the LPP using SVM. The time window for the LPP was ranging from 350-750 ms after stimulus onset [6]. Furthermore, the results of [7] served as a guide, as they show that, among others, the data of the EEG channel Fz are particularly effective in separating the three affective states. After the abovementioned preprocessing of EEG data from the Fz channel and subsequent epoching of all data of all subjects within the mentioned time window, every epoch was baseline corrected with a time segment of 350-400 ms after stimulus onset in order to make them more comparable. This step should create a distribution of the values around the baseline. The remaining data resulted in a 89 samples array (350ms measured at 250Hz). Finally the epochs were labeled according to the pleasure information (positive, negative or neutral). Thus, for every subject remained a data set with 54 epochs of 90 values each (89 time samples - corresponds to 89 features + 1 label attribute). No further features were added.

The SVM was developed as a binary classifier, but since this work intends to differentiate three states (negative, positive and neutral), the use of the LIBSVM learner developed by Chang and Lin was utilized, since it extends the principle of the traditional SVM and is able to differentiate multiple classes [23]. To obtain the influence of individuality on affective computing, optimal SVM parameters a systematic grid search was performed for C and γ with concluding leave-one-out cross-validation. Individual pairs of C - and $-\gamma$ values are taken, plugged into the SVM and their classification accuracy is calculated using the leave-one-out cross-validation. After explorative testing of all combinations, the pair with the highest accuracy was finally selected as the optimal parameter set.

When choosing the parameter values, we followed the procedure of Hsu, Chang and Lin. [21], who recommend exponentially growing sequences for C and γ . In the first processing step, all steps of the classification procedure were carried out with the combined data set of all subjects (global), and the corresponding optimal parameter pair (C_{global} and γ_{global}) was determined (see Classification results). In a further processing step, the parameters C_{global} and γ_{global} of the SVM already identified by means of the global sample were applied to the data sets of the individuals (individual). The results are shown in Fig. 2. In an exploratory study, a parameter optimization on an individual level ($C_{individual}$ and $\gamma_{individual}$) was also performed, and the results of this optimization are also shown in Fig. 2. All classification experiments were performed on a laptop using the high-performance data mining software RapidMiner.

F. Calculating effect sizes

Effect sizes [24] were calculated for comparison of individual vs. interindividual classifiers using (5):

$$D = \frac{|\mu_1 - \mu_2|}{\sigma} \quad (5)$$

III. RESULTS

In this subsection, results are shown of a) preprocessed data and b) the classification procedure.

A. EEG Preprocessing

Fig. 1 shows the evolution of the grand averages (grand average across all subjects) of the three conditions.

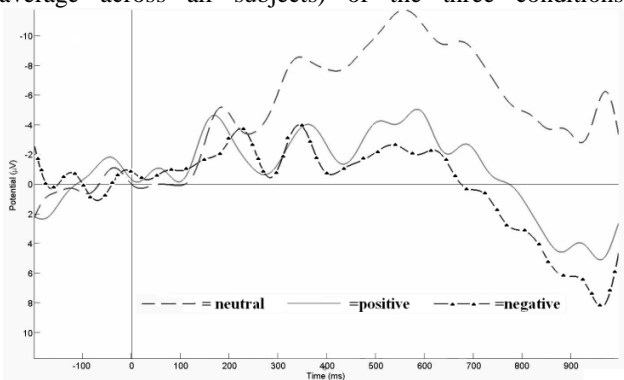


Figure 1. Grand averages of the evoked potentials on Fz for the three different conditions neutral(---), positive(—) and negative(-·-·).

Further statistical analyses illustrated significant differences for the neutral versus negative and neutral versus positive conditions. A t-test for negative versus positive did not show any significant differences in the time frame of interest. Results of the Tukeys test for Fz electrode showed a significant difference for positive vs. neutral [$t(11.4) = 3.59, p < 0.01$] and negative vs. neutral [$t(11.4) =$

$3.25, p < .05$]. No significant differences were found for the conditions negative vs. positive [$t(11.4) = 0.45, p = 0.661$].

B. Classification results

Using the obtained optimal parameters C_{global} ($= 2^{15}$) and γ_{global} ($= 2^{-11}$), the classification across all subjects (global) using leave-one-out cross-validation, resulted in an accuracy (relative number of correctly classified epochs) of 38.77%. The outcome of using global optimal parameters for calculating the detection rate at the individual level is shown in Fig. 2 for the respective subjects. However, if one calculates the optimal parameters specifically for each individual and uses them for classification, classification rate for each individual increases significantly.

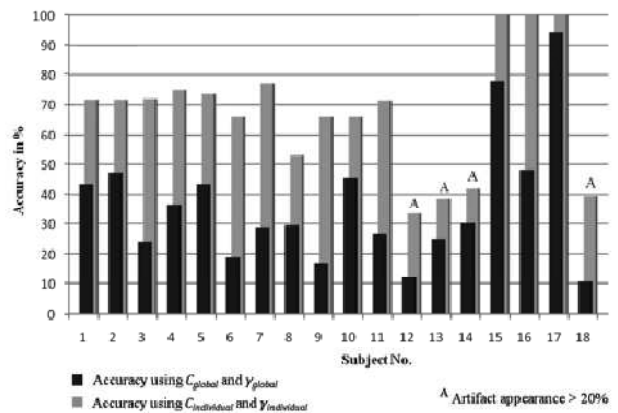


Figure 2. Comparison of classification rates with global and individually determined optimal parameters: classification rates with globally determined optimal parameters applied to each individual (black bars); classification rates with optimal parameters calculated separately for each individual (gray bars) term in traditional approaches. The improvement of the classification demonstrated here is based on the use of intracellular variance of CNS activity.

IV. DISCUSSION

Although statistical analysis was not able to show a difference between the classes positive and negative, classification rates were mostly above chance level.

A. Conclusion of aims and scopes

Objectives of this study were a) to classify emotional categories positive, neutral and negative using EEG signals and b) to demonstrate the influence of individual specificities on affective computing. Classification of the respective categories was performed with SVMs for each individual subject. In contrast to state of the art classification studies [6], this study used only filtered EEG data without any additional feature extraction. We did not use any special feature extraction due to the research question of individual differences and their impact on classification. Using pre-defined settings for detecting emotions (a global approach), some accuracy gets lost compared to use of a special trained classification (individual approach) process. This loss of accuracy may

have several origins. On the one side, there is the accuracy of the classifier itself, which is more specified to unique patterns of an individual when it is trained only on responses of this particular person. On the other side there are the influences of the person itself, of their body and mind. These influences are known as individual specificities [9] and shall be discussed in the following subsection.

Using this knowledge of the origin of the variance caused by individual specificities, a model can be found, which provides more accuracy in the prediction of the emotional state than it would be possible by using further and further improved predefined settings.

B. General discussion

Using global determined optimal parameters for classification, detection rates that are not much higher than the mathematically random chance rates of 33.33% were calculated. If one determines the optimal parameters specifically for each individual, detection rates of over 40% up to 100% are possible (Fig. 2). This improvement is statistically significant [F(19,498), $p < .001$] with an effect size of $d=1.47$. Despite of the obtained individual, optimal parameters, there can be no question of overfitting. It is not, due to the fact that in the majority of data, an influence of variance caused by false true detection can be seen. The exceptions, which show a classification rate of 100% are owed to an extraordinary good physiological response of the subjects.

If one wants to deduce emotions of a person from their psychobiological reactions, it is necessary to keep the individual patterns, with which that person responds to emotional stimuli, in mind. This information would not be needed if all people would react equally to emotional stimuli. Since this is not the case, the individual variance of the psychobiological reaction enters into the error term. The theoretical starting point of this approach goes back to Lacey and colleagues, who were the first to empirically research the concept of response specificity (RS) [25]. The concept of RS is based on the assumption that variance of psychobiological reactions is due to situational, individual and motivational influences [26]. According to Lacey there are two types of individual response specificities (IRS) – intra stressor specificity, which can be observed in moments of stressful stimulation like showing a picture of a snake to a woman who is sensitive for this kind of fear.

The second concept is Symptom-stereotypy, which is characterized by the form of the maximal physiological response to a stimulus. The fact, that these responses are stable within the individual user is of great interest for interpretation of the physiological signal by a technical system. RS and especially IRS have been shown to have an impact on psychobiological empirically by Marwitz and Stemmler [27]. In the context of the results shown in this study, this means that there are response patterns to emotional stimuli, which are user-specific and therefore help to increase classification accuracy within the individual

subject. If it is tried to generalize these findings to a between subject design, the classifier is over-fitted and prediction accuracy is decreasing, which would not be the case, if everyone would be responding in the same way. Using this knowledge, one can think of a sort of calibration technique, which supports the classifier to find a unique setting for a unique user.

Stemmler and Wacker [9] showed in their experiments that individual variance can be found in both the central and the peripheral nervous system. Therefore, the results of this study should not only be of interest for EEG analysis, but also for peripheral channels such as heart rate or skin conductance. But there are other sources of variance, too. Gender for example is known to have an influence on the shape of an ERP signal [28]. And there is even more, age, or the state of physical- and mental-health. All these factors are confounding the signal of one particular person and therefore decrease the accuracy of a classifier system.

As far as we know, the effect of individual variance is well known but the strength of the effect, which is of great interest for technical use, has not been quantified yet. Therefore we calculated the effect size, which is a much more reliable predictor for comparing these conditions than a simple correlation could be [24]. In the related literature, classifications using EEG data are quiet common, Schaaff & Schultz [29] for example were also using SVMs for the classification of EEG-data recorded by an EEG-Headband to recognize emotions for a humanoid robot the recognition-rate of 47,11% was achieved by a separated training and classification for each subject (N=5). If a relatively small group-size is used, the chance of measuring a homogenous group-effect is quite high. To get a more representative sample, we used a larger group consisting of both genders at heterogeneous age. In addition we used an Easy-cap, which is standard in EEG-research and therefore very reliable. Using these setting, we found the effect reported above, which plays an important role in the variance of the psychophysiological signal. This leads to several new questions for further research. According to the approach of individual specificities, one can try to quantify the different variances-sources and separate the error term in an individual manner, which will be more reliable than training on a steadily changing signal. This is economical as well. Due to the change of these individual factors, the training of the classifier will have to be done several times again, if the accuracy should not drop. But the more variance is solved in terms of known individual factors, the less is changing over time and situations.

We suggest that there has to be some sort of calibration, where the variance, caused by individual specificities can be identified and therefore gets solved. In general, it is likely that the classification rate in this study could have been improved by using an increased number of features; for example by adding means, variances or amplitudes and latencies of certain peaks, etc. see [20] for a detailed overview. In contrast to other studies [4] [5] [6] [8], further

optimization of the classification rate was not the objective of this study. These sorts of techniques can be used additionally to explain the variance of the signal. What should be shown in this study is that there is a big effect, which has not been used yet that provides the opportunity to extract a more stable and more precise prediction of the affective state of a user. In future work, we will try to identify factors that explain the individual variance in a stable way. Therefore, a sample has to be chosen, which is big enough and heterogenic enough to vary the most common ways of individual specificities in a controlled paradigm.

ACKNOWLEDGMENT

This research was supported in part by grants from the Transregional Collaborative Research Centre SFB/Transregio 62 "Companion-Technology for Cognitive Technical Systems" funded by the German Research Foundation (DFG). We also like to thank Henrik Kessler for helpful discussions.

REFERENCES

- [1] Gross, T. 2010: Towards a new human-centred computing methodology for cooperative ambient intelligence. *J Ambient Intell Human Comput* 1, 31-42.
- [2] Picard, R.W. 1987: Future affective technology for autism and emotion communication. *Philos Trans R Soc Lond B Biol Sci.* 12,364(1535), 3575-84
- [3] Bradley, M.M., Codispoti, M., Cuthbert, B.N., and P.J. Lang 2001: Emotion and motivation I: defensive and appetitive reactions in picture processing. *Emotion* 1(3), 276-298
- [4] Lang, P.J., Greenwald, M.K., Bradley M.M., and A.O. Hamm 1993: Looking at pictures: affective, facial, visceral, and behavioral reactions. *Psychophysiology* 30(3), 261-273.
- [5] Kim, J. and Andre E. 2008: Emotion Recognition Based on Physiological Changes in Music Listening. *IEEE Transactions on Pattern Analysis and Machine Intelligence.* 30(12), 2067-2083
- [6] Schupp, H.T., Cuthbert B.N., Bradley M.M., Cacioppo J.T., Ito T., and P.J. Lang 2000. Affective picture processing: the late positive potential is modulated by motivational relevance. *Psychophysiology* 37(2), 257-261
- [7] Cuthbert, B.N., Schupp, H.T., Bradley, M.M., Birbaumer, N., and P.J. Lang 2000: Brain potentials in affective picture processing: covariation with autonomic arousal and affective report. *Biological Psychology* 52(2), 95-111
- [8] Fahrenberg, J. and Foerster, F. 1982: Covariation and consistency of activation parameters. *Biol Psychol* 15(3-4), 151-169
- [9] Stemmler, G. and Wacker, J. 2009: Personality, emotion, and individual differences in physiological responses. *Biological Psychology* 84(2), 541-551
- [10] Lang, P.J., Bradley, M.M., and B.N. Cuthbert 2005: International Affective Picture System (IAPS): Affective ratings of pictures and instruction manual. *Technical Report A-6.* University of Florida, Gainesville, FL.
- [11] Schuster T, Gruss S, Kessler H, Scheck A, Hoffmann H, Traue H C (2010) "EEG: pattern classification during emotional picture processing" In *Proceedings of the 3rd International Conference on Pervasive Technologies Related to Assistive Environments (PETRA '10)* Samos, Greece
- [12] Schoellkopf, B., Smola, A.J., Williamson, R.C., and Bartlett, P.L. 2000: New support vector algorithms. *Neural Comput.* 12(5), 1207-45
- [13] Bradley, M.M. and Lang, P.J. 1994: Measuring emotion: the Self-Assessment Manikin and the Semantic Differential. *Journal of Behavior Therapy and Experimental Psychiatry* 25(1), 49-59
- [14] Jasper, H.H. 1958: The ten-twenty electrode system of the International Federation. *Electroencephalography and Clinical Neurophysiology* 10, 371-375
- [15] Scheck, A. 2009: Implementierung eines Systems zur Erfassung psychophysiologischer Vorgänge im Körper und deren Auswertung bezüglich möglicher Zusammenhänge mit emotionalem Erleben *Diploma Thesis University of Ulm, Ulm, Germany.*
- [16] Delorm, A. and Makeig, S. 2004: EEGLAB: an open source toolbox for analysis of single-trial EEG dynamics including independent component analysis. *Journal of Neuroscience Methods* 134(1), 9-21
- [17] Miller, G.A., Gratton, G., and C.M. Yee 1988: Generalized implementation of an eye movement correction procedure. *Psychophysiology* 25, 241-243
- [18] Kapoor, A., Bursleson, W., and R.W. Picard 2007: Automatic prediction of frustration. *International Journal of Human-Computer Studies* 65(8), 724-736
- [19] Shin, Y., Kim, Y., and Kim, E. Y. (2010). Automatic textile image annotation by predicting emotional concepts from visual features. *Image and Vision Computing*, 28(3), 526-537.
- [20] Frantzidis, C.A., Bratsas C., Papadelis, E., Konstantinidis E., Pappas C., and Bamidis, P.D. 2010: Towards emotion aware computing: an integrated approach using multichannel neurophysiological recordings and affective visual stimuli. *IEEE Transactions on Information Technology in Biomedicine* 14(3), 589-597.
- [21] Chang, C.-chung and Lin, C.-jen. (2011). LIBSVM: a library for support vector machines. *ACM Transactions on Intelligent Systems and Technology*, 2(3), 1-39.
- [22] Hsu, C.-wei, Chang, C.-chung, and Lin, C.-jen. (2010). A Practical Guide to Support Vector Classification. *Bioinformatics*, 1(1), 1-16.
- [23] Chang, C.-chung and Lin, C.-jen. (2011). LIBSVM: a library for support vector machines. *ACM Transactions on Intelligent Systems and Technology*, 2(3), 1-39.
- [24] Cohen, J 1992: A power primer. *Psychological Bulletin* 112, 155-159
- [25] Lacey, J.I, Bateman, D.E., and R. Vanlehn 1953: Autonomic response specificity, an experimental study. *Psychosomatic Medicine* (15(1), 8-21.
- [26] Fahrenberg, J., Foerster, F., and F. Wilmers 1995: Is elevated blood pressure level associated with higher cardiovascular responsiveness in laboratory tasks and with response specificity? *Psychophysiology* 4(2), 865-73.
- [27] Marwitz, M. and Stemmler, G. 2010: On the status of individual response specificity. *Psychophysiology* 35(1), 1-15
- [28] Lithari C., Frantzidis C.A., Papadelis C., Vivas Ana B., Klados M.A., Kourtidou-Papadeli C., Pappas C., Ioannides A., and P. D. Bamidis Are females more responsive to emotional stimuli? A neurophysiological study across arousal and valence dimensions. *Brain topography*, Vol. 23, No. 1. (31 March 2010), pp. 27-40
- [29] Schaaff, K. and Schultz, T. (2009). Towards an EEG-based emotion recognizer for humanoid robots. *ROMAN 2009 The 18th IEEE International Symposium on Robot and Human Interactive Communication*, pp. 792-796.

Impact of Stimulus Configuration on Steady State Visual Evoked Potentials (SSVEP) Response

Chi-Hsu Wu

Bioengineering Unit
University of Strathclyde
Glasgow, United Kingdom
e-mail: chihsu.wu@strath.ac.uk

Heba Lakany

Bioengineering Unit
University of Strathclyde
Glasgow, United Kingdom
e-mail: heba.lakany@strath.ac.uk

Abstract— We investigate the impact of configuration of multi-stimuli presented in computer monitor to steady-state visual evoked potential response. The configuration of stimuli is defined by three parameters—the size of stimuli, the separation distance between the stimuli and the layout. Two 4 by 4 checkerboards in twelve configurations were presented to the subjects. 9 subjects participated in this study. Subjects' electroencephalography (EEG) data was off-line analyzed by using Fast Fourier Transform (FFT). The mean classification rates of configuration with bigger size and larger separation distance is higher than those configurations with smaller size and shorter separation distance. These results suggest that the stimulus size is the most important parameter of three, followed by the separation distance and layout.

Keywords- Steady-State Visual Evoked Potential (SSVEP); Brain Computer Interface (BCI); Electroencephalography (EEG).

I. INTRODUCTION

Brain computer interfaces (BCIs) give their users communication and control channels that do not depend on the brain's normal output channels of peripheral nerves and muscles [1]. BCIs allow people with severe motor disabilities to communicate with the environment or control device through an alternative channel, which does not depend on normal motor output of the nervous system [2][3].

BCI requires an input brain signal from the user in order to interpret his or her intent and translate it into a command. BCIs can use invasive or non-invasive methods to access the brain signal. Non-invasive electroencephalography (EEG) based methods are most commonly used due to their properties: ease of use, flexibility, high time resolution, low cost and low risk [4][5]. Several EEG-based BCI paradigms have been successful in conveying EEG signals to control devices [6].

Many brain signals can be recorded with EEG and used as the input of BCIs. One of these is Steady-state-visual-evoked-potential (SSVEP), which some recent studies have shown its advantages of higher accuracy rate, speed, scalability and no/less training required compared to other BCI paradigms [3][7][8].

A practical SSVEP based BCI should enable more than one command, which in turn necessitates the presentation of more than one visual stimulus concurrently. In this study, we

focused on the use of the computer monitor as the visual stimulator, which provides greater flexibility and user friendly features in graphic interface than LED.

Current SSVEP BCI studies focus on the comparison of different stimulators [9][10] and signal classification methods [8][11][12][13][14]. The impact of the unattended target to the response of attended target is rarely discussed.

The aim of this study is to investigate the impact of the properties of multi-stimuli in terms of their size, separation distance and their layout on SSVEP response. The results of this study will help the practical SSVEP based BCI design.

The rest of the paper is organized as follows: Section II presents the setup and protocol of the experiment and a description of the data acquisition method. The results are discussed in Section III. The conclusion is presented in Section IV.

II. METHODS

This section explains the setup and protocol of the experiment.

A. Stimulus configurations and parameters

The visual stimuli used in this study were generated by Matlab® and Psychophysics Toolbox Version 3 (PTB-3) [17]. The functions of PTB can create accurately controlled visual stimuli for the experiment. To evaluate the impact of stimuli configurations experiment, two black and white 4x4 checkerboards were presented to the subject on a CRT or LCD computer monitor. Twelve configurations were tested in the experiment.

A configuration is defined by three parameters,

- (1) Size of stimulus,
- (2) Separation distance between two stimuli and
- (3) Layout of the stimuli.

The details of 12 configurations (C1 to C12) and the parameters are listed in Table I.

In this experiment, three criteria were used to select the stimulation frequencies.

- (1) The selected frequencies can elicit strong SSVEP,
- (2) The selected frequencies cannot be harmonics to each other or have common harmonics under 50Hz and
- (3) The frequency pair should have stable frequency output in the stimulation.

We pair all sub-frequencies of the monitor refresh rate to simulate the experiment and get the frequency output.

TABLE I. PARAMETERS OF 12 CONFIGURATIONS USED IN THE EXPERIMENT

Configuration		C1	C2	C3	C4	C5	C6	C7	C8	C9	C10	C11	C12
SIZE	Big	●	●			●	●			●	●		
	Small			●	●			●	●			●	●
SEPARATION DISTANCE	Close	●		●		●		●		●		●	
	Far		●		●		●		●		●		●
LAYOUT	Horizontal	●	●	●	●								
	Vertical					●	●	●	●				
	Diagonal									●	●	●	●

Following these criteria, the simulation results and 75Hz of the refresh rate of the monitor (CRT and LCD), 15Hz and 12.5Hz were used in the experiment.

B. Data Acquisition

A 128 channels EEG cap was placed at each subject’s scalp. The middle line of the cap is lined up with nasion andinion. To eliminate the dead skin, EEG abrasive skin prepping gel (Nuprep Gel) was applied to the electrode sites first. To reduce the impedance between scalp and electrode, EEG conductive gel (Electro-Gel) was applied to the same sites. The impedance was kept under 5kΩ. The EEG acquisition hardware and software were SynAmps2 (amplifier) and NeuroScan 4.5 (recording software).

The most significant SSVEP can be recorded at the channels over the visual cortex. 11 channels over visual cortex were selected as signal channels while Cz was chosen as the ground and Fz was chosen as the reference channel. The channel selection is shown in Figure 1. The electrode is AgCl type. The EEG sampling frequency was 2,000 Hz.

C. Protocol

Two 4x4 checkerboards were presented to each subject on a CRT or a LCD screen. Both CRT and LCD monitors can elicit SSVEP responses [9]. There was no significant difference in SSVEP response between these two stimulators. CRT is widely used in BCI studies. However, due to the popularity of LCD, an LCD monitor was also used in this study.

Each configuration had 30-45 trials. Each trial had three phases, fixation phase, stimulation phase and resting phase. During the fixation phase, there is a white cross appearing in the centre of the monitor. During the stimulation phase, two 4x4 checkerboards flickering in different frequencies were presented to the subject. In the resting phase, the screen is blank. The information of last stimulation phase (e.g., the time of the stimulation, mean frequency output of the stimuli, etc.) is displayed on the left upper corner. Three phases are illustrated in Figure 2.

One of the challenges to use monitor as visual stimulator is that the frequencies of the stimuli are restricted to the monitor refresh rate. The stimulating frequencies have to be the sub-frequencies of the monitor refresh rate. This limits the selections of the frequencies.

To avoid visual adaptation, fixation phase takes 2 or 3 seconds randomly. Resting phase takes 7 or 8 seconds randomly. The stimulation phase takes 7 seconds. The sequence of the configuration shown to subject was in fixed order (C1 to C12) for the first 3 subjects but become random in the rest configuration evaluation experiment.

Subjects were asked to attend the left stimulus in horizontal layout, upper stimulus in vertical layout and left upper stimulus in diagonal layout. Each configuration took up to 9 minutes (for 30 trials). There is a break between each configuration.

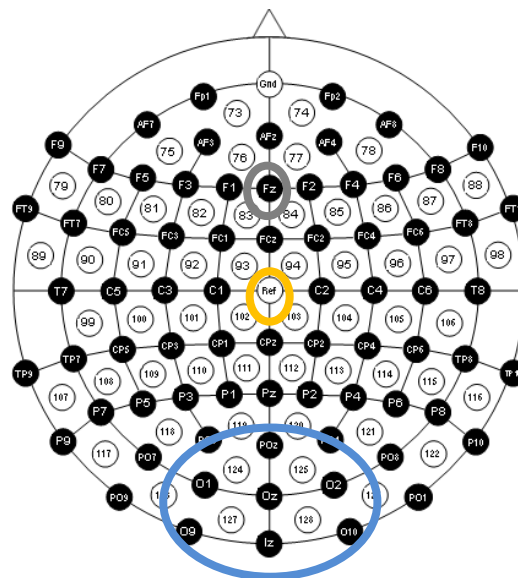


Figure 1. Channel selections. 11 channels inside blue circle were selected as signal channels. Cz (yellow circle) was selected as ground and Fz (grey circle) was selected as reference circle. Channel location is from [18].

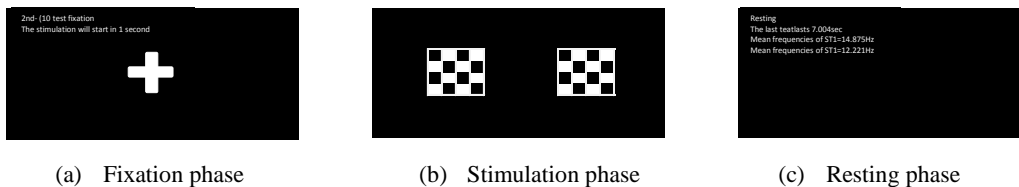


Figure 2. Three phases in a stimulation trial. (a): fixation phase: a white cross appeared in the centre of the screen (2 or 3 seconds). (b): stimulation phase: two 4x4 checkerboards were presented (7 seconds). (c): Resting phase: blank screen showed information on left upper corner of the screen (7 or 8 seconds).

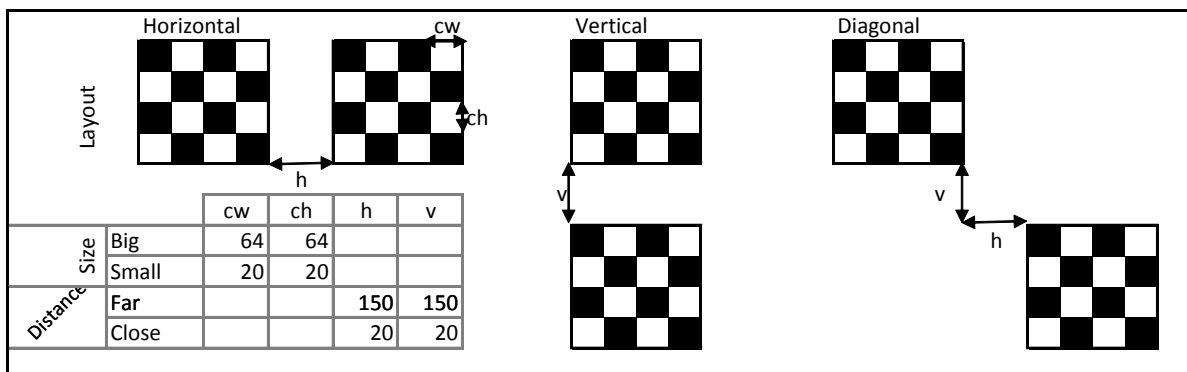


Figure 3. Illustration of the layout and the values of the parameters of configuration

SSVEP based BCI interprets users’ intents by analyzing SSVEP response. In order to achieve high accuracy, time length is an important factor. A SSVEP study [15] showed that it requires 2.8 seconds to achieve an average 95% accuracy. Some of the signal classification methods, e.g., FFT requires a longer time window to prevent turbulence caused by spontaneous EEG [16]. The stimulation phase of this study took 7 seconds as we also investigated the impact of time length.

The values of configuration of stimuli are illustrated in Figure 3. The unit of the parameters (e.g., cell width (*cw*), cell height (*ch*), horizontal distance (*h*) and vertical distance (*v*)) is pixel.

The resolutions of CRT and LCD used in the experiment are 1600x1200 and 1440x900 respectively. Figure 3 shows the setup of CRT. The setup of LCD was slightly different, but the physical visual of size and layout on the screen were similar.

III. DATA ANALYSIS AND RESULT

FFT was applied to the time domain EEG signal. FFT was performed on a single trial/epoch of EEG with different epoch time varying from 1 second to 5 seconds. After FFT was performed, the power of the frequency spectrum at all SSVEP response frequencies will be extracted. The harmonics of SSVEP response frequency, which range from 5Hz to 50Hz were also considered.

Four types of signal combinations used in the analysis: (1) Fundamental: Using the fundamental frequency response only. (2) Fundamental + Sub: Using a combination of the fundamental frequency and the sub-harmonics, which is no

lower than 5 Hz. (3) Fundamental + High: Using a combination of the fundamental frequency and the higher harmonics, which is no higher than 50Hz. (4) Fundamental + all: Using a combination of the fundamental frequency and all harmonics between 5 to 50 Hz.

Figure 4 is the average classification rates of all subjects in different configurations. Figure 4 is based on 3 seconds epoch time. Figure 4 shows that, in general, the configurations of big size of stimuli have the higher classification rates than those configurations of smaller size stimuli. The configurations of large separation distance also have higher classification rates than close separation distance if the other two parameters are the same, except C3 and C4. Horizontal layout has higher average classification rates than vertical and diagonal layouts. The results of 4 and 5 second epoch are similar.

A one-way ANOVA analysis was performed to evaluate the effect of configurations to classification rates based on an epoch time of 3 seconds. The classification rates were further divided into four groups. The first three groups are the classification rates of C6, C2 and C1, the configurations, which resulted in the top three highest classification rates, the fourth group is the average classification rates of the remaining 9 configurations, CR. (C2, CR), (C6, CR) and (C1, CR) are compared. The values of *F*(1, 6) are 27.78, 23.98 and 22.38 respectively with *p* values 0.0019, 0.0027 and 0.0032. The differences of classification rates between C2, C6, C1 and the rest configurations are significant.

Figure 5 illustrates the classification rates of one subject in different configurations using different signal combinations. Figure 5 is the result of a 4-second epoch.

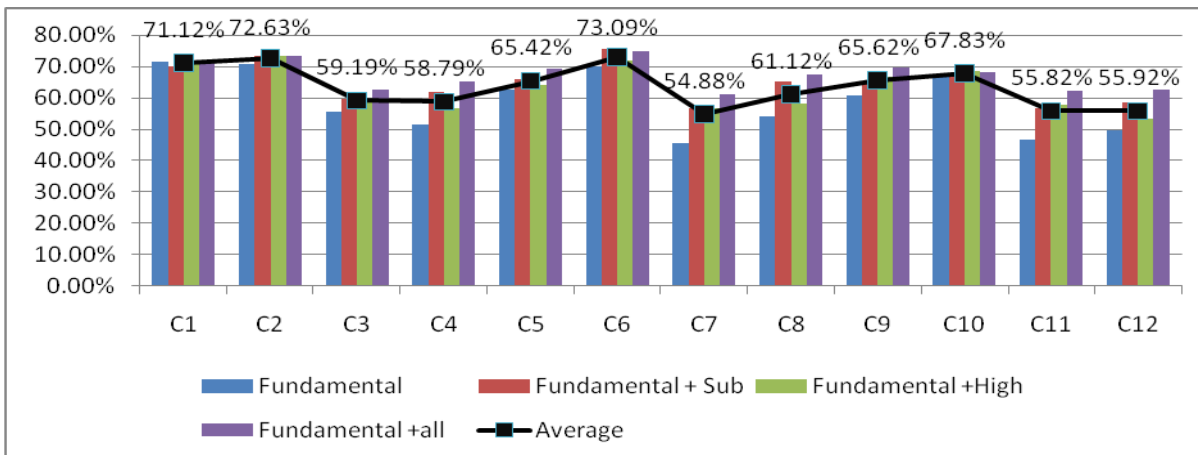


Figure 4. Average classification rates of all subjects of different signal combinations in different configurations. This figure is based on 3 seconds epoch.

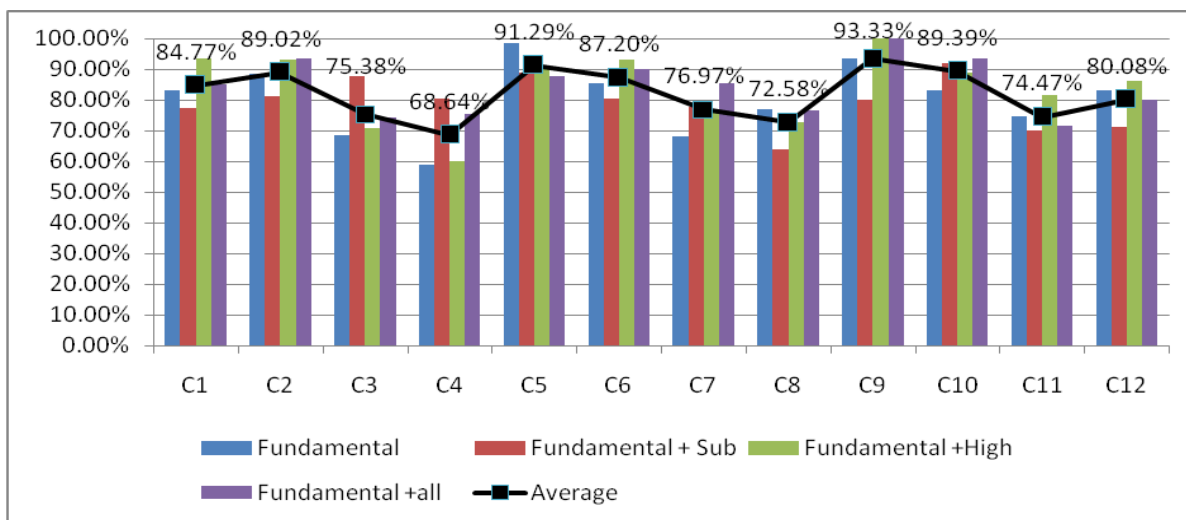


Figure 5. Classification rates of one subject of different signal combinations in different configurations.

Generally speaking, the configurations of a big size stimulus can yield a higher classification rate than the small size regardless of the layouts and separation distances. Large separation distance has higher rates if the size of stimulus is the same and layout is the same. The results from other subjects show a similar trend.

In order to understand the configuration better, four possible outcomes are further defined as following.

(1) True positive. This is when the response of the selection is the highest of the responses, which exceed the threshold. The number of true positives is referred to as a_{11} .

(2) Aliasing. This is when both responses at the stimulating frequencies exceed the threshold but the response at un-attended target is stronger than the one selected. The Aliasing is referred to as a_{12} .

(3) False positive. Only the response at the un-attended exceeds the threshold. The number of false positive is referred to as a_{21} .

(4) No response. None of the responses exceed the threshold. No response is referred to as a_{22} .

These four parameters provide another perspective view on the impact of the configurations on elicited SSVEP. The same elements of the matrix of each subject using the same signal combinations were added. a_{11} is used to examine the number of proper SSVEP responses; we use a_{12} to examine the number of aliasing responses caused by un-attended frequency; use a_{21} to examine the number of false positive and use a_{22} to examine the number of no SSVEP responses.

Table II shows the grand total of true positive, aliasing, false positive and no response of all subjects of all different epoch time (1 to 5 seconds).

It is clearly seen from Table II that C2 and C6 have the overall best performance in all configurations with more true positive and less aliasing, false positive and no response.

Table III is one subject's analysis result in all configurations with different signal combinations. This table is based on an epoch time of 4 seconds.

TABLE II. GRAND TOTAL OF TRUE POSITIVE, ALIASING, FALSE POSITIVE AND NO RESPONSE OF ALL SUBJECTS OF ALL DIFFERENT EPOCH TIME (1 TO 5 SECONDS).

overall	Fundamental				Fundamental + sub				Fundamental + high				Fundamental + all			
	a_{11}	a_{12}	a_{21}	a_{22}	a_{11}	a_{12}	a_{21}	a_{22}	a_{11}	a_{12}	a_{21}	a_{22}	a_{11}	a_{12}	a_{21}	a_{22}
C1	7,520	3,748	602	505	7,741	4,289	261	84	7,976	3,557	393	449	8,071	4,011	228	65
C2	8,048	3,777	459	421	8,255	4,095	199	156	8,386	3,715	368	236	8,428	4,091	139	47
C3	6,692	4,961	820	727	7,293	5,533	214	160	7,057	4,768	819	556	7,369	5,445	211	175
C4	6,009	4,762	1,272	662	7,447	4,816	239	203	6,540	4,588	949	628	7,592	4,751	236	126
C5	7,116	4,518	616	455	7,663	4,645	248	149	7,311	4,395	486	513	7,863	4,490	206	146
C6	7,597	4,038	573	497	8,134	4,238	197	136	8,340	3,519	429	417	8,482	3,930	216	77
C7	5,236	5,071	1,451	947	6,390	5,603	481	231	5,860	4,752	1,140	953	6,751	5,313	390	251
C8	5,704	4,557	1,347	1,097	7,087	4,767	524	327	6,117	4,424	1,089	1,075	7,292	4,530	511	372
C9	6,886	4,153	807	859	7,214	4,720	392	379	7,170	3,920	532	1,083	7,666	4,252	399	388
C10	7,445	3,602	614	1,044	7,551	4,243	464	447	7,464	3,643	513	1,085	7,746	3,979	359	621
C11	5,319	4,676	1,314	1,396	6,499	4,935	622	649	5,843	4,555	902	1,405	6,845	4,709	401	750
C12	5,232	4,396	1,437	1,640	6,106	4,954	797	848	5,689	4,337	1,075	1,604	6,534	4,679	643	849

TABLE III. NO OF TRUE POSITIVE, ALIASING, FALSE POSITIVE AND NO RESPONSE OF ONE SUBJECT IN DIFFERENT CONFIGURATION

	Fundamental				Fundamental + sub				Fundamental + high				Fundamental + all			
	a_{11}	a_{12}	a_{21}	a_{22}	a_{11}	a_{12}	a_{21}	a_{22}	a_{11}	a_{12}	a_{21}	a_{22}	a_{11}	a_{12}	a_{21}	a_{22}
C1	233	64	33	0	242	88	0	0	315	15	0	0	286	44	0	0
C2	275	55	0	0	286	44	0	0	297	33	0	0	286	44	0	0
C3	214	77	11	28	231	86	13	0	281	38	0	11	253	77	0	0
C4	176	117	26	11	220	99	11	0	252	78	0	0	242	88	0	0
C5	231	66	33	0	168	129	33	0	242	78	10	0	206	124	0	0
C6	220	88	22	0	187	143	0	0	280	50	0	0	220	110	0	0
C7	111	163	34	22	121	165	44	0	185	145	0	0	176	154	0	0
C8	222	97	11	0	207	103	20	0	275	55	0	0	275	55	0	0
C9	132	112	53	33	111	179	29	11	209	90	9	22	184	124	22	0
C10	148	87	45	50	133	142	44	11	231	77	22	0	206	124	0	0
C11	90	44	99	97	143	102	74	11	255	64	11	0	224	84	22	0
C12	154	54	89	33	154	109	67	0	231	77	22	0	202	115	13	0

This table indicates that the configurations of big size stimulus and large separation distance can produce more true positive while reduces the number of aliasing, false positive and no response, e.g., C2. While the configurations of small size stimulus, has less true positive and produce more aliasing and/or false positive and/or no response, e.g., C7, C11.

IV. CONCLUSION

From the analyzed in last session, it is clear that the size of stimulus plays the most important role in the configuration parameters, followed by separation distance and followed by the layout. We conclude that the configurations with big stimulus size, like C1, C2 and C6 can result in better SSVEP response with less aliasing.

ACKNOWLEDGMENT

The authors would like to thank all the subjects who participated in the experiment.

REFERENCES

- [1] Jonathan R. Wolpaw, Niels Birbaumer, William J. Heetderks, Dennis J. McFarland, P. Hunter Peckham, Gerwin Schalk, Emanuel Donchin, Louis A. Quatrano, Charles J. Robinson, and Theresa M. Vaughan, "Brain-Computer Interface technology: A review of the first international meeting," IEEE Transactions on Rehabilitation Engineering. vol. 8, no. 2, pp. 164-173, 2000.
- [2] Pfurtscheller, Gert, and Scherer, Reinhold, "Brain-computer interfaces used for virtual reality control," Venice, Italy, ICABB, 2010.
- [3] Ivan Volosyak, "SSVEP-based Bremen-BCI interface—boosting information transfer rates," Journal of Neural Engineering. vol. 8, no. 3, doi:10.1088/1741-2560/8/3/036020, 2011.
- [4] Jonathan R. Wolpaw, Niels Birbaumer, Dennis J. McFarland, Gert Pfurtschellere, and Theresa M. Vaughana, "Brain-computer interfaces for communication and control," Clinical Neurophysiology. vol. 113, no. 6, pp. 767-791, 2002.

- [5] Ivan Volosyak, Diana Valbuena, Tatsiana Malechka, Jan Peuscher, and Axel Gräser, "Brain-computer interface using water-based electrodes," *Journal of Neural Engineering*. vol. 7, no. 6, doi:10.1088/1741-2560/7/6/066007, 2010.
- [6] Ou Bai, Peter Lin, Sherry Vorbach, Mary Kay Floeter, Noriaki Hattori, and Mark Hallett, "A high performance sensorimotor beta rhythm-based brain-computer interface associated with human natural motor behaviour," *Journal of Neural Engineering*. vol. 5, no. 1, pp. 24–35, 2007.
- [7] Pablo Martinez, Hovagim Bakardjian, and Andrzej Cichocki, "Fully online multicommand brain-computer interface with visual neurofeedback using SSVEP paradigm," *Computational Intelligence and Neuroscience*. vol. 2007, doi:10.1155/2007/94561, 2007.
- [8] An Luo, and Thomas J Sullivan, "A user-friendly SSVEP-based brain-computer interface using a time-domain classifier," *Journal of Neural Engineering*. vol. 7, no. 2, doi: 10.1088/1741-2560/7/2/026010, 2010.
- [9] Zhenghua Wu, Yongxiu Lai, Yang Xia, Dan Wu, and Dezhong Yao, "Stimulator selection in SSVEP-based BCI," *Medical Engineering & Physics*, vol. 30, issue 8, pp. 1079–1088, October 2008.
- [10] Danhua Zhu, Jordi Bieger, Gary Garcia Molina, and Ronald M. Aarts, "A Survey of Stimulation Methods Used in SSVEP-Based BCIs," *Computational Intelligence and Neuroscience*, vol. 2010, doi:10.1155/2010/702357, 2010.
- [11] Zhonglin Lin, Changshui Zhang, Wei Wu, and Xiaorong Gao, "Frequency recognition based on canonical correlation analysis for SSVEP-based BCIs," *IEEE Transactions on Biomedical Engineering*, vol. 54, no. 6, pp. 1172-1176, 2007.
- [12] Cheng M, Gao S, Gao S, and Xu D, "Design and implementation of a brain-computer interface with high transfer rates," *IEEE Transactions on Biomedical Engineering*. vol. 49, issue 10, pp. 181–186, 2002.
- [13] Ola Friman, Ivan Volosyak, and Axel Gräser, "Multiple channel detection of steady-state visual evoked potentials for brain-computer interfaces," *IEEE Transactions on Biomedical Engineering*. vol. 54, no. 4, pp. 742-750, 2007.
- [14] Guangyu Bin, Xiaorong Gao, Zheng Yan, Bo Hong and Shangkai Gao, "An online multi-channel SSVEP-based brain-computer interface using a canonical correlation analysis method," *Journal of Neural Engineering*. vol. 6, no. 4, doi: 10.1088/1741-2560/6/4/046002, 2009.
- [15] I. Volosyak, H. Cecotti, and A. Gräser, "Steady-State Visual Evoked Potential Response - Impact of the Time Segment Length," 7th IASTED International Conference on Biomedical Engineering, 2010.
- [16] Zhenghua Wu and Dezhong Yao, "Frequency detection with stability coefficient for steady-state visual evoked potential (SSVEP)-based BCIs," *Journal of Neural Engineering*. doi:10.1088/1741-2560/5/1/004, 2008
- [17] <http://www.psychtoolbox.org>, Brainard, 1997, Pelli, 1997.
- [18] <http://www.easycap.de>.

A Basic Study for Grasping Movement on Cognitive Task

Shunji Shimizu / Tokyo University of Science, Suwa
Department of Electric Systems Engineering
Chino-city, Japan
shun@rs.suwa.tus.ac.jp

Hiroaki Inoue / Tokyo University of Science, Suwa
Research course of Engineering/Management
Chino-city, Japan
jgh12701@ed.suwa.tus.ac.jp

Noboru Takahashi / Tokyo University of Science, Suwa
Research course of Engineering/Management
Chino-city, Japan
srl@rs.suwa.tus.ac.jp

Abstract—The analysis of human grasping movement is important in developing methodologies for controlling robots or understanding human motion programs. In analyzing human grasping movement, it is advantageous to classify movements. In previous papers, classifications of grasping patterns were proposed according to the posture. Among these classifications of grasping patterns, no unified view has been reached as yet. The measured quantities in grasping have included only the posture of the hand, force and its distribution. Few have pertained to classifications based on grasping force and its distribution. This paper first tries to analyze the effect of visual information on grasping movements, and then attempts to classify grasping movements broadly according to their purpose. For the elements of the purposes of grasping movements, movements that were decided upon were those which require attention, snapping or the adjustment of the wrist or movements which do not require any special action to achieve their purpose. Secondly, we focus on the tactile information to predict with a limitation of movement. Finally, we attempted to discuss the relation between human brain activity and grasping movement on cognitive tasks.

Keywords—human hand; grasping force; grasping pattern; brain activity; NIRS.

I. INTRODUCTION

Human hands are so dexterously controlled that they can manipulate almost anything freely. Observations obtained from analyzing the grasping patterns of human hands will be useful in the control of robot hands. For example, it may be possible for industrial robots to deal flexibly with and solve unexpected problems which may occur. In the construction of more sophisticated interface systems the analysis of the grasping patterns of human hands is also suggested as an important subject for controlling robot hands by remote control.

For analysis of grasping patterns, many researchers, including Schlesiger [1] have proposed and reported methods to classify grasping patterns [2][3]. However, these classifications of grasping modes depend for many parts on

the researcher's personal definitions, and no unified view has been reached at present.

The measured quantities in grasping include the posture of the hands, and force and its distribution. However, most of the classifications have been based on the posture of the hands, and little has been reported on classification based on grasping force and its distribution.

From the point of the view of the grasping task, Napier broadly divided grasping patterns into "power grip" and "precision grip" [4]. In addition, Cutkosky classified more grasping patterns by incorporating details of the objects and the precision of the task in Napier's concept [5]. Meanwhile, Kamakura et al. presented a classification based on the contact pattern between the grasped object and grasping hand [6]. Kang et al. proposed the technique of the "contact web" which estimated information and classified grasping based on the resulting contact pattern [7]. For the theory of multi-fingered hands Yokokawa is proposing the dynamic multi-fingered manipulability measurement under the concept of the dynamic manipulability [8]. Another new approach to control the robots is the Programming by Demonstration done (PbD)[9]. A late report is proposed by Bernardin et al. [10]. Shimizu et al. described the Sensor Glove MKIII which is useful in analyzing grasping patterns and shows the potential of measuring grasping force distribution for classification [11].

Many kinds of research have been proposed for classification, but there are only a few areas such industry that are using the classifications, indicating a need for more useful grasping classification for use in engineering. We thus considered using new elements to broadly classify grasping movements. We set grasping movement purposes for the new elements, elements which are movements that require attention, snapping or adjustment of wrist or do not require any special action to achieve their purpose. Therefore, it was necessary to find a place in which position and direction had little effect when measuring grasping movements. We subsequently deliberated the possibility of broadly classifying grasping patterns according to the purpose of the grasping movement. A report about the importance of grasping task is proposed by Shiraishi, et al. [12], too.

This paper first tries to analyze the effect of visual information on grasping movements and then considers the potential for using the elements described above in classification. Lastly, we focus on the tactile information to predict with a limitation of movement.

II. EXPERIMENT 1

A. Experimental Method 1

To measure grasping movement with minimal effect from the position and object’s direction for classification, it is necessary to ascertain the proper position and direction from which to do so. The next step is to discover the role visual information plays in grasping patterns. In this experiment, USB cameras from three directions measured grasping patterns. The cameras used had a resolution of over 0.3 megapixels.

B. Range of Movement

To find the area which would not need to be considered in regard to its effect on grasping shape; subjects were made to grasp a pointer directed toward them. Then the area in which they could move without changing the direction was measured. Fig. 1 shows the range of movement. Subjects were four healthy, right-handed men aged 22 to 24.

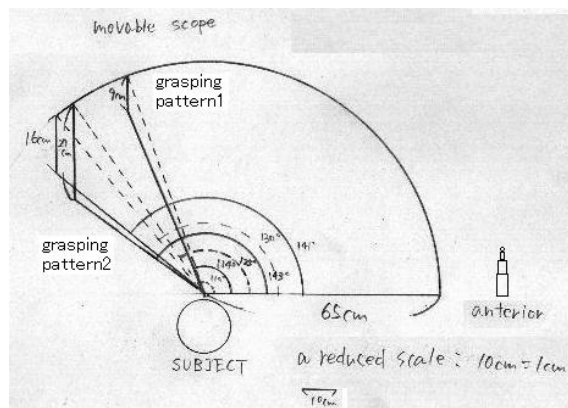


Figure 1. Range of movement (object: pointer)

The range of movement seems to depend on their flexibility and grasping patterns. As can be seen in Fig. 1, a 15 cm margin has been set, and the objects have been placed to check their effect on grasping. Fig. 2 shows the position in which the objects were placed. Grasping patterns differed little according to position; here, Position C was used for classification. However, if the object is placed in direction (4), the grasping patterns change for right-handed people. The next step was to look at the relationship between direction and grasping

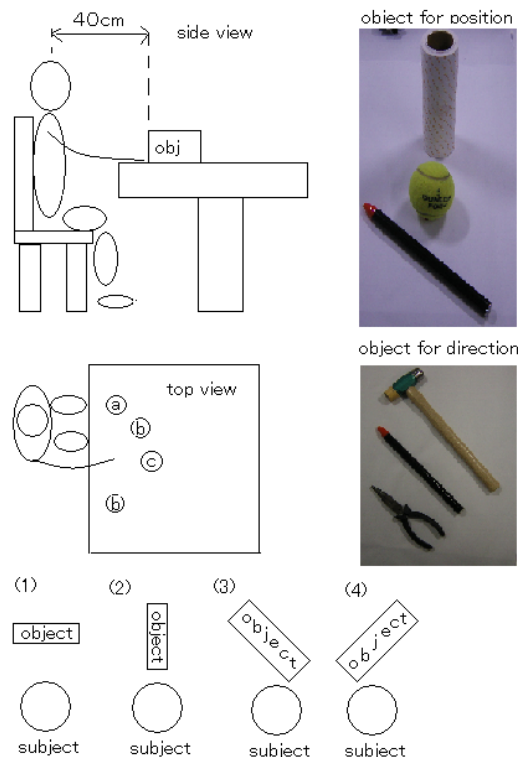


Figure 2. Object’s position and direction

C. Effect of Direction on Grasping

To analyze the relationship between direction and grasping pattern, the angle of the underarm and the angles in Fig. 3 were measured by changing the object's direction. The directions of (1) to (3) were measured by changing the angle 30 degrees. Subjects were told to grasp the object and put it onto another table. The subjects were five right-handed healthy men aged 22 – 24.

Increases in the angle of the wrist and the angle of the finger baseline are seen to be related to the angle of the object. The angle of the underarm decreased as the angle of the object increased. However, as the angle of the underarm is influenced by reaching, the displacement is not uniform. Fig. 4 exemplifies the difference between grasping patterns and the object’s directions.

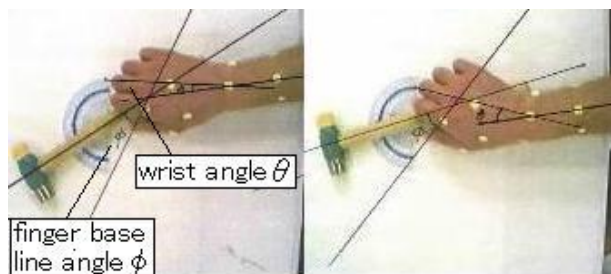


Figure 3. Angle measured, θ and ϕ

III. EXPERIMENT 2

A. Experimental Method 2

Comparing the difference of grasping movement based on “purpose of grasping movement”. We set elements which are movements that require attention, snapping or adjustment of wrist or do not require any special action to achieve their purpose. And considering the potential for using the elements described above in classification [13]

B. Experiment for the Classification of Grasping Movements

To classify grasping movements, the purpose of grasping was used as an element that is determined at a certain point, i.e., before or after grasping. In this experiment, five kinds of tasks were used to consider the relation between grasping patterns and their purpose. The tasks are to move the object to another place (Task 1), to put the object onto a small box (Task 2), to throw the object (Task 3), to make the object pass through a small hole (Task 4), to use the object as you usually do (Task 5) after grasping. These tasks were created to measure a simple grasping movement (Task 1), a movement requiring attention (Task 2), the movement which requires snapping (Task 3), a movement which requires attention and adjustment of wrist (Task 4), a movement that is imagined to be associated with the object (Task 5). And checked that the grasping movements would change with these tasks.

The purpose of the first experiment was to measure grasping shapes according to their purpose. The next step was to measure grasps without a prescribed purpose. The purpose was given only after the subject first grasped the object. The subjects were six right-handed healthy men aged 22 – 24.

C. Result of Classification Experiment

The results showed two movements involved in grasping and taking action when checking the difference between the first grasping shape and the next grasping shape. One is a change in grasping shapes before picking up. The other one is a change in the grasping shapes after picking up. Fig 6 shows the first movement; the grasping shape changes according to its purpose. T shows the second movement; the grasping shape changes according to its purpose. Such cases might be difficult to classify only by force distribution. Such movements were not seen in the case of every object. Therefore we attempted to discover out the difference between them and use it with the force distribution to classify grasping movements.

This experiment showed that one seems to make space between the palm and object or change the grasping shape into a more flexible form when they try to do something sensitive like Task 4. Probably, such a tendency has some relation to degree of freedom in movement.

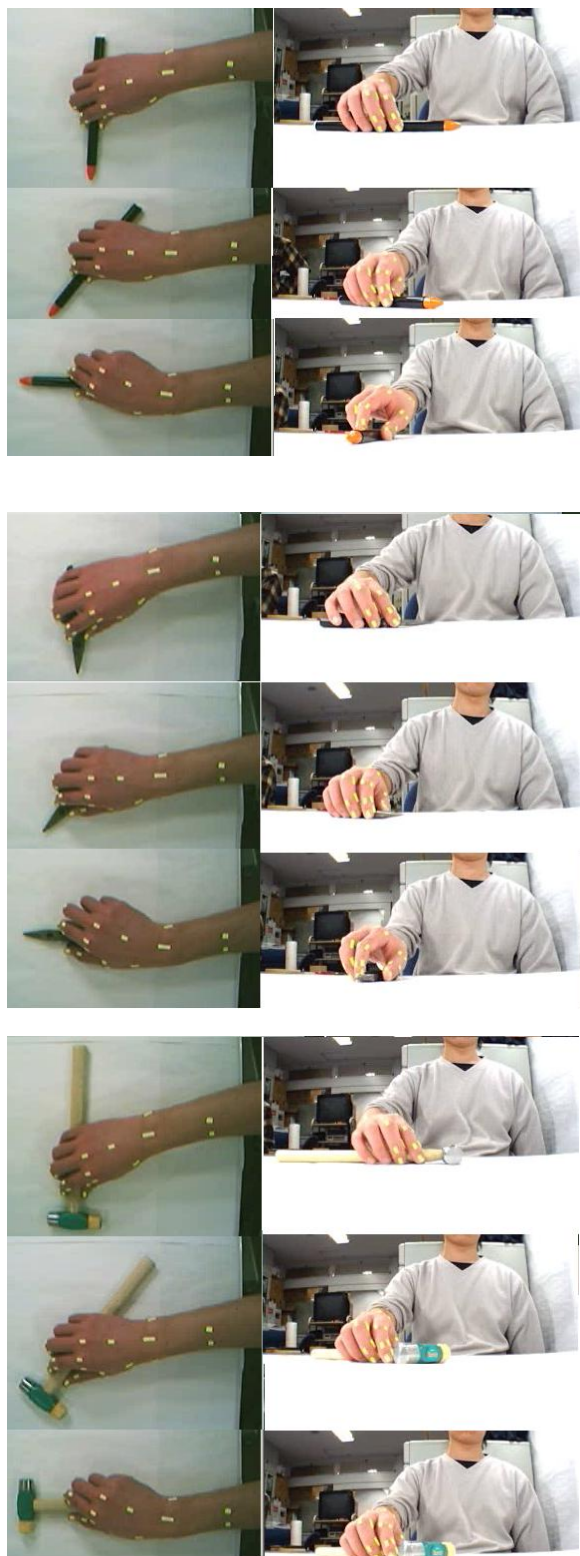


Figure 4. Grasping patterns for each object

(Top: pointer, Middle: pincher, Bottom: hammer)

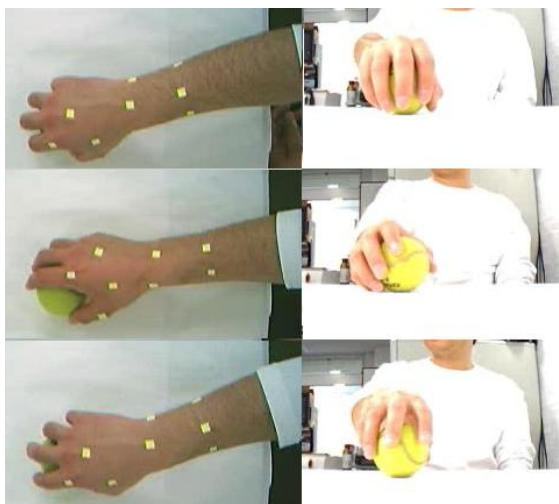


Figure 5. Changing the shape when grasping
(Top: Task 1, Middle: Task 3, Bottom: Task 4)

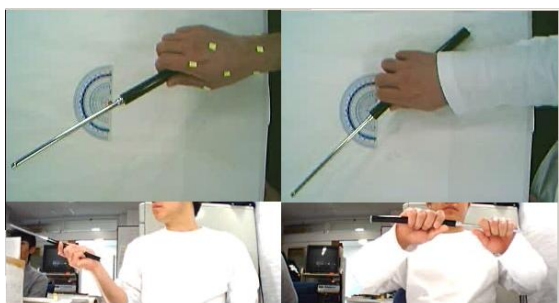


Figure 6. Changing the shape after grasping
(left:task4, right:task5)

IV. TACTILE INFORMATION

Looking into the tactile information and degree of freedom in hand movement, we first tried to check how correctly we could imagine the shape only from tactile information. Therefore, did the relation of such information to the degree of freedom in movement was considered in conducting this experiment [14]

A. Experiment Method for Tactile Information

Three limitations were made to analyze the effect. One was wearing an eye mask to shut out the visual information. Another one was a pinching movement to control the tactile information. The last one aluminum fingertip cover to reduce the tactile information and to make the surface like robot hand because we are thinking to use the results for robot's hands. The fingertip cover used in this experiment was enclosed in aluminum sheeting and the finger cushion's side was flattened. Limitations in pinching movement are shown in Fig 7.

The test was to guess the object with eyes masked and fingertip limitations. After that, same tests were conducted without using the fingertips. Fig 7, 8, 9 shows the objects

used. Objects in 8 were stuck to board. The objects in Fig. 8 (lower right) can be spun using the stick that is standing on the small plate. The objects in Fig. 9 can be pinched freely.

TABLE I. LIMITATION OF PINCH

freedom degree number	Limitation
1	Not allowed to pinch again
1'	allowed to grasp again just a little
2	allowed to move up and down
3	allowed to go over lateral side
4	allowed to grasp freely

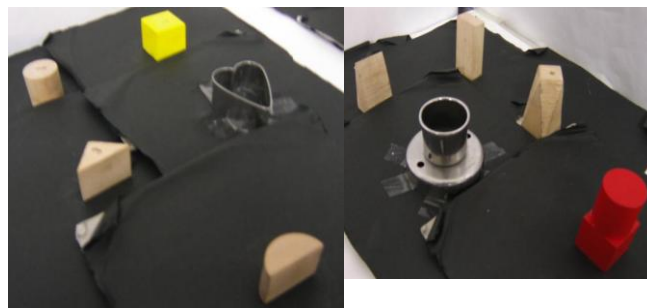


Figure 7. Object for tactile information test



Figure 8. Object for tactile information test

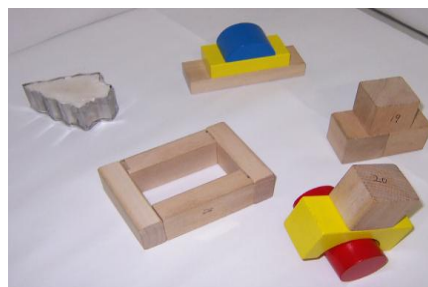


Figure 9. Object for tactile information test

B. Result of the Experiment in Tactile Information

Fig. 10 is the result of this test. The answers were checked by a majority decision of three observers. The subjects for this experiment were six men and two women, all healthy, right-handed and aged 20 – 60.

In Fig. 10, the accuracy rate was higher when the fingertip covers were not used, and the accuracy rate basically increased with the degree of freedom, but it increased only slightly when the fingertip covers were not used, or when there was a high degree of freedom. From the aspect of object identification only with tactile information, the difference in fingertip cover suggests the importance of the ridges in the fingers’ skin and the plasticity of the finger surface, probably because they are enhancing the signals. Furthermore, Degree of Freedom 4 was lower than that of 1 when they tried without the fingertip cover. This seems to have occurred when they lost track of direction when they moved their hands. This suggests that the relation between accuracy rate and freedom digger is not a simple proportional relation.

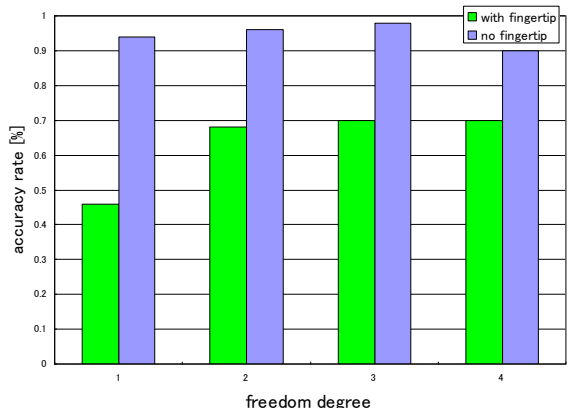


Figure 10. Degree of freedom and accuracy rate

V. GRASPING MOTION AND HUMAN BRAIN ACTIVITY

We are trying to process experimental measuring and discuss human brain activity on grasping movement and cognitive task. So, we measured brain activity from the viewpoint of blood flow changes when subject performed grasping movement including reaching. Six subjects were healthy males who were right handed. They were asked to read and sign an informed consent regarding the experiment. In measurement, f-NIRS(Functional Near Infrared Spectroscopy) made by SHIMADZE Co. Ltd. were used.

A. Experimental Method

Subjects were asked to grasp the piece of wood, pointer, column-shaped metallic bar and hammer based on instructions from operator (Fig. 11). Brain activity was measured under four conditions. Subjects grasped objects actively with their eyes open (1) or close (2), and passively with their eyes open (3) or close (4). In addition, subjects

were told to perform simple grasping motion or do it with imaging motion for using object.

Subjects took a rest during 10 seconds at least with their eye close before starting task and the time design was rest (5 seconds) – task (10 seconds) – rest (5 seconds). Finally, subject closed their eyes for 10 seconds again after task. Then, the brain activity was recorded from the first eyes-closed rest to the last eyes. The part of measurement was the frontal lobe.

B. Experimental Results

Fig. 12 shows one subject’s measuring result. At the first, Hb-oxy was increased in overall frontal lobe after start of grasping task. This tendency was common among subjects. After that, Hb-oxy was increased and decreased in synchronization with task and rest. Also, there was remarkable tendency like this during task with imaging and their eyes open.

Analysis was performed one-sample t-test and sample was variation in brain activity during about four seconds after starting tasks.

As a result, there was not significant differences at frontal lobe. However, it was shown as common tendency among subjects that there was adifference in variation of oxy-Hb density due to presence or absence of existence or non-existence imaging motion and eyesight. It was thought that this result was derived from planning for grasping and visuals stimulation.

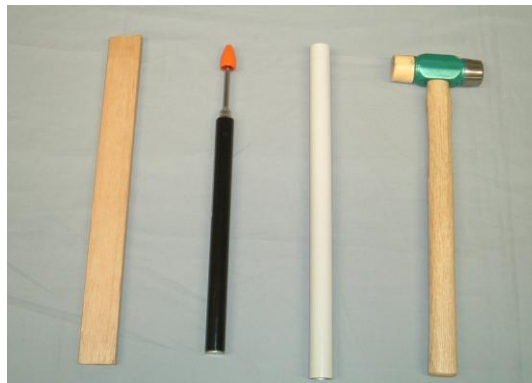


Figure 11. Grasping object

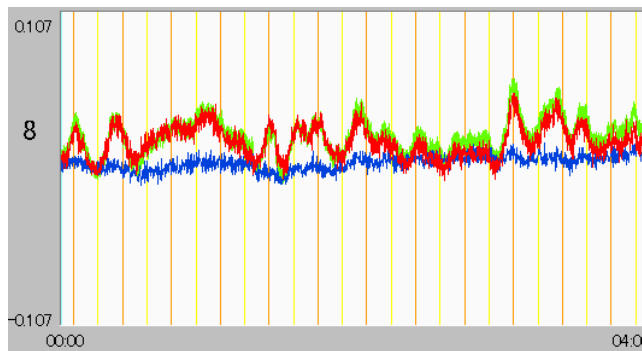


Figure 12. Measuring Result of grasping steering wheel

VI. CONCLUSION AND FUTURE WORK

This paper first studies that the grasping angle changes. From the results, it was determined that basically the wrist angle and finger baseline angle are proportionally related. In this report we attempted to classify the grasping patterns based on "purpose of grasping movement". And in the results described in Section III.B, found two movements related to "purpose of grasping movement". Some grasping movements change when you give them a purpose before grasping, but some grasping movements do not change until the object is lifted and the action accomplished. These results suggest the possibility of the classification of grasping movements according to "purpose of grasping movement". Furthermore it would be useful to classify the grasping Movements that have similar grasping forms or distributions but have different actions after grasping. At a later stage, we would like to classify grasping movements according to the "purpose of grasping movement" and use the results of the distribution in grasping patterns to create more useful classifications for grasping movements in engineering.

The results in Section IV.B are important, in using the classification. The relation between accuracy rates basically increases with the degree of freedom, but if the degree of freedom increases with no useful feedback, the results would differ from expectation. Therefore, the challenge which lies ahead is to find effective ways to use the tactile information.

In terms of measuring brain activity, we plan to examine change of brain activity due to shape of hand and object as well as a review of experimental design.

REFERENCES

- [1] Schlesinger, G: "Der Mechanische Aufbau der kunstlichen Glieder [The mechanical structure of artificial limbs]", In M.Borchardt et al. (Eds.), *Ersatzglieder und Arbeitshilfen für Kriegsbeschädigte und Unfallverletzte*, pp. 21-600, Berlin: Springer, 1919.
- [2] Christine L. Mackenzie and Thea Iberall: "The Grasping hand." G.e. Stelmach, P.A. Vroom (Eds.), *Advances in psychology*, no.104, pp. 15-46, Amsterdam, 1994.
- [3] M.A. Arbib, T.Iberall, and D.M.Lyons: "Coordinate control programs for movements of the hand," In A.W.Goodwin & I.Darian-Smith (Eds.), *Hand function and the neocortex*, pp. 111-129
- [4] J.R.Napier: "The prehensile movement of the human hand," *The journal of bone and joint surgery*, vol.38 B, no.4, pp. 902-913, 1956.
- [5] M.R. Cutkosky: "On grasping choice, grasping models, and the design of hands for manufacturing task," *IEEE Trans. Robotics and Automation*, vol.5, no.3, pp. 269-279, 1989.
- [6] N.Kamakura, M.Matsuo, H.Ishii, F.Mitsuboshi, and Y.Miura: "Pattern of static prehension in normal hands," *The American journal of occupational therapy*, vol.34, no. 7, pp. 437-445, 1980
- [7] S.B.Kang and K.Ikeuchi: "Towed automatic robot instruction from perception - recognizing a grasping from observation," *IEEE Trans. Robotics and Automation*, vol.9, No.4, pp. 432-443, 1993.
- [8] Masaki Fujiwa, Yasuyoshi Yokokohji, and Tsuneo Yoshikawa: "Dynamic Multi-Fingered Manipulability for Articulated Hands and its Extension to a Design Index for Master-Slave Hands," *Journal of the Robotics Society of Japan*, vol.22, No.2, pp. 264-272, 2004
- [9] S.Ekval and D.Kragic; "Grasp Recognition for Program by Demonstration" *IEEE International Conference on Robotics and Automation* 2005, pp. 748-753, 2005
- [10] K.Bernardin, K.Ogawara, K.Ikeuchi, and R.Dillmann; "A Sensor Fusion Approach for Recognizing Continuous Human Grasping Sequences Using Hidden Markov Models" *IEEE Trans. Robotics*, 21(1):pp. 47-57, 2005.
- [11] S.Shimizu, M.Shimojo, S.Sto, Y.Seki, A.Takahashi, Y.Inukai, and M.Yoshioka; "The Relationship between Human Gripping Types and Force Distribution Pattern in Grasping," *8th International Conference on Advanced Robotics*, pp. 299-304, 1997
- [12] K.Shiraishi, T.Kondo, and K.Ito; "Analysis on the Task Dependency of Human Grasp Movements and Application to Robot Control" *SICE Symposium on Systems and Information*, pp. 283-286, 2002
- [13] S. Matsuzawa, S. Shimizu, S. Kikuchi, E. Watanabe, H. Kina, H. Hurata, N. Takahashi, and T. Ehara, "Proposal for a New Classification Method for Grasping Movement," *The 13th International Conference on Advanced Robotics*, 2007, Jeju Island, Korea.
- [14] N. Takahashi, S. Shimizu, Y. Hirata, H. Nara, H. Inoue, N. Hirai, S. Kikuchi, E. Watanabe, and S. Kato, "Basic study of Analysis of Human Brain Activities during Car Driving," *the 14th International Conference on Human-Computer Interaction*, 2011, Orlando, Florida, USA.
- [15] S. Matsuzawa, S. Shimizu, S. Kikuchi, E. Watanabe, H. Kina, H. Hurata, N. Takahashi, and T. Ehara, "A Basic Study of Grasping Motion for Advanced Interface," *the 12th International Conference on Human-Computer Interaction*, 2007, Beijing, China.

The Relationship between Human Brain Activity and Movement on the Spatial Cognitive Task

Shunji Shimizu / Tokyo University of Science, Suwa
Department of Electric Systems Engineering
Chino-city, Japan
shun@rs.suwa.tus.ac.jp

Hiroaki Inoue/ Tokyo University of Science, Suwa
Research course of Engineering/Management
Chino-city, Japan
jgh12701@ed.suwa.tus.ac.jp

Hiroyuki Nara/ Hokkaido University
Graduate School of Information Science and
Technology
Sapporo-city, Japan
nara@ssc.ssi.ist.hokudai.ac.jp

Noboru Takahashi/ Tokyo University of Science, Suwa
Research course of Engineering/Management
Chino-city, Japan
srl@rs.suwa.tus.ac.jp

Fumikazu Miwakeichi/ The Institute of Statistical
Mathematics
Spatial and Time Series Modeling Group
Tachikawa-city, Japan
miwake1@ism.ac.jp

Nobuhide Hirai / Jichi Medical University
Department of Psychiatry
Shimotsuke-city, Japan City
nobu@nobu.com

Senichiro Kikuchi / Jichi Medical University
Department of Psychiatry
Shimotsuke-city, Japan
skikuchi@jichi.ac.jp

Eiju Watanabe/ Jichi Medical University
Department of Neurosurgery
Shimotsuke-city, Japan
eiju-ind@umin.ac.jp

Satoshi Kato/ Jichi Medical University
Department of Psychiatry
Shimotsuke-city, Japan
psykato@jichi.ac.jp

Abstract—Final purpose in this research is to contribute to developing of assistive robot and apparatus. Recently, there is a pressing need to develop a new system which assists and acts for car driving and wheelchair for the elderly as the population grows older. In terms of developing a new system, it is thought that it is important to examine behaviors as well as spatial recognition. Therefore, experiments have been performed for an examination of human spatial perceptions, especially right and left recognition, during car driving using NIRS. In previous research, it has been documented that there were significant differences at dorsolateral prefrontal cortex at left hemisphere during virtual driving task and actual driving.

In this paper, brain activity during car driving was measured and detailed analysis was performed by segmentalizing brain activity during car driving on the basis of subjects' motion. So, we report the relationship between brain activity and movement concerned with perception during driving in this paper.

Keywords-brain information processing during driving task; spatial cognitive task; determining direction; NIRS.

I. INTRODUCTION

Human movements change relative to his environment. Nevertheless, he/she recognizes a new location and decides what behavior to take. It is important to analyze the human spatial perception for developing autonomous robots or automatic driving.

The relation of the theta brain waves to the human spatial perception was discussed in [1][2]. When humans perceive space, for example, try to decide the next action in a maze, the theta brain waves saliently appear. This means we have a searching behavior to find a goal at an unknown maze. From the side of human navigation Maguire et al. measured the brain activations using complex virtual reality town [3]. But every task is notional and the particulars about the mechanism that enables humans to perceive space and direction are yet unknown. Also, Brain activities concerned with cognitive tasks during car driving have been examined. For example, there was a report about brain activity when disturbances were given to subjects who manipulated driving simulator. Also, power spectrums increased in beta and theta

bands [4]. However, there is little report on the relationship among right and left perception and driving task.

So, we performed experiments in which perception tasks were required during virtual car driving using NIRS(Near Infrared Spectroscopy). From experimental results, there were significant differences at dorsolateral prefrontal cortex in left hemisphere via one-sample t-test when subjects watched driving movie and moving their hand in circles as if handling a steering wheel [5].

In addition, we conducted experiments in real space, which were performed by taking f-NIRS in the car, and measured the brain activity during actual driving. A purpose in this experiment was to measure and analyze the brain activity during actual driving to compare results between virtual and actual results. As a result, there were significant differences at similar region [6][7]. In addition, we measured the brain activity of frontal lobe, which is related to behavioral decision-making, during car driving in different experimental design from previous one to verify previous results [8][9].

It is well known that higher order processing is done such as memory, judgment, reasoning, etc in the frontal lobe [10]. We tried to grasp the mechanism of information processing of the brain by analyzing data about human brain activity during car driving. Also, the goal of this study is to find a way to apply this result to new assist system.

So, with the aim of increasing number of subjects and examining more closely the brain activity concerned with spatial perception and direction determination during car driving, we performed additional experiments.

In this time, the brain activity of same lobe with human spatial perception and direction determination was discussed on the basis on changing direction of the gaze and starting to turn the steering wheel. Furthermore, we examined the mechanism of information processing of the brain and human spatial perception during car driving.

II. EXPERIMENT

A. Brain activity on virtual driving

1) Brain activity on driving movie is shown

The subjects for this experiment were eight males who were right handed. They were asked to read and sign an informed consent regarding the experiment.

An NIRS (Hitachi Medical Corp ETG-100) with 24 channels (sampling frequency 10 Hz) was used to record the density of oxygenated hemoglobin (oxy hemoglobin) and deoxygenated hemoglobin (de-oxy hemoglobin) in the frontal cortex area.

The movie is included two scenes at a T-junction in which it must be decided either to turn to the right or left. In the second scene, there is a road sign with directions. We used nine kinds of movies in about one minutes. Before showing the movie, subjects were given directions to turn to the right or left at the first T-junction. They were also taught the place which was on the road sign at the second T-Junction. They had to decide the direction when they looked



Fig. 1. Recorded movie during measurement

at the road sign. They were asked to push a button when they realized the direction in which they were to turn.

2) Brain activity on handling motion

In this experiment, measuring was performed by f-NIRS(Functional Near Infrared Spectroscopy), made by SHIMADZU Co. Ltd with 44ch. Five subjects were healthy males in their 20s, right handed with a good driving history. They were asked to read and sign an informed consent regarding the experiment.

The subject was asked to perform simulated car driving, moving their hand in circles as if using a steering wheel. A PC mouse on the table was used to simulate handling a wheel, and NIRS (near-infrared spectroscopy) to monitor oxygen content change in the subjects' brain. NIRS irradiation was performed to measure brain activities when the subject sitting on a chair make a drawing circle line of the right/left hand 1) clockwise, and 2) counterclockwise. The part of measurement was the frontal lobe. The subject was asked to draw on the table a circle 30 cm in diameter five times consecutively, spending four seconds per a circle. The time design was rest (10 seconds at least) – task (20 seconds) – rest (10 seconds) - close rest.

B. Brain activity during actual car driving

1) Brain activity during actual car driving

In general roads, experiments were performed by taking f-NIRS in the car, and measuring the brain activity when car driven by subjects was went through two different intersections. Six subjects were a healthy male in their 20s, right handed with a good driving history. They were asked to read and sign an informed consent regarding the experiment. In all experiments, measuring was performed by f-NIRS (Functional Near Infrared Spectroscopy), made by SHIMADZU Co. Ltd [11].

Subjects took a rest during 10 seconds at least with their eye close before driving task and they drove a car during about 600 seconds. Finally, subject closed their eyes for 10 seconds again after task. Then, the brain activity was recorded from the first eyes-closed rest to the last eyes

Subjects were given directions to turn to the right or left at the first T-junction during driving task. They were also taught the place which was on the road sign at the second T-junction. And, they were given the place where they have to



Fig. 2. Sample of first T-Junction



Fig. 3. Sample of second T-Junction

go to. So, they had to decide the direction when they looked at the road sign.

A trigger pulse was emitted on stop lines at T-Junctions to use as a measuring stick for the analysis. Also, we recorded movie during the experiment from a car with a video camera aimed toward the direction of movement (Fig. 1). Recorded movies were used to exempt measurement result including disturbances, such as foot passengers and oncoming cars, from analysis. Figure.2 and figure.3 shows one sample of T-junction.

2) Verification Experiment

To conduct verification for experimental results in previous experiment, we performed additional experiment which was achieved in a similar way.

In this experiment, experimental course was different from previous one. While previous one was included two T-junctions in which there was road sign at second one and not at first one per a measurement, there were multiple T-junctions. Three were 5 T-junction without road sign and 4 T-junctions with road sign.

Subjects were twelve males who were all right-handed. They drove a car during about 20 minutes after a rest during 10 seconds at least with their eyes close. Subjects were enlightened about turning direction and the place on which road signs was at T-junction during measurement. And, they arbitrarily decided the direction to turn when they confirmed road signs. Also, a trigger pulse was emitted in the same way.

3) Detailed analysis based on driving behavior

In this analysis, movies aimed toward the direction of movement as well as ones aimed subject movement like ocular motion and arm movement were recorded. This is to analyze brain activity using ocular motion in looking at road signs as a trigger. In previous research we performed, stop line at T-junction was used as a trigger. But, brain activity in T-junction involved movement task such as turning steering wheel, changing neck direction, hitting the brake. So, it is thought that brain activity derived from cognitive tasks was overwritten with brain activity due to movement tasks. Therefore, we tried to analyze brain activity on the basis of ocular motions to examine significant differences with cognitive tasks.

III. EXPERIMENTAL RESULT

A. Brain activity on virtual driving

1) Brain activity on driving movie is shown

On the whole, the variation in de-oxy hemoglobin was smaller than in the oxy hemoglobin. However, there was a great increase in channel 18(around #10 area of the dorsolateral prefrontal cortex of the right hemisphere). This might be the variation based on the spatial perceptions

Next, differences were investigated concerning the subject's brain activity. As the first case, it was when the vision was directed after having been told the direction. As the Second, it was when the vision was directed after having been decided the direction under the road sign.

Here, d1 and d2 were defined to analyze measurement data. d1 is the variation of hemoglobin turning of one second at the first T-junction. And d2 is variation of hemoglobin at the second one. From the measurement result, d1 and d2, all of the 269 times of each subject, there were significant differences in oxy hemoglobin 3ch. ($p < 0.02$: paired t test) and 20ch. ($p < 0.03$) using NIRS. These regions were corresponded to around #46 area of the dorsolateral prefrontal cortex of the left hemisphere and around #10 area of the dorsolateral prefrontal cortex of the right hemisphere, respectively.

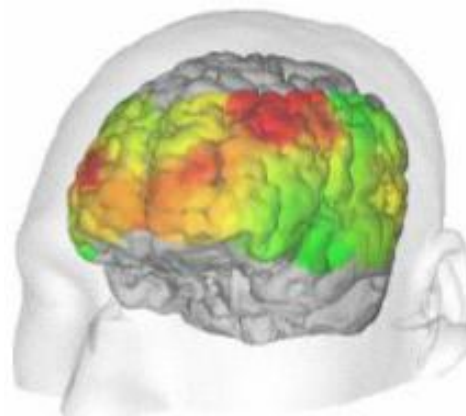


Fig. 4. Brain activity (clockwise)

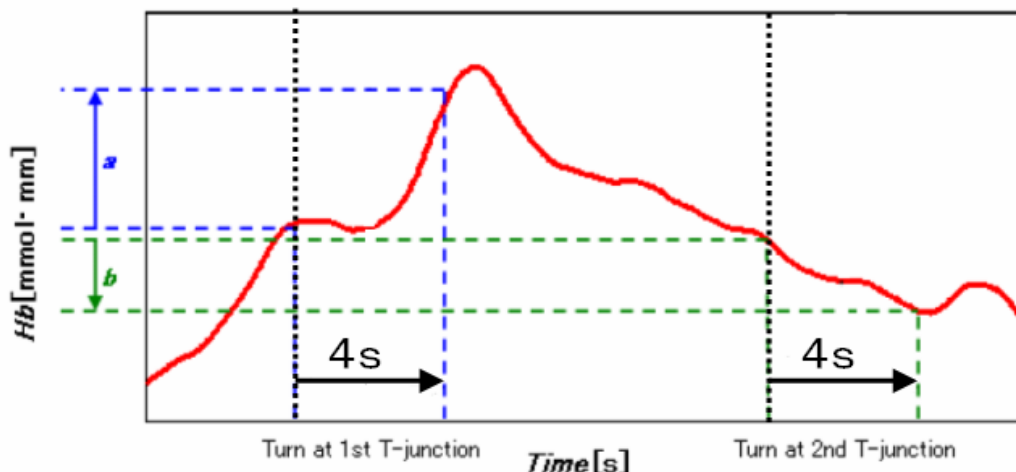


Fig. 5 Analysis method

Subjects pushed a button before turning at the second T-junction, so it influenced brain activities. The possibility of a correlation between d2 and the time until the movie was turned at the second T-junction after each subject pushed a button was investigated. Each correlation coefficient of hemoglobin channel was calculated. There was significant difference at only de-oxy hemoglobin 10ch(around #10 area of the dorsolateral prefrontal cortex of the right hemisphere) using paired t test. In only this result, the relationship between pushing a button and d2 cannot be judged.

2) *Brain activity on handling motion*

During the motion, the increase of oxy hemoglobin density of the brain was found in all subjects. The different regions of the brain were observed to be active, depending on the individual. The subjects were to be observed 1) on starting, and 2) 3-5 seconds after starting moving their 3) right hand 4) left hand 5)clockwise 6)counterclockwise. Although some individual variation existed, the result showed the significant differences and some characteristic patterns. The obtained patterns are shown as follows. Regardless of 1), 2), 3) and 4) above, the change in the oxy hemoglobin density of the brain was seen within the significant difference level 5% or less in the three individuals out of all five subjects. The part was the adjacent part both of left pre-motor area and of left prefrontal cortex. Especially, in the adjacent part of prefrontal cortex a number of significant differences were seen among in four out of five subjects. Next more emphasis was put on the rotation direction: 5) clockwise or 6) counterclockwise. No large density change was found in the brain with all the subjects employing 6). But, the significant difference was seen in four out of five subjects employing 5) (Fig.4). It is well known that in the outside prefrontal cortex higher order processing is done such as of behavior control. It is inferred that the pre-motor area was activated when the subjects moved the hand in the way stated above because the pre-motor area is responsible for behavior control, for transforming visual information, and for generating neural impulses controlling.

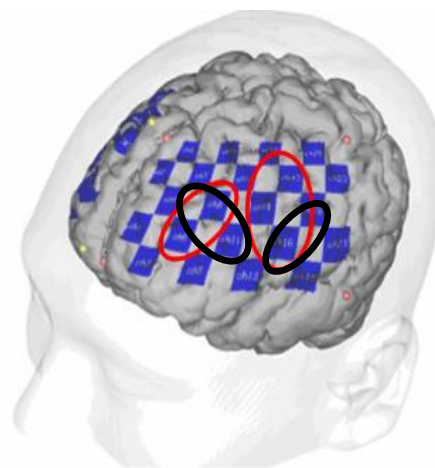


Fig. 6 Significant differences at the turn left

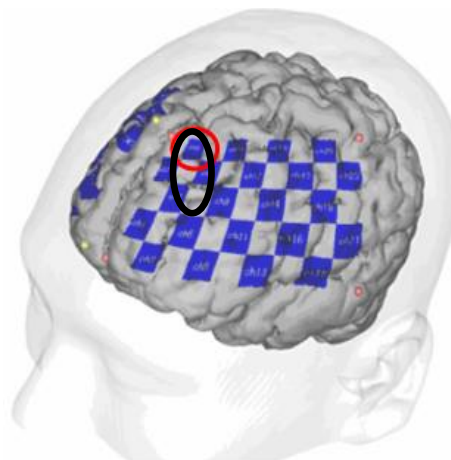


Fig. 7. Significant differences at the turn right

B. Brain activity during actual car driving

1) Brain activity during actual car driving

At the first, Hb-oxy was increased in overall frontal lobe after start of operation. This tendency was common among subjects. After that, Hb-oxy was decreased as subjects adjusted to driving the car. This meant that the brain activity changed from collective to local activities.

In this experiment, being considered time as zero when experimental vehicle reached stop line at T-junction. The analysis was performed one-sample t-test using a and b within the significant difference level 5% or less between zero and about four seconds (Fig.5). Here, a is the variation of hemoglobin turning of one second at the first T-junction. And b is variation of hemoglobin at the second one. As the results, there were significant differences around #46 area of the dorsolateral prefrontal cortex and the premotor area of the left hemisphere brain in turning left (Fig. 6:red). Also, there were significant differences #9 of the dorsolateral prefrontal cortex of the left hemisphere brain at the turn right (Fig. 7: red).

2) Verification Experiment

Various tendencies among individuals were observed in comparison with results in B. However, there were tendency that oxy-Hb was increased when car turned left or right at T-junctions and oxy-Hb was decreased during going straight

Analysis method was the same as previous one. Though Gaps were shown regions at which there were significant differences, there were significant differences in common region, too (Fig. 6,7: black). In the analysis, measurement results including disturbance at T-junctions were excluded as analysis object.

3) Detailed analysis based on driving behavior

The analysis was performed one-sample t-test within the significant difference level 5% or less between brain activity before and after looking at road sign. Each of sample data for analysis was 1 second. Also, analysis was performed with respect to each direction which subject had to go at next T-junction. As a consequence of analysis, there were significant differences at interior front gyrus of frontal lobe of left hemisphere without reference of direction (Fig. 8 and Fig. 9).

IV. CONCLUSION AND FUTURE WORK

The hemoglobin density change of the human subjects' frontal lobe was partly observed in the experiments we designed, where three kinds of tasks were performed to analyze human brain activity from the view point of spatial perception.

The NIRS measures of hemoglobin variation in the channels suggested that human behavioral decision-making of different types could cause different brain activities as we saw in the tasks: 1) taking a given direction at the first T-junction, 2) taking a self-chosen direction on a road sign at the second T-junction and 3) turning the wheel or not. Some significant differences (paired t test) on NIRS's oxy-hemoglobin and less interrelated results between "pushing a button" and brain activity at the second T-junction are obtained.

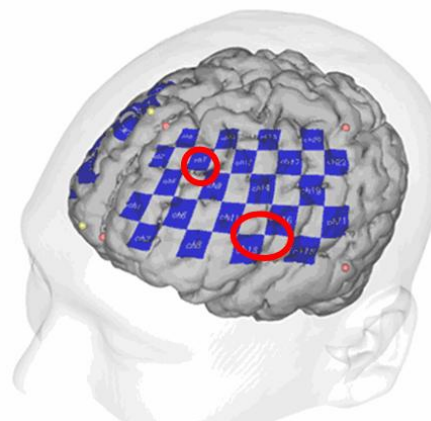


Fig. 8. Significant difference at left direction of road sign

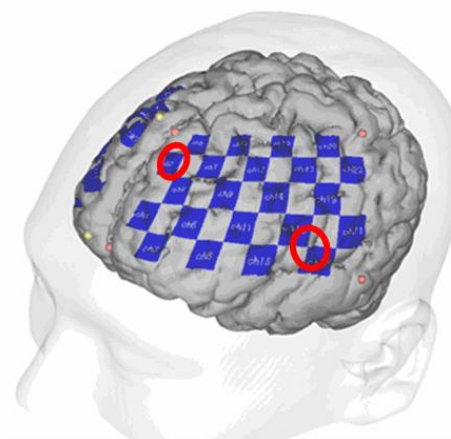


Fig. 9. Significant difference at right direction of road sign

Furthermore, experimental results indicated that with the subjects moving their hand in circle, regardless of right or left, 1) the same response was observed in the prefrontal cortex and premotor area, and 2) different patterns of brain activities generated by moving either hand clockwise or counterclockwise.

The regions observed were only those with the 5% and less significance level. Possible extensions could be applied to other regions with the 10% and less significance level for the future study. With a larger number of subjects, brain activity patterns need to be made clear. In addition, it is thought to take particular note of participation concerning working memory when car is driven.

Furthermore, it was found that there were significant differences around #44-45 area. It is well known that this region is corresponding to language area. So, it is thought

that subjects look at road map to determine direction that they have to go according to word described in road sign.

From results of these experiments, there was significant difference around working memory. So, experiments focusing on relationship turning wheel and working memory will be performed. On the other hand, experiments as to actual driving were required a broad range of perception and information processing. Especially, subjects had to determine behaves depending on various information at T-junctions, that is, the color of the traffic light, presence or absence foot passengers and so on. And so, we plan to perform more static experiments. we attention to differences on the basis of turning direction and dominant hand. In addition, we will conduct the experiments in which subjects were narrowed down to left-handedness. Furthermore, researches into other human brain activities than spatial perception are to be necessary with accumulated data from fMRI (functional magnetic resonance imaging), EEG (Electroencephalogram), etc.

When compared virtual result to actual ones, there were significant differences around #46 area in both experiments, which were performed in virtual and actual condition, as a common result. It is thought that this result is due to activities of working memory because subjects must to recall memories of movements required for car driving and turning steering wheel. Conversely, there were significant differences around #10 in virtual experiments and around premotor area in actual driving, respectively. In the virtual case, it is thought to result from inhabitation of task without movement. In the actual case, subjects had to perceive space information in real time. So, it is considered that there were significant differences around premotor area because they always ready up to manipulate steering wheel.

As a future plan, we aim to apply these results to assistive human interface. As a matter of course, we plan to performed additional experiments including the verification of these results. And final purpose is to develop a new system for manipulating wheelchair and information presentation system to assist recognition of information including spatial one during car driving.

REFERENCES

- [1] M.J. Kahana, R. Sekuler, J.B. Caplan, M. Kirschen, and J.R. Madsen: "Human theta oscillations exhibit task dependence during virtual maze navigation.", *Nature*, 1999, 399, pp. 781-784.
- [2] N. Nishiyama and Y. Yamaguchi: "Human EEG theta in the spatial recognition task", *Proceedings of 5th World Multiconf. On Systemics, Cybernetics and Informatics (SCI 2001)*, Proc. 7th Int. Conf. on Information Systems, Analysis and Synthesis (ISAS 2001), pp. 497-500 (2001).
- [3] E.A. Maguire, N. Burgess, J.G. Donnett, R.S.J. Frackowiak, C.D. Frith, and J.O' Keefe: "Knowing Where and Getting There: A Human Navigation Network," vol. 280 *Science* 8/may/1998.
- [4] Chin-Teng Lin, Shi-An Chen, Tien-Ting Chiu, Hong-Zhang Lin, and Li-Wei Ko: "Spatial and temporal EEG dynamics of dual-task driving performance." *Journal of NeuroEngineering and Rehabilitation*, vol. 8-11, 2011
- [5] S. Shimizu, N. Hirai, F. Miwakeichi, and et al: "Fundamental Study for Relationship between Cognitive task and Brain Activity during Car Driving," *Proc. the 13th International Conference on Human-Computer Interaction*, (San Diego, CA, USA, 2009), Springer Berlin / Heidelberg, 434-440.
- [6] N. Takahashi, S. Shimizu, Y. Hirata, H. Nara, F. Miwakeichi, N. Hirai, S. Kikuchi, E. Watanabe, and S. Kato: "Fundamental Study for a New Assistive System during Car Driving," *Proc. International Conference on Robotics and Biomimetics*, 2010, China.
- [7] N. Takahashi, S. Shimizu, Y. Hirata, H. Nara, H. Inoue, N. Hirai, S. Kikuchi, E. Watanabe, and S. Kato, "Basic study of Analysis of Human Brain Activities during Car Driving," the 14th International Conference on Human-Computer Interaction, 2011, Orlando, Florida, USA.
- [8] S. Shimizu, N. Takahashi, H. Nara, H. Inoue, and Y. Hirata, "Fundamental Study for Human Brain Activity Based on the Spatial Cognitive Task," the 2011 International Conference on Brain Informatics-BI 2011, China.
- [9] S. Shimizu, H. Nara, N. Takahashi, H. Inoue and, Y. Hirata, "Basic Study for Human Brain Activity Based on the Spatial Cognitive Task," *The Third International Conference on Advanced Cognitive Technologies and Applications*, 2011, Italy.
- [10] J. Cockburn: "Task interruption in prospective memory: "A frontal lobe function?." *Cortex*, vol. 31, 1995, pp. 87- 97.
- [11] E. Watanabe, Y. Yamashita, Y. Ito and, H. Koizumi, "Non-invasive functional mapping with multi-channel near infra-red spectroscopic topography in humans," *Heurosci Lett* 1996, Feb 16, 205(1), 41-4.

EEG-controlled Table Bike for Neurorehabilitation Based on Sensorimotor-rhythm BCI

Jin-Chern Chiou^{1,2,3}, Sheng-Chuan Liang¹, Chia-Hung Yen¹, Chun-Jen Chien¹, Yung-Jiun Lin^{1,3}, Tien-Fu Chang²,
Nei-Hsin Meng^{3,4}, Ching-Hung Lin³, Jeng-Ren Duann^{1,3,5,6}

¹Biomedical Engineering Research and Development Center, China Medical University, Taichung Taiwan

²Institute of Electrics and Control Engineering, National Chiao Tung University, Hsinchu, Taiwan

³Biomedical Electronics Translational Research Center, National Chiao Tung University, Hsinchu, Taiwan

⁴Department of Physical Medicine and Rehabilitation, China Medical University Hospital Taichung Taiwan

⁵Institute of Clinical and Medical Science, China Medical University, Taichung Taiwan

⁶Institute for Neural Computation, University of California San Diego, La Jolla, CA 92093 USA

t17988@mail.cmuh.org.tw, t19362@mail.cmuh.org.tw, asusm6nb@gmail.com, t20840@mail.cmuh.org.tw,
t18628@mail.cmuh.org.tw, stevechang10000@yahoo.com.tw, nsmeng@ms13.hinet.net, eandy924@gmail.com,
duann@scen.ucsd.edu

Abstract—This work demonstrates an EEG-controlled table bike for neurorehabilitation based on the sensorimotor rhythm (SMR) BCI using a wearable ultra light-weighted 4-ch wireless EEG device designed and developed by our group. The 4-ch wireless EEG module was used to acquire high quality EEG signals from the scalp locations of C3 or C4 or both. The acquired EEG data were then processed and analyzed using an EEG translation module, also designed by our group, to extract the SMR features. Consequently, the SMR features were used to turn ON and OFF a commercially available table bike for neurorehabilitation process. Finally, the feasibility of the devised EEG-controlled table bike was tested on normal subjects using a motor imagery experiment, in which the subjects were asked to perform a motor imagery task every time a ‘go’ cue was displayed at the center of a computer screen and move the table bike without physical hand movement. In total, 12 healthy normal subjects and one chronic stroke patient participated in this study. The success rate at which the subjects/patient could successfully move the table bike after the cue onsets was used to evaluate the feasibility of the device. Our result showed that most of the subjects and patient could easily learn how to operate the EEG-controlled table bike with only few sessions of training (no more than 30 minutes) and achieve around 80% success rate.

Keywords-neurorehabilitation; sensorimotor rhythm (SMR); brain-computer interface; EEG.

I. INTRODUCTION

In order to put the brain in the loop of neurorehabilitation process [1], this work devised a brain-computer interface (BCI)-based electroencephalography (EEG) controlled table bike for training patients after stroke attack and restoring

their motor control potentially through reorganizing the otherwise missing or degenerated fiber tracts directly or indirectly caused by stroke. Recent development of BCI-based neurorehabilitation has proved beneficial in helping the patients to restore their motor control, which was damaged by stroke and/or other brain injury or degeneration [2, 3]. Among all the BCI-based neurorehabilitation mechanisms, motor imagery induced sensorimotor rhythm (SMR) is probably the most pronounced brain signature, which has been largely applied to interface with rehabilitation hardware or robots for neurorehabilitation process [1, 4]. Although such SMR feature is ubiquitous across different brain imaging modalities, such as functional magnetic resonance imaging (fMRI), electroencephalography (EEG), and magnetoencephalography (MEG), EEG is so far the most preferable modality for this purpose, due mainly to the cost and availability [4, 5].

However, the form factor of most currently available EEG devices is still too bulky for portable or even wearable requirement for neurorehabilitation process. In addition, the wires connecting the EEG electrodes and the signal acquisition computer could be an obstacle to the EEG-based neurorehabilitation device as they can accidentally be caught by the moving arms of the device and thus disrupt the rehabilitation process. As a result, wireless transmission of digitized EEG data to the feature extraction module for looking for SMR patterns can be valuable to make the rehabilitation process smooth [6]. On the other hand, given that the source of SMR is known to be present in the sensorimotor and superior parietal cortices and can be extracted using scalp EEG with electrodes placed on the locations near C3 or C4 or both [7, 8]. Therefore, an EEG system with three to four channels should be more than enough for the SMR-based BCI neurorehabilitation application. It is thus possible to devise a light-weighted, wearable wireless EEG acquisition and analysis system to monitor the onsets and offsets of SMR features and integrate into a rehabilitation device or robot for controlling the ON

and OFF of the movement of the device. Such a combination might largely alleviate the limitations on the degree of freedom of rehabilitation hardware or robot and allow more versatile rehabilitation processes.

II. METHODS

A table bike was connected to a newly developed high-quality wireless 4-ch EEG recording system and an EEG signal translation module to continuously record high-quality EEG from the scalp at C3/C4 region, extract the motor-imagery induced sensorimotor rhythm (SMR) feature in the EEG data, and translate the EEG feature into control signal to turn on/off the table bike. The wireless 4-ch EEG system samples EEG signal at 2K Hz with 24-bit resolution and transmits the digitized EEG signals wirelessly through Bluetooth 2.0 protocol to a signal acquisition module, such as a laptop or a smart phone. In addition, the wireless EEG device provides extremely high quality EEG signals with input referred noise of 1.5 μ V, which outperforms most of the existing wireless EEG systems. The device itself weights about 22 g, suited for the applications in need of portable or even wearable EEG device.

The brain signal translation module receives digitized EEG signals from the wireless 4-ch EEG system and extracts the motor imagery induced event-related desynchronization of EEG sensorimotor rhythm as features. Finally, it translates result of detection into control commands to turn ON and OFF the table bike. The speed of the table bike movement was preprogrammed by the rehabilitation physician to fit the different requirements for different stroke patients. Although the current form factor of the table bike might not be optimal for neurorehabilitation process for stroke patients, the light-weighted wireless EEG and brain signal translation module can be easily adapted to any forms of rehabilitation devices. As a result, it can fit the requests of most rehabilitation physicians for devising the most suitable rehabilitation protocol for each individual stroke patient.

To evaluate the feasibility of the mind-controlled table bike, we conducted a pre-clinical test on 12 healthy normal subjects (5 female and aged 30 +/- 5 yrs., recruited from National Chiao Tung University campus) and one young (30 yr.) chronic stroke patient (6 mo. after stroke attack, recruited from China Medical University Hospital, CMUH). The experimental protocol was as follows: First, a 2-sec resting period was cued with a white cross at the center of a computer screen to ask subject to pay attention to the study as the task cue would be delivered any time soon. Then an execution cue (green disk) was delivered at the center of computer screen for 6 secs to ask subject to start motor imagery by imagining he/she is pushing the table bike forward using his/her hands without physical hand movements. If the subject could successfully move the table bike in the motor imagery trial, it was counted as a successful move; otherwise, it was counted as a failed move. The percentage of successful movement was used to evaluate the feasibility of the devised mind-controlled table bike. Informed consents were obtained from all subjects before the experiment. CMUH IRB approved the experimental protocol.

III. RESULT

For the 12 healthy normal subjects, the success rate was 80.06%. Among the 12 subjects, 7 of them had finished 4 additional runs of experiments in separate occasions (within two-month duration). The average success rates for all subjects were 82%, 86%, 92%, 67%, 79%, 74%, 74%, respectively. For the young stroke patient recruited from CMUH, fMRI of the same type of motor imagery task and diffusion tensor images (DTI) of this patient were used to determine the optimal scalp channel location. After the channel location had been determined, the patient participated in the motor imagery task and finished one session of experiment. The success rate of this patient was higher than 81%.

IV. DISCUSSION

In this study, we demonstrated an integrated work to interface a commercially available table bike for neurorehabilitation process with an ultra light-weighted, wearable wireless 4-ch EEG device and an EEG translation module to extract SMR signatures from the digitized EEG signals. Both the wearable wireless EEG module as well as the EEG translation module were designed and developed by our group. The output of the EEG acquisition and translation modules could be used to trigger ON and OFF the table bike for facilitating the BCI-based neurorehabilitation process. Finally, we conducted a motor imagery experiment to evaluate the feasibility of the devised BCI-based EEG-controlled table bike. The percentage of successfully detecting the SMR induced by the motor imagery and moving the table bike accordingly was used to rate the performance of the devised EEG-controlled table bike. Although the current study was mainly tested on the normal subjects, it is possible to translate the results of this work to clinical settings and help the patients after stroke attacks to regain the controls, at least in part, over their peripheral muscles.

The previous study showed that the accuracy of sensorimotor rhythm (SMR) feature detection might vary from subject to subject due partly to individual differences in the anatomies of sensorimotor cortex [2]. In our result, we did show individual differences in the performance in terms of success rate across different subjects. However, within the same subjects, the success rates were quite reproducible across different visits. It is also worth noting that the average success rate for this study was higher than the results as reported previously. This is mainly because that in our test result, only the 'move' condition was used and thus could bias the performance toward higher success rate for moving the device. That is, subjects and/or patients could maintain their performance to move the table bike without switching to the OFF mode for stopping movement. It was relatively easier for the subjects/patient to perform continuously the motor imagery task without alternating their mind between 'move' and 'stop' conditions as was reported in previous study. Nonetheless, the protocol with such a high success rate might be preferable from the standpoint for encouraging stroke patients and easing their training.

Although the reported wireless EEG-based neurorehabilitation device achieved such a high success rate among the normal subjects participated in this study, two major problems associated with the report device still largely concerned us: (1) what type of stroke patients can most benefit from the reported device, and (2) where is the best site on the scalp to place the EEG electrode such that the SMR features can be easily extracted for controlling the rehabilitation device? To answer the first question, we are currently incorporating the diffusion tensor imaging (DTI) technology to evaluate the integrity of the fiber tracts after stroke onset. We hypothesize that only the patients with the downstream fiber tracts intact or less contaminated by stroke attack might best benefit from the wireless EEG-based neurorehabilitation device. Thus, we are evaluating the integrity of the downstream fiber tracts of stroke patients and trying to establish a protocol for screening patients for the proposed rehabilitation process.

On the other hand, we are also testing the process to determine the best EEG electrode placement to extract the SMR features from the patients' scalp with either whole-head EEG or functional magnetic resonance imaging (fMRI) or even their combination. For EEG process, we are to wire patient with a 64-channel EEG device with whole-head coverage and run through the motor imagery and/or motor observation tasks (depending on if the patient is able to perform motor imagery task or not). As the C3 and C4 locations might become suboptimal after stroke attack, we will then search among the whole head and find out which channel(s) contains most promising SMR features for the further use. This can be the most straightforward way to figure out the best channel location(s) for the proposed neurorehabilitation process, but the process can be tedious given that patients might have some difficulties and concerns about capping for EEG recordings. Alternatively, we are to determine the best location(s) to place the EEG channels using fMRI examination, where patients are placed in an MRI scanner and asked to perform motor imagery and/or motor observation tasks. The scalp locations correspond to the fMRI activation patterns can be the target channel locations for extracting the SMR features. However, such an examination can be expensive and may add extra loading to the patients and their families. Incorporating the fMRI session with the regular follow-up examinations might be a potential solution.

Although the devised rehabilitation table bike with wearable wireless EEG frontend has been successfully

applied to one young chronic stroke patient, it is still too early to draw a conclusion regarding the effectiveness of the rehabilitation device. First, given that the patient participated in this test was young and thus with above average motivation to involve in any possible training protocol so as to help her recover from the stroke attack as much as she can. As a result, the test on this patient only might favor the reported wireless EEG-based neurorehabilitation device. As a result, the conclusion can only be drawn after a large-scale clinical trial. In this end, we are to propose a clinical trial protocol to our hospital to conduct a large-scale clinical trial with well-controlled patient population, stroke phase, and protocol. In so doing, we hope to prove the effectiveness of the reported neurorehabilitation device on improving the recovery from the disabilities in the limbs caused by stroke attack.

ACKNOWLEDGMENT

This work has been supported in part by the "Aim for the Top University Plan" of National Chiao Tung University and Ministry of Education of Taiwan.

REFERENCES

- [1] J. J. Daly and J. R. Wolpaw, Brain-computer interface in neurological rehabilitation, *Lancet Neurol.*, vol. 7, pp. 1032-1043, 2008.
- [2] G. Pfurtscheller, C. Neuper, G. R. Muller, Graz-BCI: state of the art and clinical applications, *IEEE Trans. Neural Syst. Rehabil. Eng.*, vol. 11, pp. 177-180, 2003.
- [3] J. N. Mak and J. R. Wolpaw, Clinical applications of brain-computer interfaces: Current state and future prospects, *IEEE Rev. Biomed. Engr.*, vol. 2, pp. 187-199, 2009.
- [4] N. Nirbaumer and L. G. Cohen, Brain-computer interfaces: communication and restoration of movement in paralysis, *J. Physiol.*, Vol. 579, pp. 621-636, 2007.
- [5] J. J. Daly, R. Cheng, J. Rogers, K. Litinas, K. Hrovat, and M. Dohring, Feasibility of a new application of noninvasive brain computer interface (BCI): A case study of training for recovery of volitional motor control after stroke, *J. Neurological Physical Therapy*, vol. 33, pp. 203-211, (2009).
- [6] C. T. Lin, L. W. Ko, J. C. Chiou, J. R. Duann, R. S. Huang, S. F. Liang, T. W. Chiu, and T. P. Jung, Noninvasive neural prostheses using mobile and wireless EEG, *Proceedings of the IEEE*, vol. 96, pp. 1167-1183, 2008.
- [7] G. Pfurtscheller, C. Neuper, C. Brunner, and F. Lopes da Silva, Beta rebound after different types of motor imagery in man, *Neurosci. Lett.* vol. 378, pp. 156-159, 2005.
- [8] A. Solodkin, P. Hlustik, E. E. Chen, and S. L. Small, Fine modulation in network activation during moroe execution and motor imagery, *Cerebral Cortex*, vol. 14, pp. 1246-1255, 2004.

How Robust the Motor Imagery Induced EEG Sensorimotor Rhythm can be Extracted: A Test from a Cohort of Normal Subjects

Jeng-Ren Duann^{1,2,3}, Tien-Fu Chang⁴, Yung-Jiun Lin¹, Jin-Chern Chiou^{1,4}

¹Biomedical Engineering Research Center, China Medical University, Taichung, Taiwan

²Institute of Clinical and Medical Science, China Medical University, Taichung, Taiwan

³Institute for Neural Computation, University of California San Diego, CA 92093, USA

⁴Institute of Electrics and Control Engineering, National Chiao Tung University, Hsinchu, Taiwan

duann@sccn.ucsd.edu, stevechang10000@yahoo.com.tw,
t18628@mail.cmuh.org.tw, t17988@mail.cmuh.org.tw

Abstract—This study tested the robustness of the sensorimotor rhythm (SMR) features induced by motor imagery task and compared the result to those of other motor tasks, such as motor execution and observation. Thirteen subjects participated in the study and performed 5 runs of motor tasks with three different motor conditions (imagery, execution, and observation). Each run consisted of 15 motor task trials (5 for each motor condition), cued in a random sequence. 64-ch EEG was recorded while subjects performed the motor tasks. The separate runs of EEG data were concatenated and processed using independent component analysis (ICA) to separate the motor components from other brain or non-brain sources (including artifacts). Equivalent independent components from different subjects were selected using a K-means clustering method based on the features summarized from dipole location, time-frequency response, as well as scalp map. Finally, the average alpha (8-13 Hz) power changes were computed according to the motor conditions. The significance level of the event-related desynchronization (ERD) as compared to the baseline prior to the motor cue onset and the duration with significant ERD were compared across different motor conditions. Our result showed that no significant difference in terms of onset of motor induced ERD among the three motor conditions (around 370 ms after motor cue onset). However, the level of ERD was most pronounced for the motor execution condition (around -8 dB from the baseline). Both motor imagery and motor observation had similar level of the motor induced ERD. For the onset duration of the motor induced ERD, motor execution also showed the longest duration of alpha power decrease as compared to two other motor conditions. Both motor imagery and motor observation had much shorter duration of alpha power decrease; however, motor imagery elicited slightly longer ERD. As a result, the SMR-based BCI-controlled neurorehabilitation using a motor imagery should be quite challenging, if not impossible, for extracting SMR feature in real time given such a limited duration of the alpha ERD induced by the motor imagery.

Keywords—sensorimotor rhythm (SMR); motor imagery; EEG; brain-computer interface (BCI); neurorehabilitation; event-related desynchronization (ERD); independent component analysis (ICA)

I. INTRODUCTION

BCI based neurorehabilitation process has been reported beneficial for the stroke patients in helping them to recover their motor control, which was damaged after stroke attack [1, 2]. Among the BCI neurorehabilitation protocol, sensorimotor rhythm (SMR) based BCI has been widely adopted in a variety of neurorehabilitation to restore the motor control function of stroke patients [3]. However, the effectiveness of the SMR-based BCI being used for controlling a rehabilitation device has yet been rigorously evaluated in the past. As a result, the outcomes of SMR-based neurorehabilitation seemed quite inconclusive in the literature [4, 5]. In this study, we empirically compared the SMR induced by motor imagery to those induced by real motor execution (grasping) as well as watching the video clip of someone grasping. The result should lend itself guidance for devising an SMR-based neurorehabilitation apparatus.

This article is organized as follows: The next section, Methods, gives the details regarding the subject population, experimental protocol, data acquisition, and data analysis. The third section presents the details of the result of the data analysis, including the ICA component selection as well as the grand average of the sensorimotor responses induced by motor imagery as compared to the other types of motor tasks. Finally, we project the future work based on our findings for devising an SMR-based BMC-controlled neurorehabilitation apparatus to improve the progress of rehabilitation for the patients after stroke attack and/or brain injury.

II. METHODS

A. Subjects

Thirteen normal healthy right-handed subjects (with mean age of 24±3 years old) participated in this study. All subjects were recruited on the campus of National Chiao Tung University, Hsinchu Taiwan and with neither history of neurological diseases nor central and peripheral nervous system injury prior to the experiment. None of them had experience with BCI neural feedback before. All subjects gave signed written consent before experiment. The

Institutional Review Board (IRB) of China Medical University and Hospital, Taichung Taiwan, approved the experimental protocol.

B. Experimental Design

To compare the differences in the SMR induced by different motor tasks, an EEG experiment consisted of three types motor tasks, namely, motor execution, motor imagery, and motor observation was used. During motor execution trials, subjects were requested to physically grasp with their left (nondominant) hand slowly within a 3-sec window. During motor imagery trials, subjects were supposed to imagine they are grasping slowly with their left hand, without physical movement, in a 3-sec window. Likewise, during motor observation trials, a video clip of someone grasping slowly with his left hand in a 3-sec window was played and subjects were requested to watch carefully the video clip without any physical movement. The video showed only a left hand portion with no other body parts.

Each EEG bout consisted of 15 trials, five for each of the three motor conditions. Each trial started with 1 sec resting period as baseline and a white cross was displayed at the center of computer screen for subjects to fixate. Then, a visual cue with one of the three conditions (“grasp”, “imagine grasping”, and “watch grasping”) was displayed at the center of a computer screen for 3 sec for subject to perform the motor tasks (motor execution and imagery) accordingly, except for motor observation condition, in which a 3-sec grasping video was played instead and subjects were requested to watch the video clip attentively. Finally, 2-sec OFF-period followed by a 1-3 s interstimulus interval (ISI) was appended to form an 8-sec window for each trial. This resulted in a 120-sec long EEG bout. Four EEG bouts comprised an EEG session and 60 trials (15 trials x 4 bouts, 20 trials for each motor condition) were collected in total.

C. EEG Acquisition

The EEG data were acquired using a Neuroscan SynAmp2 (Compumedics Ltd., Victoria, Australia) with 64 channels, including two EOG channels. To monitor eye movements, the horizontal EOG was recorded from electrodes at the outer canthi of both eyes; the vertical EOG was recorded from the electrodes above and below the left eye. All electrodes were referenced to the linked mastoids and the ground electrode was placed at the location AFz. Electrode impedances were maintained below 5 K Ω before recordings. The EEG was recorded with a pass-band of 0.1 - 250 Hz and digitized at 1000 Hz sampling rate.

D. Data Preprocessing

An experienced EEG experimenter first inspected the acquired EEG signals from each individual subject and removed bad channels and the EEG portions that are highly contaminated. After being band-pass filtered with pass band of 0.1 - 50 Hz, data from the four EEG bouts were downsampled to 100 Hz and concatenated into one unified EEG data. The preprocessed EEG data were then segmented

into 4-sec epochs, -1 sec prior to and 3 sec after motor cue onsets.

E. ICA and Clustering

For each of the individual subjects, all 60 motor event-related EEG epochs were concatenated and the two eye channels were excluded from the further independent component analysis (ICA). The ICA decomposition was conducted using an infomax ICA algorithm as implemented in EEGLAB (<http://scn.ucsd.edu/EEGLAB>) [6]. It was to separate the independent brain EEG processes from those of artifactual components, such as eye artifacts (blinking and lateral eye movements), muscle activities, environmental noises, etc. The EEG data of 12 out of the 13 subjects were decomposed into 62 independent components (ICs) and one with 61 channels, due to one bad EEG channel having been removed prior to ICA decomposition.

After ICA decomposition, source localization process using the DIPFIT2 toolbox in the EEGLAB was used to select the SMR components [7]. Given that the independent EEG components are mostly dipolar, the ICs with residual variance larger than 15% using a single dipole fit were removed from the further data analysis [8]. This process removed 525 ICs from the original 805. The removed ICs were those with single-channel activation topography or EEG topography could not be accounted for by single dipoles. It should not affect the identification of right SMR components because, in general, the SMR component can be well explained by a single dipole.

The remaining 280 ICs from all 13 subjects were then clustered into equivalent component clusters to investigate the common EEG processes from the group of subjects. Here, we mainly used the feature of cluster analysis in EEGLAB study function. First, the feature variables (FVs), consisted of component topography, component event-related time-frequency (TF) plot (defined as event-related spectral perturbation, ERSP, in EEGLAB), and x -, y -, and z -coordinates of dipole location, were computed. Among the FVs, the component map was the inverse of the unmixing matrix obtained in ICA decomposition; the ERSP was computed by wavelet transformation with 3-cycle window lengths and 50% window overlap to convert the time-domain signals to a time-frequency plot. The FVs of component topography and ERSP were then summarized using principal component analysis (PCA) to reduce the dimension to 10 principal components for each FV. Finally, K-mean clustering algorithm was used to categorize, based on the 23-dimension feature space (10 each for component topography and ERSP and 3 for dipole location), the ICs into 15 clusters with an additional outlier cluster to put those ICs without being assigned into any of the 15 clusters [9].

The 15 clusters were visually inspected to find the cluster with average component topography mainly covering the right motor areas. Then, average component ERSPs across all the ICs within the same clusters were computed such that to determine the main frequency band for SMR components. As a result, one cluster best represented the right SMR activity was selected. In the selected right SMR cluster, some subjects may contribute more than one component. Thus, a

final adjustment was performed by comparing the mean ERD profiles in the alpha band (8-13 Hz) derived from the component ERS of each component. The purpose was to ensure each subject only contributed one equivalent IC to the selected cluster.

F. Statistical Analysis

After SMR component cluster had been identified, the conditional ERDs in the alpha frequency were computed according to the types of motor tasks for each individual subject. Then, the grand mean conditional ERDs were averaged across all 13 subjects. The level and duration of alpha power decrease from the baseline before the cue onset of the right SMR EEG components were compared across different motor conditions. Further, the onset timings of the alpha power decrease were computed for the conditional ERDs of each individual subject by finding the time (in ms) at which the ERD reach half of the amplitude of alpha power decrease from the baseline. The significance of the differences in onsets of alpha power decrease between any two of the motor conditions was estimated using a paired two-sample t-test.

III. RESULT

After ICA decomposition and component clustering, one of the 62 ICs (one of the 13 subjects came only with 61 components because one bad channel had been removed before ICA decomposition) was selected into the right SMR cluster from all 13 subjects. Finally, the average power changes of all three motor conditions within the alpha frequency band (8-13 Hz) were computed for each subject.

The results showed that all three motor conditions elicited significant alpha power decrease (event-related desynchronization, ERD) starting around 370 ms as compared to the baseline. The onset timings of alpha power ERD for all three motor conditions were comparable. However, motor execution condition elicited the largest ERD (around -8 dB from baseline) and the ERD lasted for up to few seconds. On the other hand, the ERD elicited by the motor imagery and motor observation conditions were quite comparable with the ERD induced by the motor imagery slightly larger and longer than that by the motor observation.

IV. DISCUSSION

To our knowledge, this is the first study rigorously testing the robustness of the ERD in alpha frequency band elicited by the motor imagery task as compared to the motor execution and motor observation. More importantly, it is also the first study using ICA to separate the sensorimotor rhythm (SMR) from other brain and non-brain sources/artifacts, so that we would be able to look into the pure SMR activity elicited by different motor conditions without interference from other unrelated components. As a result, this study lends itself a standard to test how robust the motor imagery induced alpha ERD as being used for BCI control.

In our preliminary result, it showed that all three motor conditions could successfully elicit ERD in the alpha frequency band with similar onset timings from the motor

cue. At the first glance, the alpha ERD elicited by motor imagery was quite limited with much lower level of suppress (almost half the amplitude) as compared to the motor execution condition. In addition, the onset duration of alpha ERD induced by motor imagery was also much shorter than that of motor execution. This means that the translation module to extract the SMR features elicited by motor imagery process will need to be sensitive enough to find the small amplitude changes within the alpha frequency band, and fast enough to determine the presence of alpha ERD after motor imagery. This should raise some difficulties over devising an SMR-based BCI-controlled neurorehabilitation apparatus.

However, the result is currently yet conclusive, as we will still need to complete the data analysis on all 13 subjects. As we expected that the result of this study gives the best scenario of SMR changes elicited by motor imagery, which is the most commonly used brain signal features for neurological rehabilitation process currently. Therefore, the result presented here should be able to provide a guideline for devising an SMR-based BCI controlled neurorehabilitation apparatus.

ACKNOWLEDGMENT

This work is supported in part by the "Aim for the Top University Plan" of National Chiao Tung University and Ministry of Education of Taiwan and NSC 100-2218-E-039 - 001.

REFERENCES

- [1] E. Buch, C. Weber, L.G. Cohen, C. Braun, M.A. Dimyan, J. Mellinger, A. Caria, S. Soekadar, A. Fourkas, and N. Birbaumer, Think to move: Neuromagnetic brain-computer interface (BCI) system for chronic stroke, *Stroke*, 39:910-917, 2011.
- [2] J.J. Daly and J.R. Wolpaw, Brain-computer interfaces in neurological rehabilitation, *Lancet Neurol.* 7:1032-1043, 2008.
- [3] G. Pfurtscheller, C. Neuper, G. R. Muller, Graz-BCI: state of the art and clinical applications, *IEEE Trans. Neural Syst. Rehabil. Eng.*, vol. 11, pp. 177-180, 2003.
- [4] G. Pfurtscheller, C. Neuper, C. Brunner, and F. Lopes da Silva, Beta rebound after different types of motor imagery in man, *Neurosci. Lett.*, vol. 378, pp. 156-159, 2005.
- [5] A. Solodkin, P. Hlustik, E. E. Chen, and S. L. Small, Fine modulation in network activation during motor execution and motor imagery, *Cerebral Cortex*, vol. 14, pp. 1246-1255, 2004.
- [6] A. Delorme and S. Makeig, EEGLAB: An open source toolbox for analysis of single-trial EEG dynamics including independent component analysis, *J. Neurosci. Method*, 134:9-21, 2004.
- [7] R. Oostenveld and P. Praamstra. The five percent electrode system for high-resolution EEG and ERP measurements. *Clin Neurophysiol*, 112:713-719, 2001.
- [8] A. Delorme, J. Palmer, J. Onton, R. Oostenveld, and S. Makeig, Independent EEG sources are dipolar, *PLoS One*, vol. 7, e30135, 2012.
- [9] D. Lelic, M. Gratkowski, K. Hennings, and A. M. Drewes, Multichannel matching pursuit validation and clustering – A simulation and empirical study, *J. Neurosci. Method*, vol. 196, pp. 190-200, 2011.

Fundamental Study to New Evaluation Method Based on Physical and Psychological Load in Care

Hiroaki Inoue/Tokyo University of Science, Suwa
Research course of Engineering/Management
Chino-city, Japan
jgh12701@ed.suwa.tus.ac.jp

Shunji Shimizu/Tokyo University of Science, Suwa
Department of Electric Systems Engineering
Chino-city, Japan
shun@rs.suwa.tus.ac.jp

Noboru Takahashi/Tokyo University of Science, Suwa
Research course of Engineering/Management
Chino-city, Japan
sr1@ed.suwa.tus.ac.jp

Hiroyuki Nara/Hokkaido University
Graduate School of Information Science and Technology
Sapporo-city, Japan
nara@ssc.ssi.ist.hokudai.ac.jp

Takeshi Tsuruga/Hokkaido Institute of Technology
Department of Clinical and Rehabilitation Engineering
Sapporo-city, Japan
tsuruga@hit.ac.jp

Fumikazu Miwakeichi/The Institute of Statistical Mathematics
Spatial and Time Series Modeling Group
Tachikawa-city, Japan
miwake1@ism.ac.jp

Nobuhide Hirai/Jichi Medical University
Department of Psychiatry
Shimotsukeshi-city, Japan
nobu@nobu.com

Senichiro Kikuchi/Jichi Medical University
Department of Psychiatry
Shimotsukeshi-city, Japan
skikuchi@jichi.ac.jp

Eiju Watanabe/Jichi Medical University
Department of Neurosurgery
Shimotsukeshi-city, Japan
eiju-ind@umin.ac.jp

Satoshi Kato/Jichi Medical University
Department of Psychiatry
Shimotsukeshi-city, Japan
psykato@jichi.ac.jp

Abstract—Recently, Japan (also world-wide countries) has become aged society, and wide variety welfare device and system have been developed. But evaluation of welfare system and device are limited only stability, intensity and partial operability. So, evaluation of usefulness is insufficient. Therefore, we will attempt to establish the standard to evaluate usefulness for objectively and quantitatively on the basis of including non-verbal cognition. In this paper, we measure load of sitting-standing operation to use EMG and 3D Motion Capture and set a goal to establish objective evaluation method. We think that establishing objective evaluation method is necessity to develop useful welfare device. We examined possibility of assessing load and fatigue from measuring brain activity to use NIRS.

Keywords- Evaluation; Movement; Exercise; 3D Motion Capture; NIRS; EMG; Care; Welfare Technology; Usefulwelfare device evaluation; Evaluation method.

I. INTRODUCTION

As increasing aging population in Japan and world-wide countries, welfare systems and devices based on the increased popularity of welfare device and system. Also the market of

welfare system and device are expanding. However, the evaluation method is limited respectively to stability, strength and a part of operability for individual system or device. It means that evaluation methodology for usefulness of them dose not established. Therefore, we will attempt to establish the standard to evaluate usefulness for objectively and quantitatively on the basis of cognition such as physical load, reduction of fatigue and postural stability. Especially, in considering universality, it is necessary to measure human movement in daily life. Movement was not measured by using particular device, but routinely-performed movement in daily life.

So, we examined the possibility of evaluation by measuring physical load due to activities of daily living with using 3D Motion Analysis System and EMG. Also, we looked into the possibility of quantitative evaluation of tiredness and load on the basis of brain activity using NIRS. Also, we consider that physical and psychological load are linked to cognition including non-verbal cognition. In this paper, the purpose of experiments are to evaluate motion focusing on sitting and standing movement which is usually done in our life by using 3D Motion Analysis System, EMG, NIRS. We consider that human feel physical and psychological load during life motion.

We tried to measure physical load by using 3D Motion Analysis System, EMG. And, we tried to measure non-verbal cognition about psychological load by using NIRS.

II. EXPERIMENTAL METHOD

A. Evaluation by using 3D Motion Analysis and EMG

We simultaneously measured 3D position and muscle potential of subject during task by using 3D Motion Analysis System (nac IMAGE TECHNOLOGY Inc. products-MAC3DSYSTEM [1]) and EMG(KISSEI COMTEC Inc. products-MQ16 [2]).

Regarding to measuring 3D position, 8 Infrared cameras were placed around subject and 27 markers of the body surface were set on the basis of Helen-Hayes(Fig. 1). In measuring muscle potential, measurement regions were tibialis anterior muscle, gastrocnemius muscle, quadriceps femoris muscle, hamstring, flexor carpi ulnaris muscle, extensor carpi ulnaris muscle, triceps brachii, latissimus dorsi muscle of the right side of the body because these muscle were deeply associated with standing and sitting movement. Also, wireless measurement was used so that subject was constrained as little as possible. Sampling frequency of 3D Motion Analysis System and EMG was 100Hz and 1kHz, respectively.

Subjects were three males aged twenties. They were asked to read and sign an informed consent regarding the experiment.

In this experiment, subject repeated one series of movement, which was to transfer from chair to seat face of welfare device (IDEA LIFE CARE Co. Ltd products-NORISUKEsan [3]) and opposite one with alternating between standing and sitting, at five times per one measurement. Seating face of welfare device, which was designed to assist transfer movement, was manipulated by simple method and appeared on the top of chair.

Subjects were heard buzzer every one second and kept a constant motion of speed to satisfy certain measuring conditions. Also, they transferred from seat face to chair or conversely every 8 seconds with consideration for movement of elderly persons. Operation of welfare device was performed by operator other than subject.



Figure 1. Experimental View of 3D motion Analysis and EMG

B. Evaluation by using NIRS

We measured brain activity during motion with the purpose of establishing evaluation method based on generality (Fig. 2).

Subjects were six males aged twenties. They were asked to read and sign an informed consent regarding the experiment. Measurement apparatus was NIRS(SHIMADZU CO. Ltd products-FOIRE3000 [4]). Measurement region was at right and left prefrontal cortex.

1) Measuring Brain Activity during transfer with Standing position(task1)

At this measurement, subject used welfare device to perform transferring in a standing position. In this measurement, subject sat on seating face of welfare device appeared on the top of chair after raising hip until kneeling position. Also, subject performed inverse transferring from seating face to chair. Time design was rest(5 seconds)-task(10 seconds)-rest(5 seconds). This time design was repeated 30 times.

2) Measuring Brain activity during transfer with half-crouching position (task2)

At this measurement, subject used welfare device to perform transferring in a half-crouch position. In this measurement, subject sat on seating face of welfare device appeared on the top of chair after raising hip until kneeling position. Also, subject performed inverse transfer from seating face to chair. Time design was rest(5 seconds)-task(10 seconds)-rest(5 seconds). This time design was repeated 30 times.

In experiments of task1 and task2, operation of welfare device was performed by operator other than subject. Before this measuring, subjects adjusted to transferring by use of welfare device.

3) Measuring brain activity during keeping a half-crouch position(task3).

Subjects performed two tasks at this measurement. During task3-1, subject sat on seating face of welfare device with eyes open. During task3-2, they kept a half-crouch position.

Subjects alternated task3-1 and task3-2. Also, subjects took resting time between two types of motion with eyes close. Therefore time design was rest(5 seconds)-task3-1(10 seconds)-rest(5 seconds) – task3-2(10 seconds)-rest(5 seconds). This time design was repeated 15 times.



Figure 2. Experimental View of NIRS

III. EXPERIMENTAL RESULT

A. Evaluation by using 3D Motion Analysis and EMG

Fig. 3 shows result of transferring which was measured by 3D motion analysis and EMG. In Fig. 3, middle trochanter is the height of midpoint between right and left trochanter from the floor. Trunk angle is the forward slope of trunk. Also, following terms are arectifying voltage wave for each eight muscles, which are Tibialis anterior muscle, Astrocnemius muscle, Quadriceps femoris muscle, Hamstring, Triceps brachii muscle, Etensor carpi ulnaris muscle, Flexor carpi ulnaris muscle and Latissimus dorsi muscle.

Next, analysis was performed by extracting muscle potential during standing and sitting movement from measuring result with reference to middle trochanter and trunk angle and calculating value of interal during movement. Table 1 shows the ratio of value integral with welfare device to one without device. Also, we compared moving distance of median point between using welfare device and not. Table 2 shows the comparison results in a manner similar to Table 1.

B. Evaluation by using NIRS

As common result of all subjects, oxy-Hb tended to increase during task and to decrease in resting state. Therefore, it was thought that change of hemoglobin density due to task was measured. Fig. 6 shows trend of the channel in which significant different was shown. Analysis was performed via one-sample t-test by a method similar to previous researches [5,6,7,8,9]. In this analysis, it was necessary to remove other than change of blood flow due to fatigue. So, our method was mainly focused on resting state to compare with the 1st trial and another trials of brain activity.

In task1 1 and 2, each of sample data for analysis was 4 seconds after the task(Fig. 4). In task 3, sample data was 4 seconds during task.(Fig. 5)

In the t-test of the same task, we performed t-test with first time trial and other trial which was from second times to thirty times, and examined relationship the number of trials and significant differences.

In task 1, significant different could be found from the about 10th trials. Fig. 9 show region confirmed significant different.

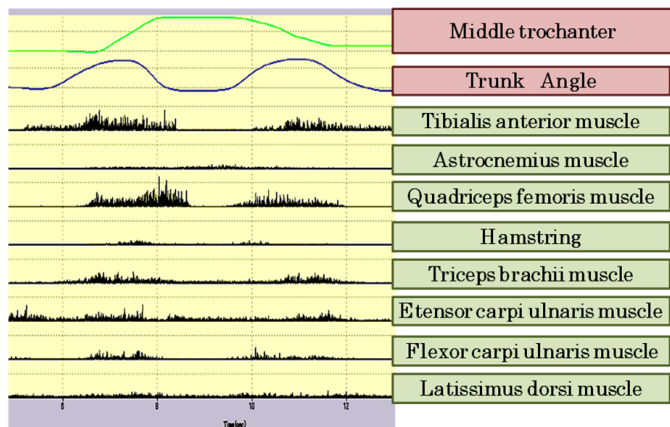


Figure 3. Result of 3D Motion Analysis and EMG

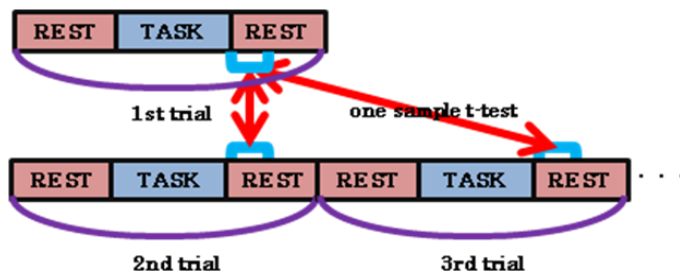


Figure 4. T-test of sample data of task1 and 2

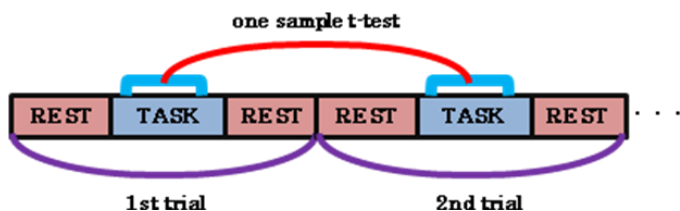


Figure 5. T-test of sample data of task3

TABLE I. COMPARISON OF INTEGRAL EMG

muscle	region	Subject1	Subject2	Subject3
Standing	Tibialis anterior muscle	0.37	0.49	0.64
	Astrocnemius muscle	0.83	0.78	0.97
	Quadriceps femoris muscle	0.66	0.36	0.81
	Hamstring	1.90	0.50	1.07
	Triceps brachii muscle	1.07	3.34	1.01
	Etensor carpi ulnaris muscle	1.08	1.31	0.96
	Flexor carpi ulnaris muscle	1.07	0.89	0.85
	Lattissimus dorsi muscle	0.98	0.87	1.20
Sitting	Tibialis anterior muscle	0.50	0.59	0.80
	Astrocnemius muscle	1.01	0.92	0.94
	Quadriceps femoris muscle	0.49	0.57	0.85
	Hamstring	2.16	1.60	0.96
	Triceps brachii muscle	0.89	0.96	1.07
	Etensor carpi ulnaris muscle	0.79	0.89	0.86
	Flexor carpi ulnaris muscle	0.79	0.86	0.95
Lattissimus dorsi muscle	1.16	1.18	0.93	

TABLE II. COMPARISON OF CHANGE IN MEDIAL POINT

	Subject1	Subject2	Subject3
Sitting	0.89	1.03	0.90
Standing	1.00	0.84	1.08

In task 2, significant different could be found from the about 10th trials too. Fig. 10 show region confirmed significant different.

Next, we performed t-test with case of standing position (task 1) and half-crouch position(task 2). In this analysis, significant different could be found at prefrontal area(14ch, 17ch, 28ch and 32ch). Fig. 11 show region confirmed significant different.

Also, two type of motion which was sitting and keeping a half-crouching position were repeated alternately in task 3. At first, we performed t-test using 4 seconds during first trial and 4 seconds during other trials which were from second to fifteenth in same position. Regarding to analysis result using sample data during sitting position and half-crouching position, there were significant different at Prefrontal area. Fig. 12 confirms significant different.

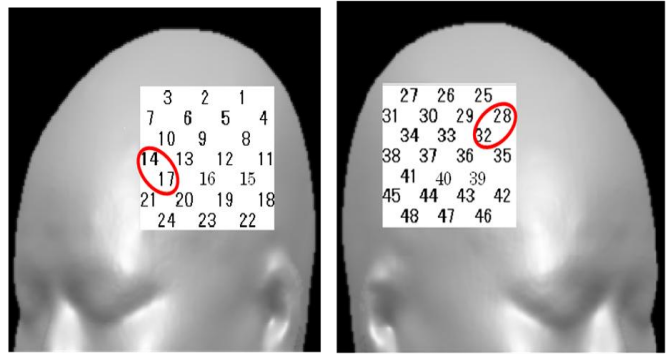


Figure 9. Signifiant Difference of task1

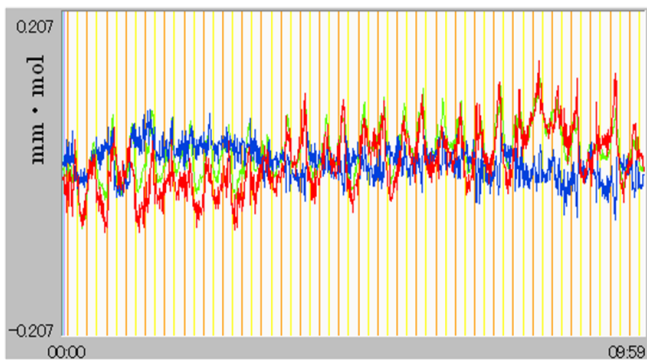


Figure 6. Measuring Result of Task1

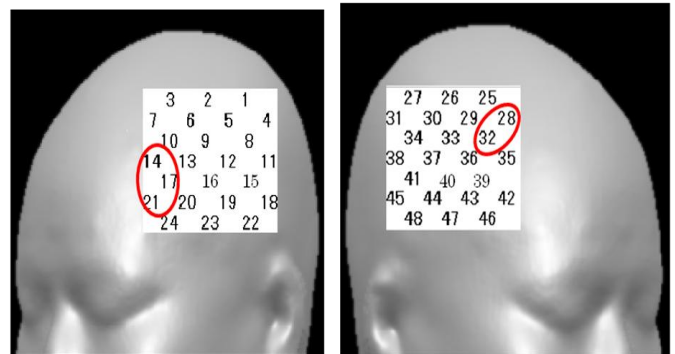


Figure 10. Significant difference of task2

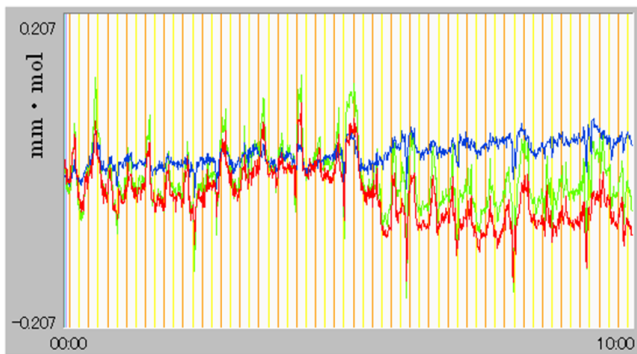


Figure 7. Measuring Result of Task2

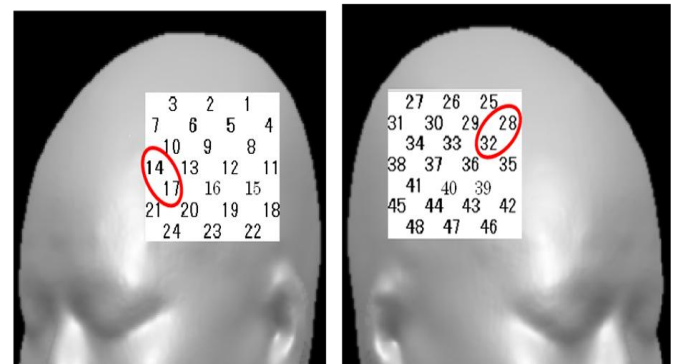


Figure 11. Significant Difference of task 1 and 2

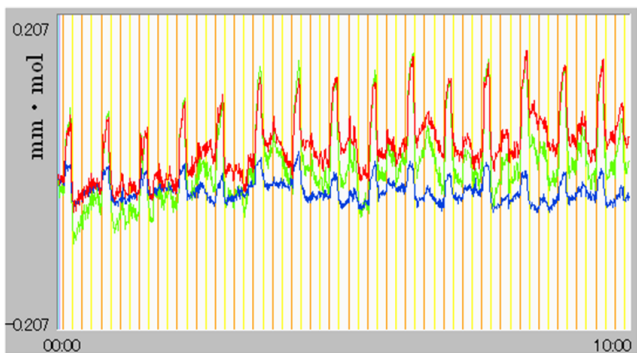


Figure 8. Measuring Result of Task3

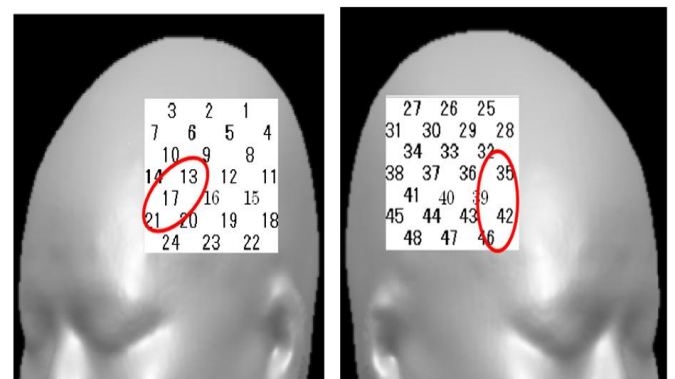


Figure 12. Significant Difference in sitting position

IV. DISCUSSION

1) Evaluation by using 3D Motion Analysis and EMG

From analysis result, it was shown that value of integral was decreased by using assistive apparatus for transfer. Especially, there was remarkable decrease in value of integral at tibialis anterior muscle, quadriceps femoris muscle. On the other hand, it was shown to be minor decrease in one at upper limb and muscles of the back. Also, moving distance of barycentric position was decreased by the use of welfare device.

On the ground of this result, it was thought to be due to difference in height between chair and seating face of welfare device. Therefore, it was thought that the use of assistive apparatus is useful to lighten burden on lower limb. Thus, it's contemplated that muscle load during standing and sitting movement was decreased and reduced centroid fluctuation to lower the possibility of turnover.

Even if subjects performed daily movements of standing and sitting with the use of assistive equipment, it was shown that the integral of muscle potential and distance of centroid change was decreased. Therefore, it was proved that there is the possibility of evaluation of daily performance except for movement with welfare device.

2) Evaluation by using NIRS

In this experiment, we tried to measure quantitatively the physical and psychological strain on the basis of brain activity. Also, we think that brain activity disclose human cognitive including non-verbal. As a result, it was shown that there were differences at brain activity due to number of trials and postural. In this time, analysis was performed via one-sample t-test using sample of brain activity in resting state during task or after task. Hence, analysis method was to remove disturbance such as body motion and angular variation of neck to the extent possible although there was the possibility to measure skin blood flow. Therefore, it was thought that strain due to tasks was quantitatively measured by being recognized significant differences

Also, in previous research, it was reported to decrease in activity in the brain around #10, 11 [10] as the result of measuring brain activity during Advanced Trial Making Test using PET [11]. Therefore, this result came out in support of previous research in no small part.

Of course, it is necessary to increase number of subject at the present stage. In addition, there are problems associated with experiment, number of subject, method and measured region. However, in terms of being recognized significant differences at brain activity due to movement, it was thought to show useful result in evaluating quantitatively daily movements.

V. CONCLUSION AND FUTURE WORK

In this experiment, our purpose was to evaluate quantitatively physical load with focusing on standing and sitting movement which was part of daily movements using 3D motion analysis system and EMG.

As the result, it was shown that the integral of lower-limb muscle, such as tibialis anterior muscle and gastrocnemius muscle, significantly decreased by the use of welfare device.

Also, it was reported that there is a positive correlation between anteversion angle of body trunk and movement duration

in previous research [12]. But, our experiment method was to estimate the possibility of falling in rising from a sitting position by calculating moving distance of median point. And, it was confirmed that the possibility of falling was decreased by using device.

Next, we tried to measure physical and psychological load quantitatively on the basis of brain activity. And there were significant differences due to number of trials, holding position. In this experiment, analysis method was to remove disturbance such as body motion and angular variation of neck to the extent possible by using measurement result in resting state as sample. Therefore, it was thought to show useful result in evaluating quantitatively load due to movement task by being recognized difference in brain activity caused by number of trials, substance of task and holding position.

Main purpose in this study is to evaluate physical load and fatigue quantitatively. So, we tried to evaluate change of muscle load due to difference of motion by simultaneous measuring with 3D motion analysis System and EMG quantitatively.

However, evaluation of psychological load is necessary, too. In terms of using welfare device, prolonged use must be taken into account. In this case, it is important to consider not only physical load but also psychological load due to prolonged use from standpoint of developing welfare device and keeping up surviving bodily function.

And, in previous research, separation between physical and psychological load has been performed. But, our view is that there is correlation with physical and psychological load. So, we tried to measure psychological load including physical one based on brain activity and quantitatively evaluate both load.

For the future, our aim is to establish method of discussing useful of welfare device by evaluating load involved in other daily movements with increasing number of subjects.

ACKNOWLEDGMENT

This research was supported as follow. There dimensional motion analysis and commodious room were provided from nac Image Techonogy Inc. EMG and analysis software were provided from KISSEI COMTEC. NIRS was provided from SHIMADZU COPPORATION. Developing welfare device was provided from IDEA SYSTEM CO., LTD. We are deeply grateful to them.

This study contributes to become the basis for one of theme of s-innovation program in Japan Science and Technology Agency which was named "Development Fatigue-reduction Technology for Social Contribution of Aged Person and Establishment System for Evaluation.

REFERENCES

- [1] Y. Shinoda, "Consideration of feature extraction based on center of gravity for Nihon Buyo dancer using motion capture system," SICE Annual Conference 2011, Tokyo Japan, pp. 1874-1878.
- [2] Y. Yamaguchi, A. Ishikawa, and Y. Ito, "Development of Biosignal Integration Analysis System for Human Brain Function and Behavior," Organization for Human Brain Mapping 2012, China.
- [3] H. Inoue, S. Shimizu, N. Takahashi, H. Nara, and T. Tsuruga "Fundamental Study for Evaluation of the Effect due to Exercise Load", Assistive Technology, Bio Medical Engineering and Life Support 2011, Japan.

- [4] E. Watanabe, Y. Yamashita, Y. Ito, and H. Koizumi, "Non-invasive functional mapping with multi-channel near infra-red spectroscopic topography in humans," *Neurosci Lett* 1996, Feb 16, 205(1), 41-4.
- [5] N. Takahashi, S. Shimizu, Y. Hirata, H. Nara, F. Miwakeichi, N. Hirai, S. Kikuchi, E. Watanabe, and S. Kato, "Fundamental Study for a New Assistive System during Car Driving," Proc. of International Conference on Robotics and Biomimetics, 2010, China.
- [6] N. Takahashi, S. Shimizu, Y. Hirata, H. Nara, H. Inoue, N. Hirai, S. Kikuchi, E. Watanabe, and S. Kato, "Basic study of Analysis of Human Brain Activities during Car Driving," the 14th International Conference on Human-Computer Interaction, 2011, USA.
- [7] S. Shimizu, N. Takahashi, H. Nara, H. Inoue, and Y. Hirata, "Fundamental Study for Human Brain Activity Based on the Spatial Cognitive Task," the 2011 International Conference on Brain Informatics-BI 2011, China.
- [8] S. Shimizu, N. Takahashi, H. Nara, H. Inoue, and Y. Hirata, "Basic Study for Human Brain Activity Based on the Spatial Cognitive Task," The Third International Conference on Advanced Cognitive Technologies and Applications, 2011, Italy.
- [9] S. Shimizu, N. Takahashi, H. Inoue, H. Nara, F. Miwakeichi, N. Hirai, S. Kikuchi, E. Watanabe, and S. Kato, "Basic Study for a New Assistive System Based on Brain Activity associated with Spatial Perception Task during Car driving," Proc. International Conference on Robotics and Biomimetics, 2011, Thailand.
- [10] Y. Watanabe, "Molecular/neural mechanisms of fatigue, and the way to overcome fatigue," *Folia Pharmacologica Japonica*, vol. 129, pp. 94-98, 2007.
- [11] H. Kuratsune, K. Yamaguti, G. Lindh, B. Evengard, G. Hagberg, K. Matsumura, M. Iwase, H. Onoe, M. Takahashi, T. Machii, Y. Kanakura, T. Kitani, B. Langstrom, and Y. Watanabe, "Brain Regions Involved in Fatigue Sensation: Reduced Acetylcarnitine Uptake in to the Brain," *Neuroimage*, vol. 17, pp. 1256-1265, November 2001.
- [12] K. Maruta, "The influence of Seat Angle on Forward Trunk Inclination During Sit-to-Stand," *Journal of Japanese Physical Therapy Association* vol. 31, No.1, pp. 21-28, 2004.

Geometry of Intentionality in Neurodynamics

Germano Resconi

Dept. of Mathematics and Physics
Catholic University
Brescia, Italy
resconi@speedyposta.it

Robert Kozma

Dept. of Mathematical Sciences
Computational Neurodynamics Laboratory
Memphis , TN 38152 USA
rkozma@memphis.edu

Abstract— Brains are the most complex systems in the known Universe and they are composed of simple neural units producing electrical impulses. The key contribution of this work is the use of geometric concepts for neural states, in terms of currents and voltages. In the introduced adaptive neuromorphic electrical circuit, we relate voltage with current using the conductance matrix or alternatively using the impedance matrix. After a change of reference system and introducing a new distance measure, we transform the initially linear relationships into a geodesic over the phase space. Every change of variables can be reproduced by a similar change of voltages into currents and vice versa with the help of the conductance or impedance matrices, respectively. Our geometric approach to neurodynamics can be applied to integrate digital computer structure with neuromorphic computing principles, which produces an efficient new computational paradigm.

Keywords- *Neurodynamics; Intentionality; Geometry of Cognition; Neuromorphic Computing ; Geodesic; Memristor.*

I. INTRODUCTION

This work proposes a mathematical formulation of intentional dynamics following Freeman's half century-long dynamic systems approach [1-4]. We consider the electrical behavior of the brain at the microscopic level and derive principle leading to higher cognition at the mesoscopic and macroscopic levels. In the past decades, artificial neural networks have been successfully employed. To model various brain functions such neural net models consist of a large number of high precision components, which leads scaling problems manifested in slow and often unstable learning, inefficient adaptation properties, and the need of external learning and control action. In this work, we aim at fast and stable learning and autonomous adaptation using low precision components. To achieve this goal we employ dynamical components, which are part of a closed feedback the loop with the outside world. The corresponding ordinary differential equations (ODEs) represent a stiff nonlinear system, which are very inefficient to solve on digital computers. An example is the IBM Blue Gene project with 4096 CPUs and 1000 Terabytes RAM [5]. To simulate the

Mouse cortex with 8×10^6 neurons, 2×10^{10} synapses at 10^9 Hz, this digital implementation requires 40 KW. The human brain has 10^{10} neurons and 10^{14} synapses; its clock frequency is 10 Hz and uses 20 W with its analog circuitry. Apparently, analog is more efficient than digital by many orders of magnitude.

The use of analog electrical circuits for neuromorphic computing with memristors could solve the problem of neural computation in the future. It is conceivable that learning effects so eloquently displayed by memristors are in fact manifestations of memristive behavior in the neural tissue [6-7]. In this case memristors indeed could be the *Holy Grail* of building brain like computers by exploiting the same mechanisms in computer memories as the ones brains employ. This possibility has enormous long-term consequences, which is difficult even to imagine from our present limited vantage point. Recall that for Turing the physical device is not computable by a Turing machine, which is the theoretical version of the digital computer. If we use analog systems, we do not need algorithms to program the neurons. Rather, the computer algorithm is substituted by the network dynamics evolving in phase space. For example, we can program the CrossNet [8-9] electrical system, which has been used to compute the parameters describing the desired trajectories. Geometrical and physical descriptions of Freeman's intentional neurodynamics are beyond algorithmic and digital computation. To clarify better the new computation paradigm, we observe that animals and humans have a very efficient mechanism to use their finite brains to comprehend and adapt to infinitely complex environment [1-3]. We show that this adaptive system conforms to a geometric interpretation. This gives us the possibility to implement the required parameters in ODE to achieve the desired intentional neurodynamics. In this work, we consider two aspects of intentionality, namely cognitive and physiological,, both are reflections of nonlinear brain dynamics. At the cognitive level, intentionality corresponds to the change of the reference system, while physiological intention is defined by neuro-dynamical processes. First we describe the brain connectivity structure as a material support or hardware that makes it possible to achieve the

required intentional transformation. The neural units are modeled by electrical circuits with capacitors and adaptive resistors and their dynamics is described by Ordinary Differential Equations (ODE). The solutions of these ODEs give the trajectory of the neural states as they evolve in time. ODEs are widely used in neural models, however they have shortcomings due to the difficulty of specifying the parameters and because their solutions cannot be found precisely in most practically relevant situations. In the introduced adaptive neuromorphic electrical circuit, we relate voltage with current using the conductance matrix or alternatively using the impedance matrix. Next, we introduce the change of reference system and a new distance measure, through which we transform the initially straight line into a geodesic over the phase space in the new reference. We show that every change of variables and reference can be reproduced by a similar change of the impedances and currents or voltages space coordinates and vice versa with the help of the conductance or impedance matrices, respectively, we can simulate by neural network (hardware) any change of reference or any change of variables (software). We conclude the work with discussion and outlining directions for future research.

II. INTENSION AND ELECTRICAL CIRCUIT

Because the brain is a complex electrical circuit with capacity and resistors, we think that it can express intentionality by suitable tune of the electrical parameters. The instrument to match intentionality with the dynamics neural mechanisms is the geometry in the space of the neural currents or voltages. We know that geometry is represented by the form of the distance in the given space. For example, in the Euclidean geometry the form is given by the straight line where the distance is the Euclidean distance; on the sphere, the form of the distance is a circle and the distance is the non Euclidean distance on the sphere. The form of the geometry in the electro dynamics neural mechanism is the trajectory of a point in the space of the currents or voltages. The distance in the geometry of the neural system is given by the square root of the instantaneous electrical power W as follows:

$$W = \sum_j i_j(v_1, v_2, \dots, v_p)v_j$$

and

$$i_j(v_1, v_2, \dots, v_p) \approx \sum_k \frac{\partial i_j}{\partial v_k} v_k = \sum_k C_{j,k} v_k \tag{1}$$

or

$$i = Cv, v = C^{-1}i = Zi, Z = C^{-1}$$

we have

$$\begin{aligned} W &= \sum_j i_j(v_1, v_2, \dots, v_p)v_j = \sum_{j,k} C_{j,k} v_k v_j = v^T Cv \\ &= (C^{-1}i)^T C(C^{-1}i) = i^T C^{-1}i = i^T Zi = \sum_{j,k} Z_{j,k} i_k i_j \end{aligned}$$

In equations (1) the first equation is the ordinary computation of the electrical power by currents and voltages. The second equation is the computation of the matrix of the conductance C for which from the current we compute the voltages. To obtain the matrix of conductance C , we expand the relation between voltages and currents in Taylor form and we stop at the first derivative. The other equations in (1) are obtained substituting the voltage current relation by the matrix C . Z is the impedance matrix. Now the power gives us the *material* aspect of the intentionality. The other part of the intentionality is the *conceptual* that is given by the wanted transformation

$$\begin{cases} y_1 = y_1(x_1, x_2, \dots, x_p) \\ y_2 = y_2(x_1, x_2, \dots, x_p) \\ \dots \\ y_q = y_q(x_1, x_2, \dots, x_p) \end{cases} \tag{2}$$

The transformation (2) can be compared with one statement in the digital computer where in input we have the x values and in output the y values. So, the (2) is a MIMO (many inputs many outputs) transformation or statement shown in Figure 1

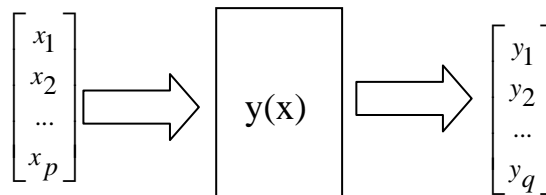


Figure 1 Transformation from input x into output y by MIMO $y(x)$,

We can have different examples of the transformation as linear transformation

$$\begin{cases} y_1 = m_{1,1}x_1 + m_{1,2}x_2 + \dots + m_{1,p}x_p \\ y_2 = m_{2,1}x_1 + m_{2,2}x_2 + \dots + m_{2,p}x_p \\ \dots \\ y_q = m_{q,1}x_1 + m_{q,2}x_2 + \dots + m_{q,p}x_p \end{cases} \quad (3)$$

where m are the linear parameters of the transformation (3). We can have also the non linear transformation as follows

$$\begin{cases} y_1 = (1 - x_1)x_2 + x_1(1 - x_2) \\ y_2 = x_1x_2 + (1 - x_1)(1 - x_2) \end{cases} \quad (4)$$

Here the first equation is connected with XOR and the second is connected with EQ logic relation. Given the system in Eq.2, the total differential of any equation in (2) are

$$\begin{cases} dy_1 = \frac{\partial y_1}{\partial x_1} dx_1 + \frac{\partial y_1}{\partial x_2} dx_2 + \dots + \frac{\partial y_1}{\partial x_p} dx_p \\ dy_2 = \frac{\partial y_2}{\partial x_1} dx_1 + \frac{\partial y_2}{\partial x_2} dx_2 + \dots + \frac{\partial y_2}{\partial x_p} dx_p \\ \dots \\ dy_q = \frac{\partial y_q}{\partial x_1} dx_1 + \frac{\partial y_q}{\partial x_2} dx_2 + \dots + \frac{\partial y_q}{\partial x_p} dx_p \end{cases} \quad (5)$$

We know that when the reference system for variables y is Cartesian, the straight line is a geodesic and the distance between two points with infinitesimal distance is the classical quadratic form

$$ds = \sqrt{dy_1^2 + dy_2^2 + \dots + dy_q^2} \quad (6)$$

After changing the reference from y to x, the same distance can be written as a function of x as follows:

$$\begin{aligned} ds &= \sqrt{\left(\frac{\partial y_1}{\partial x_1} dx_1 + \dots + \frac{\partial y_1}{\partial x_p} dx_p\right)^2 + \dots + \left(\frac{\partial y_q}{\partial x_1} dx_1 + \dots + \frac{\partial y_q}{\partial x_p} dx_p\right)^2} \\ &= \sqrt{\sum_{j,k} G_{j,k} dx^j dx^k} \quad (7) \end{aligned}$$

where the down indices are the covariant components and the indices up are the contravariant indices In the new

reference x the distance is the same minimum value so is again a geodesic. The metric tensor is given as:

$$G_{j,k} = G_{k,j} = \sum_p \frac{\partial y_p}{\partial x_j} \frac{\partial y_p}{\partial x_k} \quad (8)$$

According to optimum property principle of differential geometry, the variation of the distance C must equal to zero:

$$\delta C = \delta \int ds = \delta \int \sqrt{\sum_{j,k} G_{j,k}(x_i) \frac{dx^j}{dt} \frac{dx^k}{dt}} = 0 \quad (9)$$

The conditions under which Eq. 8 gives the minimum distance is given by Euler's differential equations

$$\begin{aligned} \frac{d}{dt} \frac{\partial \sqrt{\sum_{j,k} G_{j,k}(x_i) \frac{dx^j}{dt} \frac{dx^k}{dt}}}{\partial \frac{dx^k}{dt}} + \\ - \frac{\partial \sqrt{\sum_{j,k} G_{j,k}(x_i) \frac{dx^j}{dt} \frac{dx^k}{dt}}}{\partial x^i} = 0 \end{aligned} \quad (10)$$

The solutions of Eq. 10 give a space with distance measure in Eq. 8. The trajectories with minimum distance in this geometry are called geodesic. The distance in Eq. 8 can be associated with a system of ordinary differential equations (ODEs), the solutions of which produce the geometry. The electrical power W defined in Eq. 1 can be written by the derivatives of charges q_j:

$$W = \sum_{j,k} Z_{j,k} \dot{q}_j \dot{q}_k = \sum_{j,k} Z_{j,k} \frac{dq_j}{dt} \frac{dq_k}{dt} \quad (11)$$

and

$$\sqrt{W} = \sqrt{\sum_{j,k} Z_{j,k} \frac{dq_j}{dt} \frac{dq_k}{dt}} \quad (12)$$

where q are the electrical charges.

Note that Eq. 9 and Eq. 11 have similar structures. Eq. 9 is the geometric expression of the conceptual intention, while Eq. 11 expresses the material intention given by electrical dynamics of the neural network. Our goal is to derive how the conceptual intention can be transformed into its material

counterpart; therefore, we require that parameters Z are equal to G:

$$\sqrt{W} = \frac{ds}{dt} \text{ and } G_{i,j} = Z_{i,j} \quad (13a)$$

Eq. 13a can be written in terms of the voltage V and conductance C as follows:

$$\sqrt{W} = \frac{ds}{dr} \text{ and } G_{i,j} = C_{i,j}, W = \sum_{j,k} C_{j,k} v_j v_k \quad (13b)$$

The geometric method to transform the abstract or conceptual part of the intention into the material part is similar to the transformation of the software into the hardware in a digital computer.

Now we illustrate the geodesic for a simple electrical circuit and its associated ODE. Given the trivial electrical circuit [10, 11],

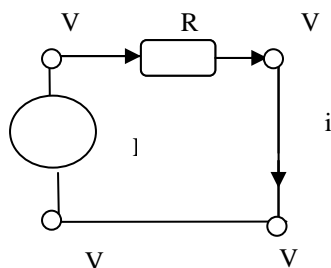


Figure 2 A simple electrical circuit with one generator E and one resistor R

we compute the power W that is dissipated by the resistance R and define the infinitesimal distance ds:

$$W = R \left(\frac{dq}{dt} \right)^2 = Ri^2$$

$$\left(\frac{ds}{dt} \right)^2 = W = R \left(\frac{dq}{dt} \right)^2 = Ri^2$$

$$ds = \sqrt{W} dt = \sqrt{R \left(\frac{dq}{dt} \right)^2} dt$$

In the electrical circuit, the currents flow in such a way as to dissipate the minimum power. The geodesic line in the one dimensional current space i is the trajectory in time. For the minimum dissipation of the power or cost C, we have

$$\delta C = \delta \int ds = \delta \int \sqrt{W} dt = \delta \int \sqrt{R \left(\frac{dq}{dt} \right)^2} dt = 0$$

We can compute the behavior of the charges for which we have the geodesic condition of the minimum cost. We know that this problem can be solved by the Euler differential equations [13]

$$\frac{d}{dt} \frac{\partial \left(\sqrt{R \left(\frac{dq}{dt} \right)^2} \right)}{\partial \frac{dq}{dt}} - \frac{\partial \left(\sqrt{R \left(\frac{dq}{dt} \right)^2} \right)}{\partial q} = 0$$

or

$$\frac{d}{dt} \frac{\partial R \left(\frac{dq}{dt} \right)^2}{\partial \frac{dq}{dt}} - \frac{\partial R \left(\frac{dq}{dt} \right)^2}{\partial q} = 0$$

When R is independent of the charges and constant in time, i.e., R has no memory, the previous equation can be written as follows:

$$\frac{d \left(\frac{dq}{dt} \right)}{dt} = \frac{d^2 q}{dt^2} = 0, q(t) = at + b, i = \frac{dq}{dt} = a = \frac{E}{R}$$

The geodesic is a straight line in the space of the charges. When the *conceptual intention* moves on a sphere given by the equation

$$y_1^2 + y_2^2 + y_3^2 = r^2 \quad (14)$$

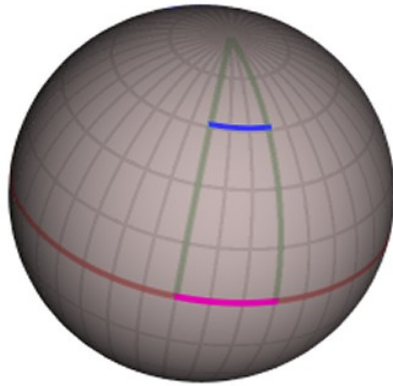


Figure 3: Illustration of the geodesic principle. In green we have the geodesic as line with minimum distance.

we have the following transformations for the *conceptual intention*:

$$\begin{cases} y_1 = r \sin(\alpha) \cos(\beta) \\ y_2 = r \sin(\alpha) \sin(\beta) \\ y_3 = r \cos(\alpha) \end{cases} \text{ or } \begin{cases} y_1 = x_1 \sin(x_2) \cos(x_3) \\ y_2 = x_1 \sin(x_2) \sin(x_3) \\ y_3 = x_1 \cos(x_2) \end{cases} \quad (15)$$

Let's compute the geodesic in the space (x_1, x_2, x_3) :

$$\begin{aligned} \left(\frac{ds}{dt}\right)^2 &= \left(\frac{dy_1}{dt}\right)^2 + \left(\frac{dy_2}{dt}\right)^2 + \left(\frac{dy_3}{dt}\right)^2 \\ &= \left(\frac{\partial y_1}{\partial x_1} \frac{dx_1}{dt} + \frac{\partial y_1}{\partial x_2} \frac{dx_2}{dt} + \frac{\partial y_1}{\partial x_3} \frac{dx_3}{dt}\right)^2 \\ &+ \left(\frac{\partial y_2}{\partial x_1} \frac{dx_1}{dt} + \frac{\partial y_2}{\partial x_2} \frac{dx_2}{dt} + \frac{\partial y_2}{\partial x_3} \frac{dx_3}{dt}\right)^2 \\ &+ \left(\frac{\partial y_3}{\partial x_1} \frac{dx_1}{dt} + \frac{\partial y_3}{\partial x_2} \frac{dx_2}{dt} + \frac{\partial y_3}{\partial x_3} \frac{dx_3}{dt}\right)^2 \\ &= \left(\frac{dx_1}{dt}\right)^2 + x_1^2 \left(\frac{dx_2}{dt}\right)^2 + x_1^2 \sin^2(x_2) \left(\frac{dx_3}{dt}\right)^2 \end{aligned} \quad (16a)$$

We want to simulate the movement of the electrical circuit over the specified surface using Eq. 12a, where the impedance is given as:

$$\begin{aligned} G_{j,k} &= \begin{bmatrix} 1 & 0 & 0 \\ 0 & x_1^2 & 0 \\ 0 & 0 & x_1^2 \sin^2(x_2) \end{bmatrix} \\ &= \begin{bmatrix} 1 & 0 & 0 \\ 0 & r_1^2 & 0 \\ 0 & 0 & r_1^2 \sin^2(\alpha) \end{bmatrix} = Z_{j,k} \quad (16b) \end{aligned}$$

Next we establish a connection between the derivative of the coordinates x and the currents i :

$$\text{for } \begin{bmatrix} i_1 \\ i_2 \\ i_3 \end{bmatrix} = \begin{bmatrix} \frac{dq_1}{dt} \\ \frac{dq_2}{dt} \\ \frac{dq_3}{dt} \end{bmatrix} \equiv \begin{bmatrix} \frac{dx_1}{dt} \\ \frac{dx_2}{dt} \\ \frac{dx_3}{dt} \end{bmatrix} = \begin{bmatrix} \frac{dr}{dt} \\ \frac{d\alpha}{dt} \\ \frac{d\beta}{dt} \end{bmatrix}$$

The power is

$$\begin{aligned} W &= Z_{1,1} i_1^2 + Z_{2,2} i_2^2 + Z_{3,3} i_3^2 \\ &= i_1^2 + r^2 i_2^2 + r^2 \sin^2(x_2) i_3^2 \\ &= \frac{dq_1}{dt} + q_1^2 \left(\frac{dq_2}{dt}\right)^2 + q_1^2 \sin^2(x_2) \left(\frac{dq_3}{dt}\right)^2 \quad (17) \end{aligned}$$

Figure 4 illustrates the connection among the charges, the currents, the derivative of the distance s and the geodesic.

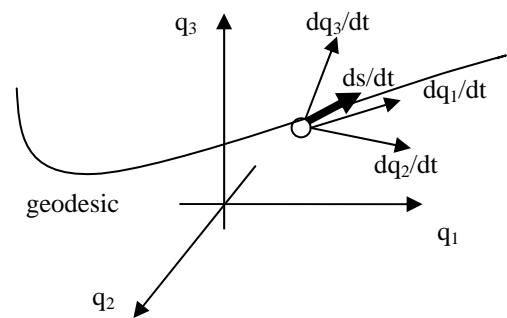


Figure 4 Geometric illustration of the geodesic with electrical charges, currents, and derivative of distance s .

Based on the conceptual transformation, we can compute the electrical parameters, impedances Z , by which the movement on the surface can be obtained by an electrical circuit whose parameters are in agreement with the conceptual intention.

III. GEODESIC OF THE NEURAL ELECTRICAL CIRCUIT

The electrical activity of the synapse is given by the circuit

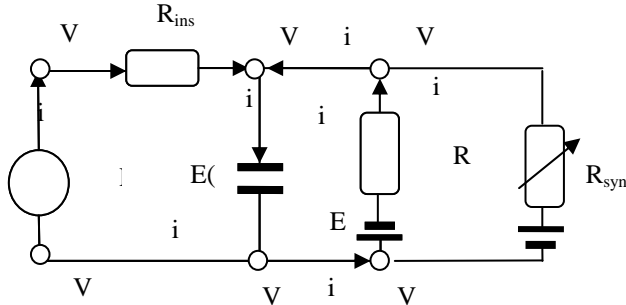


Figure 5 : Electrical circuit of synapses.

The impedance matrix is

$$Z = \begin{bmatrix} R_{ins} + 3 & 1 & 0 \\ 1 & R_m + 3 & R_m \\ 0 & R_m & R_{syn} + R_m + 2 \end{bmatrix}$$

The geodesic trajectory for a synapse is written as:

$$W = \left(\frac{ds}{dt}\right)^2 = (R_{ins} + 3)i_2^2 + (R_m + 3)i_5^2 + (R_m + R_{syn} + 2)i_8^2 + 2i_2i_5 + 2R_m i_5i_8$$

For more complex neural networks, we can derive the corresponding geodesics in a similar fashion. For example, we could consider have the electrical representation of a neural network as shown in Fig. 6. The axon circuitry is shown in Fig. 7. The geodesic can be derived for these networks as well, but we do not give the details in this brief paper.

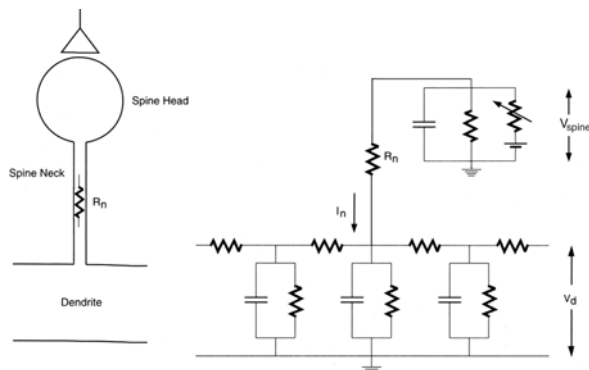


Figure 6 Complex electrical circuit of neural network system

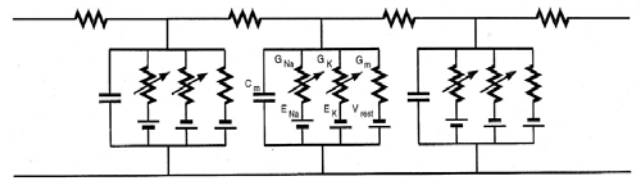


Figure 7. Example of axon and the electrical circuit

IV. CONCLUSION AND FUTURE WORK

In this work, we employed geometric concepts for states of a neural network represented using an electrical circuitry. In the introduced neuromorphic electrical circuitries, we relate voltage with current using the conductance matrix or the impedance matrix. After a change of reference system and introducing a new distance measure, we transform the initially linear relationships into a geodesic over the phase space. With the introduced neural network, we can simulate the geodesic movement for any transformation of the reference system. For a given transformation of reference, we can build the associated geodesic, which allows implementing the transformation of reference in the neural network. The neural network as an analog computer gives the solution of the ODE of the geodesic in the wanted reference. Our work is closely related to Freeman's work [1] on intentional neurodynamics, according to which intentionality can be studied in its manifestations of goal-directed behaviors. The goal-directed behavior is the reflection of the cognitive transformation, which is manifested through the neural mechanisms that construct the mesoscopic amplitude modulation (AM) space-time patterns of cortical activity. AM patterns related to intentionality emerge through the neural interactions in the limbic system and neocortical regions, including the sensory and motor cortices. Intentionality in brain dynamics can be modeled by nonlinear dynamic systems, focused on the construction of meaning rather than representations [1- 4].

In this paper, we described the brain and its parts as complex electrical circuits. Intention has two different aspects, namely, the *conceptual* part and the *material* part. The *conceptual* part of intentionality is given by a nonlinear transformation of the brain states. We introduce a new reference system, in which the geodesic, the transformed image of a straight line satisfies the condition that the minimum distance between two points in the state space is realized along the geodesic. The other aspect of intentionality is its *material* part. We observe that any part of the brain can be modeled by an electrical circuit and that the transformations between the voltages and currents define the change of the reference. Therefore, we conclude that the

actual transformation in the brain states is the *material* part of the intention.

In a working intentional system, the *conceptual* and *material* parameters of intentionality should be equal. When the two parts are equal, we have the brain dynamic in agreement with the required transformation in the conceptual space. This means that brains realize the required transformation in the material world. If a task is defined in the conceptual domain, then the task can be realized in the material neural network using suitable parametric structures. In terms of the traditional digital computer paradigm, the conceptual part of intention can be viewed as the software, while the material part of intention corresponds to the hardware [12]. The difference between the geometric theory of intentionality and the traditional digital computer paradigm is in the way the software and hardware is described. In digital computers, there are logic statements for the software and logic gates for the hardware. In the geometric approach to intentionality, the “hardware” and “software” of brains are inseparable. Namely, we have geometric changes of the references in the multidimensional space as “software” and corresponding transformations in neuromorphic computing as “hardware.” Further studies toward geometric approach to intentionality are in progress .

ACKNOWLEDGMENT

This work has been supported in part by a grant of FedEx Institute of Technology, University of Memphis.

REFERENCES

- [1] W. J. Freeman (1975) “*Mass Action in The Nervous System*” Academic Press, New York.
- [2] R.Kozma and W.J. Freeman (2008) “Intermittent spatial – temporal desynchronization and sequenced synchrony in ECoG signal “ *Chaos* Vol. 18, 037131 pp. 1-8.
- [3] B. Bollobas , R. Kozma and D. Miklos (2009) (Eds) “*Handbook of Large –Scale Random Networks* “ Bolyai Society Mathematical Studies , Springer Verlag New York ISBN 978 -3 – 540 – 69394-9.
- [4] W.J. Freeman (2008) “A pseudo-equilibrium thermodynamic model of information processing in nonlinear brain dynamics.” *Neural Networks*, doi:10.1016/ j.neunet.2007.12.011.
- [5] H. Makram (2006) “The blue brain project,” *Nature Reviews Neuroscience*, Vol.7, pp. 153-160.
- [6] M.D. Pickett, D.B. Strukov JL Borghetti, JJ Yang G.S. Snider GS, DR Stewart, and RS Williams (2009) “Switching dynamics in titanium dioxide memristive devices.” *J Appl Phys* 106:074508R.
- [7] R. Kozma, R. Pino and G. Paziienza (2012) “*Advances in Memristor Science and Technology*,” Dordrecht, Springer Verlag.
- [8] T. Kohno and K. Aihara, “A Design Method for Analog and Digital Silicon Neurons Mathematical-Model-Based Method-,” *Proc. AIP Conference*, Vol. 1028, pp. 113–128.
- [9] J. Rinzel and B. Ermentrout (1998) “Analysis of Neural Excitability and Oscillations,” in “*Methods in Neural Modeling*”, ed. C. Koch and I. Segev, pp. 251–291, MIT Press.
- [10] G. Resconi (2007) “Modelling Fuzzy Cognitive Map by Electrical and Chemical Equivalent Circuits,” *Joint Conf. Inf. Science*, July8-24 2007 Salt lake City Center USA.
- [11] G. Resconi and V.P.Srini (2009) “Electrical Circuit As A Morphogenetic System,” *GEST Int. Trans. Comp. Sci. Engng*, Vol. 53(1), pp.47-92.
- [12] A.A. Mandzel and T. Flach (1999) “Geometric methods in the study of human motor control,” *Cognitive Studies*, 6 (3), pp. 309 – 321.
- [13] S.V Fomin., and I.M.: Gelfand, *Calculus of Variations*, Dover Publ., 2000

Co-adaptivity in Unsupervised Adaptive Brain-Computer Interfacing: a Simulation Approach

Martin Spüler, Wolfgang Rosenstiel
Wilhelm-Schickard-Institute for Computer Sciences
University of Tübingen
Tübingen, Germany
Email: {spueeler,rosen}@informatik.uni-tuebingen.de

Martin Bogdan
Computer Engineering
University of Leipzig
Leipzig, Germany
Email: bogdan@informatik.uni-leipzig.de

Abstract—A Brain-Computer Interface (BCI) allows a user to control a computer by pure brain activity. Due to the non-stationarity of the recorded brain signals, the BCI performance tends to decrease over time. Recently, adaption of the BCI has been proposed as a means to counter non-stationarity and help to stabilize the BCI performance. Since most adaption methods for BCI are analysed in an offline setting, one important factor is not taken into account: that also the user is adapting. While online experiments take into account the adaptive user, a comparison of different classifiers with the same data is always biased towards the method that was used for feedback and thereby does not allow a proper evaluation of the classifier in a co-adaptive environment. To solve this problem, we propose a simulation approach that simulates an adapting BCI user and allows to test and compare different adaptive algorithms considering the co-adaptivity between BCI and user. With this approach we can also show, under which conditions an adaption of the BCI improves performance and when the adaptive BCI and the adaptive user hinder each other and lead to a decrease in BCI performance.

Keywords—Brain-Computer Interface(BCI); unsupervised adaption; co-adaptivity.

I. INTRODUCTION

A Brain-Computer Interface (BCI) classifies the brain signals of a user, thereby giving him the possibility to communicate or control a computer by pure brain activity. One problem for current BCI systems is the high non-stationarity of the recorded brain signals, which causes the BCI performance to deteriorate over time. Adaption of the BCI classifier has been proposed as a means to counter these non-stationarities and to stabilize or even improve the BCI performance [1]. There exist numerous publications that show different adaption methods for BCI to increase performance in an offline analysis [2]–[5]. But an evaluation of adaptive algorithms in an offline setting is not advisable, since it does not take the user into account, who learns and adapts to the BCI. Thereby it is unclear if the adaptive BCI makes it harder for the user to learn BCI control or if the learning of the user, who adapts his control strategy, might hamper the learning of the adaptive BCI algorithm.

To overcome this problem and to take into account the learning user, online experiments have to be performed. This

was already done with a supervised adaption of the classifier [6]–[8], which is not practical, since supervised adaption can not be used in practical BCI applications due to the missing class labels. So far, Vidaurre et al. are the only ones to show an unsupervised online adaption of a BCI classifier [9] with the result that an unsupervised adaption might not be feasible for all subjects. While these online experiments allow a suitable evaluation of a BCI adaption, they still do not allow a fair comparison between adaptive and non-adaptive methods to assess the benefit of BCI adaption, since the non-adaptive methods were evaluated offline on the data recorded from the online experiments. The results are thereby biased towards the adaptive method used during the online experiment.

To compare two different adaptive and non-adaptive methods for BCI, both have to be evaluated online. Due to external factors like inter- and intra-subject variability in BCI performance and learning, a large subject-population would be needed that goes beyond what is used in today's BCI research.

So far, there is no work that specifically addresses this aspect of co-adaptivity in a BCI.

As an approach to test different adaptive methods in an online setting with a learning user, we propose the use of a simulation method, that allows to simulate online BCI sessions with an adaptive user under different environments with different parameters in a fast and cost-efficient way.

In the following, we will explain, how the simulation works, what parameters are available to adjust the user's behaviour, and the environmental influences and we will demonstrate the influence of parameter changes. Based on an adaptive BCI classifier, we will show how the simulations can be used to evaluate the mutual influence between the user and the BCI, and under which conditions the user benefits from an adaptive BCI classifier or which conditions lead to decreasing BCI performance.

In addition, we will show, that this simulation approach can also be used to answer other questions like: can the user learn to control an adaptive BCI, if neither the user nor the BCI have any prior knowledge?

II. METHODS

To simulate the interaction between an (adaptive) BCI and the user, a genetic algorithm was used to simulate the learning user and the BCI classifier was used as a fitness function for the genetic algorithm. An overview of the general concept is depicted in Figure 1. A motor imagery BCI, where the BCI was controlled by left hand motor imagery and right hand motor imagery was used as archetype for the simulated BCI.

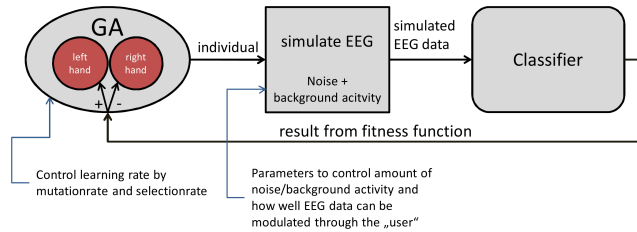


Figure 1. Overview of the simulation of two adaptive systems

The genetic algorithm consists of two populations: population P_L belonging to *left hand motor imagery* and population P_R belonging to *right hand motor imagery*. Both populations are filled with individuals, which can be seen as representations of the specific state of brain activity. Each individual $I_N = (i_N, f_N)$ consists of a vector $i_N \in \mathbb{R}^n$ and a fitness value $f_N \in \mathbb{R}$.

To control the BCI, a new individual I_N is created for each trial. Depending on the target class for this trial, the I_N is either created out of P_L if the target is the class associated with *left hand motor imagery* or vice versa. For the creation of a new individual, two parent individuals (I_1, I_2) are drawn randomly from the population, with individuals with higher fitness having a higher probability to be chosen. For the creation of the new vector i_N , it is chosen randomly, which parts are filled from i_1 and which from i_2 . On average, i_1 and i_2 fill half of i_N . Depending on the parameter settings for the mutation rate, a noise vector is added to i_N to introduce mutations. The amplitude of the noise vector also depends on the mutation rate. Since I_N will be added to the population later, a random I_D is selected out of the population, from which the parents of I_N were drawn, and removed. Individuals with lower fitness have a higher probability to be drawn.

I_N is then used to generate an artificial EEG signal according to i_N . The EEG signal is then preprocessed and classified by the BCI classifier. The BCI classifier outputs $c_N \in \mathbb{R}$ with $c_N \geq 0$ when *left hand motor imagery* is classified and $c_N < 0$ when *right hand motor imagery* is classified. The BCI classifier then serves as a fitness function for the genetic algorithm with $f_N = c_N$ being the fitness value if the individual stems from P_L and $f_N = -c_N$ when the individual stems from P_R . At last the individual $I_N = (i_N, f_N)$ is added to its population.

A. Simulation of EEG data and preprocessing

For the generation of the EEG data, the vector $i_N \in \mathbb{R}^{20}$ is used as current state of brain activity. For the simulation of the EEG data a samplingrate of 100 Hz is used and the two electrodes C3 (located over the left motor cortex) and C4 (located over the right motor cortex) are simulated. The values $i_{Nx}, x = \{1, 3, 5, \dots, n-1\}$ represent the brain activity in the left motor cortex, while the values $i_{Nx}, x = \{2, 4, 6, \dots, n\}$ represent the brain activity in the right motor cortex.

The brain activity in the left motor cortex is used for generation of EEG data for C3 and the activity in the right motor cortex for the generation of EEG data for C4. The 10 values are used to modulate the frequency spectrum in the range from 3 to 30 Hz. To simulate background activity and noise as it is typically present in real EEG recordings, pink ($1/f$) noise and white noise are added with amplitudes that can be predefined in the settings. Also the noise can change over time to simulate a covariate shift [10].

After generation of the EEG signal, the frequency spectrum for both electrodes is extracted by an autoregressive model with order 10. The power spectrum in the range from 1 to 50 Hz in bins with width of 1 Hz are used as features for the classification.

An example for the different steps of simulation of the EEG data and preprocessing is visualized in Figure 2.

B. BCI classifier

In the following, the two methods are introduced, that have been used for classification in the simulated BCI.

1) *SimpleMu*: SimpleMu is a very simple classifier that was used to test the parameters settings of the genetic algorithm with a simple non-adaptive classifier. It outputs the difference in the power spectrum between C3 and C4 in the Mu range (7 to 12 Hz). Assume $A_{i,b}$ is the power for channel i at frequency bin b , with $i = 1$ for C3 and $i = 2$ for C4, the output of the classifier is calculated as follows:

$$c_N = \sum_{b=7}^{12} A_{1,b} - A_{2,b} \quad (1)$$

2) *K-means*: K-means clustering [11] was chosen as an algorithm that allows an unsupervised adaption of the BCI, as well as an unsupervised calibration.

Given a $k \in \mathbb{N} \setminus \{0, 1\}$ and n datapoints (x_1, x_2, \dots, x_n) with $x_i \in \mathbb{R}^d$, k-means tries to partition the n datapoints into k ($k \leq n$) cluster or sets $\mathbf{S} = \{S_1, S_2, \dots, S_k\}$, while minimizing the within-cluster sum of squares:

$$\arg \min_{\mathbf{S}} \sum_{i=1}^k \sum_{\mathbf{x}_j \in S_i} \|\mathbf{x}_j - \boldsymbol{\mu}_i\|^2 \quad (2)$$

$\boldsymbol{\mu}_i$ represent the mean of all datapoints in cluster S_i . For the initialisation of k-means an initial set of k means

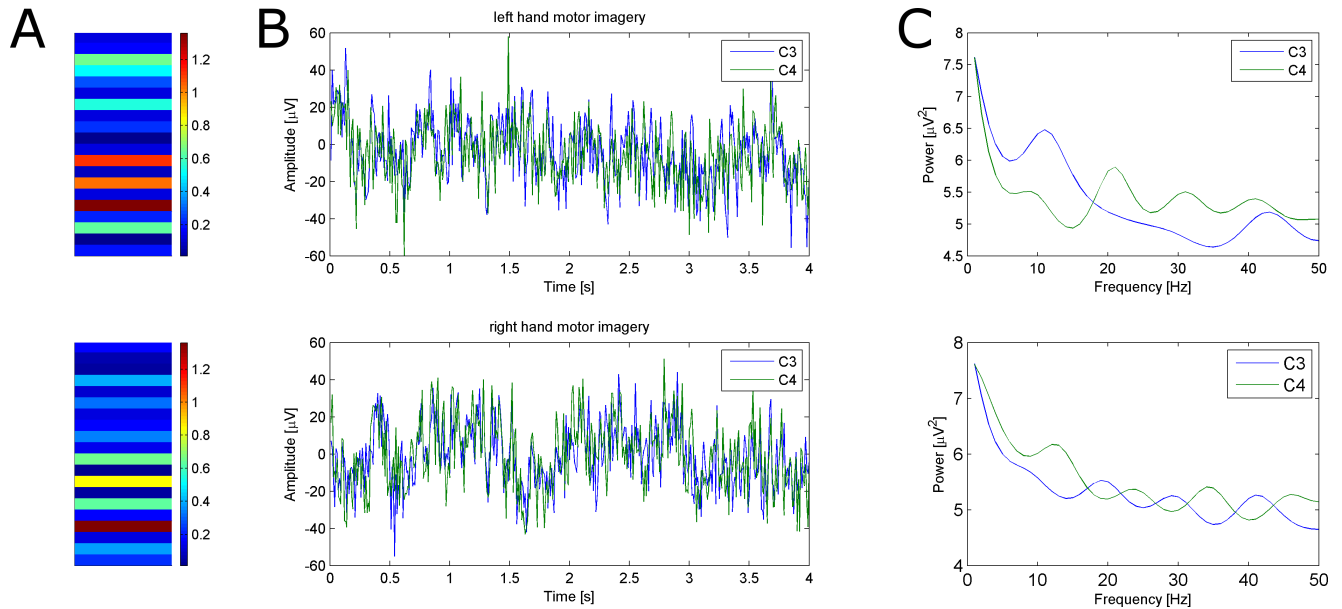


Figure 2. Simulation of EEG data: A) Vector for one individual of population for left hand imagery (top) and right hand imagery (bottom) B) Corresponding EEG-signal at electrodes C3 and C4 C) Corresponding frequency spectrum at electrodes C3 and C4

$(m_1^{(1)}, m_2^{(1)}, \dots, m_k^{(1)})$ has to be given. When a new data-point x_{n+1} is added to adapt the classifier, it has to be ensured, that the mean of the existing clusters are adapted and no new clusters are created from scratch. Therefore the means $(\mu_1^{(n)}, \mu_2^{(n)}, \dots, \mu_k^{(n)})$ from the previous result of k-means are used as initial set $(m_1^{(n+1)}, m_2^{(n+1)}, \dots, m_k^{(n+1)})$.

In the following, $k = 2$ is used, since the BCI control is simulated with only 2 classes.

For the unsupervised calibration, the initial means are chosen randomly. Due to the fact, that k-means is a pure clustering approach without any knowledge of the true class labels, the clusters can represent the classes correctly, but the clusters can be associated with the wrong class label. In this case the BCI would always choose the wrong class and do exactly the opposite of what the user is intending to. Since a human user would recognize this fact and just correct the mistake of the BCI by switching the two imagery classes himself, such a behaviour had to be implemented into the genetic algorithm. Therefore, the individuals of the two populations P_L and P_R were completely switched if the accuracy fell below a threshold of 30 %, which should mimic the behaviour of the human user switching his mental imagery classes.

Although k-means does not offer a supervised calibration of the BCI by default, k-means can be performed on all individuals in P_L and P_R . The initial means $m_1^{(1)}$ and $m_2^{(1)}$ are set to the mean of all individuals of P_L and P_R , respectively, and the clusters can be associated with the correct class labels, to simulate a supervised calibration of the BCI.

A new trial x_t is then classified by calculating

$$c_N = \|\mathbf{x}_t - \boldsymbol{\mu}_L\| - \|\mathbf{x}_t - \boldsymbol{\mu}_R\| \quad (3)$$

where $\boldsymbol{\mu}_L$ is the mean of the cluster for left hand motor imagery and $\boldsymbol{\mu}_R$ the mean of the cluster for right hand motor imagery.

III. PARAMETER CHANGES AND THEIR EFFECT

Different parameters can be used to test different settings and adjust the behaviour of the genetic algorithm. In the following, the important parameters are presented and their effect is demonstrated with the non-adaptive simpleMu classifier. It is assumed that the genetic algorithm has prior knowledge how to control the BCI, since it is also explained to BCI users, that they should control the BCI by motor imagery.

If not stated otherwise, a BCI session with 2000 trials was simulated, where both classes were evenly distributed. 10 sessions were simulated resulting in a vector for each session, where the outcome of each trial was marked with 1 if correct and 0 if wrong. The accuracy for one time point during this session was calculated by sliding a Hanning window with length 251 over the result-vector.

A. Learning rate

One parameter that strongly influences the behaviour of the genetic algorithm is the so called *learning rate*. It is one parameter, to be set ≥ 0 , which is proportional to the mutation rate and to the weighting of the fitness function, when individuals with the highest or lowest fitness are

randomly selected either for reproduction or elimination. While the algorithm will not learn at all with a learning rate of 0, it should learn faster and adapt faster to the BCI with a higher learning rate.

The effect of two exemplary learning rates is displayed in Figure 3.

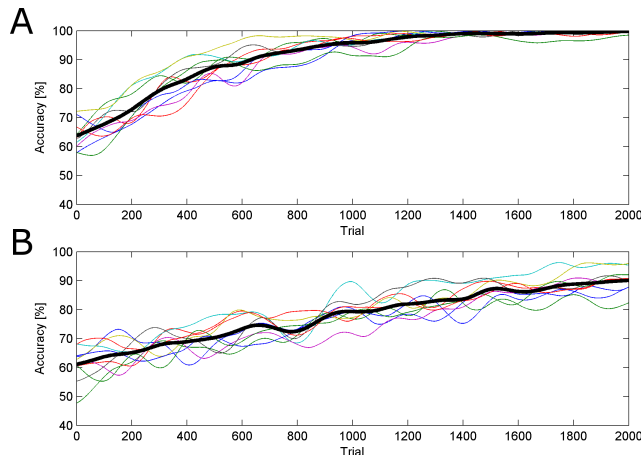


Figure 3. Result of a simulation with two different learning rates of 2 (A) and 0.5 (B). The thin colored lines represent different simulated sessions and the thick black line represents the average accuracy over all simulation runs.

A comparison of different learning rates with values ranging from 0.01 to 2 is shown in Figure 4. It is clear that the simulated user learns and adapts to the BCI and that it adapts faster to the BCI with a higher learning rate.

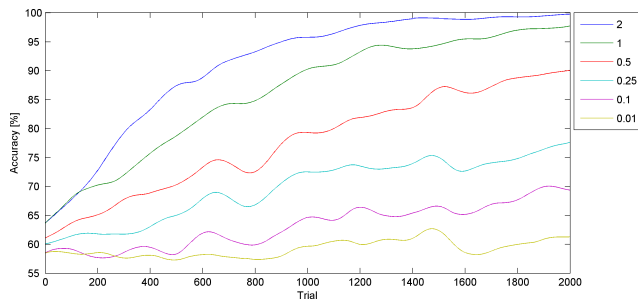


Figure 4. Average accuracy during simulations with different learning rates.

B. Initial performance

Another parameter that can be changed for the simulations is the initial performance of the BCI user. The initial performance is modeled by drawing the initial individuals for the populations P_L and P_R from two different distributions. Each distribution has 20 dimensions and for 18 dimensions the mean and standard deviation of these dimensions is equal across both distributions. For 2 dimensions, which roughly correspond to the alpha-band in the left or right motor cortex, the mean of the distributions differs by d_x

times the standard deviation. The higher the d_x , the higher is the initial performance.

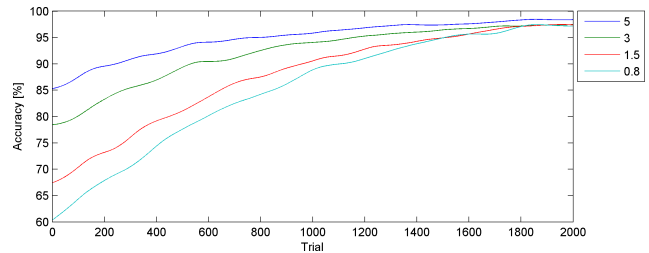


Figure 5. Average accuracy during simulations with different distance d_x between the two populations P_K and P_R , which results in different initial performance. Learning rate was set to 1.

Figure 5 shows results from simulations with learning rate 1 and different values for d_x . For each parameter combination 50 sessions were simulated and the average is displayed.

C. Signal-to-noise ratio

One problem when recording EEG for controlling a BCI, is the amount of noise and background activity, that is picked up by the EEG. Therefore EEG has a bad signal-to-noise ratio. To evaluate the adaption of the simulated user under different signal-to-noise ratios, signal-to-noise ratio was introduced as another parameter that affected how well the genetic algorithm was able to modulate the brain activity compared to the amplitude of the noise in the EEG signal. The result of simulations with different signal-to-noise ratios is shown in Figure 6. Due to these results, a value of 0.2 was chosen as a realistic value to be used for all following simulations.

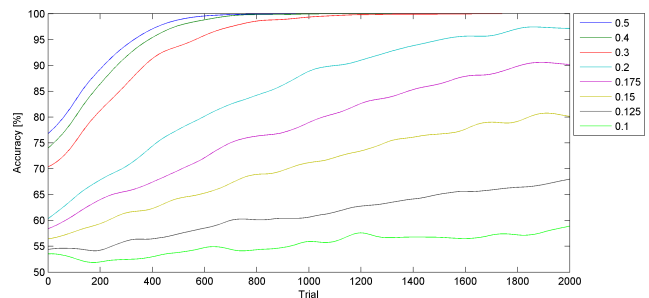


Figure 6. Results of simulations with different signal-to-noise ratios. For each value 50 sessions have been simulated and the average is displayed.

D. Covariate shift

To simulate the effect of non-stationarity in EEG signals, a covariate shift [10] of the data was introduced by increasing the amount of pink noise every trial by a specified value. To test how well the simulated user adjusts to the covariate shift, different extents of covariate shift were tested with 50 simulated sessions per value and a learning rate of 1. To

simulate the effect of a covariate shift on BCI users with low initial performance and high initial performance, simulations were conducted with $d_x = 0.8$ and $d_x = 5$. The results for this simulations are shown in Figure 7.

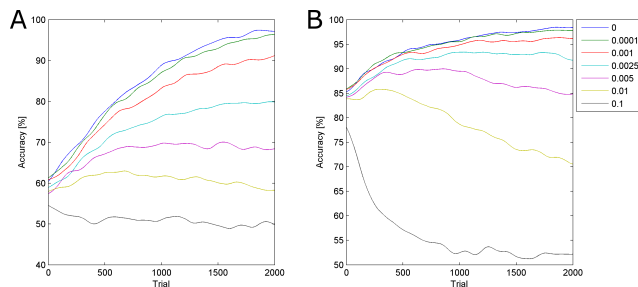


Figure 7. Results of simulations with different values for the amount of covariate shift and a learning rate of 1. A) for users with low initial performance B) for users with high initial performance

It can be seen that a higher covariate shift makes it harder for the BCI user to adapt to the changes and if the covariate-shift is too large, the user can't adapt and the BCI performance drops. This drop in BCI performance is especially visible for BCI users with high initial performance.

IV. RESULTS

A. Adaptive vs. non-adaptive classifier

To simulate the effect of classifier adaption on the BCI performance, k-means was used as a classifier and a supervised calibration was simulated. For the adaptive case, the classifier was adapted in an unsupervised manner, while the classifier was static for the non-adaptive case.

To evaluate the benefit of adaptive classification, 500 sessions were simulated each with different values d_x and different learning rates whereas the mean accuracy over the whole session was taken as performance measure. The average performance difference between the adaptive classifier and the non-adaptive one, is shown in Table I. While the performance gets worse for low d_x with low learning rate and high d_x with high learning rate, the user benefits from the adaptive classifier when d_x is high with a low learning rate or with a high d_x and a low learning rate. To check if there is a significant difference between the results for the adaptive classifier and the results for the non-adaptive classifier, Wilcoxon's ranksum test was performed for each combination of d_x and learning rate. The parameter combinations with significant effects ($p < 0.01$) are marked in bold in Table I.

A 3-way ANOVA was applied to the values and shows, that the use of the adaptive classifier significantly ($p < 0.0001$) increases the total average performance by 1.41 %. The 3-way ANOVA also shows, that there are significant interactions between the factors learning rate and adaption ($p < 0.0001$), as well as a significant interaction between the factors d_x and adaption ($p < 0.0001$).

d_x	learning rate						
	0.1	0.25	0.5	1	2	4	8
0.8	-0.020	-0.021	-0.021	0.000	0.029	0.085	0.192
1.5	-0.001	0.031	0.021	0.020	0.011	0.026	0.085
3	0.014	0.018	0.020	-0.002	-0.014	-0.043	0.006
5	0.026	0.020	0.016	0.005	-0.025	-0.074	-0.005

Table I
DIFFERENCE BETWEEN ADAPTIVE AND NON-ADAPTIVE BCI CLASSIFIER. POSITIVE DIFFERENCE MEANS A HIGHER ACCURACY WITH THE ADAPTIVE CLASSIFIER. IF THERE IS A SIGNIFICANT DIFFERENCE ($p < 0.01$) BETWEEN THE RESULTS FOR THE ADAPTIVE CLASSIFIER AND THE RESULTS WITH THE NON-ADAPTIVE CLASSIFIER, THE VALUE HAS BEEN MARKED BOLD.

B. Influence of covariate shift

To evaluate the effect of covariate shift on the benefit of adaptive classification, simulations were run with different amounts of covariate shift. For different combinations of d_x and learning rates 100 sessions were simulated each with a covariate shift ranging from 0 to 0.1. Since a 4-way ANOVA shows no significant ($p > 0.05$) interaction between learning rate and adaption, when considering different amounts of covariate shift, the results were averaged over the learning rates. Figure 8 shows the average performance improvement by adaptive classification with different amounts of covariate shift. It can be seen that it depends on the learning rate and the amount of covariate shift if BCI performance is increased by adaption of the classifier.

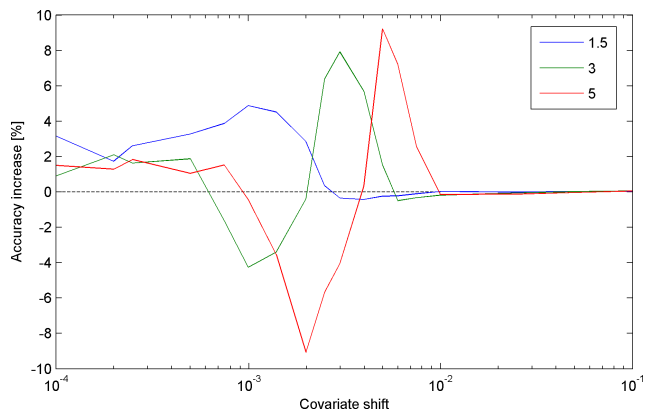


Figure 8. Results from simulations with different amounts of covariate shift with different initial performance.

C. Co-adaptivity without prior knowledge

There still is the question to be answered, if BCI control can be achieved if neither the user nor the BCI have any prior knowledge on how control might work or how the two classes can be differentiated. Therefore, simulations were run, in which the individuals for both populations P_L and P_R were drawn from the same distribution ($d_x = 0$) simulating that the user has no prior knowledge on how to control the BCI. Since the k-means classifier is initialized randomly,

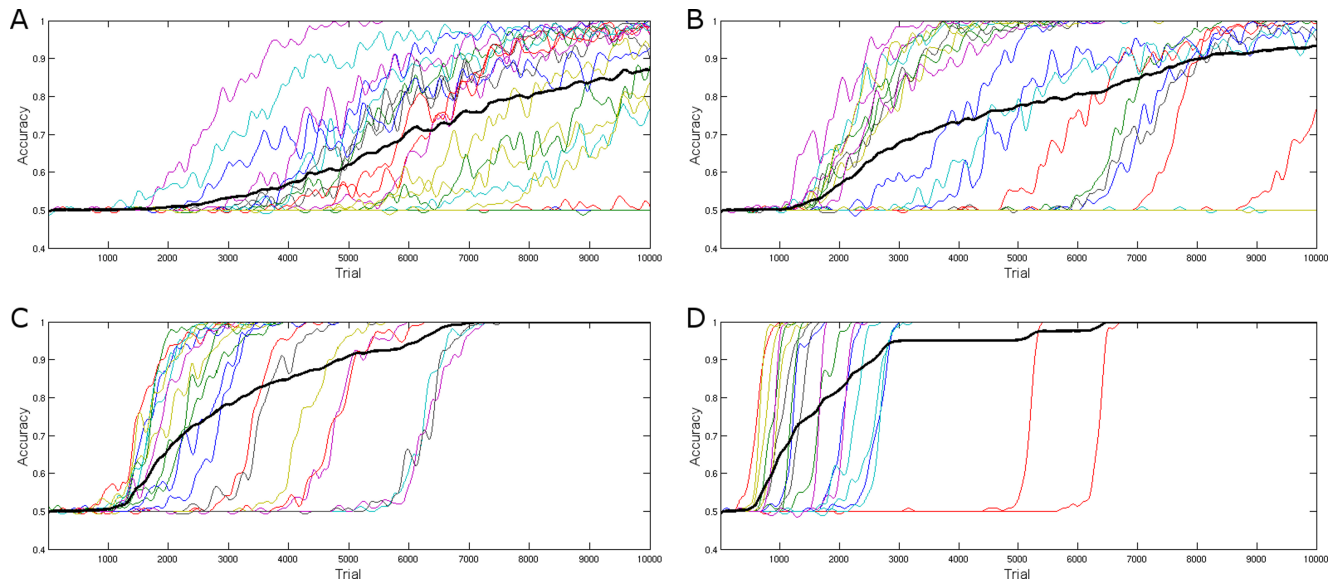


Figure 9. Co-adaptivity without prior knowledge. Performance during the first 10000 trials with a learning rate of A: 0.5 B: 1 C: 2 D: 4. Colored lines show the result of one session, while the black line shows the average performance.

the classifier has also no prior knowledge on what data to expect.

For different learning rates 20 sessions were simulated, with one session having 10000 trials. The results show, that regardless of the learning rate, performance can be achieved, but with a higher learning rate BCI control is achieved earlier. While with the same learning rate in some sessions BCI control was achieved very fast, it took longer in other sessions. At the end of the session significant BCI control was achieved in 45 % of the sessions with learning rate 0.25, 80 % with learning rate 0.5, 90 % with a learning rate of 1 and 100 % with learning rates of 2 and 4. Although BCI control was not achieved in all sessions with lower learning rate, the results show that the simulated user would still gain BCI control if more trials were performed i.e., for longer BCI sessions. The results from the simulations with different learning rates are displayed in Figure 9.

V. DISCUSSION

At first it needs to be discussed, why we used the presented approach and think of it to be an appropriate model for a learning user. The approach by using a genetic algorithm does not try to resemble the biological processes involved in learning, but tries to model the behavioural processes and aspects involved in human learning. Learning to control a BCI is skill learning [12], which is learned by a human through reinforcement [13]. So, a human learns to control a BCI by trying different strategies and keeping those strategies that maximize the reward, which is a high BCI accuracy. Slight variations in the human’s actions are introduced either voluntarily or involuntarily. If these varia-

tions lead to higher reward they are positively reinforced and thereby used more often, while variations which decrease the reward are negatively reinforced and thereby used less often. The genetic algorithm essentially does the same [14]; slight variations are introduced through mutation. Individuals with lower fitness are removed, which negatively reinforces behaviour that leads to poor BCI control and individuals with higher fitness are allowed to reproduce, whereby behaviour that leads to good BCI control is positively reinforced.

With this simulation approach we have presented a method that allows to simulate a BCI user that learns to control the BCI and adapts. By changing the parameters of the simulation it allows to adjust the simulations closer to real-life conditions. While a learning rate of 0.1 to 0.25 seems to be suitable to simulate learning of EEG-based BCI control [15], ECoG allows for faster learning of BCI control [16] and learning rates of 0.5 to 1 could be used to simulate ECoG-based BCIs.

The parameter d_x can be used to adjust the initial performance and $1.5 \leq d_x \leq 5.0$ can be used to set the initial BCI accuracy to a value that resembles the average performance reached by most users [17], [18].

Comparing simulation results for an adaptive and a non-adaptive classifier shows that most users will benefit from an adaptive classifier. But for user with low initial BCI performance ($d_x = 0.8$, respectively a BCI accuracy < 65%) an unsupervised adaption does not increase or even decrease the BCI performance, which is in line with the findings by Vidaurre et al. [9].

Regarding the use of unsupervised adaption as a means to alleviate non-stationaries and thereby improve BCI accuracy

under a covariate shift, the simulations show that adaption of the classifier can be used to alleviate non-stationarity and thereby improve BCI performance. But unsupervised adaption can also have a negative effect depending on the amount of covariate shift and the initial BCI performance of the user. The simulations also show that BCI control can be achieved if neither the BCI nor the user has any prior knowledge.

VI. CONCLUSION

In this paper, we have proposed a method that uses genetic algorithms to simulate the mutual interaction between a learning user and an adaptive BCI. We have shown the presented approach to be a viable method to study the interaction of 2 learning systems, namely the adaptive BCI and the learning user. It can be used to test and evaluate new adaptive classification methods in a co-adaptive environment and test if the use of a specific adaptive method is always beneficial or under which conditions a specific adaptive method should not be used. Due to the rather simple approach of generating artificial EEG data, it cannot replace an offline analysis on real human EEG data. But, simulations can be used in addition to an offline analysis, to investigate the behaviour of a specific adaptive algorithm in a co-adaptive environment and optimize adaptive algorithms to perform better in cooperation with a learning BCI user.

ACKNOWLEDGMENT

This study was funded by the German Federal Ministry of Education and Research (BMBF, BFNT F*T, Grant UTü 01 GQ 0831).

REFERENCES

- [1] J. d. R. Millán, "On the need for on-line learning in brain-computer interfaces," in *Proceedings of the International Joint Conference on Neural Networks*, Budapest, Hungary, 7 2004, iDIAP-RR 03-30.
- [2] J. Blumberg, J. Rickert, S. Waldert, A. Schulze-Bonhage, A. Aertsen, and C. Mehring, "Adaptive classification for brain computer interfaces," in *Engineering in Medicine and Biology Society, 2007. EMBS 2007. 29th Annual International Conference of the IEEE*, aug. 2007, pp. 2536–2539.
- [3] A. Satti, C. Guan, D. Coyle, and G. Prasad, "A covariate shift minimisation method to alleviate non-stationarity effects for an adaptive brain-computer interface," in *Pattern Recognition (ICPR), 2010 20th International Conference on*, Aug. 2010, pp. 105–108.
- [4] C. Vidaurre, A. Schlögl, B. Blankertz, M. Kawanabe, and K. r. Müller, "Unsupervised adaptation of the lda classifier for brain-computer interfaces," in *Proceedings of the 4th International Brain-Computer Interface Workshop and Training Course 2008*, 2008, pp. 122–127.
- [5] G. Liu, D. Zhang, J. Meng, G. Huang, and X. Zhu, "Unsupervised adaptation of electroencephalogram signal processing based on fuzzy c-means algorithm," *International Journal of Adaptive Control and Signal Processing*, 2011. [Online]. Available: <http://dx.doi.org/10.1002/acs.1293>
- [6] J. DiGiovanna, B. Mahmoudi, J. Fortes, J. Principe, and J. Sanchez, "Coadaptive brain-machine interface via reinforcement learning," *Biomedical Engineering, IEEE Transactions on*, vol. 56, no. 1, pp. 54–64, 2009.
- [7] G. Gage, K. Otto, K. Ludwig, and D. Kipke, "Co-adaptive kalman filtering in a naive rat cortical control task," in *Engineering in Medicine and Biology Society, 2004. IEMBS '04. 26th Annual International Conference of the IEEE*, vol. 2, sept. 2004, pp. 4367–4370.
- [8] C. Vidaurre, C. Sannelli, K.-R. Müller, and B. Blankertz, "Co-adaptive calibration to improve bci efficiency," *Journal of Neural Engineering*, vol. 8, no. 2, p. 025009, 2011.
- [9] C. Vidaurre, M. Kawanabe, P. von Bünau, B. Blankertz, and K. Müller, "Toward Unsupervised Adaptation of LDA for Brain-Computer Interfaces," *Biomedical Engineering, IEEE Transactions on*, vol. 58, no. 3, pp. 587–597, March 2011.
- [10] M. Sugiyama, M. Krauledat, and K.-R. Müller, "Covariate shift adaptation by importance weighted cross validation," *J. Mach. Learn. Res.*, vol. 8, pp. 985–1005, Dec. 2007. [Online]. Available: <http://dl.acm.org/citation.cfm?id=1314498.1390324>
- [11] J. A. Hartigan, *Clustering Algorithms*, 99th ed. New York, NY, USA: John Wiley & Sons, Inc., 1975.
- [12] E. Curran, "Learning to control brain activity: A review of the production and control of EEG components for driving braincomputer interface (BCI) systems," *Brain and Cognition*, vol. 51, no. 3, pp. 326–336, Apr. 2003.
- [13] W. T. Fu and J. R. Anderson, "From recurrent choice to skill learning: a reinforcement-learning model." *J Exp Psychol Gen*, vol. 135, no. 2, pp. 184–206, May 2006.
- [14] J. J. Grefenstette, D. E. Moriarty, and A. C. Schultz, "Evolutionary algorithms for reinforcement learning," *Journal Of Artificial Intelligence Research*, vol. 11, pp. 241–276, 1999.
- [15] J. R. Wolpaw and D. J. Mcfarland, "Control of a two-dimensional movement signal by a noninvasive brain-computer interface in humans," vol. 101, no. 51. National Academy of Sciences, Dec. 2004, pp. 17 849–17 854.
- [16] G. Schalk, K. J. Miller, N. R. Anderson, J. A. Wilson, M. D. Smyth, J. G. Ojemann, D. W. Moran, J. R. Wolpaw, and E. C. Leuthardt, "Two-dimensional movement control using electrocorticographic signals in humans," *Journal of Neural Engineering*, vol. 5, no. 1, p. 75, 2008.
- [17] C. Vidaurre and B. Blankertz, "Towards a Cure for BCI Illiteracy," *Brain Topography*, vol. 23, no. 2, pp. 194–198, 2010.
- [18] B. Blankertz, C. Sannelli, S. Halder, E. M. Hammer, A. Kübler, K.-R. Müller, G. Curio, and T. Dickhaus, "Neurophysiological predictor of smr-based bci performance," *NeuroImage*, vol. 51, no. 4, pp. 1303 – 1309, 2010.

Handling of Deviations from Desired Behaviour in Hybrid Central/Self-Organising Multi-Agent Systems

Yaser Chaaban and Christian Müller-Schloer

Institute of Systems Engineering
Leibniz University of Hanover
Hanover, Germany
chaaban,cms@sra.uni-hannover.de

Jörg Hähner

Institute of Organic Computing
University of Augsburg
Augsburg, Germany
joerg.haehner@informatik.uni-augsburg.de

Abstract—The ever increasing complexity of today’s technical systems embodies a real challenge for their designers. This complexity can be regarded as the major source of unexpected system failures. Organic Computing (OC) is concerned with this complexity aiming to build robust, flexible and adaptive systems. In previous papers, we proposed a hybrid system for coordinating semi-autonomous agents using the Organic Computing concept. In this paper, we extend our prototype implementation with the aim of making it capable of handling deviations from planned (desired) behaviour. Therefore, we introduce different types of deviation that can arise. Deviations should be detected as soon as possible after their occurrence so that the controller can re-plan accordingly. In this way, the hybrid central/self-organising concept tolerates that some agents behave in fully autonomous way in the central architecture. Here, the autonomy of the agents is recognised as a deviation from the plan of the central algorithm, if the agents are not respecting this plan. Consequently, the system performance remains robust despite the occurrence of deviations.

Keywords—Organic Computing; Hybrid Coordination; Robustness; Multi-Agent Systems

I. INTRODUCTION

The Organic Computing initiative introduces an OC system as follows [3]: "a technical system which adapts dynamically to the current conditions of its environment. It is self-organizing, self-optimizing, self-configuring, self-healing, self-protecting, self-describing, self-explaining and context-aware". Therefore, the goal of this initiative is to develop systems that are robust, flexible and adaptive at the same time utilising advantage of the organic properties of OC. In other words, OC has the objective to use principles that are detected in natural systems. In this case, nature can be considered as a model aiming to cope with the increasing complexity of the recent technical systems [3].

Organic systems use the "controlled self-organisation" design paradigm, in which the unwanted behaviour should try to be prevented, whereas the desired behaviour should be rewarded. In this regard, the robustness of OC systems is a key property, because the environments of such systems are dynamic.

Since OC systems are self-organising systems that exhibit some degrees of autonomy, the behaviour of these systems should be observed in order to take an appropriate

intervention timely if necessary. The different degrees of autonomy are necessary for OC systems, so that they can adapt their behaviour to new environmental situations, where environments of such complex systems change dynamically.

This autonomy as well as disturbances, deviations in the system behaviour from that expected, and other reasons may cause an unwanted emergent behaviour [4] or the whole system may fail unexpectedly. Therefore, the system should be observed (e.g., by an observer) and controlled (e.g., by a controller), so that this emergent behaviour or the complete system failure can be prevented. Consequently, the system performance remains effective and will not deteriorate significantly or at least the system will not fail.

For this purpose, OC uses an observer/controller (o/c) architecture as an example in system design. Using the (o/c) design pattern proposed in [5], the behaviour of OC systems can be observed and controlled. A generic o/c architecture was presented in [6] to establish the controlled self-organisation in technical systems. This architecture is able to be applied to various application scenarios.

In previous papers, we introduced a system for coordinating vehicles at a traffic intersection using an o/c architecture [1][2]. The traffic intersection is regulated by a controller, instead of having physical traffic lights. Figure 1 shows a screenshot from our project.

In both earlier papers, we implemented the generic o/c architecture adapted to our traffic scenario and accomplished our experiments assuming that no deviations from plan occur in the system. In this paper, we continue with the implementation of the case when deviations from desired or planned behaviour arise in the system to completely realise our vision. Therefore, we present different types of deviation that can occur.

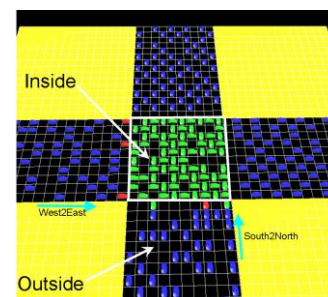


Figure 1. The traffic intersection without traffic lights

This paper is organised as follows. Section 2 describes our original system introduced in [1][2]. Section 3 presents a survey of related work concerning agent-based approaches used for fully autonomous vehicles within an intersection without traffic lights. Section 4 is the main part of this paper. Firstly, it describes how the observer detects deviations. The employing of neighbourhood to determine the location of deviations is depicted secondly. After that, the situation parameters including the specification of deviations and disturbances (accidents) will be explained. Accordingly, the decision making process will be presented. Section 5 introduces different metrics, which can be used to measure and test the system performance, followed by the evaluation of the system performance by means of experimental results. Section 6 draws the conclusion of this work. Finally, the future work is explicated in Section 7.

II. THE ORIGINAL SYSTEM

Previously, we proposed a new multi-agent approach which deals with the problem occurring in the system wherever multiple agents (vehicles) move in a common environment (traffic intersection without traffic lights). We presented the desired system architecture together with the technique that is to be used to cope with this problem. This architecture was an o/c architecture adapted to the scenario of traffic intersection.

The system under observation (vehicles within the centre of the intersection) is considered as a set of elements possessing certain attributes in terms of Multiagent systems. This means that every vehicle in the system is an agent. Every vehicle by itself is assumed to be egoistic (because the driver here is autonomous and he tries quickly to cross the intersection and probably he does not obey his trajectory). Therefore competition situations arise due to the egoistic behaviour (competition-based behaviour) of vehicles, which in turn leads to a traffic jam in the centre of the intersection.

A. Path Planning

Our work introduced in [1] solves a coordination problem by a central algorithm (a central-planning algorithm), using an adapted A*- algorithm that was used for path planning. Here, the path planning is considered as a resource allocation problem (resource sharing problem) where multiple agents (vehicles) move in a shared environment (traffic intersection) and need to avoid collisions.

Path planning delivers collision-free trajectories for all vehicles. Path planning has to be done only for vehicles inside the centre of the intersection. A vehicle outside the centre of the intersection has only local rules, through which this vehicle tries to move forward avoiding collisions with other vehicles.

B. Observation

The observer concentrates only on the intersection. Therefore, other observers in order to observe the agents (vehicles) on the way are not considered. In the centre of the intersection every vehicle has to obey its planned trajectory. Since deviations from the planned trajectories are possible,

the monitoring is done in order to detect the deviations and to intervene dynamically through re-plan trajectories of the affected vehicles. The observer of the intersection aggregates its observations as a vector of situation parameters. These parameters are then sent to the controller.

C. Controlling

Our work presented in [2] introduced the control process of our system. The decision maker is the central part of the controller. The controller uses the decision maker to take a decision how it can intervene most suitable when it is necessary, so that the system can be influenced with respect to the given goal by the user.

However, it is worth recalling that our implementation in [1][2] assumed that all agents (vehicles) obey their planned trajectories, and consequently no deviations from plan will arise. Conversely, this paper deals with deviations aiming to complete our ambitious target (building a hybrid robust multi-agent system).

III. STATE OF THE ART

In the literature, there are enormous works concerning safety properties of usual traffic intersections that concerns only human-operated vehicles. Additionally, there are some works in connection with safety measures of autonomous vehicles within an intersection. In this paper, we focus the discussion of related work on agent-based approaches used for fully autonomous vehicles within an intersection without traffic lights.

In this regard, according to our knowledge, there are no projects that focus on the robustness of autonomous vehicles within an intersection without traffic lights, where deviations from desired (planned) behaviour occur.

A study of the impact of a multi-agent intersection control protocol for fully autonomous vehicles on driver safety is presented in [7]. In this study, the simulations deal only with collisions in intersections of autonomous vehicles. This means that the study deals only with the problem after an accident has already happened aiming to minimise the losses and to mitigate catastrophic events. It assumes that the colliding vehicle sends a signal and the intersection manager becomes aware of the situation immediately. However, it can be noted that the study has not considered the robustness of the intersection system.

Other related work to cope with the coordination problem of autonomous cars at intersection was introduced in [8]. The work proposed a priority-based algorithm that produces a collaborative behaviour between cars of an intersection without traffic lights. In this context, priorities for cars will be allocated according to the waiting times of these cars in the intersection so that car A will take a higher priority than car B if car A has a higher waiting time than car B [8].

To the best of our knowledge, this paper represents the first study towards fault-tolerant (deviation-tolerant) robust hybrid central/self-organising multi-agent systems in intersections without traffic lights using the organic computing (OC) concept.

The work in [7] deals only with collisions, whereas in this paper, the observer observes the autonomous vehicles

within an intersection without traffic lights in order to detect deviations. Additionally, the autonomy in this paper is recognised as a deviation, if the agents are not respecting the central plan. Consequently, the controller intervenes when it is necessary, so that the system remains demonstrating robustness.

IV. THE APPROACH

This section describes the realisation of the observation step of this paper. It presents the detection of deviations, the employing of neighbourhood to determine the location of deviations, the situation parameters which will be collected including the specification of deviations and disturbances (accidents) occurred in the system under observation, and the decision making step.

Robust systems should be fault-tolerant in order to deal with faults, deviations or disturbances and to continue working effectively and fulfilling their major tasks. In the context of this paper, fault tolerance avoids system failures in the presence of deviations from plan that occur in the system allowing the agents (vehicles) of the system to move reliably in their environment (traffic intersection without traffic lights).

The main goal of our project is keeping a multi-agent system robust when disturbances and deviations occur in the system behaviour. Agents (vehicles) have to be observed within the shared environment (intersection) through an observer (the observer of the o/c architecture), because the agents are autonomous (decentral) and they are allowed to behave in a completely autonomous way, therefore deviations from the planned trajectories (central plan) are possible.

This concept introduces a robust hybrid central/self-organising multi-agent system (hybrid coordination) solving the conflict between a central planning algorithm and the autonomy of the agents (decentral, self-organised). Here, the autonomy of the agents is recognised as a deviation from the plan of the central algorithm, if the agents are not respecting this plan (the plan is given to agents as a recommendation).

A. Detection of deviations

The observer concentrates only on the agents (vehicles) within the shared environment (centre of the intersection).

Figure 2 shows how such deviations are detected through the observer (through the detector of deviation and detector of collision) in the system.

The observer reads the planned trajectory of an agent from the trajectories-memory (should-be state), only when this agent is located within the shared environment (within the intersection). At the same time, it reads also the current travelled trajectory (actual state) of this agent, including (x_i, y_i, t_i) , where the agent is at location (x_i, y_i) at time t_i . The detector of deviation in the observer compares the two states (should-be, actual) of every agent in order to detect whether any deviation from the plan occurred as in the next equation:

$$\text{(should-be state)} \text{ XOR } \text{(actual state)}$$

When any deviation from the plan occurs, the detector of collision performs the next process. This process detects whether the deviation led to a collision and finds the

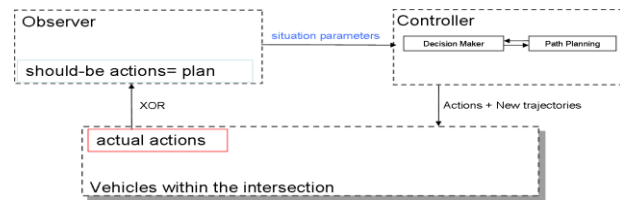


Figure 2. Detection of deviation

deviation class. The possible classes of deviation, which could be detected through the observer in this system, are: autonomy (a deviation from plan), accident (a disturbance) or autonomy with accident (a deviation with a disturbance).

Afterwards, the observer aggregates its observations as a vector of situation parameters describing the actual states and sends it to the controller which selects the more suitable actions and sends it to the system with the new trajectories.

It is important to mention that the controller will decide whether the detected deviations can be tolerated with respect to the safety distance around the agents (vehicles) as described in section (Decision Making).

The deviation detector uses the idea of neighbourhood in order to compare the two states (should-be and actual states) of every agent as described in the next section.

B. Neighbourhood

The term neighbourhood is used in this paper. It is used wherever multiple agents (e.g., robots, vehicles, etc.) move in a common environment (intersection). This paper reaps the benefit of employing “neighbourhood” so that the places of occurred deviations can be determined (the direct neighbourhood, or the second neighbourhood, etc).

Here, the neighbourhood is a square-shaped neighbourhood which can be used to define a set of cells (C) surrounding a given cell c_0 with (x_0, y_0) coordinates; whereas the common environment (the intersection) is a square grid.

When an agent A (vehicle V) is located in a cell c_0 (x_0, y_0) of the intersection, then the neighbourhood N_{c_0} of this cell is the set of cells $C = \{c_i(x_i, y_i)\}$ that can be seen by this agent (vehicle) from the central cell c_0 (x_0, y_0) . Consequently, the neighbours of this agent A (vehicle V) is a set of agents A_i (vehicle V_i) which are located in this neighbourhood N_{c_0} .

The neighbourhood has a distance (radius) which determines to which extent is this neighbourhood limited. This extent represents the view of an agent (vehicle). In a metric space of cells $M = (C, d)$, a set $N_r(c_0)$ is a neighbourhood of a cell c_0 if there exists another set of cells with centre c_0 and radius r , so that

$$N_r(c_0) = N(c_0; r) = \{c \in C \mid d(c, c_0) < r\}$$

Figure 3 shows the idea of neighbourhood which is used in this paper. This definition of neighbourhood can be seen as the well-known Moore neighbourhood (also known as the 8-neighbors) where the distance (radius) is 1. In reference [9], the Moore neighbourhood of range r is defined by:

$$N^M_{(x_0, y_0)} = \{(x, y) \mid |x - x_0| \leq r, |y - y_0| \leq r\}$$

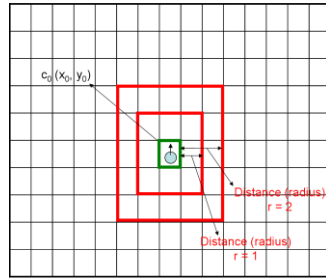


Figure 3. The used neighbourhood

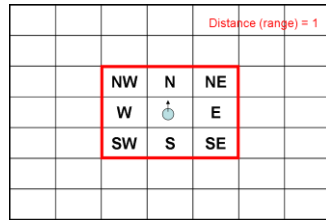


Figure 4. The direct (first) neighbourhood

Here, the neighbourhood is a set of cells surrounding a given cell (x_0, y_0) . Moore neighbourhoods for ranges $r = 0, 1$, and 2 are illustrated in Figure 3. It can be inferred that the number of cells in the Moore neighbourhood of range r is the odd squares $(2r + 1)^2$.

It can be seen that the number of cells in the Moore neighbourhood of range $r=0$ is 1, i.e., it contains only the cell $c_0(x_0, y_0)$ where the agent (vehicle), whose neighbourhood is under search, is located. However, it contains 9 cells in the Moore neighbourhood of range $r=1$, i.e., it contains 8 neighbours and the cell $c_0(x_0, y_0)$ itself. In this case of Moore neighbourhood ($r=1$), the neighbourhood can be called the first or direct neighbourhood. The direct neighbourhood is used as depicted in Figure 4.

Here, the agent (vehicle) is located in the central cell and the 8 neighbours of this agent are named according to the direction in which there are the following neighbours:

N: North, E: East, S: South, W: West.

NW: North West, NE: North East, SE: South East, SW: South West.

Therefore, the neighbourhood of the central cell c_0 , where the agent (vehicle) is located, can be defined as follows:

$$N_1(c_0) = N(c_0; 1) = \{c \in C \mid d(c, c_0) < 1\}$$

$$N_1(c_0) = \{c_0, N, E, S, W, NW, NE, SE, SW\}$$

By the range $r=2$, the Moore neighbourhood contains 24 neighbours and the cell $c_0(x_0, y_0)$ itself (the second neighbourhood).

When the observer detects that an agent (vehicle) is located (the actual state) in a cell (e.g., the cell N), which belongs to the direct neighbourhood $N_1(c_0)$, instead of in their planned cell (e.g., the central cell c_0 that is the should-be state), then it sends to the controller that the deviation of the agent (vehicle) is within the first (direct) neighbourhood $N_1(c_0)$. In a similar way, the observer sends to the controller that the deviation of the agent (vehicle) is within the second neighbourhood, if it detects that the agent (vehicle) is located in a cell which belongs to the second neighbourhood $N_2(c_0)$ instead of in their planned cell c_0 .

C. Situation Parameters

The situation parameters contain the class of the detected deviation and the (x, y, t) of the deviation (the new state), if the observer has detected a deviation. When the controller gets the situation parameters containing a deviation message, then it activates the decision maker and plans new trajectories, if needed, and sends to the system the more suitable actions with the new trajectories.

The situation parameters represent the global description of the current situation of the system under observation and include five parameters:

[Deviations, Accidents, Exceptions, predictions, confidence interval]

- Specification of the detected deviations (unplanned autonomous behaviour).
- Specification of the detected disturbances (accidents).
- Exceptions: e.g., an emergency car.
- Predictions: e.g., the arrival time of the emergency car to the intersection (that is future consequences).
- Confidence interval: e.g., currently normal planning but after two minutes, a special plan for the emergency car shall be activated (that is future consequences).

D. Deviation specification

In this paper, we focus only on deviations from planned behaviour (disturbances, accidents, will be considered in future work). The specification of the deviations includes the following features:

- If any deviation from plan was detected: {true, false}.
- If a deviation was occurred (true), then the begin time of the deviation occurrence, Start (t) and the end time if it's over, End (t).
- The location of the deviation where it occurred, the coordinates (x, y) .
- The type of the deviation (deviation from the planned trajectories).
- The result of the deviation. If the deviation caused an accident or not: {Accd, No. Accd}.

In this regard, there are four possible deviation types. According to the time of the deviation occurrence, it can recognise two deviation types. First, vehicles can change its speed (change speed) trying for example to cross the intersection more quickly than planned. Second, vehicles can stop (making stop) trying to avoid a potential collision with another vehicles in the intersection. However, according to the location of the deviation, two other deviation types can be recognised. First, vehicles can change its lane (change lane) trying for example to leave a full lane of vehicles in order to drive quickly as long as possible. Second, vehicles can change its direction (change direction) trying for example to avoid a potential collision with another vehicles in the intersection or trying to avoid a traffic jam in the intersection.

E. Decision Making

The controller uses the decision maker to take a decision how it can intervene most suitable when it is necessary, so that the system can be influenced with respect to the given goal by the user. The given goal of the user in the introduced application scenario (the intersection) is to keep the system demonstrating robustness in spite of fully autonomous behaviour (causes deviations from plan) and disturbances (accidents) which could appear in the intersection system. In addition, it aims to get autonomous traffic as possible with low delays.

The decision maker is activated when the controller gets the situation parameters from the observer containing a deviation message. On the other side, when there is no deviation, this means that everything is as planned and the decision maker will not be used in this case.

The controller has to intervene on time if it is necessary (decision maker unit) and to select the best corrective action (it makes a decision whether a replanning is required and it uses also the path planning unit if needed) that corresponds to the current situation so that the system performance remains acceptable and the target performance of the system is maintained. Here, the controller has the capability of fault-tolerance (deviation-tolerance) and consequently it decides whether the detected deviations can be tolerated with respect to the free positions (safety distance) around the agents (vehicles). It tolerates a deviation unless the limit of the safety distance is not exceeded through the deviated agent (vehicle). The controller sends to the system the appropriate actions with the new planned trajectories according to the actions table.

V. PERFORMANCE EVALUATION

In this section, we present an initial evaluation of our system using the model of a traffic intersection, which was designed and described in our earlier paper [1]. We include only our main result aiming to deal with deviations from planned (desired) behaviour of agents (vehicles). In future work, we intend to present a more complete empirical evaluation including experiments for measuring the robustness of the system, in which deviations from plan occur and disturbances (accidents) appear in the intersection system.

A. System Performance Metrics

This section will prove the performance of the intersection system presenting an empirical evaluation including experiments with three metrics: throughput, main waiting time and main response time. Here, the first metric, the throughput, is required for estimating the overall reduction of the system's performance, in which deviations from the plan of the controller occur. According to the intersection system, throughput is the total amount of vehicles that left the intersection (simulation area) over time, whereas the mean waiting time is the mean waiting time (ticks or iterations) needed by vehicles to traverse the intersection. The response time has two parts. Firstly, the path planning time, it is the time to search for trajectories,

i.e., the time between the moment when the path planning unit in the controller of the o/c architecture gets messages (requests) from the system (vehicles) and the moment when it sends appropriate trajectories to the system (vehicles). Secondly, the observation/controlling time, it is the needed time by the observer to detect a deviation and the needed time by the controller to re-plan the affected trajectories.

The measurement of the three metrics will be made using several values of the simulation parameter, the maximum number of vehicles, employing the evaluation scenario I (Equal-Equal) described in [1]. Accordingly, the traffic flow rates (traffic levels) of vehicles in south-north and west-east directions is equal, namely 5 vehicles/tick. However, the measurement has been repeated in the cases that the maximum number of vehicles in each direction is equal, namely 20, 40, 80, and 100 vehicles (40, 80, 160, 200 vehicles in both directions). The three used metrics have been measured after 3000 ticks.

B. Test environment

As a test environment, a Pentium 4 personal computer with 2.8 GHz speed and 2 GB RAM has been used to perform the simulation of the traffic application scenario.

C. Test situation

In order to deal with deviations from plan, we assume that vehicles violate (do not obey) their planned trajectories in the centre of the intersection but there are no accidents in the intersection.

In this paper, the desired type of potential deviations in the simulation of the traffic system is (change speed). That means, vehicles can change its speed trying for example to cross the intersection more quickly than planned. With respect to this type of deviations, vehicles that can only make one move (its planned speed is one move) in one tick (a single time step) are trying to make two moves in the same length of simulation time (one tick). For example, a vehicle moves two steps forward, if there is no vehicle in the next two cells in front of it in the intersection. Otherwise, it moves only one step (as its planned speed) if no vehicle only in the next cell in front of it. However, deviations do not cause any accident.

Then, we will measure the system performance and compare the two cases, the system performance with and without deviations. This comparison was managed between the measured values of the first case (without deviations) and the measured values of the second case (with deviations) using the three metrics mentioned above: throughput, mean waiting time and mean response time.

Such comparison can lead to discover the effect of non-compliance with the central plan (planned trajectories of vehicles). Consequently, the comparison here is between the first case (without deviations), which is full central planning and the second case (with deviations), which is hybrid coordination (central and decentral). Therefore, this comparison will be used to determine whether the system performance remains acceptable (will not deteriorate considerably) despite the occurrence of deviations.

# Vehicles (Max. Number of Vehicles)	Si1 Without Deviations (vehicles)	Si2 With Deviations (vehicles)
40	989	989
80	1950	1951
160	3849	3864
200	4800	4786

TABLE I. THE COMPARISON OF THE SYSTEM THROUGHPUT

D. Results of throughput measurement

Table I shows the comparison of the system throughput measured after 3000 ticks between the first case Si1 (without deviations) and the second case Si2 (with deviations) with varying amounts of the maximum number of vehicles in both directions from 40 to 200 vehicles.

In this regard, the same behaviour of the system throughput applies to both cases Si1 (without deviations) and Si2 (with deviations) can be seen. Consequently, the values are roughly identical in both cases. That means, the system throughput by the second case Si2 increases almost always linearly with the number of vehicles despite deviations from the planned trajectories (due to the autonomous vehicles).

This emphasises that no degradation of the system throughput was established when vehicles make deviations (drive more speedily than the plan) and thus do not obey their planned trajectories. Therefore, it is inferred that the central plan (the path planning by means of a central planning algorithm) was optimal. However, no improvement of the system throughput was found. The reason for this is that the vehicles which drive more speedily than planned block other vehicles in the neighbourhood to obey their planned trajectories. Therefore, increase the speed of a vehicle will be at the expense of the speed of other vehicles in the next neighbourhood and thus it may lead to delays of these vehicles.

E. Results of mean waiting time measurement

Table II shows the comparison of the mean waiting times and the standard deviations of all vehicles, that left the intersection measured after 3000 ticks between the both cases Si1 and Si2 with varying amounts of the maximum number of vehicles in both directions from 40 to 200 vehicles. Additionally, Figure 5 shows the same comparison of the mean waiting time as diagram.

Here, it can be seen the same behaviour of the waiting times applies to both cases Si1 and Si2. Consequently, the mean waiting times are roughly identical by both cases. More accurately, there is very small increase by Si2 due to deviations. That means, the mean waiting times by the second case Si2 increase but very slightly despite the deviations from the planned trajectories (due to the autonomous vehicles).

The very small increase of the mean waiting times by Si2 can be traced back to the deviations of vehicles (drive more speedily than planned) which lead in turn to block other vehicles in the neighbourhood causing longer delays than those intended (planned). This confirms the conclusion that the central plan (the path planning for the vehicles) was optimal.

# Vehicles	Si1 Without Deviations		Si2 With Deviations	
	Mean Waiting Time (Ticks)	Std. Deviation	Mean Waiting Time (Ticks)	Std. Deviation
40	0.59	0.80	0.59	0.80
80	0.84	0.53	0.89	1.09
160	1.13	1.16	1.21	1.23
200	1.43	1.39	1.50	1.32

TABLE II. THE COMPARISON OF THE MEAN WAITING TIMES AND THE STANDARD DEVIATION OF ALL VEHICLES THAT LEFT THE INTERSECTION

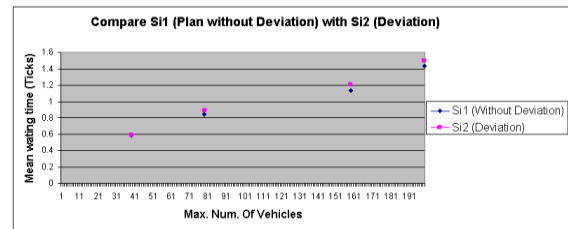


Figure 5. The comparison of the mean waiting times and the standard deviation of all vehicles that left the intersection

Here, it can be seen the same behaviour of the waiting times applies to both cases Si1 and Si2. Consequently, the mean waiting times are roughly identical by both cases. More accurately, there is very small increase by Si2 due to deviations. That means, the mean waiting times by the second case Si2 increase but very slightly despite the deviations from the planned trajectories (due to the autonomous vehicles).

The very small increase of the mean waiting times by Si2 can be traced back to the deviations of vehicles (drive more speedily than planned) which lead in turn to block other vehicles in the neighbourhood causing longer delays than those intended (planned). This confirms the conclusion that the central plan (the path planning for the vehicles) was optimal.

F. Results of mean response time measurement

Figure 6 shows the comparison of the mean response time between the both cases Si1 and Si2 with varying amounts of the maximum number of vehicles in both directions from 40 to 200 vehicles. This comparison was made by the evaluation scenario I (Equal-Equal) after 3000 ticks using the reservation way (AllTrajectoriesVector) described in [1].

Here, different behaviour of the response times between Si1 (without deviations) and Si2 (with deviations) is clearly seen. More accurately, there is an increase by Si2 due to deviations. That means, the mean response times by Si2 increase clearly but reasonably despite deviations from the planned trajectories (due to the autonomous vehicles).

The reasonable increase of the mean response times by Si2 can be attributed to the long time (comparing with the Si1 without deviations) needed to detect deviations occurred in the system and to re-plan all affected trajectories. It can be seen that by (100-100) vehicles in the intersection the mean response time is less than 15 ms, which can be considered a reasonable value for the today's modern computing devices.

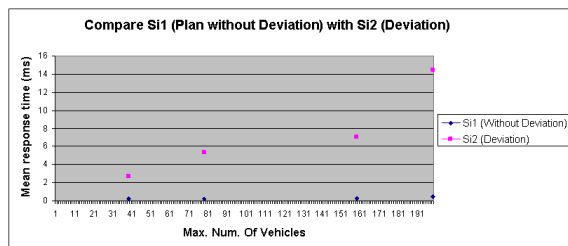


Figure 6. The comparison of the mean response time after 3000 ticks between the first and second cases

VI. CONCLUSIONS

In this work, the hybrid central/self-organising concept aims to increase the autonomy of agents in the central architecture. This means, the hybrid concept tolerates that some agents behave in fully autonomous way in the central architecture. It solves the conflict between a central planning algorithm (a component in the controller) and the autonomy of the agents (the entities of the system under observation and control).

In this paper, deviations from the plan occur but there are no accidents occur in the intersection. That means, vehicles do not obey their planned trajectories (i.e., decentral due to autonomous vehicles). Here, actual trajectories of vehicles will be observed identifying any deviations from plan in order to make replanning by means of the path planning algorithm. Here, vehicles try to change its speed crossing the intersection more quickly than planned (deviation type is change speed). Therefore, we extended our prototype implementation with the aim of making it capable of handling potential deviations.

In this regard, a comparison was made between the first case Si1 (without deviations) and the second case Si2 (with deviations). So, the comparison here was between Si1, which is fully central planning and Si2, which is hybrid coordination (central and decentral). This comparison was made using three metrics, throughput, mean waiting time and mean response time.

The present implementation shows high success potential by detecting deviations from desired (planned) behaviour and consequently to make replanning. By this comparison, the system of central planning shows approximately the same performance as the system of decentral planning when only deviations from the central plan occur but no disturbances (accidents) occur. Based on this, it can be concluded that a local problem (e.g., small deviation from plan) can be solved at local level.

VII. FUTURE WORK

In this paper, we implemented the generic o/c architecture adapted to our traffic scenario and accomplished our experiments assuming that no accidents (disturbances) occur in the system environment (intersection). Therefore, the next step is to continue with the implementation of the

case when accidents arise, in addition to deviations from plan, in the intersection aiming to completely realise our vision. Then, we will measure the system performance and compare the two cases, the system performance with deviations and accidents (disturbances) on one side and the system performance without deviations or accidents from the other side. This comparison will be used to determine whether the system performance remains effective (robust) despite disturbances and deviations occurred in the system (intern) or in the environment (extern). Simultaneously, an appropriate metric for the quantitative determination of the robustness will be developed.

REFERENCES

- [1] Yaser Chaaban, Jörg Hähner, and Christian Müller-Schloer. "Towards fault-tolerant robust self-organizing multi-agent systems in intersections without traffic lights". In *Cognitive09: proceedings of The First International Conference on Advanced Cognitive Technologies and Applications*, November, 2009, pp. 467-475, Greece. IEEE.
- [2] Yaser Chaaban, Jörg Hähner, and Christian Müller-Schloer. "Towards Robust Hybrid Central/Self-organizing Multi-agent Systems". In *ICAART2010: proceedings of the Second International Conference on Agents and Artificial Intelligence*, Volume 2, pp. 341-346, January 2010 Spain.
- [3] CAS-wiki: Organic Computing. http://wiki.cas-group.net/index.php?title=Organic_Computing, [retrieved: February, 2012]
- [4] Moez Mnif, Urban Richter, Jürgen Branke, Hartmut Schmeck, and Christian Müller-Schloer. "Measurement and control of self-organised behaviour in robot swarms". In Paul Lukowicz, Lothar Thiele, and Gerhard Tröster, editors, *Proceedings of the 20th International Conference on Architecture of Computing Systems (ARCS 2007)*, volume 4415 of LNCS, pp. 209-223. Springer, 2007.
- [5] Christian Müller-Schloer. "Organic computing: on the feasibility of controlled emergence". In *CODES+ISSS '04: Proceedings of the 2nd IEEE/ACM/IFIP international conference on Hardware/software codesign and system synthesis*, pp. 2-5. ACM, 2004.
- [6] Urban Richter, Moez Mnif, Jürgen Branke, Christian Müller-Schloer, and Hartmut Schmeck. "Towards a generic observer/controller architecture for organic computing". In Christian Hochberger and Rüdiger Liskowsky, editors, *INFORMATIK 2006 - Informatik für Menschen!*, volume P-93 of GI-Edition - Lecture Notes in Informatics (LNI), pp. 112-119. Bonner Köllen Verlag, 2006.
- [7] Kurt Dresner and Peter Stone. "Mitigating catastrophic failure at intersections of autonomous vehicles". In *AAMAS '08: Proceedings of the 7th international joint conference on Autonomous agents and multiagent systems*, pp. 1393-1396, Richland, SC, 2008. International Foundation for Autonomous Agents and Multiagent Systems.
- [8] Emre Cakar, Jörg Hähner, and Christian Müller-Schloer. "Creating collaboration patterns in multi-agent systems with generic observer/controller architectures". In *Autonomics '08: Proceedings of the 2nd International Conference on Autonomic Computing and Communication Systems*, pp. 1-9, Belgium, 2008.
- [9] Moore Neighborhood in the WolframMathworld. <http://mathworld.wolfram.com/MooreNeighborhood.html>, [retrieved: March, 2012].

Fuzzy Weights Representation of AHP for Inner Dependence among Alternatives

Shin-ichi Ohnishi

Faculty of Engineering
Hokkai-Gakuen University
Sapporo, Japan
ohnishi@eli.hokkai-s-u.ac.jp

Takahiro Yamanoi

Faculty of Engineering
Hokkai-Gakuen University
Sapporo, Japan
yamanoi@eli.hokkai-s-u.ac.jp

Abstract - The Analytic Hierarchy Process (AHP) proposed by T. L. Saaty has been widely used in decision making. Inner dependence method AHP is used for cases in which criteria or alternatives are not independent enough and using the original AHP or inner dependence AHP may cause results to lose reliability because the comparison matrix is not necessarily sufficiently consistent. In such cases, fuzzy representation for weighting criteria or alternatives using results from sensitivity analysis is useful. We present local weights of normal AHP alternatives via fuzzy sets, and then calculate modified fuzzy weights. We also get overall weights of alternatives based on certain assumptions. Results show the fuzziness of inner dependence AHP if the comparison matrix is not sufficiently consistent and individual alternatives do not have enough independence.

Keywords - decision making; AHP; fuzzy sets; sensitivity analysis.

I. INTRODUCTION

The Analytic Hierarchy Process (AHP) proposed by T.L. Saaty in 1977 [1][2][3] is widely used in decision making, because it reflects humans feelings “naturally”. A normal AHP assumes independence among criteria and alternatives, although it is difficult to choose enough independent elements. Inner dependence method AHP [4] is used to solve this problem even for criteria or alternatives having dependence.

A comparison matrix may not, however, have enough consistency when AHP or inner dependence is used because, for instance, a problem may contain too many criteria or alternatives for decision making, meaning that answers from decision-makers, i.e., comparison matrix components, are ambiguous or fuzzy [5]. To solve this problem, we consider that weights should also have ambiguity or fuzziness. Therefore, it is necessary to represent these weights using fuzzy sets.

Our research applies sensitivity analysis [6] to inner dependence AHP to analyze how much the components of a pairwise comparison matrix influence the weights and consistency of a matrix [7]. This may enable us to show the magnitude of fuzziness in weights. We previously proposed new representation for criteria and alternatives weights in AHP [8][9], also representation for criteria weights for inner dependence, as L-R fuzzy numbers [10]. In this paper, we propose a fuzzy representation of overall alternative weights for double inner dependence structure AHP, using results from

sensitivity analysis and fuzzy operations. We then represent fuzziness as a result of double inner dependence AHP when a comparison matrix among alternatives does not have enough consistency.

In Section 2, we introduce AHP and its inner dependence method. The sensitivity analyses for AHP are described in Section 3. Then the fuzzy weight representation is defined in Section 4, and Section 5 is a conclusion.

II. INNER DEPENDENCE AHP

In this section, we introduce steps of normal AHP and its inner dependence method.

A. Process of Normal AHP

(Process 1) Representation of structure by a hierarchy. The problem under consideration can be represented in a hierarchical structure. The highest level of the hierarchy consists of a unique element that is the overall objective. At the lower levels, there are multiple activities (i.e., elements within a single level) with relationships among elements of the adjacent higher level to be considered. The activities are evaluated using subjective judgments of a decision maker. Elements that lie at the upper level are called parent elements while those that lie at lower level are called child elements. Alternative elements are put at the lowest level of the hierarchy

(Process 2) Paired comparison between elements at each level. A pairwise comparison matrix A is created from a decision maker's answers. Let n be the number of elements at a certain level. The upper triangular components of the comparison matrix a_{ij} ($i < j = 1, \dots, n$) are 9, 8, .., 2, 1, 1/2, ..., or 1/9. These denote intensities of importance from activity i to j . The lower triangular components a_{ji} are described with reciprocal numbers as follows

$$a_{ji} = 1/a_{ij} \quad (1)$$

in addition, for diagonal elements, let $a_{ii} = 1$. The lower triangular components and diagonal elements are occasionally omitted from the written equation as they are evident if upper triangular components are shown. The decision maker should make $n(n-1)/2$ paired comparisons at a level with n elements.

(Process 3) Calculations of weight at each level. The weights of the elements, which represent grade of importance among each element, are calculated from the pairwise comparison matrix. The eigenvector that corresponds to a positive eigenvalue of the matrix is used in calculations throughout in this paper.

(Process 4) Priority of an alternative by a composition of weights. The composite weight can be calculated from the weights of one level lower. With repetition, the weights of the alternative, which are the priorities of the alternatives with respect to the overall objective, are finally found.

B. Consistency

Since components of the comparison matrix are obtained by comparisons between two elements, coherent consistency is not guaranteed. In AHP, the consistency of the comparison matrix A is measured by the following consistency index (C.I.)

$$C.I. = \frac{\lambda_A - n}{n - 1}, \tag{2}$$

where n is the order of matrix A , and λ_A is its maximum eigenvalue.

It should be noted that $C.I. \geq 0$ holds. Also, if the value of C.I. becomes smaller, then the degree of consistency becomes higher, and vice versa. The comparison matrix is consistent if the following inequality holds.

$$C.I. \leq 0.1 \tag{3}$$

Also consistency ratio (C.R.) is defined as

$$C.R. = \frac{C.I.}{M}, \tag{4}$$

where M is random consistency value. However we only employ C.I., since we mainly use 4 or 5-dimensional data whose random consistency value is not far from 1

C. Inner Dependence Structure

The normal AHP ordinarily assumes independence among criteria and alternatives, although it is difficult to choose enough independent elements. Inner dependence AHP [4] is used to solve this type of problem even for criteria or alternatives having dependence.

In the method, using a dependency matrix $F = \{f_{ij}\}$, we can calculate modified weights $w^{(n)}$ as follows,

$$w^{(n)} = Fw \tag{5}$$

where w is weights from independent criteria or alternatives, i.e., normal weights of normal AHP and dependency matrix F is consist of eigenvectors of influence matrices showing dependency among criteria or alternatives.

If there is dependence among alternatives, we can calculate modified weights of alternatives $u_i^{(n)}$ with only respect to

criterion i . Then we composite these 2 weights to calculate overall weights of alternative k , $v_k^{(n)}$ as follow:

$$v_k^{(n)} = \sum_i^m w_i u_{ik}^{(n)}$$

where m is number of criteria.

III. SENSITIVITY ANALYSES

When we actually use AHP, it often occurs that a comparison matrix is not consistent or that there is not great difference among the overall weights of the alternatives. In these cases, it is very important to investigate how components of the pairwise comparison matrix influence on its consistency or on the weights. To analyse how results are influenced when a certain variable has changed, we can use sensitivity analysis.

In this study, we use a method that some of the present authors have proposed before. It evaluates a fluctuation of the consistency index and the weights when the comparison matrix is perturbed. It is useful because it does not change a structure of the data.

Since the pairwise comparison matrix is a positive square matrix, Perron-Frobenius theorem holds [11]. From Perron-Frobenius theorem, following theorem about a perturbed comparison matrix holds.

Theorem 1 Let $A = (a_{ij})$, $(i, j = 1, \dots, n)$ denote a comparison matrix and let $A(\varepsilon) = A + \varepsilon D_A$, $D_A = (a_{ij}d_{ij})$ denote a matrix that has been perturbed. Let λ_A be the Frobenius root of A , v be the eigenvector corresponding to λ_A , and w be the eigenvector corresponding to the Frobenius root of A' . Then, a Frobenius root $\lambda(\varepsilon)$ of $A(\varepsilon)$ and a corresponding eigenvector $w(\varepsilon)$ can be expressed as follows

$$\lambda(\varepsilon) = \lambda_A + \varepsilon \lambda^{(1)} + o(\varepsilon), \tag{6}$$

$$w(\varepsilon) = w + \varepsilon w^{(1)} + o(\varepsilon), \tag{7}$$

where

$$\lambda^{(1)} = \frac{v^T D_A w}{v^T w}, \tag{8}$$

$w^{(1)}$ is an n -dimension vector that satisfies

$$(A - \lambda_A I)w^{(1)} = -(D_A - \lambda^{(1)} I)w, \tag{9}$$

where $o(\varepsilon)$ denotes an n -dimension vector in which all components are $o(\varepsilon)$.

A. Analysis for consistency of pairwise comparison

About a fluctuation of the consistency index, following corollary can be obtained from Theorem 1.

Corollary 1 Using appropriate g_{ij} , we can represent the consistency index C.I.(ε) of the perturbed comparison matrix $A(\varepsilon)$ as follows

$$C.I.(\varepsilon) = C.I. + \varepsilon \sum_i \sum_j^n g_{ij} d_{ij} + o(\varepsilon). \quad (10)$$

To see g_{ij} in the equation (10) in Corollary 1, how the components of a comparison matrix impart influence on its consistency can be found.

B. Analysis for weights of AHP

About the fluctuation of the weights, following corollary also can be obtained from Theorem 1.

Corollary 2 Using appropriate $h_{ij}^{(k)}$, we can represent the fluctuation $w^{(1)}=(w_k^{(1)})$ of the weight (i.e., the eigenvector corresponding to the Frobenius root) as follows

$$w_k^{(1)} = \sum_i \sum_j^n h_{ij}^{(k)} d_{ij}. \quad (11)$$

From the equation (7) in Theorem 1, the component that has a great influence on weight $w(\varepsilon)$ is the component which has the greatest influence on $w^{(1)}$. Accordingly, from Corollary 2, how components of a comparison matrix impart influence on the weights, can be found, to see $h_{ij}^{(k)}$ in the equation (11).

Calculations or proofs of these theorem and corollaries are shown in [7].

IV. FUZZY WEIGHTS REPRESENTATIONS

A comparison matrix often has poor consistency (i.e., $0.1 < C.I. < 0.2$) because it encompasses several criteria or alternatives. In these cases, comparison matrix components are considered to be fuzzy because they are results from human fuzzy judgment. Weights should therefore be treated as fuzzy numbers.

A. L-R Fuzzy Numbers

To represent fuzziness of weights, an L-R fuzzy number is used.

L-R fuzzy number

$$M = (m, \alpha, \beta)_{LR} \quad (12)$$

is defined as fuzzy sets whose membership function is as follows.

$$\mu_M(x) = \begin{cases} R\left(\frac{x-m}{\beta}\right) & (x > m), \\ L\left(\frac{m-x}{\alpha}\right) & (x \leq m). \end{cases}$$

where $L(x)$ and $R(x)$ are shape function .

B. Fuzzy Weights of Criteria or Alternatives of normal AHP

From the fluctuation of the consistency index, the multiple coefficient $g_{ij}h_{ij}^{(k)}$ in Corollary 1 and 2 is considered as the influence on a_{ij} .

Since g_{ij} is always positive, if the coefficient $h_{ij}^{(k)}$ is positive, the real weight of criterion or alternative k is considered to be larger than w_k . Conversely, if $h_{ij}^{(k)}$ is negative, the real weight of criterion or alternative k is considered to be smaller. Therefore, the sign of $h_{ij}^{(k)}$ represents the direction of the fuzzy number spread. The absolute value $g_{ij} |h_{ij}^{(k)}|$ represents the size of the influence.

On the other hand, if C.I. becomes bigger, then the judgment becomes fuzzier.

Consequently, multiple C.I. $g_{ij}|h_{ij}^{(k)}|$ can be regarded as a spread of a fuzzy weight concerned with a_{ij} .

Definition 1 (fuzzy weight) Let $w_k^{(n)}$ be a crisp weight of criterion or alternative k of inner dependence model, and $g_{ij} |h_{ij}^{(k)}|$ denote the coefficients found in Corollary 1 and 2. If $0.1 < C.I. < 0.2$, then a fuzzy weight \tilde{w}_k is defined by

$$\tilde{w}_k = (w_k, \alpha_k, \beta_k)_{LR} \quad (13)$$

where

$$\alpha_k = C.I. \sum_i \sum_j^n s(-, h_{kij}) g_{ij} |h_{kij}|, \quad (14)$$

$$\beta_k = C.I. \sum_i \sum_j^n s(+, h_{kij}) g_{ij} |h_{kij}|, \quad (15)$$

$$s(+, h) = \begin{cases} 1, & (h \geq 0) \\ 0, & (h < 0) \end{cases}, \quad s(-, h) = \begin{cases} 1, & (h < 0) \\ 0, & (h \geq 0) \end{cases}$$

C. Fuzzy Weights for Inner dependence among Alternatives

For inner dependence structure among alternatives, we can define and calculate modified fuzzy local weights of alternatives $\tilde{u}_i^{(n)}=(\tilde{u}_{ik}^{(n)})$, $k=1, \dots, m$ with only respect to criterion i using an dependence matrix F_A as follows,

$$\tilde{u}_k^{(n)} = (u_{ik}^{(n)}, \alpha_{ik}^{(n)}, \beta_{ik}^{(n)})_{LR} \quad (16)$$

where

$$u_i^{(n)} = (u_{ik}^{(n)}) = F_A u_i \quad (17)$$

u_i is crisp local alternative weights with only respect to criterion i and α_{ik}, β_{ik} are calculated by fuzzy multiple operations, equation(5) and definition 1.

Fuzzy overall weights of alternative k for inner dependence among alternatives can be also calculated as follows, using fuzzy multiple \otimes and fuzzy summation operations:

$$\tilde{v}_k^{(n)} = \sum_i^m w_i \otimes \tilde{u}_{ik}^{(n)}$$

where $w = (w_i)$ is crisp weights of criteria.

Then we can evaluate fuzzy overall weights of alternatives with their centers and spreads.

V. CONCLUSIONS

We proposed a kind of modified local fuzzy weight by use of sensitivity analyses for inner dependence AHP in case of the dependence among alternatives exist. Moreover we can also calculate overall alternative weights for the inner dependence by fuzzy sets.

Our approach shows how to represent weights and how the result of AHP has fuzziness when data is not sufficiently consistent or reliable.

We now plan to investigate the properties of these fuzzy weights more and apply it to real data. In the future work, we will use this idea for not only inner dependence but also outer dependence structure.

REFERENCES

- [1] T. L. Saaty, "A scaling method for priorities in hierarchical structures," *J. Math. Psy.*, 15(3), 1977, pp. 234—281.
- [2] T. L. Saaty, *The Analytic Hierarchy Process*. McGraw-Hill, 1980, New York..
- [3] T. L. Saaty, "Scaling the membership function," *European J. of O.R.*, 25, 1986, pp. 320-329.
- [4] T. L. Saaty, *Inner and Outer Dependence in AHP*, 1991, University of Pittsburgh.
- [5] S. Ohnishi, D. Dubois, H. Prade, and T. Yamanoi, "A Fuzzy Constraint-based Approach to the Analytic Hierarchy Process," *Uncertainty and Intelligent Information Systems*, 2008, pp. 217-228.
- [6] Y. Tanaka, "Recent advance in sensitivity analysis in multivariate statistical methods," *J. Japanese Soc. Comp. Stat.*, 7(1), 1994, pp. 1-25.
- [7] S. Ohnishi, H. Imai, and M. Kawaguchi, "Evaluation of a Stability on Weights of Fuzzy Analytic Hierarchy Process using a sensitivity analysis," *J. Japan Soc. for Fuzzy Theory and Sys.*, 9(1), 1997, pp. 140-147.
- [8] S. Ohnishi, H. Imai, and T. Yamanoi, "Weights Representation of Analytic Hierarchy Process by use of Sensitivity Analysis," *IPMU 2000 Proceedings*, 2000.
- [9] S. Ohnishi, T. Yamanoi, and H. Imai, "A Fuzzy Representation for Weights of Alternatives in AHP," *New Dimensions in Fuzzy Logic and Related Technologies*, Vol.II, 2007, pp. 311-316.
- [10] S. Ohnishi, T. Yamanoi, and H. Imai, "A Fuzzy Weight Representation for Inner Dependence AHP," *Journal of Advanced Computational Intelligence and Intelligent Informatics*, Vol.15, No.3, 2011, pp. 329-335.
- [11] M. Saito, *An Introduction to Linear Algebra*, Tokyo University Press, 1966.

APPENDIX

[Proof] (Theorem 1)

From Perron-Frobenius theorem [11], the Frobenius root λ_A is the simple root. Thus, expansions (6) and (7) are valid. And then, characteristic equations become

$$\begin{aligned} (A + \varepsilon D_A)(w_1 + \varepsilon w^{(1)} + o(\varepsilon)) \\ = (\lambda_A + \varepsilon \lambda^{(1)} + o(\varepsilon))(w_1 + \varepsilon w^{(1)} + o(\varepsilon)), \end{aligned}$$

$$Aw_1 = \lambda_A w_1.$$

From these two equations, (9) can be obtained. Further, by Perron-Frobenius theorem, eigenvalue of A and transposed A' is same, therefore

$$v'A = \lambda_A v$$

holds, and it becomes

$$v'w \lambda^{(1)} = v'D_A w.$$

Thus, equation (8) holds. (Q.E.D)

Measuring Robustness in Hybrid Central/Self-Organising Multi-Agent Systems

Yaser Chaaban and Christian Müller-Schloer

Institute of Systems Engineering
Leibniz University of Hanover
Hanover, Germany
chaaban,cms@sra.uni-hannover.de

Jörg Hähner

Institute of Organic Computing
University of Augsburg
Augsburg, Germany
joerg.haehner@informatik.uni-augsburg.de

Abstract—It is noteworthy that the definition of system robustness varies according to the context in which the system is used. Therefore, manifold meanings of system robustness were introduced in literature. Additionally, various formal measures and metrics were presented to achieve the system robustness. In previous papers, we proposed a new concept to keep a multi-agent system robust when deviations from planned (desired) behaviour occur in the system. This concept introduces a robust hybrid central/self-organising multi-agent system. The scenario used in this work is a traffic intersection without traffic lights. In this paper, we extend our prototype implementation with the aim of making it capable of handling disturbances (accidents) occur in the system environment (intersection) aiming to completely realise our vision. Simultaneously, we develop an appropriate metric for the quantitative determination of the robustness.

Keywords-Robustness; Organic Computing; Hybrid Coordination; Multi-Agent Systems

I. INTRODUCTION

Organic Computing (OC) has the objective to use principles that are detected in natural systems. In this case, nature can be considered as a model aiming to cope with the increasing complexity of the recent technical systems [3]. Consequently, OC tries to develop systems that are adaptive, flexible and robust at the same time utilising advantage of the organic properties of OC. In this regard, the robustness of OC systems is a key property, because the environments of such systems are dynamic.

In organic systems, the design of the system architecture plays a main role in achieving a robust system so that its performance has to remain acceptable in the face of deviations or disturbances occurred in the system (intern) or in the environment (extern). That means, the developing of robust systems needs to take into account that degradation of the system's performance in the presence of such disturbances should be limited in order to maintain a satisfying performance. Therefore, a robust system has the capability to act satisfactorily even when conditions change from those taken into account in the system design phase. Nevertheless, this capability has to be retained, because of the increasing complexity of novel systems where the environments change dynamically. As a result, fragile systems may fail unexpectedly even due to slightest disturbances. Thus, a robust system will continue working in

spite of the presence of disturbances by counteracting them with corrective interventions.

Considering the system design paradigm, it should be decided whether the system architecture will be centralised or decentralised. Centralised approach is the paradigm where the system is based on a centralised architecture (there is a central controller and the components of the system are not fully autonomous). On the other hand, decentralised approach means that the system has a distributed (there is no central controller and all components of the system are autonomous) or a hierarchical architecture (the components of the system are semi-autonomous in which they are locally centralised) [4]. Based on this, distribution possibilities of system architecture have important implications for system robustness.

Although the decentralised approach would have some advantages over the centralised one, especially scalability, the hybrid approach containing both centralised and decentralised at the same time is applicable and even may be much better than the use of each one separately. The hybrid approach should be robust enough against disturbances, because robustness is an indispensable property of novel systems. Additionally, it represents the interaction between decentralised mechanisms and centralised interventions. In other words, the hybrid approach exhibits the central/self-organising trait simultaneously. This means that a conflict between a central controller (e.g., a coordination algorithm) and the autonomy of system's components should be solved in order to achieving the robustness of the system.

For this purpose, OC uses an observer/controller (o/c) architecture as an example in system design. Using the (o/c) design pattern proposed in [5], the behaviour of OC systems can be observed and controlled. A generic o/c architecture was presented in [6] to establish the controlled self-organisation in technical systems. This architecture is able to be applied to various application scenarios.

During the last years, the progress in communication and information technologies was significant. Consequently, a lot of investigations were done aiming to improve transport systems so that the "Intelligent Transportation System (ITS)" was developed. ITS have several applications in traffic and automotive engineering. According to ITS, numerous notions were distinguished such as, among other, intelligent vehicles, intelligent intersections, and autonomous vehicles. In this context, a traffic intersection without traffic lights can be considered as a main testbed to apply the hybrid

approach, where autonomous agents are autonomous vehicles, and the controller of the intersection is the central unit.

II. THE ORIGINAL SYSTEM

In previous papers, we introduced a system for coordinating vehicles at a traffic intersection using an o/c architecture [1][2]. The traffic intersection is regulated by a controller, instead of having physical traffic lights. Figure 1 shows a screenshot from our project. In this regard, we proposed a new multi-agent approach which deals with the problem occurring in the system wherever multiple agents (vehicles) move in a common environment (traffic intersection without traffic lights). We presented the desired system architecture together with the technique that is to be used to cope with this problem. This architecture was an o/c architecture adapted to the scenario of traffic intersection.

In both earlier papers, we implemented the generic o/c architecture adapted to our traffic scenario and accomplished our experiments assuming that no deviations from plan occur in the system. The evaluation of the concept was carried out based on the basic metrics: throughput, waiting time and response times [1] [2].

In this paper, we continue with the implementation of the case when disturbances (accidents) arise in the system (intersection) to completely realise our vision. Consequently, the system performance remains effective and will not deteriorate significantly or at least the system will not fail.

Additionally, an appropriate metric for the quantitative determination of the robustness will be developed and presented in this paper.

This paper is organised as follows. Section 2 describes our original system introduced in [1][2]. Section 3 presents a survey of related work concerning robust agent-based approaches used for fully autonomous vehicles within an intersection without traffic lights, in addition to various methods for measuring robustness. Section 4 is the main part of this paper. Firstly, it describes the interdisciplinary methodology, “Robust Multi-Agent System” (RobustMAS), developed in this paper. After that, it presents the measurement of robustness and gain according to the RobustMAS-concept. Section 5 introduces the evaluation of the system performance by means of experimental results. Section 6 draws the conclusion of this work. Finally, the future work is explicated in Section 7.

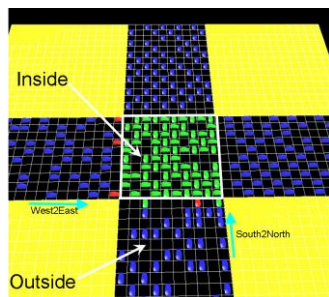


Figure 1. The traffic intersection without traffic lights

III. STATE OF THE ART

Keeping a system robust in presence of disturbances or deviations from plan was investigated by researchers for years. Consequently, many approaches or architectures were introduced towards building robust systems.

In the literature, there are enormous works concerning safety properties of usual traffic intersections that concerns only human-operated vehicles. Additionally, there are some works in connection with safety measures of autonomous vehicles within an intersection. In this paper, we focus the discussion of related work on robust agent-based approaches used for fully autonomous vehicles within an intersection without traffic lights. Furthermore, we consider various methods for measuring robustness.

In this regard, according to our knowledge, there are no projects that focus on the robustness of autonomous vehicles within an intersection without traffic lights, where disturbances occur.

A study of the impact of a multi-agent intersection control protocol for fully autonomous vehicles on driver safety is presented in [7]. In this study, the simulations deal only with collisions in intersections of autonomous vehicles aiming to minimise the losses and to mitigate catastrophic events. However, it can be noted that the study has not considered the robustness of the intersection system.

A. Measures for robustness

Many research projects deals with system robustness and they make an effort to measure the robustness and to find an appropriate metric for it. These projects are in various kinds of science. Robustness metrics play the role to mitigate the expected degradation of the system performance when disturbances occur.

There is a clear lack of study of these metrics in designing robust multi-agent systems. This paper raises the question: “How the robustness can be guaranteed and measured in technical systems?”

In literature, there are diverse potential measures of system robustness. Every measure of robustness is based and designed according to the definition of the robustness concept in a specific context. The most common robustness measure uses the robustness definition related to definition of performance measure. Some robustness measures estimate the system performance using the average performance and its standard deviation, the signal-to-noise ratio, or the worst-case performance. Other robustness measures take into account the probability of failure of system as well as the maximum deviation from benchmark where the system has still the ability to deal with failures [8].

B. Generalised robustness metric

Viable quantitative approaches in order to measure robustness are required. Some approaches were introduced, among others, in [9][10][11]. Both approaches; the FePIA procedure in [9] and the statistical approach in [10] are general approaches and consequently can be adapted to specific purposes (arbitrary environment). In both approaches, diverse general metrics were used to quantify robustness. This metrics estimate specific system features in

the case of disturbances (perturbations) in components or in environment of the system. Additionally, this metrics were mathematically described. Both approaches in [9] and in [10] are applicable in embedded systems design [11] where embedded systems are designed as Systems on Chip (SOC). These both approaches do not comply with the RobustMAS-concept we use to characterise robustness.

To the best of our knowledge, this paper represents the first study towards measuring the robustness of hybrid central/self-organising multi-agent systems in intersections without traffic lights using the organic computing (OC) concept.

IV. THE APPROACH

The Organic Computing initiative aims to build robust, flexible and adaptive systems. Future system shall behave or act appropriately according to situational needs. But this is not guaranteed in novel systems which are complex and their environments change dynamically.

The focus of this paper is to investigate and measure the robustness of coordination mechanisms for multi-agent systems in the context of organic computing. As an application scenario, a traffic intersection without traffic lights is used. Vehicles are modelled as agents.

A. Robust Multi-Agent System (RobustMAS)

An interdisciplinary methodology called “Robust Multi-Agent System” (RobustMAS), has been developed and evaluated regarding different evaluation scenarios and system performance metrics.

The new developed methodology (RobustMAS) has the goal of keeping a multi-agent system robust when disturbances (accidents, unplanned autonomous behaviour) occur. The result is an interaction between decentralised mechanisms (autonomous vehicles) and centralised interventions. This represents a robust hybrid central/self-organising multi-agent system, in which the conflict between a central planning and coordination algorithm on one side and the autonomy of the agents on the other side has to be solved.

The hybrid coordination takes place in three steps:

- A course of action with no disturbance: central planning of the trajectories without deviation of the vehicles.
- Observation of actual trajectories by an Observer component, identifying deviations from plan.
- Replanning and corrective intervention.

In the scenario of this paper, an intersection without traffic lights, the participants are modelled as autonomous (semi-autonomous) agents (Driver Agents) with limited local capabilities. The vehicles are trying as quickly as possible to cross the intersection without traffic lights.

An intersection manager is responsible for coordinating tasks. It performs first a path planning to determine collision-free trajectories for the vehicles (central). This path planning is given to vehicles as a recommendation. In addition, an observation of compliance with these trajectories is done; because the vehicles are autonomous (decentralised) and thus deviations from the plan in principle are possible.

Of particular interest is the ability of the system, with minimal central planning intervention, to return back after disturbances to the normal state (robustness).

For the path planning, common path search algorithms are investigated in our earlier paper [1]. Particularly interesting here is the A*- algorithm. The path planning is considered as a resource allocation problem (Resource Allocation Conflict), where several agents move in a shared environment and have to avoid collisions. The implementation was carried out under consideration of virtual obstacles. Virtual obstacles model blocked surfaces, restricted areas (prohibited allocations of resources), which may arise as a result of reservations, accidents or other obstructions. In addition, virtual obstacles can be used for traffic control.

Different types of deviations from the plan of vehicles were examined in our previous paper [1]. The controller is informed by the observer about the detected deviations from the plan, so that it can intervene in time. The controller selects the best corrective action that corresponds to the current situation so that the target performance of the system is maintained.

In this paper, we introduce an appropriate metric for the quantitative determination of the system robustness. The robustness measurement will be made when disturbances (accidents) occur in the system (intersection).

B. Measurement of robustness and gain according to the RobustMAS-concept

Since RobustMAS aims to keep a multi-agent system robust even though disturbances and deviations occur in the system, a new appropriate method to measure the robustness of a multi-agent system is required. The equivalent goal of RobustMAS by the application scenario, a traffic intersection without traffic lights, is to keep the traffic intersection robust even though deviations from the planned trajectories and accidents occur in the intersection. Therefore, a new concept will be introduced in order to define the robustness of multi-agent systems. Additionally, the gain of RobustMAS will be defined and used to show the benefit of the system that can be obtained through using the hybrid central/self-organising concept, which is a hybrid coordination (central and decentral), compared to using only a decentral planning.

According to the RobustMAS-concept, the robustness of a multi-agent system can be defined as follows:

“The robustness of a multi-agent system is the degradation of the system performance under disturbances that take place in the system environment and under deviations from the plan (central) that occur in the behaviour of the agents (autonomous, decentral)”.

Consequently, RobustMAS-concept assumes that a robust system keeps its performance acceptable after occurrence of disturbances and deviations from the plan.

In order to measure the robustness of RobustMAS in the traffic intersection system, the throughput metric is used for determining the reduction of the performance (system throughput) of RobustMAS after disturbances (accidents) and deviations from the planned trajectories occur. That is because throughput is one of the most commonly used

performance metrics. Therefore, the comparison of the throughput values is required in the three cases: without disturbance, with disturbance with intervention and with disturbance without intervention.

Figure 2 illustrates this comparison where (t_1) is the simulation time step at which the disturbance (accident) will occur and remain until the simulation time step (t_2). This figure shows cumulative performance (throughput) values of the system before and after disturbance occurrence comparing the three mentioned cases.

The black curve is the performance (throughput) of the system if no disturbance occurs during the simulation. The green curve is the performance of the system when a disturbance at time (t_1) occurs and the central planning intervenes on time. The simulation lasts until time (t_2). The red curve is the performance of the system when a disturbance at time (t_1) occurs and the central planning does not intervene. Here, two areas can be distinguished: Area1 and Area2 in order to measure the robustness of RobustMAS as depicted in Figure 3.

This figure shows the idea of how the robustness of the system as well as the gain of the system can be determined according to the RobustMAS-concept.

The robustness (R) of a system (S) can be determined as described in the next formula:

$$R_s = \frac{\text{Area2}}{\text{Area1} + \text{Area2}} = \frac{\int_{t_1}^{t_2} Per(t)_{(with\ Intervention)} d(t)}{\int_{t_1}^{t_2} Per(t)_{(No\ Disturbance)} d(t)}$$

This means that the robustness is the surface area 2 divided by the sum of the two surface areas 1 and 2. The Area2 is the integral of the green curve (disturbance with intervention) between $t = t_1$ and $t = t_2$. The sum of Area1 and Area2 is the integral of the black curve (no disturbance) between $t = t_1$ and $t = t_2$.

Additionally, the gain of the system can be used as a secondary measure. In this context, the gain of a system can be defined according to the RobustMAS-concept as follows:

“The gain of a system is the benefit of the system through central planning (compared to decentral planning). Accordingly, the gain of a system represents the difference between the system performance (throughput) in the two cases, with and without intervention of the central planning algorithm”. This issue is expressed by the following equation:

$$\text{Gain} = \Delta Per (\text{Intervention}) - \Delta Per (\text{NoIntervention})$$

As depicted in Figure 3, the gain of the system can be calculated using the values of the system performance (throughput values) at the end of the simulation time ($t=t_2$). Here, $\Delta Per(\text{Intervention})$ represents the difference between the system performance in the two cases, without disturbance and disturbance with intervention of the central planning algorithm; whereas $\Delta Per(\text{NoIntervention})$ represents the difference between the system performance in the two cases,

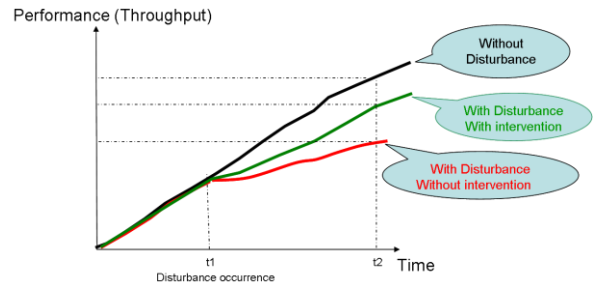


Figure 2. The comparison of system performance (throughput) by the situation (without disturbance) to the situation disturbance in both cases (with and without intervention)

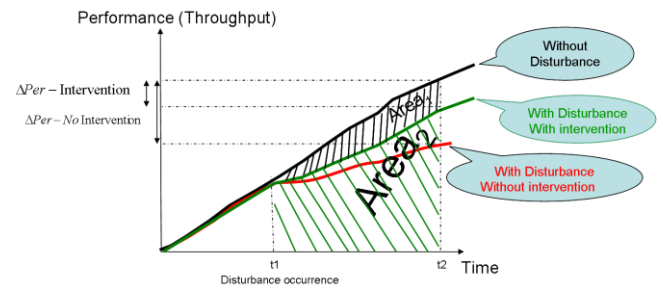


Figure 3. Measuring robustness and gain according to the RobustMAS-concept

disturbance with and without intervention of the central planning algorithm.

The discussion of the robustness measurement using the system throughput metric will be based on the simulation parameter, the disturbance strength. This parameter represents the size of the accident in the used traffic system.

Obviously the disturbance strength influences the system performance which in turn leads to different degrees of system robustness. When the disturbance strength is increased, then the system robustness will reduce. This means that the increase of the disturbance strength is inversely proportional to the degree of the system robustness.

According to the used application scenario, the size of the accident influences the intersection throughput (the number of vehicles that have left the intersection area) which in turn leads to different degrees of the robustness of the intersection. When the size of the accident increases, then the intersection robustness will decrease. This can be justified simply on the ground that accidents will cause obstacles for the vehicles in the intersection. These obstacles will impede the movement of vehicles which are behind the accident location. Additionally, the central plan algorithm considers the accidents as virtual obstacles (restricted areas) and therefore it limits the planned trajectories of potential traffic. The autonomous vehicles which do not obey their planned trajectories have to avoid the accident location by performing a lane change (to the right or to the left of the accident location) if it is possible. Certainly, autonomous vehicles have to check the possibility to avoid the accident by pulling into another lane before they take this evasive action. So, the vehicle behind the accident location tries to overtake the accident location on the right if the intended position is not occupied by another vehicle. Otherwise, if the intended

position is occupied by another vehicle, then the vehicle tries to overtake the accident location on the left if the intended position is not occupied by another vehicle. If all potential intended positions are occupied, then the vehicle stops (doesn't change its position) and repeats this behaviour (the evasive action) again in the next simulation step.

V. PERFORMANCE EVALUATION

In this section, we present a complete empirical evaluation of our system using the model of a traffic intersection, which was designed and described in our earlier paper [1]. This evaluation includes experiments for measuring the robustness of the system, in which deviations from plan occur and disturbances (accidents) appear in the intersection system. That means, it deals with deviations from planned (desired) behaviour of agents (vehicles), in addition to disturbances (accidents).

A. Test situation

In this test situation, the vehicles do not obey their planned trajectories (the central plan) and thus deviations from the plan will occur as well as accidents in the intersection.

In this regard, an observation of actual trajectories by the observer will be made in order to detect any deviations from plan and to detect potential accidents in the intersection allowing the controller to make replanning for all affected trajectories using the path planning algorithm. This will be carried out via the deviation detector component and the accident detector component in the observer [1][2].

The test situation serves to measure the robustness of the intersection system and to assess the degree of the robustness of RobustMAS during disturbances (e.g., accidents) and deviations (e.g., unplanned autonomous behaviour).

B. Measuring robustness and gain

As mentioned above, the throughput metric is used to determine the reduction of the performance (system throughput) of RobustMAS after disturbances (accidents) occur and consequently to measure the robustness of RobustMAS in the traffic intersection system. Additionally, the discussion of the robustness measurement is based on the simulation parameter, the disturbance strength (the size of the accident). The measurement has been repeated in the cases that the disturbance strength is 1, 2, and 4. That means, the accident occupies an area of size 1, 2 and 4 cells in the traffic intersection. The results were obtained in an interval between 0 und 3000 ticks.

It can be concluded that the increase in the size of the accident is inversely proportional to the degree of the intersection robustness.

RobustMAS tries to guarantee a relatively acceptable reduction of the intersection robustness when the size of the accident increases. RobustMAS ensures at least that increasing of size of the accident will not lead to failure of the intersection.

Because the location of the accident within the intersection plays a major role in the performance of the intersection system, the simulation was repeated 10 times.

Each time of repetition, an accident will be generated in a random position of the intersection by choosing a random (x, y) coordinate pair within the intersection. This (x, y) coordinate pair represents the central cell of the accident. The other cells which represent the whole accident location will be chosen also randomly depending on the value of the simulation parameter "size of accident", so that the chosen cells will surround the central cell (x, y) of the accident. So, it can be ensured that accidents will be generated in different parts of the intersection achieving more realistic study. The average values of the system throughput will be calculated from several repetitions of the simulation (random accident locations), so that a picture of how an accident would affect the system performance is created.

The simulation parameter "Disturbance occurrence time" (Accident occurrence time) represents the time (the time step in the simulation) at which the accident will be generated. The time is measured by ticks. In the simulation, the "Accident tick" was adjusted to the value of the tick "1000", i.e., an accident should be generated at tick "1000". That means, the simulation has no accident in the interval [0-1000]; whereas it has an accident in the remaining simulation interval [1000-3000] as depicted in Figure 4. Here, the system performance is the intersection throughput. The throughput is measured by the number of vehicles that left the intersection area (cumulative throughput values).

The robustness and the gain of the traffic intersection system can be determined using the two formulas of the robustness and the gain of the system described above.

In order to see the effect of the disturbance strength (size of the accident), Table I compares the obtained results of the robustness and the gain of the system for various values of disturbance strength after 3000 ticks.

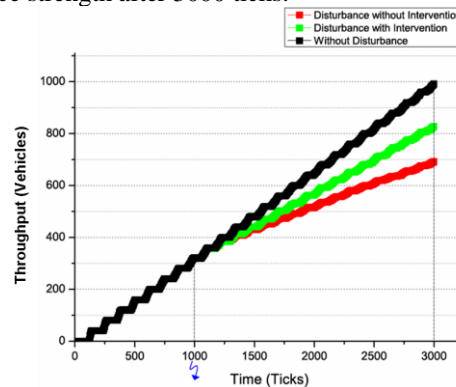


Figure 4. The "Disturbance occurrence time" adjusted to the tick (1000) and the simulation length is (3000) ticks

Disturbance strength (Accident size)	Robustness (%)	Gain (Vehicles)
1	87	137
2	86	161
4	83	169

TABLE I. THE ROBUSTNESS AND THE GAIN OF THE SYSTEM FOR VARIOUS VALUES OF DISTURBANCE STRENGTH

It can be concluded that when the disturbance strength increases, the robustness of the system decreases, but very slightly showing a high degree of robustness. This emphasises that a degradation of the system throughput was established when an accident was occurred in the intersection and the vehicles made deviations violating their planned trajectories. Therefore, in case of disturbances (accidents), the intervention of the central plan (a central planning algorithm) led to better system performance than the decentralised solution in which agents (vehicles) have to plan locally their trajectory.

On the other hand, when the disturbance strength increases, the gain of the system increases. This confirms the conclusion that the intervention of the central plan was better demonstrating an improvement of the system throughput.

Therefore, it is inferred that a global problem (e.g., an accident in the intersection) should be solved at global level, because there is a central unit (the o/c architecture) that has the global view of the system. This central unit can plan better than a decentral unit. A central unit needs only longer time than a decentral unit. This issue can be solved simply by providing central units that have plenty of resources, e.g., CPU capacity (real-time requirements), memory capacity, etc, as well as the management of these resources.

VI. CONCLUSIONS

In this paper, we extended the implementation of the generic o/c architecture adapted to our traffic scenario and accomplished our experiments assuming that accidents (disturbances), in addition to deviations from plan, occur in the system environment (intersection).

Additionally, we introduced an interdisciplinary methodology called "Robust Multi-Agent System" (RobustMAS). We developed and evaluated RobustMAS aiming to keep a multi-agent system robust when disturbances (accidents, unplanned autonomous behaviour) occur. RobustMAS represents a robust hybrid central/self-organising multi-agent system, in which the conflict between centralised interventions (central planning) and the autonomy of the agents (decentralised mechanisms, autonomous vehicles) was solved.

In this regard, we measured the system performance and compared the two cases, the system performance with disturbances on one side and the system performance without disturbances from the other side. This comparison showed that the system performance remains effective (robust) despite disturbances and deviations occurred in the system. Furthermore, we presented an appropriate metric for the quantitative determination of the robustness of such hybrid multi-agent systems. Subsequently, we measured the robustness and gain of a multi-agent system using the RobustMAS-concept. The experiments showed a high degree of robustness of RobustMAS.

VII. FUTURE WORK

One aspect that may be of interest for future work is the fairness between the system's agents (vehicles). In order to achieve this fairness, there are different approaches that deal with this issue. The other aspect that will be an important issue in future is the coordination and cooperation of multiple intersections without traffic lights.

REFERENCES

- [1] Yaser Chaaban, Jörg Hähner, and Christian Müller-Schloer. "Towards fault-tolerant robust self-organizing multi-agent systems in intersections without traffic lights". In *Cognitive09: proceedings of The First International Conference on Advanced Cognitive Technologies and Applications*, November, 2009, pp. 467-475, Greece. IEEE.
- [2] Yaser Chaaban, Jörg Hähner, and Christian Müller-Schloer. "Towards Robust Hybrid Central/Self-organizing Multi-agent Systems". In *ICAART2010: proceedings of the Second International Conference on Agents and Artificial Intelligence*, Volume 2, pp. 341-346, January 2010 Spain.
- [3] CAS-wiki: Organic Computing. http://wiki.cas-group.net/index.php?title=Organic_Computing, [retrieved: February, 2012].
- [4] Y. Uny Cao, Alex S. Fukunaga, and Andrew B. Kahng. *Cooperative Mobile Robotics: Antecedents and Directions*. Autonomous Robots, pp. 4:226-234, 1997.
- [5] Christian Müller-Schloer. "Organic computing: on the feasibility of controlled emergence". In *CODES+ISSS '04: Proceedings of the 2nd IEEE/ACM/IFIP international conference on Hardware/software codesign and system synthesis*, pp. 2-5. ACM, 2004.
- [6] Urban Richter, Moez Mnif, Jürgen Branke, Christian Müller-Schloer, and Hartmut Schmeck. "Towards a generic observer/controller architecture for organic computing". In *Christian Hochberger and Rüdiger Liskowsky, editors, INFORMATIK 2006 - Informatik für Menschen!*, volume P-93 of GI-Edition - Lecture Notes in Informatics (LNI), pp. 112-119. Bonner Köllen Verlag, 2006.
- [7] Kurt Dresner and Peter Stone. "Mitigating catastrophic failure at intersections of autonomous vehicles". In *AAMAS '08: Proceedings of the 7th international joint conference on Autonomous agents and multiagent systems*, pp. 1393-1396, Richland, SC, 2008. International Foundation for Autonomous Agents and Multiagent Systems.
- [8] H. Schmeck, C. Müller-Schloer, E. Cakar, M. Mnif, U. Richter. "Adaptivity and Self-organisation in Organic Computing Systems". *ACM Transactions on Autonomous and Adaptive Systems*, 2009, pp. 10:1-10:32.
- [9] V. Shestak, H. J. Siegel, A. A. Maciejewski, and S. Ali. "The robustness of resource allocations in parallel and distributed computing systems". In *Proceedings of the International Conference on Architecture of Computing Systems (ARCS 2006)*, pp. 17-30, 2006.
- [10] D. England, J. Weissman, and J. Sadagopan. "A new metric for robustness with application to job scheduling". In *IEEE International Symposium on High Performance Distributed Computing 2005 (HPDC-14)*, Research Triangle Park, NC, July 24-27, 2005.
- [11] Waldschmidt, K., Damm, M., "Robustness in SOC Design", *Digital System Design: Architectures, Methods and Tools*, 2006. DSD 2006. 9th EUROMICRO Conference on Digital System Design, pp. 27-36, Volume: Issue: , 0-0.

Some New Concepts in MCS Ontology for Cognitics;

Permanence, Change, Speed, Discontinuity, Innate versus Learned Behavior, and More

Jean-Daniel Dessimoz and Pierre-François
Gauthey

HEIG-VD, School of Business and Engineering
HES-SO, Western Switzerland University of Applied
Sciences

CH-1400 Yverdon-les-Bains, Switzerland

e-mail: {jean-daniel.dessimoz, pierre-
francois.gauthey}@heig-vd.ch

Hayato Omori

Department of Mechanical Engineering
University of Chuo
Tokyo, Japan

e-mail: h_omori@bio.mech.chuo-u.ac.jp

Abstract—Paving the way for advanced cognitive technologies and applications, an ontology for automated cognition, cognitics, has been proposed. Starting in a pragmatic way from where we stand, in particular with humans creating robots, progressing with distributed axioms, navigating through small contexts in direction of selected goals (design of high performance machines, of robots cooperating with humans, and better understanding of cognition in humans), we adopt an incremental, constructivist approach, in conceptual and operational frameworks. Discussion is made in the current paper of a number of cognitive notions including those of reality, time and revisited “speed”, change and discontinuity, innate and learned behaviors, as well as the human-inspired basics of communication in a group. These newly defined notions conveniently complement the existing Model for Cognitive Sciences ontology. All these elements confirm the rightness of our current approaches in solving concrete Artificial Intelligence problems and this is illustrated below by some concrete examples taken in domestic context, including robots capable of learning.

Keywords- cognitive robotics; MCS ontology for cognition; cognitive speed; discontinuity; reality; innate behavior; communication basics

I. INTRODUCTION

In the past century, a major step in evolution has been made when information has been formally defined, and infrastructure has been provided for communication and processing of information in a massive scale.

In the early days of signal processing, in technical terms, information was neatly provided by some transmitters, originating from some other electronic devices, control panels, microphones or other sensors yet. Machine-based sources of information were limited to signal generators, such as for sine-waves or pseudo-random sequences.

Then, however, things have become much more complex and cognition is the new domain to domesticate, where pertinent information is autonomously created by expert agents (e.g. , [1]). It is with this very relevant goal that the MCS theory for cognitive sciences has been created (Model for Cognitive Sciences [2, 3] and the cognitive pyramid (Fig. 1). This has been published and has already brought

interesting benefits in terms of understanding the core cognitive properties, assessing quantitatively their values, and allowing for convincing implementation of cognitive robots in selected areas [4]. So far, people have developed context-dependant expertise indicators (e.g. Elo points for chess-players, Association of Tennis Professionals points for tennis-players, or IQ scores), but unfortunately no other work, in our knowledge, has addressed the formal, technically-prone definitions of cognitive entities with associated units, beyond the concept of information.

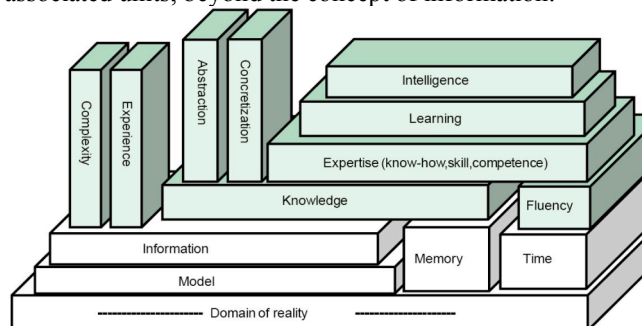


Figure 1. Main cognitive entities in MCS theory. Important cognitive concepts, defined in MCS theory, are colored in green (left). They are based on a few classic entities, including reality and time, which, though classic, also need a discussion from a cognitive perspective

Fig.1 schematically presents the main cognitive entities in MCS theory context. Without giving here again the equations for their quantitative assessments, let us briefly review their definitions.

The top group is green, referring to MCS essentials. Knowledge is, for an agent (human or possibly machine-based) the property to deliver the right information; fluency, the cognition speed; expertise, the property to deliver information right and fast, the product of knowledge and fluency; learning, the ability to increase expertise levels; intelligence, the capability to learn, and quantitatively, the ratio of learning to experience; experience, the amount of information witnessed in terms of input and output associations (“examples”, “experiments”); complexity, the amount of information necessary to exhaustively describe an object; abstraction, the property of delivering less

information than it is incoming; concretization is the inverse of abstraction.

The lower group is white. Even though in principle the corresponding concepts are classical, experience shows that their limits are not well understood, and this is especially disturbing as the new, green concepts are built on them. Thus information is very much time-dependant, the delivery of it essentially making its repetition useless; information is essentially subjective, which means that the same message may convey different quantities to different users; memory is considered here as a support for the permanence of messages, such as an engraved stone, i.e. without the typically associated writing and reading processes; the last 3 quoted concepts, reality, model and time, are further discussed in the sequel of this paper.

In general, commonsense, classical concepts, and corresponding MCS concepts are quite synonymous and can be described by the same words; nevertheless, there remain often subtle differences, and in the sequel of this article, when the respective distinctions should be made, the “c-” prefix will be added for the terms defined in MCS Ontology; for example c-speed (1/s unit) is not the usual displacement, motion speed (m/s unit).

Today another step is considered, whereby artificial cognitive agents should effectively approach human cognitive capabilities for three complementary reasons: better functional services (including those involving human-machine cooperation), better understanding of human nature, and implementation possibility of theories in order to make them operational, and thereby possibly validate them. Proceeding should now be done in incremental steps along two complementary ways: the understanding of concepts, and the operationalized implementation of cognition in machines.

In this endeavors, a first surprise had been to experience that the prerequisites, the basis on which the MCS theory was built, were not at all as widely understood as expected (re. general surveys [5,6] and focused discussions below). A complement had been progressively brought, re-discussing classical topics, namely those relating to the notions of information, models and memory.

Now, at the moment of addressing in its “generality” the cognitive faculty of humans, another necessary pre-condition for implementing it in machine-based agents appears. A further analysis, of deeper foundations yet on which the MCS theory is grounded, cannot be escaped. What is reality? What is time? How to cope with the infinite complexity of reality? How much innate or wired can be the cognitive capability we are considering?

The paper addresses these questions in successive sections: Section II for reality; Section III for time; Section IV for ways to cope with the infinite complexity of reality, in particular including the innate versus learning paradigms for producing new cognitive agents. Finally, the general presentation made so far will be illustrated in Section V with detailed concrete examples, taken in the field of cooperative robotics, addressing both human and machine-based cognitive aspects and operations.

II. WHAT IS REALITY?

In MCS theory, reality is in principle viewed as everything, including not only physical objects but also immaterial ones, including information repositories, models, assumptions, novels and if-worlds. It corresponds to the universal definition of Parmenides: What is, is. As illustrated in Fig. 2, reality is infinitely complex (re. the definition of complexity in MCS ontology: an infinite amount of bits or megabytes of information would be required for the exhaustive description of reality), so much so that even any tiny part of it, in practical terms, is infinitely complex as well. Reality, including self, is also always the ultimate reference. All subjects facing reality are bound to adopt a constructivist approach [7], relying on means initially self-provided, as innate or “wired”, and later on, hopefully improving those means, in particular by proceeding with exploration and learning by experience (Concretely, a human starts in particular with DNA; a typical robot of ours is given in particular a computer and an executable program; then they explore and learn and ultimately successfully achieve many new, unforeseen operations).

This position is similar to the one of Kant [5], for whom innate, pre-existing “categories” are initially required, allowing cognitive agents to perceive. And simultaneously, by careful axiomatic contributions, complex cognitive structures including possible collective, shared models (culture) can be elaborated.

In summary, in a first stage where a single individual is considered, we do not need to know what is reality, as we benefit from the beginning, of an innate (or “wired” in machines) capability to cope with it (models). Nevertheless, rational processes can also develop in parallel, which, with automated cognition, possible exploration tasks, and on the basis of acquired experience, should yield various improvements.

At the next stage, where the creation of a new capacity to cope with reality is considered, ingenuity is the key, as defined in MCS ontology [3].

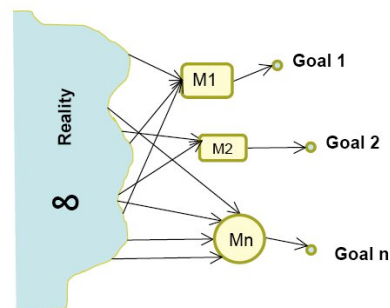


Figure 2. Experience strongly suggests that reality is infinitely complex. Models may be simple and validly serve singular goals, but they should always be considered as very specific for those goals and infinitely lacunary with respect to reality

III. WHAT IS TIME?

Strangely, time is far from well defined in classical terms. The proposal of Kant is interesting with his

complementary attitudes, leaning on one hand towards intuition, whereby everyone has a spontaneous understanding of the time concept; and leaning on the other hand towards rationality (Weltweisheit, philosophy), by which a rigorous, “mathematical”, definition could be elaborated – with no guarantee but chance however to have this latter construct coincide with the former one. Similarly, St-Augustine claims to know very well what is time - as long as noone asks for a formal definition of it! Even in the contemporary time where philosophy and science have both well developed, Rosenberg apologizes for simply defining time as follows: “time is duration” and “duration is the passage of time” [6].

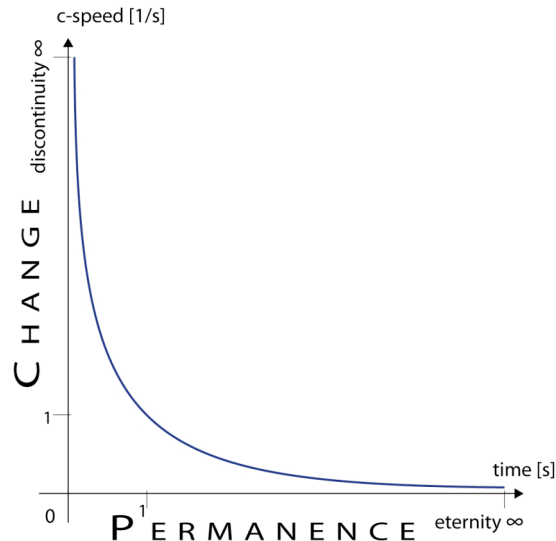


Figure 3. Time characterizes permanence, and speed as defined in MCS ontology, i.e., “c-speed”, does it for change.

It is well-known that dictionaries tend to have circular definitions. This should be accepted for at least two reasons: as clearly stated by Kant, reality and cognitive world are disconnected; in this sense, a “first” definition, i.e., relating directly to reality is impossible (convenient complements to circumvent this obstacle include visits to museums, science parks, touring and lab experiments). Now, with circular definitions, the cognitive world appears as a maze with multiple entry points. In a chain of 10 so-related concepts, the reader has ten chances to hop with his/her/its intuition from reality to the cognitive world (which includes libraries, languages, dictionaries and Wikipedia).

Time has already been addressed in MCS ontology, as well two other closely-related concepts fluency and agility. Here, however, things improve: a clearer articulation is made between time and change; speed is defined in a universal way, which then helps, with appropriate, specific complements, better handle changes in a variety of domains. Fluency, thus, becomes the speed of expert information delivery and agility the speed of action.

We propose here to define time as a distributed axiom, in a cloud of 6 interconnected concepts: time, permanence, eternity, change, speed, and discontinuity (re. Fig. 3):

- Time is a measure of permanence, and is quantified by the “second” as a unit.

- Permanence is the property of things that do not change.

- A permanence that is persistent for an infinite amount of time is eternity.

- Speed is a measure of change, and is quantified, in MCS ontology (“c-speed”), by the inverse of a second (notice that this is more general than the usual motion speed, assessed in meter per second; it can also apply to all dimensions other than linear in distance, e.g. speed of rotation, heating, speech, sedimentation, or general cognitive operations).

- Change is the property of things that do not remain same, stable, permanent over a certain time.

- A change that occurs at an infinite speed is a discontinuity.

If any single one of the six previous statements is intuitively understood, this evidence can be rationally propagated to all the other 5 associated concepts.

Changes can be of different orders: the speed of change may be permanent, constant over a certain time (1st order change); or the speed itself may change at constant speed, yielding the notion of permanent acceleration (2nd order change), etc. (re. “jerk” for 3rd order change).

IV. HOW TO COPE WITH THE INFINITE COMPLEXITY OF REALITY?

Section II has shown that reality should be considered as infinitely complex. Yet, it appears that much can often be achieved in practice. So, what paradigms allow for such positive outcomes? The current section presents 5 of them, including the selection of (prioritized) goals, the pragmatic exploration of local circumstances, the generation of agents with some innate or wired initial capabilities, an iterative process improving performance, and the accelerated progress resulting from setting multiple, coordinated actions in parallel.

A. Necessity of selecting a goal

As illustrated in Fig. 2, experience shows that numerous goals can be reached while ignoring most aspects of reality. Numerous simple ad hoc models prove effective. To the point where even bacteria not only survive in our often-hostile world, but even usually live well and multiply.

A basic paradigm consists in focusing attention on selected contexts, successively considering them with as many constraints as possible. A good example of this approach is notably the famous “hic et nunc – here and now” framework in Jesuits’ case studies. Here, are some other typical cases: “under assumption”, “with abstract and holistic views”, “with more detailed analytical representations”, etc.

Critical for success is the proper selection of a goal. A goal in practice always has a number of peculiarities that open possibilities for effective and simple modeling (re. also Fig. 2). In AI, it is often said in substance that experts know what to ignore in a given situation.

For example, we have stated above what is the main goal of the research we refer to in this paper: to make possible the design of artificial cognitive agents effectively approaching

human cognitive capabilities, with further possible positive impacts in three areas (see Introduction section). Toward this goal, an effective model implies in particular the proposed extensions of MCS ontology.

Some other, more intuitive arguments for selecting a goal include the following two:

- It may be useful to map in cognitive context the well established A* algorithm for navigation in space [8]; crucial elements are the location of goal-site and the one of current position.
- As reality is infinitely complex, non-oriented efforts would get as diluted and ineffective as curry powder in a river (re. Thai word recommending humans to focus on selected goals).

B. Pragmatic approach adapted to circumstances

Then care must be given to current status. In a pragmatic way, we propose to start with the world as is, modeled as simply as necessary for reaching the considered goals. In cognition, backtracking is the rule. From the selected goal, specifications are derived, which then lead the cognitive process, and in particular an active perception (“exploration”) faculty capable of acquiring useful information and the possible experience elements eventually allowing for improvements (re. Fig. 4).

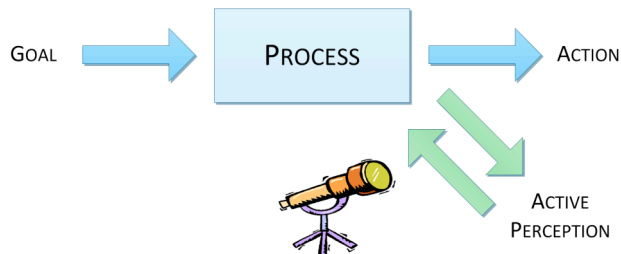


Figure 4. In cognition, backtracking is the rule. From the selected goal, specifications are derived, which then lead the cognitive process, and in particular an active perception (“exploration”) faculty capable of acquiring the experience necessary for improvements.

C. Innate goal and capabilities

A prominent place is initially given to innate and current capabilities (re. Fig. 5).

In practice, it is precious to be aware that even humans do not start, individually, from scratch. At birth time, they already know for example how to grasp, crawl, find their food; these tasks are not necessarily obvious for a robot.

Some chicken for example have such an elaborate pre-design that they can be industrially grown without any social assistance; they can get out of their egg and develop without the help of previous generations.

It is therefore legitimate also for machine-based agents under study to start from some predefined (let us say “wired”, or pre-programmed) initial state. And humans have created robots.

D. Improved goal and capabilities

In the paragraph about reality, care had been taken to keep things as simple as possible. Nevertheless, multiple

cognitive processes, including some innate capabilities, and possibly newly acquired experience elements could already been mentioned, opening the way for improvements and learning.

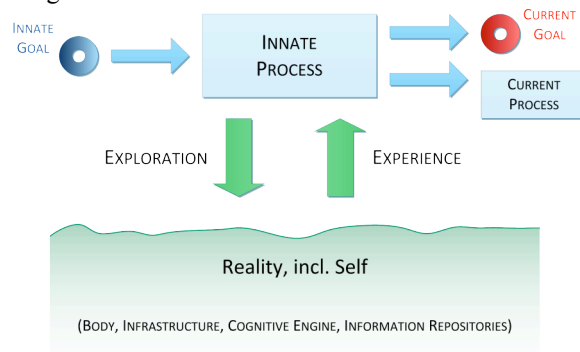


Figure 5. Current goals and processes may result from exploration performed and/or experience acquired by an agent running a given cognitive process in a certain domain of reality. Initial goals and processes are innate (or “wired”).

The next interesting stage occurs when the design and creation of a new capacity to cope with reality is considered (Fig. 6). For connecting directly to reality, chance (as in Darwin’s theory,) or ingenuity (as defined in MCS ontology [3]) are the main keys.

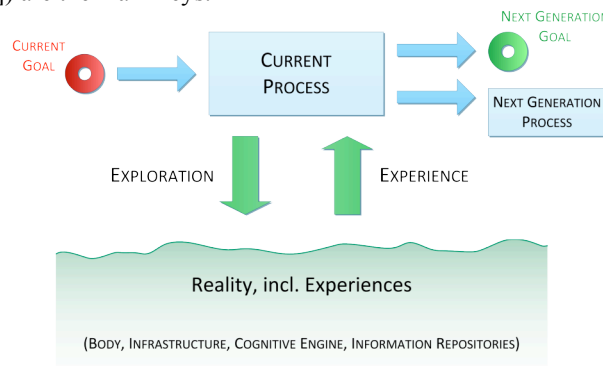


Figure 6. Current goals and processes may lead to improvements in next generation system (in particular for humans or machines).

E. Collective approach; elements of communication, credibility, reputation, and trust

Experience shows that the coordinated forces of multiple agents – groups- increase the possibilities of successful actions in the world.

This paradigm can be exploited in a multiplicity of ways. Of particular interest for our context, we find groups of humans, of robots, and of hybrid resources – robots cooperating with humans.

Groups have already been defined in MCS ontology. In this context a critical ingredient has been identified as the culture of the group, and, in reference to it, the communication channel and some kind of formalism, protocol or language.

Two new elements come now under scrutiny. The first one, is, for inspiration, the case of baby communication, a case reasonably simple for the purpose of progressive

transfer of approach to machine-based systems. The second one is the sharing of error probability of a source, among humans, which expands at group-level a feature already taken into account for individual cognitive agents.

In their early months of existence, babies appear to have at least 4 types of communication capabilities. In some circumstances, babies can express strongly (high arousal) their emotions [9], their states of happiness and unhappiness (positive or negative valence); they cry, or smile, which typically leads to corresponding correcting or sustaining actions from their parents. They also test the good understanding and adequacy of key behaviors and gestures by imitating, and mimicking; they also sometimes just synchronize with others in their attitudes and actions (they join in or trigger yawning, and laughing).

The MCS theory has introduced a value, in terms of probability of error, for cognitive agents delivering information. This affects the quantitative estimation of knowledge characterizing these sources. Now we can add a similar, interesting property at group level, which allows for appropriate propagation of the expected error-rate. In this framework, agents would take into consideration the credibility of sources and in particular of other group members; if shared at group level, this credibility could form the basis for, collectively, building up a reputation. Thus when receiving a message, such agents could associate to it a trust value, based on reputation. Improvements would result in terms of modulation of risk-taking and in the respective weighting of multiple conflicting sources being integrated (fused).

V. DETAILED EXAMPLES IN COOPERATIVE ROBOTICS

Let us consider a typical test task of Robocup@Home (RaH) competitions, “Fetch and Carry” (F&C). In substance, team members can in particular talk to their robots, giving a hint about what to fetch (e.g., “a grey box”), and where it stands (e.g., “near the front door”); the robot should by then know enough about topology and navigation to be able to autonomously reach there, locate the object accurately enough to get it in the “hand”, grasp it, lift it up, and transport it back to the starting location (re. Fig. 7).

The results of Sections II and IV, including §A to E in the latter case can be illustrated here, both in human and in machined contexts.

A. Illustration in human context

In a first stage, a group of international experts have elaborated a rulebook where the general goal of designing systems useful for humans (SII) is focused towards a domestic goal (SIV.A), and then backtracked into the specification of even more focused subgoals : elementary capabilities to be devised. One of them is the task called “Fetch and Carry”, addressing a “natural” way for a robot to find, grasp and transport an object (SIV.A). This intermediary goal is then searched in parallel by multiple teams (SIV.E). This task adapts to local infrastructure (SIV.B) and is iteratively considered, year after year (SIV.C-D).

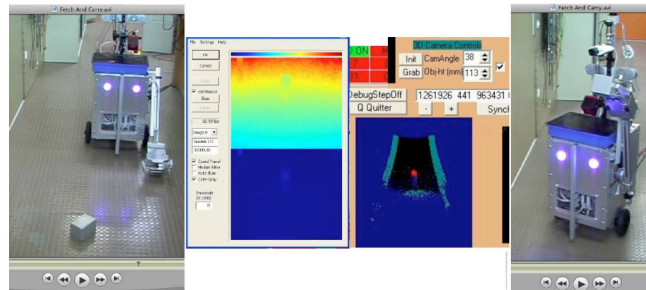


Figure 7. In the F&C task, our proprietary robot RH-Y uses in particular a vocal dialogue, a navigation capability typically using a ranger for navigation purpose, a time-of-flight camera for recognising and locating objects (center) and position and force controlled arm and gripper (left and right).

B. Illustration in robotic context

The demonstration system is real and thus very complex. An overview of the task can be seen on a video available online (e.g., [10]) and multiple aspects are presented elsewhere. Here we shall discuss a minimum of aspects for purpose of example.

Consider first as an analogy, the problem for a human to jump over a wall. This can be easily achieved, or may remain totally impossible, depending on how high is the wall; the metric height is critical. Similarly, in the cognitive world, properties must be precisely defined and metrically quantified in order to allow for meaningful descriptions and effective requirement estimation.

For the F&C test task, referees typically retain about 20 objects, which may be randomly put in 20 possible locations. Robots may more or less be wired with initial expertise, e.g., in terms of topologies and functions; a common culture is also defined (“names” of standard objects and locations are published on a wall one day or more before the test). Let us practice a quantitative estimation of requirements in terms of cognitive entities (re. concepts of Fig. 1). Ignoring here many processes, such as e.g. word perception and recognition, or navigation and handling, let us focus on the cognitive task of understanding which object is where. The input space would consist in about 10 bit of information for each object and rough location specified. On this basis, at the most abstract level, one out of $20 \times 20 = 400$ possibilities should be resolved (i.e. about 9 bit) to know which object is to be fetched, and where it is roughly located. In this very minimal form, the necessary knowledge for correctly understanding the vocal dialogue amounts to approximately $K=14$ lin. With a dialogue lasting for 5 s, the amount of expertise for this cognitive task amounts to $E=14/5=2.8$ lin/s. Learning is demonstrated and can be quantitatively estimated on this domain: without dialogue the task cannot be achieved in the 5 min allotted to the task (roughly, $K=0$ lin, and therefore, $E=0$ lin/s), while with a successful dialogue, lasting for, say 5 s, E increases to about 3 lin/s. The MCS intelligence index is thereby of $i=3/5=0.6$ lin/s².

In the specified location (e.g. “near the door”) the object is manually moved by referees by +/- 20cm just before the test, making it impossible for robots to have it fully (pre-)

wired. Therefore exploration as in SIV.B is performed, using Time-of-Flight (TOF, distance) perception. Notice that here, as in most usual cases, the perception process features (or requires) a lot more knowledge and expertise than the above cognitive operation: in particular the input space includes here 176x144 samples, each with 1cm accuracy in a 500cm range, i.e., about 150'000 bit of information; similarly, the output stage is relatively large for successful trajectory specification (about 10'000 bit of output information), and the processing time is short (say, 0.1s).

Time is a very important feature for success, in many contexts of this applications (motor control, parallel agent management, sensor-based exploration process, etc.). In our proprietary "Piaget" environment [11], agents run in parallel, with very short, individually granted, time slots, lasting for about 100 nanoseconds each in average. Therefore, at low level, Piaget defines its own time basis ("TicksPerSecond"); nevertheless, at higher level and for longer time increments (>10 ms) time is managed on the basis of the system clock, and is thereby compatible with the general culture, common to multiple robots and humans, that makes effective cooperation possible.

VI. CONCLUSION

Starting in a pragmatic way from where we stand, in particular with humans creating robots, progressing with distributed axioms, navigating through small contexts in direction of selected goals (the design of high performance machines, of robots cooperating with humans, and a better understanding of cognition in humans), we adopt a constructivist approach in conceptual framework and validate them gradually by making them operational in test tasks. The paper has first briefly revised MCS, an ontology for cognition, both for the case when it is embedded in humans, and also for the case when it is machine-based, automated (re. « cognitics » in this latter case). Past works had taken for granted that reality and time were notions evident for everyone. Now, at the moment of attempting a practical implementation of those notions in robots, the situation is quite different. Early results in the context of MCS theory had made it clear that reality is infinitely complex, practically out of reach for cognition, under condition of exhaustivity. Further research has therefore been performed and the current paper could nevertheless sketch ways to cope with the infinite complexity of reality. Several other cognitive notions could also be newly discussed, including those of time and revisited "speed"; change and discontinuity; innate and learned behaviors; as well as the human-inspired basics of communication in a group. On the basis of the proposed MCS ontology, and taking often advantage of innate/wired expertise, it can be concluded that robots can be effectively deployed in quantitatively bound domains, as illustrated in several concrete examples.

ACKNOWLEDGMENTS

The authors wish to thank the reviewers for several useful suggestions. They also acknowledge the contributions of numerous engineers and students, as well as members of technical services, at HEIG-VD, who have more or less directly contributed to the reported project. In particular, this year, the following persons can be mentioned: Sudarat "Amy" Tangnimitchok, Promphan "Kim" Ounchanum, and So Mi Kang.

REFERENCES

- [1] Bernard Claverie, "Cognirique - Science et pratique des relations à la machine à penser", Editions L'Harmattan, 2005, pp. 141.
- [2] Jean-Daniel Dessimoz, "Cognition Dynamics; Time and Change Aspects in Quantitative Cognitics", Second International Conference on Intelligent Robotics and Applications. Singapore, 16 - 18 December, 2009; also in Springer Lecture Notes in Computer Science, ISBN 978-3-642-10816-7, pp. 976-993.
- [3] Jean-Daniel Dessimoz, "Cognitics - Definitions and metrics for cognitive sciences and thinking machines", Robotics Editions, Cheseaux-Noréaz, Switzerland, ISBN 978-2-9700629-1-2, pp. 169, January 2011.
- [4] Wisspeintner, T., T. van der Zant, L. Iocchi, and S. Schiffer, "RoboCup@Home: Scientific Competition and Benchmarking for Domestic Service Robots", Interaction Studies, vol. 10, issue Special Issue: Robots in the Wild, no. 3: John Benjamin Publishing, pp. 392--426, 2009.
- [5] Frederick Charles Copleston, "A history of philosophy", Volume 6, Continuum International Publishing Group Ltd.; Edition : New edition (June 5, 2003), pp. 528.
- [6] Alexander Rosenberg, "Philosophy of science: a contemporary introduction", Routledge contemporary introductions to philosophy, 2005
- [7] George E. Hein, "Constructivist Learning Theory", The Museum and the Needs of People CECA (International Committee of Museum Educators) Conference, Jerusalem Israel, 15-22 October 1991, Lesley College. Massachusetts USA.
- [8] Hart, P. E.; Nilsson, N. J.; Raphael, B., "A Formal Basis for the Heuristic Determination of Minimum Cost Paths", IEEE Transactions on Systems Science and Cybernetics SSC4 4 (2), pp. 100-107, 1968.
- [9] Julie A. Jacko (Ed.), "Human-Computer Interaction. Novel Interaction Methods and Techniques" 13th Internat. Conf., HCI Internat. 2009, Proc. Part II, San Diego, CA, USA, Springer.
- [10] <http://rahe.populus.ch /rub/4> , last downloaded on June 3rd, 2012.
- [11] Jean-Daniel Dessimoz, Pierre-François Gauthey, and Hayato Otori, "Piaget Environment for the Development and Intelligent Control of Mobile, Cooperative Agents and Industrial Robots", accepted for publication, ISR 2012, International Symposium for Robotics, Internat. Federation of Robotics, Taipei, Taiwan, Aug.27-30, 2012.

Experiencing and Processing Time with Neural Networks

Michail Maniadakis and Panos Trahanias

Institute of Computer Science, Foundation for Research and Technology Hellas (FORTH)

Heraklion, Crete, Greece

Email: {mmaniada, trahania}@ics.forth.gr

Abstract—The sense of time is directly involved in most of the daily activities of humans and animals. However, the cognitive mechanisms that support experiencing and processing time remain unknown, with the assumption of the clock-like tick accumulation dominating the field. The present work aims to explore whether temporal cognition may be developed without the use of clock-like mechanisms. We evolve ordinary neural network structures that (i) monitor the length of two time intervals, (ii) compare their durations and (iii) express different behaviors depending on whether the first or the second duration was larger. We study the mechanisms self-organized internally in the network and we compare them with leading hypothesis in brain science, showing that tick-accumulation may not be a prerequisite for experiencing and processing time.

Keywords-time perception, temporal cognition, brain-inspired cognition, robotic system

I. INTRODUCTION

The interaction of humans and animals with the environment is supported by multiple sensory modalities such as audition, vision and touch, each one mapped on a specific region of our brain. Interestingly, our sense of time relies on radically different working principles breaking the rule of using a dedicated brain region for processing. Humans and animals lack “time sensors”, as well as a primary sensory brain area devoted explicitly to the sense of time [1].

Time experiencing has attracted significant research interest in brain science, with several works considering where and how time is processed in our brain [2], [3]. An extensive number of brain areas have been reported to contribute in time experiencing such as the cerebellum [3], the right posterior parietal cortex [4], the fronto-striatal circuits [5], the insular cortex [6] and the medial temporal lobes [7].

There are now two main explanations on how our brain experiences time [8]. The oldest and most influential approach assumes the existence of pacemakers producing tick sequences which are counted by an accumulator. A modern version of this assumption assumes coincidence detection circuits to operate as timekeepers [9]. The alternative approach assumes that time may be encoded in the dynamic state of neuron populations that support ordinary cognitive processes. This implies that our brain does not need pacemakers or timekeepers to experience the flow of time. Still, it remains unclear whether such a neural-state-based mechanism may robustly support the accomplishment

of behavioral and cognitive tasks.

The present work aims to investigate the reliability of the latter clock-free approach with respect to a time-based behavioral task, exploring also the possible benefits that a cognitive system may gain from adopting such a dynamical state approach. To address this issue, we employ self-organized computational cognitive systems embodied in artificial agents. Our study focuses on a task that considers comparing the length of two time intervals. The underlying task assumes agents capable of experiencing the flow of time, monitoring and measuring the time elapsed, encoding the duration of the first interval in working memory and contrasting the first and second temporal durations, in order to choose between alternative response activities. To develop such a capacity, we evolve Continuous Time Recurrent Neural Networks and we investigate the dynamics self-organized in the networks in order to reveal the mechanisms encoding and comparing the two temporal intervals. This is expected to promote one of the alternative hypothesis of time processing in the brain. Note that brain scientists have recently considered embodiment as a key feature for the emergence of time perception capacity (e.g., [6], [8]), therefore making robotic experiments particularly appropriate for investigating time processing mechanisms.

In the field of artificial intelligence the role of time in cognition is currently not adequately appreciated [10]. More than a decade ago, F. Varela discussed the fundamental role of time flow experiencing in cognition [11], without however accomplishing to direct scientific interest on artificial time perception. Existing systems can only superficially consider time in their cognitive loop. For example, a turn-taking task with two agents accomplishing to synchronize their behavior, changing roles periodically is studied in [12]. In another experiment, an artificial cognitive system self-organizes mechanisms that consider and exploit time, in order to develop high level cognitive skills such as executive control [13]. However, to the best of our knowledge, no artificial cognitive system has been implemented capable to explicitly process time in order to accomplish a behavioral task. The present study aims to fill this gap, paving the way for artificial agents with human-like time processing capacity (e.g., perceive synchrony and ordering of events, mentally travel in the past and future, share with humans temporal views about the dynamic world).

In the following sections we first describe the task consider in our study and the method used to design neural network based cognitive systems. Subsequently, we present the obtained results and the mechanisms self-organized in neural networks. Finally, we discuss how our findings may compare to time-related brain processes and we provide directions for future work.

II. EXPERIMENTAL SETUP

The present experiment investigates mechanisms capable of (i) experiencing the flow of time and (ii) comparing temporal intervals. We have implemented a simulated environment which involves a two wheeled simulated robotic agent equipped with 8 uniformly distributed distance and light sensors. The agent experiences a light cue for two different intervals A and B. A Continuous Time Recurrent Neural Network (CTRNN) is used to provide the artificial agent with cognitive capacity. The CTRNN is evolved to experience the flow of time, compare the two intervals A and B, and implement alternative robotic behaviors depending on whether A or B was longer. Note that the robotic behaviors considered in our experiments are kept in rather low levels of complexity in order to direct focus on the mechanisms supporting the experience and processing of time.

A. Behavioral Task

The experiment starts with a simulated mobile robot located at the beginning of a corridor environment (see Figure 1). The artificial agent remains at the initial position where it experiences the same light cue for two different time intervals A and B. The agent has to consider and compare the durations of A and B to decide which one is longer. Then, in order to successfully complete the task, the agent has to navigate to the end of the corridor and turn right when the A interval was longer, or, turn left when the A interval was shorter (than B).

The temporal structure of the experimental procedure is illustrated in Figure 2. The trial starts with a short preparation phase making the internal state of the CTRNN obtain a non-random initial value before light experience begins. Just after that, the first light experience is provided to the agent, which last for a randomly specified number of simulation steps (in the range [10,100]), corresponding to the length of the temporal interval A. Subsequently the agent rests for ten simulation steps and then it experiences light for a second time, which corresponds to the second time interval B (that is again randomly specified in the range [10,100]). Then the agent is provided 20 simulation steps to decide the response direction. At the end of the wait period the agent is provided a “go” signal and then it starts navigating to the end of the corridor turning left or right. We note that we preserve a minimum distance of 15 simulation steps between the A and B intervals, to ensure that the agent will be capable of comparing all randomly generated pairs of A and B.

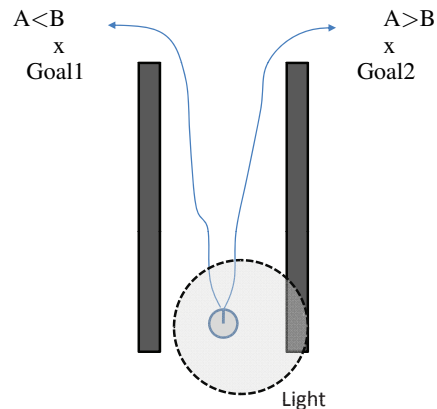


Figure 1. Graphical illustration of the experimental setup . The agent experiences light for two temporal intervals A, B and depending on which one was longer it has to drive either leftwards, or rightwards.

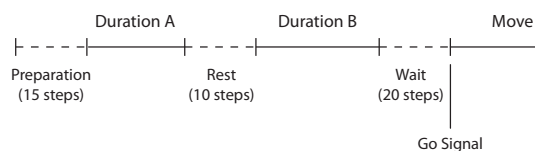


Figure 2. The temporal structure of the experiment.

B. CTRNN Model

We use a Continuous Time Recurrent Neural Network (CTRNN) model to investigate how time experiencing and processing mechanisms self-organize in neuronal dynamics. The implementation of the CTRNN is based on the well known leaky integrator neurons as it is described in previous studies [14]. Interestingly, in CTRNNs information is implicitly encoded using internal neurodynamics. Thus, in our experimental setup, the neuronal state is initialized only once in the beginning of the trial, and then neuronal dynamics continue without resetting.

In the present work we use a two-layer neural network (with full connectivity within and among layers), as shown in Figure 4(a). The upper layer receiving sensory information is expected to monitor environment changes self-organizing a time processing capacity, and additionally implement the mechanism for comparing A and B. For the purposes of the present study this layer is considered as the core component of the CTRNN. The lower part of the network aims to combine the result of the A and B comparison with the current sensory input in order to effectively drive the robotic agent along the corridor.

C. Evolutionary Procedure

We employ a Genetic Algorithm (GA) to explore cognitive dynamics enabling the artificial agent to perceive the flow of time and additionally compare the length of the two time intervals A and B. We use a population of

1000 artificial chromosomes encoding different CTRNN configurations (their synaptic weights and neural biases). Each candidate CTRNN solution is tested on eight randomly initialized versions of the task described in the previous section (randomness regards the lengths of A and B intervals). In the first four tasks, the duration of A was longer than B, while the opposite relation holds for the last four tasks. The evaluation of CTRNNs in multiple random tasks has been shown to significantly improve the validity of the evaluation metric, while at the same time it increases the robustness of the evolved cognitive system against difficult exemplar scenarios.

To evaluate the capacity of the artificial agent in comparing the length of temporal intervals A and B, we mark two different positions in the environment which are used as goal positions for agent's behavior, as shown in Figure 1. Depending on whether A has been actually longer than B or not, we select the appropriate goal position and we measure the minimum distance D of the agent's path from that goal (i.e., when $A > B$ the agent should approximate Goal1, while when $A < B$ the agent should approximate Goal2). Additionally, during navigation, we consider the number B of robot bumps on the walls. Overall, the success of the agent to accomplish a given task i is estimated as:

$$S_i = \frac{100}{D \cdot B} \quad (1)$$

By maximizing S_i , we aim at minimizing the distance from the goals producing responses at the correct side of the corridor, as well as avoid bumping on the walls. Then, the total fitness of the individual for the combination of eight randomly initialized tasks is estimated by:

$$fit = \prod_{i=1}^8 S_i \quad (2)$$

The afore mentioned measures guide the evolution of the randomly initialized population consisting of 1000 individuals, each one encoding a complete CTRNN configuration. Real-value encoding is used to map synaptic weights and neural biases into chromosomes. We have used a standard GA process with survival of the fittest individual along consecutive generations. During reproduction, we have used as a basis the best 30 individuals of a given generation, which randomly mate with the 70% of the rest individuals using a single point crossover. Mutation corresponds to the addition of up to 25% noise, in the parameters encoded to the chromosome, while each parameter has a probability of 4% to be mutated. In each evolutionary run the randomly initialized population is evolved for a predefined number of 500 generations.

III. RESULTS

We have evolved CTRNN controllers running eight different GA processes. Five of the evolutionary procedures

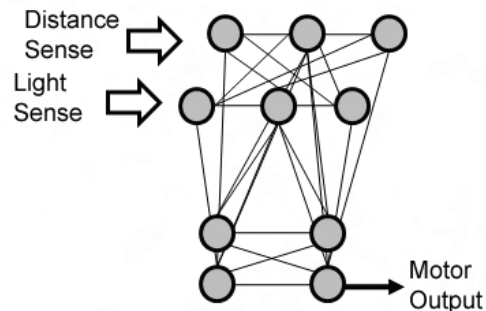


Figure 3. The CTRNN used in the present study.

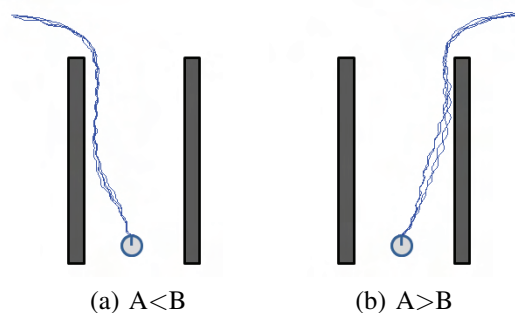


Figure 4. Parts (a) and (b) correspond to the results of the evolutionary procedure showing the two different types of responses provided by the agent when $A < B$, or $A > B$.

converged successfully configuring CTRNNs capable of comparing temporal intervals, accomplishing the behavioral task described in the previous sections. Interestingly, the results obtained from the statistically independent evolutionary procedures exhibit common characteristics, which are discussed below using as a working example one representative solution. The performance of the agent in comparing two time intervals successfully driving to the correct side of the corridor, is demonstrated in Figure 4 (a) and (b).

Note that the experience of time intervals and the estimation of their length is mainly implemented in the upper component of the CTRNN. The motor component of the network seems to have no contribution in measuring the length of time intervals being mainly involved in implementing the motor response. Therefore, we concentrate on the upper part of the CTRNN for the rest of our study.

In order to obtain insight in the dynamics self-organized internally in the CTRNN, we have conducted tests revealing the memorization and comparison mechanisms. Following the symbolization $[A \text{ vs } B]$ to denote the durations of A and B intervals considered in a particular test case, we have examined the following exemplar tests with A shorter than B: $[10 \text{ vs } 25]$, $[20 \text{ vs } 40]$, $[20 \text{ vs } 70]$, $[40 \text{ vs } 60]$, $[80 \text{ vs } 95]$ as well as test cases where A is longer than B: $[25 \text{ vs } 10]$, $[40 \text{ vs } 20]$, $[70 \text{ vs } 20]$, $[60 \text{ vs } 40]$, $[95 \text{ vs } 80]$. The

activation of neurons in the upper part of the CTRNN for the aforementioned pairs of [A vs B] tests is depicted in Figure 5. We see that the obtained solution is sufficiently robust, dealing successfully with the cases of A and B being both short or both long, as well as with other intermediate comparisons. In all shown plots we can easily identify the A and B period that the agent experiences light, followed by a sinusoidal activation which corresponds to the navigation of the agent to the end of the corridor turning either left or right. For example, in the second plot of the first column of Figure 5 considering [20 vs 40] the agent experiences the first period of light from step 15 to step 35, then rests for 10 steps, and experiences the second period of light from step 45 to step 85. In the next 20 steps it has to decide the direction of the given response, and implements the underlying response from step 105 until the end of the trial.

Monitoring the Elapsed Time. With a close look into the dynamics implemented in the upper component of the CTRNN, we see that three neurons are employed to measure the length of temporal intervals. This corresponds to the neurons plotted in red, green and magenta in Figure 5. We observe that these three neurons start diminish their activities one after the other as time passes, which suggests that the agent segments the time flow at bins of approximately 25 simulation steps (see for example the last plot in Figure 5). This type of segmentation facilitates counting the length of the experienced light intervals and the aggregation of the time elapsed. We note that similar time related ramping activity (in fact, it is an inverse ramp in our model) has been observed in many brain areas being probably involved in time processing [15], [16].

Note that measuring the elapsed time for the case of interval B, is affected by the length of interval A. For example, compare the way that the 40-steps interval is experienced in the second plot of Figure 5 (a) and in the fourth plot of Figure 5 (b). Clearly, the given interval of 40 simulation steps is experienced in two different ways. This is because the internal state of the network as it is shaped at the end of A, modulates the experience of B. As it is explained below, this perceptual adjustment is implemented in order to facilitate comparison.

Decision Making. In order to obtain insight on how the CTRNN decides the longest of the two intervals, we conduct principal component analysis in the neural activity of the upper level. The activity of the first principal component (PC1) for the test cases discussed above is illustrated in Figure 6. Clearly, the longer interval (either A or B) is the one that implements the lower PC1 values. Note that the shortest the length of the first interval, the steepest the decrease of PC1 in the beginning of the second interval, while in contrast when the first interval is long then PC1 diminishes slowly when B is experienced. This means that the network memorizes the length of the A period by undertaking neural states that properly modulate the ways

the second interval is experienced. In other words, a 20 steps interval is not the same when it is experienced first or second in order. This is in agreement to the subjective experience of time and the modulation of duration perception in humans by external factors such as attention, or emotions.

Turning back to Figure 5, we observe that the neurons being responsible for comparing the two temporal intervals and deciding the direction of robot's motion are mainly the ones plotted in red and black. Every time that the agent concludes "B is longer" the black neuron activity is high and the red activity low (Figure 5 (a)). However, when "A is longer" these two neurons do not have enough time to take extreme high and low values (Figure 5 (b)). Interestingly, the same neurons hold also an estimate of the final decision at the intermediate rest period of the agent. When the first interval is short, then the neurons predict that a probably longer one will follow decreasing the activity of the underlying neurons at the beginning of B (see for example the first and second plot in Figure 5(a)). In contrast when the agent has experienced a long A, the agent predicts that the second period will be probably shorter, setting both neurons to relatively high values at the beginning of B (see for example the last plot in Figure 5(b)).

Adjustable Duration Comparison. When A is short, it is easy for the network to compare it with a long B, but it is difficult to compare it with a short B. To address this issue, the network adjusts the way B is experienced. In particular, a short A results into fast neural changes in the early B steps, magnifying possible differences between a short A and a short B. See for example neural activities in the first plot of the Figure 5 (a) where both A and B are short. The other case of B being long, can be easily handled with clear neural differences as it is shown in the third plot of Figure 5(a).

In the other extreme case where both A and B are long, we see that neural changes are slow at the early steps of B making the network shift focus at a later time, magnifying the difference between the two intervals when the length of B approximates the length of A. See for example the last plot in Figure 5(a) where fast neural changes are observed mainly at the end of the B interval. The case of A being long and B short can be easily handled with clear neural differences, as it is shown in the third plot of Figure 5(b).

Overall, following the above described adjustments, depending on the length of A, the network accomplishes to direct focus on the moments that are more critical for a given comparison.

Motion Planning and Action Implementation. The direction of the motor response is decided by the upper part of the CTRNN. Note that the main difference in neural activity between the cases that the agent moves left-wards or right-wards, is the unfolding of the neuron plotted in blue (compare the plots shown in Figs 5(a) and 5(b)). We observe a clear oscillation of the underlying neuron when the agent drives left, while the activity of the neuron vanishes when

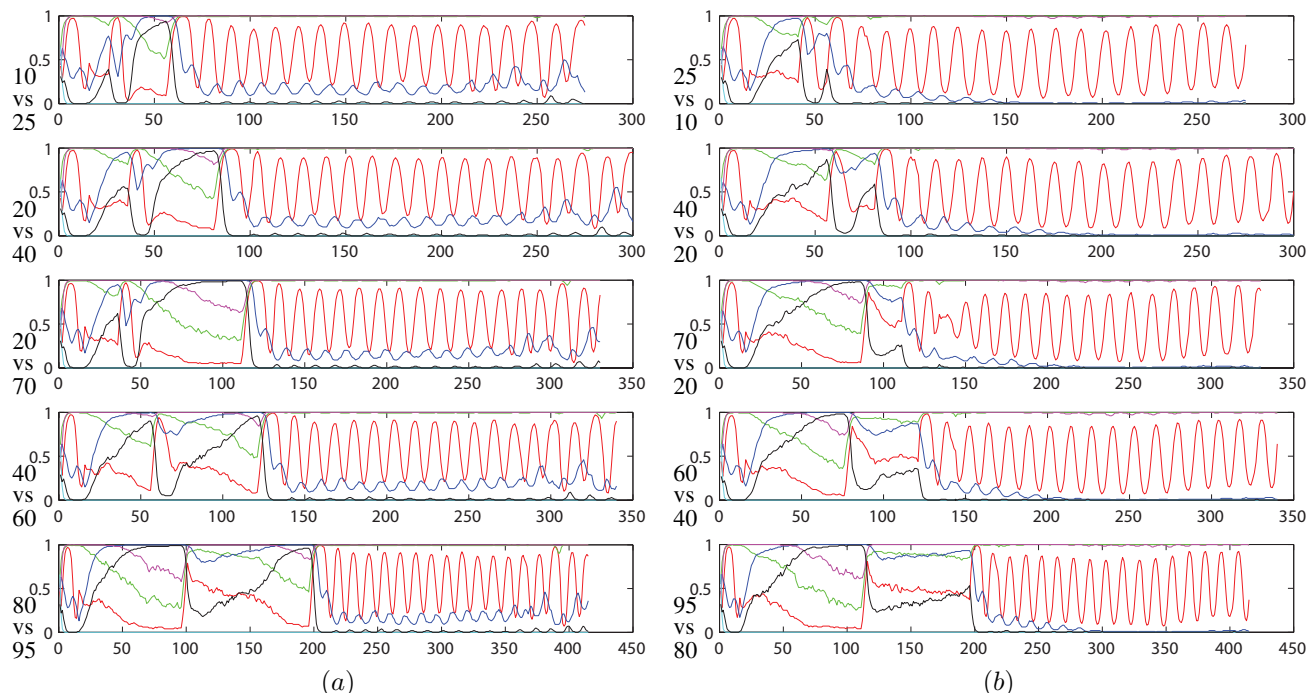


Figure 5. The activity of neurons in the upper level of the CTRNN for several test cases with the duration of interval A being shorter than B in column (a) and A being longer than B in column (b).

the agent moves right.

IV. DISCUSSION

The present work explores time processing cognitive mechanisms considering whether they require clock-like “tick” signals to work. According to our findings, cognitive systems can solve duration comparison tasks without using any tick-based mechanism. Our model has developed another time measurement mechanism with an (inverse) ramp functionality similar to the one observed in the brain [15], [16]. Despite the fact that the implemented system adopts oscillation-based internal mechanisms for driving the robot, the experience of time is based on rate coding rather than a mixture of oscillations. This contrasts the neuroscientific assumption arguing that time experiencing relies on monitoring the neurons oscillating in our brain at different rates [2].

As it is explained above, the CTRNN model implements an adjustable way to experience time, which facilitates duration comparison. This is in agreement with modern approaches explaining time-experience on the basis of dynamic neural states [17]. According to our results, experiencing a given time interval is not accomplished in a universal, flat way and is not always the same, but it is rather modulated by the state of the network at the beginning of time experiencing. The present work reveals a beneficial characteristic of such a flexible time experiencing mechanism which regards the ability of the network to properly focus on the most critical moments of a given comparison accomplishing to

solve the task for difficult exemplar cases (i.e., compare A and B having small duration difference).

V. CONCLUSIONS

The current work investigates possible mechanisms for time perception in cognitive systems. We show that ordinary neural schemes can self-organize robust mechanisms for monitoring, representing and comparing two different temporal intervals developing at the same time biologically reliable characteristics. Our findings suggest (i) that pace-makers is not the only possible solution for experiencing and processing time, and (ii) that adaptive time perception may be beneficial for the functionality of the overall system enabling to direct attention on the most critical time moments.

The current work may serve as a basis for more sophisticated computational models developing the full extent of time processing skills. In the near future we intend to extend the implemented model in the direction of ordering perception, and time-based recall.

Interestingly, time processing models may be also embodied in robotic systems to improve their cognitive capacities. Due to the central role of time in a range of different modalities, such as experience encoding and learning, the use of tenses in natural language, long term action planning, etc., the implementation of artificial agents that perceive and process temporal information has a great potential towards the seamless integration of robots in human societies.

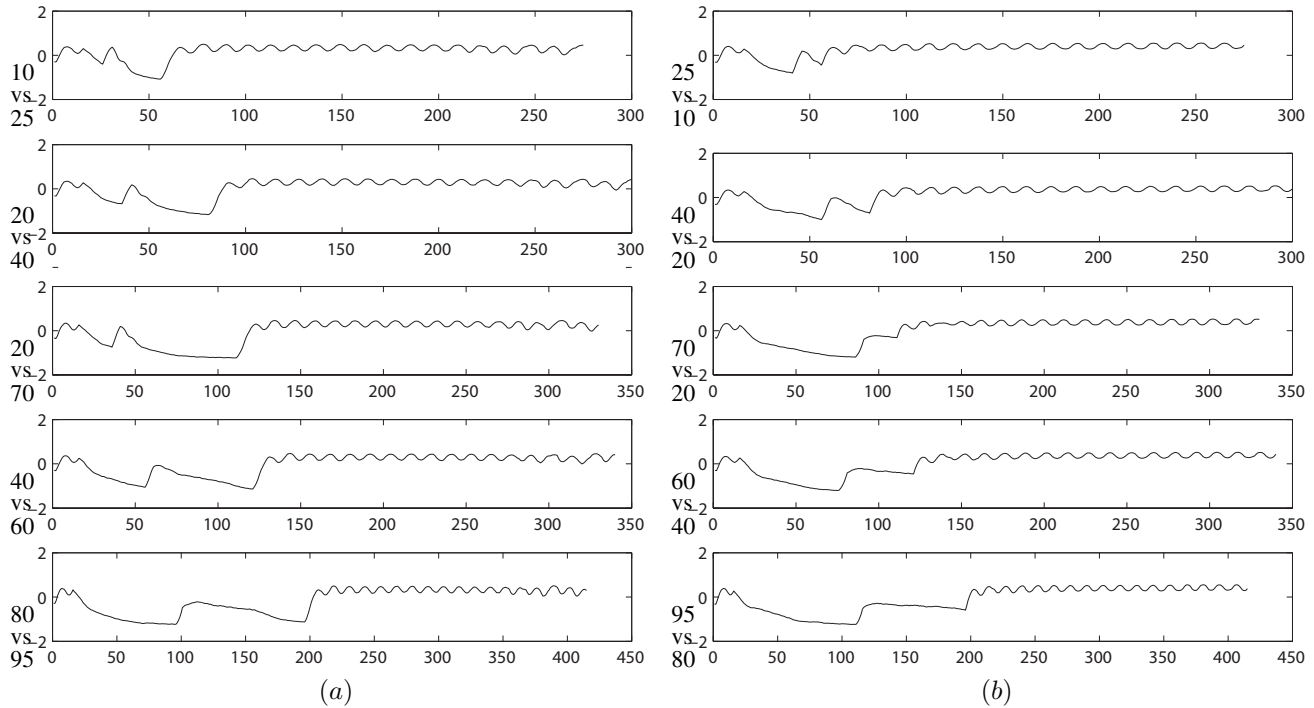


Figure 6. The activity of the first principal component in the upper level of the CTRNN, shown for several test cases with the duration of interval A being shorter than B in column (a) and A being longer than B in column (b).

REFERENCES

- [1] M. Wittmann and V. van Wassenhove, "The experience of time: neural mechanisms and the interplay of emotion, cognition and embodiment," *Phil. Trans. Royal Society B*, vol. 364, pp. 1809–1813, 2009.
- [2] W. Meck, "Neuropsychology of timing and time perception," *Brain & Cognition*, vol. 58, no. 1, 2005.
- [3] R. Ivry and J. Schlerf, "Dedicated and intrinsic models of time perception," *Trends in Cogn. Science*, vol. 12, no. 7, pp. 273–280, 2008.
- [4] D. Buetti, B. Bahrami, and V. Walsh, "The sensory and association cortex in time perception," *Journal Cognitive Neuroscience*, vol. 20, pp. 1054–1062, 2008.
- [5] S. Hinton and H. Meck, "Frontal-striatal circuitry activated by human peak-interval timing in the supra-seconds range," *Cognitive Brain Research*, vol. 21, pp. 171–182, 2004.
- [6] M. Wittmann, "The inner experience of time," *Phil. Tran. Royal Soc. B*, vol. 364, pp. 1955–67, 2009.
- [7] A. Botzung, E. Denkova, and L. Manning, "Experiencing past and future personal events: functional neuroimaging evidence on the neural bases of mental time travel," *Brain and Cognition*, vol. 66, pp. 201–212, 2008.
- [8] D. Buonomano and R. Laje, "Population clocks: motor timing with neural dynamics," *Trends in Cognitive Science*, vol. 14, no. 12, pp. 520–527, 2010.
- [9] C. Buhusi and W. Meck, "What makes us tick? functional and neural mechanisms of interval timing," *Nature Rev. Neuroscience*, vol. 6, pp. 755–765, 2005.
- [10] M. Maniadakis and P. Trahanias, "Temporal cognition: a key ingredient of intelligent systems," *Frontiers in Neurobotics*, vol. 5, 2011.
- [11] F. Varela, "Present-Time Consciousness," *Journal of Consciousness Studies*, vol. 6, no. 2-3, pp. 111–140, 1999.
- [12] H. Iizuka and T. Ikegami, "Adaptive coupling and intersubjectivity in simulated turn-taking behaviours," *Advances in Artificial Life*, pp. 336–345, 2003.
- [13] M. Maniadakis, P. Trahanias, and J. Tani, "Explorations on artificial time perception," *Neural Networks*, vol. 22, pp. 509–517, 2009.
- [14] B. M. Yamauchi and R. D. Beer, "Spatial learning for navigation in dynamic environment," *IEEE Trans. Syst. Man Cybern.*, vol. 26, no. 3, 1996.
- [15] M. Leon and M. Shadlen, "Representation of time by neurons in the posterior parietal cortex of the macaques," *Neuron*, vol. 38, no. 2, pp. 317–327, 2003.
- [16] A. Mita, H. Mushiake, K. Shima, Y. Matsuzaka, and J. Tanji, "Interval time coding by neurons in the presupplementary and supplementary motor areas," *Nature Neuroscience*, vol. 12, no. 4, pp. 502–507, 2009.
- [17] U. R. Karmarkar and D. V. Buonomano, "Timing in the absence of clocks: Encoding time in neural network states," *Neuron*, vol. 53, no. 3, pp. 427 – 438, 2007.

A Predictive System for Distance Learning Based on Ontologies and Data Mining

Boufardea Evangelia

University of Patras

CTI "Diophantus" Computer Technology Institute &
Press

Patras, Greece

mpoufard@ceid.upatras.gr, mpoufard@westgate.gr

Garofalakis John

University of Patras

CTI "Diophantus" Computer Technology Institute &
Press

Patras, Greece

garofala@ceid.upatras.gr, garofala@cti.gr

Abstract— The development of distance learning, e-learning and online learning, has increased exponentially in recent years. Lately, researchers have begun to investigate various data mining techniques in order to improve the quality of this type of education. However, although distance learning in education is well established, there are a few attempts to extract educationally useful information during the course and before the final evaluation. In this paper, we propose an ontology based on the structure of a distance learning environment which enriches a recommendation system with rules generated by data mining techniques. Tutors can use this recommendation system in order to predict learners' progress and their final performance. This application will enhance the efficiency of any distance learning or e-learning platform and will be beneficial for learners as well as for tutors in the learning process.

Keywords: *ontology; protégé; RDF; data mining; weka; classification; J48 algorithm; distance learning; HOU*

I. INTRODUCTION

The rapid spread of Internet has caused significant changes in many sectors of the economy and society worldwide. From these changes, education could not be left out. With the increasing development of information technologies, a new form of education appears, e-learning (distance education), which revolutionized the educational process.

Furthermore, while the World Wide Web gradually transforms into Semantic Web, new standards and models such as Extensible Markup Language (XML) [20], Resource Description Framework (RDF) and OWL Web Ontology Language are evolving in order to enhance this technology.

The storage, presentation, transmission and search of information according to those standards open up new horizons in the utilization of the Web. Ontologies are increasingly get used for knowledge representation.

A large ontology contains useful data for a system of distance education and thus it is deserved to investigate the "hidden knowledge", i.e., to discover possible associations or to find repeated patterns and forms or extreme events.

This paper proposes a data mining approach to discover relationships between the learning resources metadata. A new recommendation system is developed for assisting tutors in distance learning to predict learners' progress and their final performance. The developed system is based on a new

framework using data mining techniques in metadata derived from an ontology. The basic idea was to design an ontology that can store knowledge about the learners' skills in relation to a specific educational purpose. We used for our research PLI23 - Telematics, Internet of the Hellenic Open University, which has a very specific subject and 4 mandatory projects per year, and then we exploited the imported data in order to discover rules and predict learners' progress. The key in distance learning is the communication between learners and tutors. With the help of the proposed system, this communication is getting better, more immediate and effective. In other words, the quality of distance learning is improved.

This paper is organized as follows: in Section II, related work, a quick reference to ontologies, data mining and distance education, which are the basis of our application, are presented. In Section III, we present our implemented application is presented. The application has three parts. The first refers to the ontology that was created in order to represent a course. The second part refers to the data mining techniques that were used in order to exploit the data from the ontology, which algorithms were used and why, which attributes were taken into account, and finally, the rules generated. The third part of the application -the predictive system- is a platform which is used by tutors in order to predict learners' progress. The platform is based on the results of the previous parts. Finally, conclusions and an outline of further work are presented.

II. TOPICS OF INTEREST

Distance learning, ontologies and data mining techniques are the topics that were studied in order to implement our decision support system. There is related work that is presented below.

A. Distance learning

Higher education systems all over the world are challenged nowadays by the new information and communication technologies (ICT). Distance education or distance learning is a field of education that focuses on teaching methods and technology with the aim of delivering teaching, often on an individual basis, to students who are not physically present in a traditional educational setting such as a classroom. It has been described as "a process to

create and provide access to learning when the source of information and the learners are separated by time and distance, or both." Distance education courses that require a physical on-site presence for any reason (including taking examinations) have been referred to as hybrid or blended courses of study [18].

Distance learning programs can fundamentally change the way schools compete for students, especially part-time students. A school that develops distance learning programs usually increases the scale and scope of its offerings. Many traditional institutions have added distance learning programs. Academic institutions and corporations are combining resources to bring distance learning programs to workplaces. Academic institutions offer courses through distance learning so students have opportunities to create a degree program that uses course offerings from multiple schools.

Hellenic Open University (HOU) is the 19th Greek State University, but the only one that provides distance education in both undergraduate and postgraduate levels via the development and utilization of appropriate learning material and methods of teaching. The HOU's mission is to provide distance education at both undergraduate and postgraduate level. For that purpose, it develops and implements appropriate learning material and methods of teaching. The promotion of scientific research as well as the development of the relevant technology and methodology in the area of distance learning falls within the scope of the HOU's objectives [22].

B. Ontology

Ontologies are widely used in Knowledge Engineering, Artificial Intelligence and Computer Science, in applications related to knowledge management, natural language processing, e-commerce, intelligent integration information, information retrieval, database design and integration, bio-informatics, education, and in new emerging fields like the Semantic Web [1].

The term is borrowed from philosophy, where ontology is a systematic account of existence.

"Ontology is an explicit specification of a conceptualization." This definition became the most quoted in literature and by the ontology community. Based on Gruber's definition, many definitions of what ontology is were proposed. Borst (1997, page 12) modified slightly Gruber's definition as follows: Ontologies are defined as a formal specification of a shared conceptualization." [7].

Several technologies have been developed for constructing and developing the Semantic Web. RDF and its extensions such as OWL have been developed to define metadata schemas, domain ontologies and resource descriptions. RDF is a W3C (World Wide Web Consortium) standard developed in 1997. It is a standard model for data interchange on the Web. RDF has features that facilitate data merging even if the underlying schemas differ, and it specifically supports the evolution of schemas over time without requiring all the data consumers to be changed [23]. Web ontology language (OWL) built on RDF is the new W3C recommendation for ontology construction with

facilitates for effective reasoning capabilities by consistency checking through inference rules such as transitivity, symmetry etc. OWL is designed for use by applications that need to process the content of information instead of just presenting information to humans. OWL facilitates greater machine interpretability of Web content than that supported by XML, RDF, and RDF Schema (RDF-S) by providing additional vocabulary along with a formal semantics. OWL has three increasingly-expressive sublanguages: OWL Lite, OWL DL, and OWL Full [24].

Eyharabide et al. [13] described an ontology that was implemented for predicting students' emotions when interacting with a quiz about Java programming. Zhuhadar et al. [9] and Pin-Yu Pan et al. [12] proposed a hybrid recommendation strategy of content-based and knowledge-based, in which aiming to filter recommended items from the available items according to the user's preferences. Sridharan et al. [3] presents a multi-level ontology - driven topic mapping approach to facilitate an effective visualization, classification and global authoring of learning resources in e-learning.

In this paper, we implemented an application ontology that contains all the definitions needed to model the knowledge required for the particular area of application. Application ontologies often extend and specialize the vocabulary of the domain for a given application such as ours. For instance in this work, we created an ontology for a system specialized in distance learning for the HOU and we adapt the particularities of HOU into the ontology.

C. Data mining techniques

Data mining involves the use of sophisticated data analysis tools to discover previously unknown, valid patterns and relationships in large data sets. These tools can include statistical models, mathematical algorithms, and machine learning methods (algorithms that improve their performance automatically through experience, such as neural networks or decision trees). Consequently, data mining consists of more than collecting and managing data, it also includes analysis and prediction [8].

Data mining is ready for application in the business community because it is supported by three technologies that are now sufficiently mature [6]:

- Massive data collection
- Powerful multiprocessor computers
- Data mining algorithms

The most commonly used techniques in data mining are: Artificial neural networks (non - linear statistical data modeling tools, usually used to model complex relationships between inputs and outputs or to find patterns in data) [15], Decision trees (a decision support tool that uses a tree-like graph or model of decisions and their possible consequences, including chance event outcomes, resource costs, and utility) [17], Genetic algorithms (a search heuristic that mimics the process of natural evolution) [19], Association Rules (popular and well researched method for discovering interesting relations between variables in large databases) [16], etc.

There are several approaches to data mining techniques in e-learning generating recommendations based on a user’s profile. Burdescu et al. [4] proposed a novel structure of a support system for e-Learning infrastructure that is based on data representing learner’s activities and processes. Markov chain modeling and classification is used as main intelligent procedure for data analysis. Hanna [10] described how we can profit from the integration of data mining and the e-learning technology. Taking into consideration the suggested methods, data mining can be used to extract knowledge from e-learning systems through the analysis of the information available in the form of data generated by their users. In this case, the main objective is to find the patterns of system usage by teachers and students and, perhaps most importantly, to discover the students’ learning behavior patterns. In this paper, we used classification process and more specific Decision Trees in order to find a set of models that describes and distinguishes data classes and concepts. The derived model is based on the analysis of a set of training data.

A dissertation also with subject “Understanding dropout of adult learners in e-learning” [2] has been also conducted, which is related, too.

III. APPLICATION

A. Building the Ontology

Nowadays, ontologies offer the ability to model the knowledge of a domain in a discrete and definite way. We used Protégé as a framework application. Figure 1 shows the design of “pli” ontology in Protégé.

As far as concerning HOU, by means of an ontology, it will be possible to describe the knowledge domain the subjects constituting it, the relations among the various subjects, as well as methodologies and means with which they are presented. The content of an ontology depends both on the amount of information and on the degree of formality that is used to express it. Generally, two main types of ontologies are distinguished: lightweight and heavyweight. In this paper, the lightweight approach is adopted according to this definition of ontology: “ontology may take a variety of forms, but it will necessarily include a vocabulary of terms and some specification of their meaning”. A lightweight ontology is a structured representation of knowledge, a taxonomy where the concepts are arranged in a hierarchy with a simple relationship between them.

In this ontology, we had to model and represent the relevant aspects and domains of knowledge for a distance learning environment which contains the knowledge about the followings:

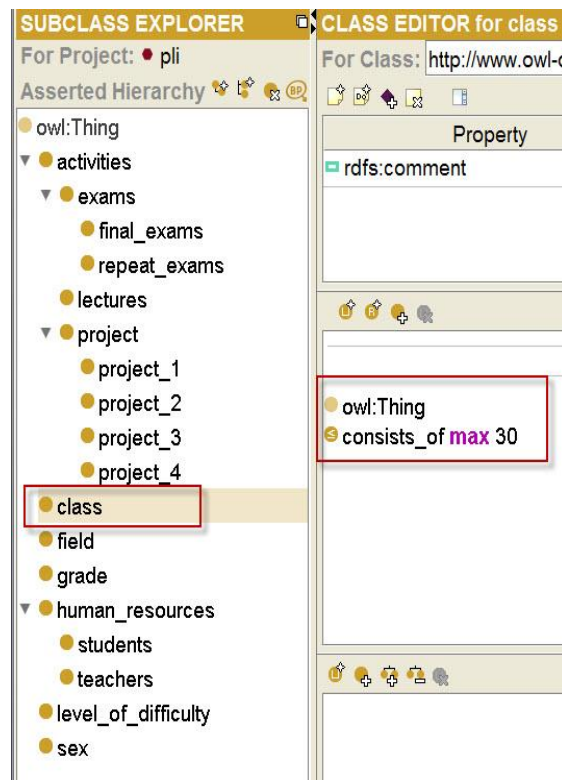


Figure 1. Pli ontology

Apart from the above classes, there are also relations, datatypes and restrictions such as following in Table I:

TABLE I. ELEMENTS OF PLI ONTOLOGY

Pli ontology	
Relations	“Students belong to a class” or “A class consists of students” “A project has level of difficulty” “Teachers teach at a class” or “A class is taught by teachers” “Students take activities” or “Activities are taken by students” “Students are of sex” “Students have grades” etc...
Datatypes	Exams_type (string) – domain: <i>exams, students</i> Grade (float) – domain: <i>students, grade</i> Pass_exams (Boolean) – domain: <i>students</i>
Restrictions	A class <= consists of max 30 (students), etc...

In our study, there were three different fields, three classes, four teachers, seventy nine students, and three level of difficulty for the projects. In order to check if there is any

inconsistency of our ontology we used a reasoner. Pellet [14] reasoner was used, which is a piece of software able to infer logical consequences from a set of asserted facts or axioms.

After the ontology building, metadata are gathered, and the title and description fields of the metadata XML/RDF files are separated. The next step is to use the produced RDF in order to take the data in an ARFF (Attribute-Relation File Format) format in order to process them with data mining techniques. An ARFF file is an ASCII text file that describes a list of instances sharing a set of attributes.

B. Data mining techniques for prediction

Data-mining techniques have been applied in order to find interesting patterns, build descriptive and predictive models from large volumes of data accumulated through the ontology. The results of data mining can be used for getting a better understanding of the underlying educational processes especially in distance learning, for generating recommendations and advices to students, for improving resource management, etc.

We used classification as it has many applications in both traditional education and modern educational technology. The best results are achieved when classifiers can be learned from real data, but in educational domain the data sets are often too small for accurate learning. Our sample was only 79 instances.

Our most important concern was to select a sufficiently powerful model, which catches the dependencies between the class attribute and other attributes, but which is sufficiently simple to avoid overfitting. Both data preprocessing and the selected classification method affect this goal. We used Weka for the extraction of rules that predict students' progress. Weka is a collection of machine learning algorithms for data mining tasks. The algorithms can either be applied directly to a dataset and Weka [21] contains tools for data pre-processing, classification, regression, clustering, association rules, and visualization. It is also well-suited for developing new machine learning schemes. It can also make comparative surveys or checks in datasets. Someone can see the errors of every classification with a popup menu, or if there is a decision tree the result can be shown as a picture.

The produced RDF from the ontology gives us the instances of the attributes that we are interested in. The attributes that are important for our predictive system are the grades of the projects, the grades of the exams, the type of exam, the gender of the student. Some other important attributes could be the age of the students, their marital status, their educational background etc. Unfortunately, due to the privacy of the personal data we could not have access to these data so we restricted in the referred attributes.

Real data is often incomplete in several ways. It can contain missing or erroneous attribute values. Erroneous values are generally called noise, but in some contexts noise means only measurement errors. Educational data is usually quite clean because it is either collected automatically (log data) or checked carefully (students' scores). In our system

we used real data based on students' grades so we avoid the noise.

All the useful needed data are in the ontology that was implemented previously, so we can extract them in an arff format, see Figure 2, via RDF schema, with the help of a parser. We need these data in arff format as it is the suitable format for processing of data through Weka. For this reason firstly we codified students' data in a tuple in order to process them if there are hidden relations among them i.e., students whose 2nd and 3rd project had grade up to 7,5 succeeded in final exams, or students who did not submit the 1st project they dropped out the course.

The following data were elaborated:

Sex (male/female)	Grade 1 st project (number)	Grade 2 nd project (number)	Grade 3 rd project (number)	Grade 4 th project (number)
Grade Final exams (number)	Grade Repeat exams (number)	Type of exams (final/repeat)	Pass (true/false)	

For example, a student can be represented as tuple at Weka as follows:

male, 5, 6, 7, -1, 4, 9, repeat, true

That is, the student is man and his grades at the first three projects are 5, 6, 7, he did not submit the fourth project, he failed at final exams with grade 4 and he gave repeat exams with grade 9 and he passed the course.

```
@relation pli

@attribute student {female,male}
@attribute grade1 real
@attribute grade2 real
@attribute grade3 real
@attribute grade4 real
@attribute gradeexam real
@attribute graderepeat real
@attribute typeofexam {final,repeat}
@attribute pass {true,false}

@data
male,9.3,7.9,7.5,6.0,7.2,-1.0,final,true
female,7.9,7.8,6.2,9.0,5.7,-1.0,final,true
male,9.1,8.8,9.6,9.4,8.1,-1.0,final,true
```

Figure 2. Arff file for pli

The dataset that was created consists of 79 instances and every record has 9 attributes. Essentially it is investigated whether a student will pass the exams of the course based on rating criteria the grades of the projects and the grades of exams.

Through the process of data, Weka extracts rules applicable to a proportion of cases (confidence). We are interested in those that apply for 100% of cases. The data

classification is a supervised learning process in which an apprentice algorithm takes a number of observations (records) as a basis for its training.

As we use the dataset in Weka, we can have immediately a visualization of all attributes depending on pass or fail status of student.

The data mining technique that was used in our application was classification. Decision trees are maybe the best-known classification paradigm. A decision tree represents a set of classification rules in a tree form. Decisions tree are a collection of nodes, branches, and leaves. Each node represents an attribute; this node is then split into branches and leaves. Decision trees work on the “divide and conquer” approach; each node is divided, using purity information criteria, until the data are classified to meet a stopping condition.

The earliest decision trees were constructed by human experts, but nowadays they are usually learned from data. One of the best known algorithms is C4.5 [11] is an algorithm used to generate a decision tree. The basic idea in all learning algorithms is to partition the attribute space until some termination criterion is reached in each leaf. Usually, the criterion is that all points in the leaf belong to one class. However, if the data contains inconsistencies, this is not possible. As a solution, the most common class among the data points in the leaf is selected. An alternative is to report the class probabilities according to relative frequencies in the node. J48 is an open source Java implementation of the C4.5 algorithm in the Weka data mining tool.

For our recommendation system we decided to use J48 algorithm since decision trees have many advantages: they are simple and easy to understand, they can handle mixed variables (i.e., both numeric and categorical variables), they can classify new examples quickly, and they are flexible. Enlargements of decision trees can easily handle small noise and missing attribute values. Decision trees have high representative power, because they can approximate nonlinear class boundaries, even if the boundaries are everywhere piecewise parallel to attribute axes [5]. The idea of classification is to place an object into one class or category, based on its other characteristics

We run our dataset using J48 algorithm and cross validation 10 folds. This means that the dataset is divided into 10 parts. The nine of them used in order to train the algorithm and the rest one is applied to trained algorithm. We made many tests giving as data only the grade of 1st project and the grade of final and repeat exams, and then giving the grade of 1st and 2nd project etc. We will present the decision tree which is resulted from the data of all the grades of projects and the sex of students. In Figure 3 you can see this decision tree. The building of the tree is shown in the Figure 4.

From the 79 instances the 63 classified correctly and 16 classified erroneously. The precision of the classification of our model is 85.2%.

- Correctly Classified Instances 63 79,7%
- Incorrectly Classified Instances 16 20,3 %

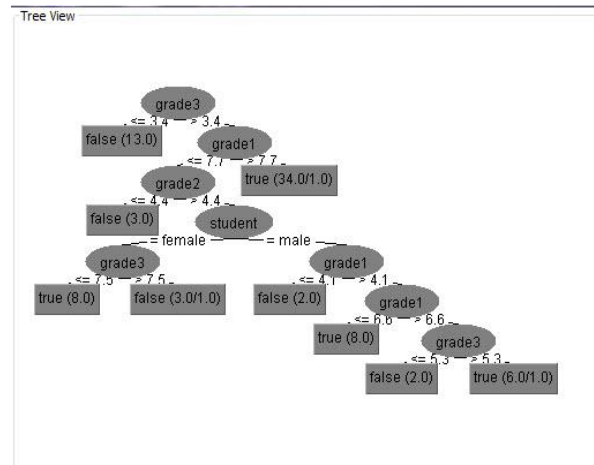


Figure 3. Decision tree

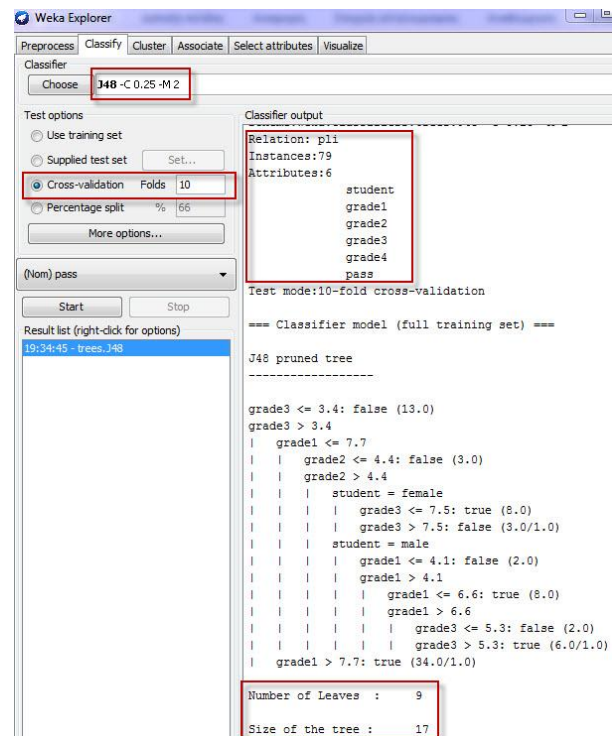


Figure 4. Building the tree with J48 (cross-validation 10 folds)

We observe that for the class “pass=true” (the course) is True Positive=0,891, False Positive=0.417, Precision=0.831, instead of the class “pass=false” is True Positive =0.583, False Positive =0.109 and Precision=0.7.

According to Confusion Matrix the 10 b instances from 24 b (b: false) classified as a (a: true) although there were b so FP=10/24=0.417. On the other hand 6 a classified as b so FP for the “pass=false” is 6/55=0,109.

- Probabilities of being correct given that your decision.
-Precision of pass=true is $49/59 = 83\%$
- Probability of correctly identifying class.
-Recall accuracy for pass=true is $49/55 = 89\%$
- Accuracy: # right/total = $63/79 = \sim 79,7\%$

We used the same dataset to train J48 algorithm with parameter percentage split 66%. The building of the tree is shown in the Figure 5.

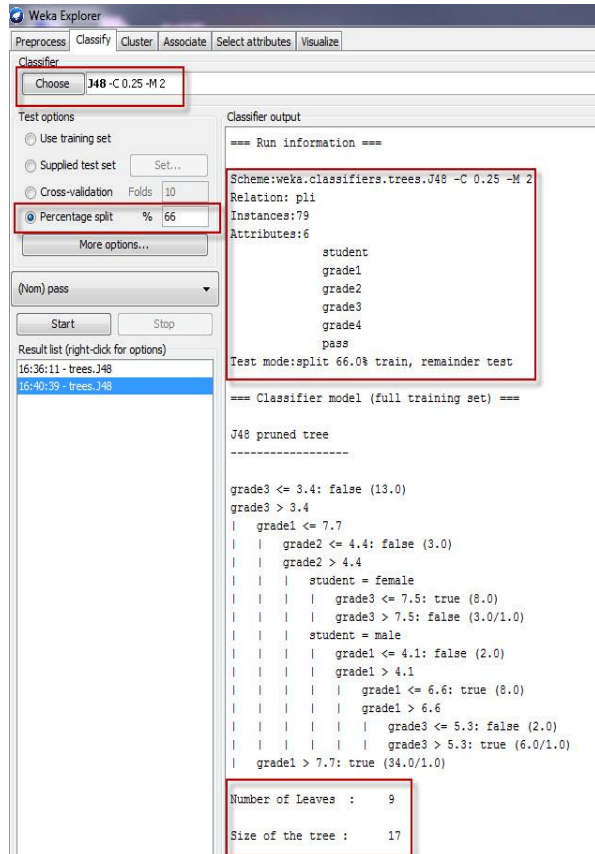


Figure 5. Building the tree with J48 (percentage split 66%)

The metrics are the following: from the 27 instances the 23 instances classified correctly and 4 classified erroneously. The accuracy of our model is 85.2%

- Correctly Classified Instances 23 85.2%
- Incorrectly Classified Instances 4 14.8%

For the class “pass=true” is True Positive=0.952, False Positive=0.5, Precision=0.87. For the class “pass=false” is True Positive =0.5, False Positive =0.048 and Precision=0.75. According to the Confusion Matrix 3 b instances out of 6b (b: false) classified as a (a: true) although there were b so $FP=3/6=0.5$. On the other hand 1 a classified as b and for “false” was $FP=1/21=0.048$.

- Probabilities of being correct given that your decision.
-Precision of pass=true is $20/23 = 87\%$
- Probability of correctly identifying class.
-Recall accuracy for pass=true is $20/21 = 95.23\%$
- Accuracy: # right/total = $23/27 = \sim 85.2\%$

Summarizing for the case of class “pass=true” the metrics for the two different parameters are shown in Table II. For the class “pass=false”, the metrics are shown in Table III. We take into account only the grades of projects and students’ sex. As we see the accuracy is the same independently of the parameter and the decision tree is the same too.

TABLE II. METRICS FOR PASS=TRUE

Pass=true	TP	FP	Precision	Recall	Accuracy
J48 (cross-validation 10 folds)	0,891	0,417	0,831	0,891	79,7%
J48 (percentage split 66%)	0,952	0,5	0,87	0,952	85,2%

TABLE III. METRICS FOR PASS=FALSE

Pass=false	TP	FP	Precision	Recall	Accuracy
J48 (cross-validation 10 folds)	0,583	0,109	0,7	0,583	79,7%
J48 (percentage split 66%)	0,5	0,048	0,75	0,5	85,2%

Based on the produced decision trees some rules were created. We used these rules in order to implement a recommendation system.

C. Recommendation system

The goal of the recommendation system is to provide a modern web based environment that will allow the timely assessment of the achievement of learning outcomes, thus supporting the realization of efficient personalized learning paths. The aims are to support the monitoring of learners’ progress and provide indicators of successfully achieving learning outcomes, to support the assessment of learning paths and to provide a means for interaction between learners and tutors.

This predictive system is a web based platform that records learners’ progress and provide tools for analyzing their performance and estimating the chances of finally achieving the planned learning outcomes based on the rules that generated through the data mining techniques. This platform will be targeted to learners, tutors of HOU.

This study examines the background information from data that impact upon the study outcome of PLI23-

Telematics students at the HOU. Classifying students based on grades information and the rules presented for each node would allow the tutors to identify students who would be “at risk” of dropping the course very soon in academic year. Then the tutor can support student with additional educational material, and give them orientation, advising, and mentoring programs, that could be used to positively impact the academic successes of such students.

Our application is a web based application implemented with open source technologies such as php, MySQL, javascript, html. Tutors and learners have access to the platform, but tutors have access in an additional functionality of platform. This functionality is the prediction of students’ progress. Tutors can log on in the platform and insert student’ data such as name, grades, etc. then they can check with the given data the probability of failing or succeeding in the exams. If the tutors see that a student is “at risk” can communicate with him/her and advise him/her, give supportive material or just make a warning. So the learner could improve his/her performance, study harder etc.

Figure 6 shows the prediction of “pass” of a student. The tutors can see the percentage of probability and if they want to see they can also see the decision tree that resulted in this percentage. Of course if we had access in more information about students such as age, occupation, marital status etc this system would give us more interesting rules. But as we already referred we could not have access to such information. However, if there are institutes or organizations which don’t face problems related to privacy, this system could cover their needs too.

The system also creates arff files automatically after the insertion of data, which means that creates a larger dataset that can be exploited by Weka and maybe it can also change the rules that have been already generated.

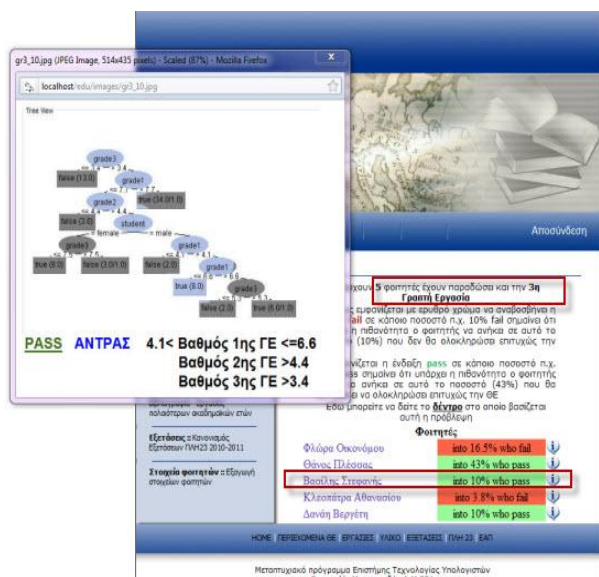


Figure 6. Prediction of a student’s final performance

The key in distance learning, as we already mentioned, is the quality of communication. A system like ours can improve the quality of this type of education since it supports the immediate communication between tutor and learner. Tutor has only to click on the name of student and send him/her an email or make a call and inform him/her for his/her progress.

We made piloting testing with real data of students of next years and the results were very satisfying. We use 31 records of students. The application firstly gave the proportion based on the grades of 1st project, then based on grades of 1st and 2nd project and finally based on grades of 1st, 2nd and 3rd project. The grade of 4th project doesn’t play any role to the generated rules from previous step of data mining. This happens because of the curricula of HOU, the 4th project is optional. If a student doesn’t have good grades in previous projects can give the 4th project in order to be able to participate in final exams. That means that the majority of students do not make the 4th project. The application seems to be very accurately as it has small deviation error i.e., for the 1st project and for the 1st and 2nd project the system predicts that all users will pass the exams. The real data show that only two students fail out from 31. So the system has accuracy 93.5%. Taking into account and the 3rd project the precision of system is getting lower. The system predicts erroneously that 2 students will succeed in exams and 2 students will fail. So the accuracy of system is 87%. However, it predicts that 2 students (women) will marginally fail but at the end they pass. So we assume that this path of the decision tree is weak and if we had a larger dataset to train the algorithm, this path would be different.

The Precision of this pilot dataset is 90.3% and the Recall is 96.6% comparing to the precision and the recall of the classifier performance we see that is more accurately. This happens as the pilot test dataset is too small and the data are too clear. Table IV shows briefly the results of pilot testing.

TABLE IV. PREDICTION OF STUDENTS’ FINAL PERFORMANCE

Results/Projects	Prediction of pass	Prediction of fail	Pass	Fail	Total
1 st	31	0	29	2	31
1 st & 2 nd	31	0	29	2	
1 st & 2 nd & 3 rd	29	2	27	4	

IV. CONCLUSIONS AND FUTURE WORK

This application can be the vehicle for improving the quality of existing distance -and not only- learning systems and it will be very helpful not only for the learners who will be able to be informed for their progress but also for the tutors who can improve their teaching process. After the study of different data mining techniques, we chose the one that was most suitable for our application and as we see is the most widespread in this field. The results were very satisfying and after pilot testing of our application we saw that the final results verified the generated rules with small

deviation error prediction. The basic idea of this system can be also applied in other distance learning or e-learning systems.

A comparison between some classification tree models would be conducted in the future in order to determine the best model for the dataset. Maybe an alternative to a classification tree should be considered in order to compare the results.

This research is based on background information only. Leaving out other important factors as previous studies, number of courses completed motivation, financial aids, age, marital status, etc.) that may affect study outcome, could distort results obtained with classification trees. For example, including the educational background of students after the submission of the first project would probably improve predictive accuracy of the model. To improve the model, more attributes could be included to obtain prediction with fewer errors.

Furthermore, an idea is to incorporate the C4.5 algorithm to our platform in order to run again and again the algorithm with the new data too. So the model will be always up to dated and new rules could be generated. These rules could be also incorporated to our ontology as restrictions. This enrichment of ontology may lead to the extraction of prediction directly from the ontology.

REFERENCES

- [1] A. Gomez-Perez, M. Fernandez-Lopez and O. Corcho, "Ontological Engineering with examples from the areas of Knowledge Management, e-Commerce and the Semantic Web", First Edition
- [2] B. A. Jusung Jun, "Understanding dropout of adult learners in e-learning", A Dissertation Submitted to the Graduate Faculty of the University of Georgia in Partial
- [3] B. Sridharan, H. Deng, B. Corbitt, "An ontology-driven topic mapping approach to multi-level management of e-learning resources", 17th European Conference on Information Systems, pp. 1187-1198
- [4] Burdescu, D.Dan Mihaescu, M. Cristian Ionascu, C. Marian Logofatu, Bogdan, "Support system for e-Learning environment based on learning activities and processes" (19-21 May 2010), Research Challenges in Information Science (RCIS), 2010 Fourth International Conference, pp. 37-42
- [5] C. Romero, S. Ventura, M. Pechenizkiy, R.S.J.d. Baker, "Handbook of Educational Data Mining, Edited", chapter 5
- [6] F. Castro, A. Vellido, À. Nebot, F. Mugica, "Applying Data Mining Techniques to e-Learning Problems", Evolution of Teaching and Learning Paradigms in Intelligent Environment In Evolution of Teaching and Learning Paradigms in Intelligent Environment, Vol. 62 (2007), pp. 183-221
- [7] Gruber, Thomas R. , "A translation approach to portable ontology specifications", (June 1993), Knowledge Acquisition 5, pp.199–220.
- [8] J. W. Seifert, "Data Mining: An Overview", National Security Issues, pp. 201-217
- [9] L. Zhuhadar, O. Nasraoui, R.Wyatt and E. Romero, "Multi-model Ontology-based Hybrid Recommender System in E-learning Domain", 2009 IEEE/WIC/ACM International Conference on Web Intelligence and Intelligent Agent Technology – Workshops, pp.91-95
- [10] M. Hanna, (2004) "Data mining in the e-learning domain", Campus-Wide Information Systems, Vol. 21 Iss: 1, pp.29 - 34
- [11] N. V. Chawla, "C4.5 and Imbalanced Data sets: Investigating the effect of sampling method, probabilistic estimate, and decision tree structure", ICML'03 Workshop on Class Imbalances
- [12] Pin-Yu Pan, Chi-Hsuan Wang, Gwo-Jiun Horng, Sheng-Tzong Cheng, "The development of an Ontology-Based Adaptive Personalized Recommender System", Electronics and Information Engineering (ICEIE), 2010 International Conference On, 1-3 Aug. 2010, pp. V1-76 - V1-80
- [13] V. Eyharabide, A. Amandi, M. Courgeon, C.Clavel, C. Zakaria, J. Martin, "An ontology for predicting students' emotions during a quiz. Comparison with self-reported emotions", Affective Computational Intelligence (WACI), 2011 IEEE Workshop on, 11-15 April 2011, pp. 1-8
- [14] <http://clarkparsia.com/pellet/protege/> [retrieved: March, 2012]
- [15] http://en.wikipedia.org/wiki/Artificial_neural_network [retrieved: May, 2012]
- [16] http://en.wikipedia.org/wiki/Association_rule_learning [retrieved: May, 2012]
- [17] http://en.wikipedia.org/wiki/Decision_tree [retrieved: May, 2012]
- [18] http://en.wikipedia.org/wiki/Distance_education [retrieved: March, 2012]
- [19] http://en.wikipedia.org/wiki/Genetic_algorithm [retrieved: May, 2012]
- [20] <http://en.wikipedia.org/wiki/XML> [retrieved: May, 2012]
- [21] <http://www.cs.waikato.ac.nz/ml/weka> [retrieved: March, 2012]
- [22] <http://www.eadtu.eu/hellenic-open-university-hou-greece.html> [retrieved: March, 2012]
- [23] <http://www.w3.org/RDF/> [retrieved: May, 2012]
- [24] <http://www.w3.org/TR/owl-features/> [retrieved: May, 2012]

An Experiment in Students' Acquisition of Problem Solving Skill from Goal-Oriented Instructions

Matej Guid, Ivan Bratko
 Artificial Intelligence Laboratory
 Faculty of Computer and Information Science, University of Ljubljana
 Ljubljana, Slovenia
 {matej.guid, ivan.bratko}@fri.uni-lj.si

Jana Krivec
 Department of Intelligent Systems
 Jožef Stefan Institute
 Ljubljana, Slovenia
 jana.krivec@ijs.si

Abstract—In this paper, we investigate experimentally the efficacy of semi-automatically constructed instructions for solving problems that require search. The instructions give advice to the student, in terms of what sub-goals should be attempted next in the process of solving a problem. Our chosen experimental problem domain was the chess endgame of checkmating with bishop and knight, which occasionally presents difficulties even to chess grandmasters. Our subjects, little more than complete beginners, were given the task of learning to win this endgame by studying the instructions. We were interested in two questions: (1) How effective were the goal-oriented instructions as an aid to the student towards mastering this domain? (2) What was the form of the students' "internal representation" of the acquired knowledge? The latter question was studied by our method for automatically identifying so-called procedural chunks from the students' games. Given the simplicity of the chunk detection method, the reconstructed chunks of students' acquired knowledge reflected the goal structure of the instructions amazingly well.

Keywords—cognitive models; procedural knowledge; procedural chunks; problem solving; perception; memory; chess.

I. INTRODUCTION

People operate under constant attacks from lots of external information. If we want to react properly and orient in the world that surrounds us, we need to use this information selectively and effectively. In doing so, we need to incorporate knowledge, stored in long-term memory, which we can recall to short-term memory when needed. Information is usually stored in the memory in the form of chunks - completed units of logically related information clusters that facilitate their retrieval and use, and allow better utilization of a limited working-memory capacity ([1], [2]). Most of the previous research efforts have been devoted to chunks in declarative knowledge, while little is known about the chunks in procedural knowledge. The nature of chunks still remains very elusive, especially with understanding chunks in procedural knowledge. Our attempt is to show the existence of chunks in procedural knowledge, define them, and see how they are incorporated in ones memory.

In this paper, we intend to verify the following claim: people learn procedural knowledge by (sub-consciously) constructing meaningful units of procedural knowledge. To

emphasize the difference with respect to well-known chunks in declarative knowledge, we will refer to these meaningful units of procedural knowledge as *procedural chunks*. In chess, for example, a procedural chunk is a sequence of chess moves that all together belong to a chess concept, and are therefore memorized by a player as a whole. We also intend to demonstrate that compared to the traditional approach that usually provides declarative knowledge, using the approach that emphasizes developing students' *procedural knowledge* can greatly improve their skills.

In our previous study [3], we indicated the existence of procedural chunks by using *reconstruction* of chess games. In the experiments presented in this paper, however, the participating students - chess beginners - were actually *playing* chess against a computer. The identification of chunks was performed by combining existing methods for chunk recognition, slightly adapted for detection of chunks in procedural knowledge. The times spent for execution of individual moves played by the students served as the most valuable information for determining chunks, similarly as in several studies related to chunks in declarative knowledge (see, for example: [4], [5], [6], and [7]).

As a case study, we considered teaching students how to play a difficult KBNK (king, bishop, and knight vs. king) chess endgame, by providing the students with goal-oriented procedural knowledge in the form of a manual (textbook instructions) supported with example games. We have chosen chess for our research domain due to the following reasons:

- because of its complexity, clearly defined rules, built-in scales for measuring chess players' knowledge (*Elo* rating system), and generalization to other areas often made possible;
- chess endgames with a few pieces have an additional benefit as an experimental domain: availability of *perfect information* in the form of chess tablebases [8], enabling optimal play by a computer and - more importantly - easier tracking of students' learning progress.

The paper is organized as follows. In Section II, we

Table I
THE 11 GOALS PRESENTED IN THE TEXTBOOK INSTRUCTIONS.

1	Deliver checkmate.
2	Prepare the knight for checkmate.
3	Restrain black to a minimal area beside the right corner.
4	Build a barrier and squeeze black king's area.
5	Approach black from the center.
6	Block the way to the wrong corner.
7	Push black towards the right corner.
8	Push black towards the edge.
9	Approach with the king.
10	Bring the knight closer.
11	Keep the kings close.

describe in more detail the domain of KBNK, the teaching materials used in the experiments, and the experimental procedure. Section III introduces the methods used for identification of procedural chunks. Section IV presents the results of our experiments, particularly in terms of students' learning progress during the playout games and procedural chunks identified. We conclude the paper and point out directions for further work in Section V.

II. EXPERIMENTAL SETUP

A. Domain Description

Our domain of choice was the KBNK (king, bishop, and knight vs. a lone king) chess endgame, which is regarded as the most difficult of the elementary chess endgames. The stronger side can always checkmate the opponent, but even optimal play may take as many as 33 moves. Several chess books give the general strategy for playing this endgame as follows. Since checkmate can only be forced in the corner of the same color as the squares on which the bishop moves, the opponent will try to stay first in the center of the board, and then retreat in the wrong-colored corner. The checkmating process can be divided into three phases: (1) driving the opposing king to the edge of the board, (2) forcing the king to the appropriate corner, and (3) delivering checkmate. However, only knowing this basic strategy hardly suffices for anyone to checkmate the opponent effectively. There are many recorded cases when strong players, including grandmasters, failed to win this endgame.

B. Textbook Instructions and Example Games

In our experiments, we used "textbook instructions" in the form of goals for delivering checkmate from any given KBNK position. These instructions were semi-automatically derived using an interactive procedure between a chess teacher (a FIDE master of chess) and the computer [9], using argument-based machine learning (ABML) approach combined with an algorithm for semi-automated domain conceptualization of procedural knowledge [10].

The textbook instructions consist of 11 goals listed in Table I (see [11] for details). The chess-player is instructed to always try to execute the highest *achievable* goal. The goals are listed in order of preference, goal 1 being the most preferred. In the textbook instructions presented to the students, these goals were supplemented with detailed explanations and illustrative diagrams.

The students also had *example games* demonstrating the checkmating procedures at their disposal. The example games were supplemented with the goals given as instructions, in terms of which is the preferable (and also achievable) goal in a particular position. An instruction is given each time the previous suggested goal was accomplished.

Figure 1 is taken from the textbook instructions. It demonstrates the execution of one of the goals. This goal is supplemented by the following explanation in the textbook instructions: "When the defender's king is already pushed to the edge of the board, the attacker's task is to constrain as much as possible the defending king's way to the wrong-colored corner. At the same time, the attacker should keep restraining the enemy king to the edge of the board."

Both the textbook instructions and the example games that were used in our experiments are available in a web appendix at [11].

C. Experimental Procedure

Three students – chess beginners of slightly different levels – were involved in the experiment. Student 1 is a *Class B* player, Student 2 is a *Class C* player (*i.e.*, slightly weaker than Student 1 in terms of his chess strength), and Student 3 is a *Class D* player (a complete beginner, however, well familiar with the rules of chess). According to the ELO rating scales, the *Class B*, *Class C*, and *Class D* represent ELO rating ranges of 1600-1800, 1400-1600, and 1200-1400, respectively [12].

Our assumption was that none of the three students possessed procedural knowledge sufficient for successfully delivering checkmate in the KBNK endgame at the beginning of the experiment. In order to verify the correctness of this assumption, the participants were first asked to try to deliver checkmate in three games against the computer. The computer was defending "optimally", *i.e.*, always randomly choosing among moves with the longest distance to mate (using chess tablebases). The time limit was 10 minutes per game. Each game started from a different starting position: mate-in-30-moves or more assuming optimal play. The moves and times spent for each move were recorded automatically using *Fritz 13* chess software by *Chessbase*.

None of the students were able to deliver checkmate at this first stage of the experiment. While the students were occasionally able to force the defending king towards the edge of the board, it turned out that the most difficult part was to block the way to the wrong corner and push the king towards the right corner – the corner where checkmate

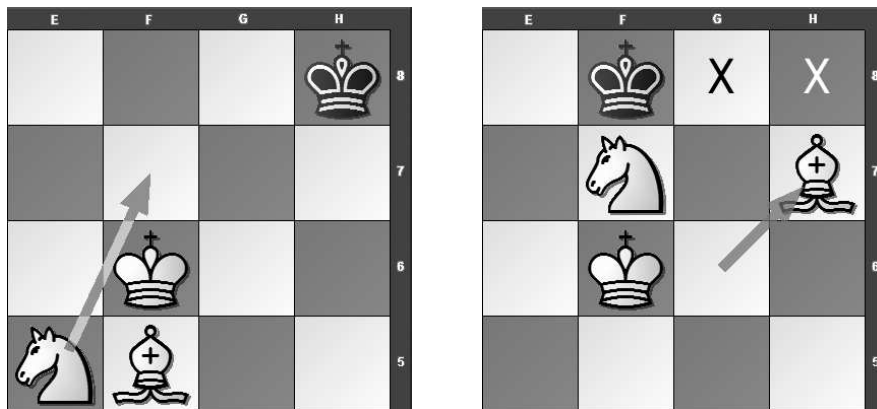


Figure 1. Demonstration of the execution of the goal 6: “Block the way to the wrong corner.” In the position on the left, white pieces lure the defending king out of the wrong corner (note that a light squared bishop cannot deliver mate in a dark square corner): 1.Ne5-f7+ Kh8-g8 2.Bf5-g6 Kg8-f8 (this is the only available square to the black king, since h8 is attacked by the knight) 3.Bg6-h7! The last move in this sequence takes under control square g8, and sets up the blockade one square farther from the wrong corner.

can be delivered. They had no idea how to establish the appropriate barrier around the right corner in order to deny the defending king an escape from there.

Then the students were given the textbook instructions and access to the example games that contain instructions as commentary to particular move sequences. The students were reading the instructions and observing the example games until they felt they are ready to challenge the computer once again. None of them spent more than 30 minutes for reading the instructions and observing the example games at this point.

In the second stage of the experiment, the students were again trying to checkmate the optimally defending computer. The time limit per game was again set to 10 minutes. The starting position of each game was chosen randomly in such way that each of the four pieces occupied one corner square, with the white bishop always being placed on a white square. Similarly as in the first stage, the moves and times spent for each move were recorded automatically. The textbook instructions and example games were not accessible to the students at this stage. If a game ended in a draw, the student was again granted the access to the textbook instructions and example games for up to ten minutes before starting a new game. This procedure was then being repeated until the first win was recorded. In order to verify the quality of the learned knowledge, the students were asked to challenge the computer again, this time with the white bishop being placed on a black square (*i.e.*, the opposite square than in their all earlier games).

Since it is our conjecture that people learn procedural knowledge by using procedural chunks, we attempted to verify whether the students learned any procedural chunks during the process of learning how to deliver checkmate in the difficult KBNK chess endgame. Thus, we needed some methods to identify procedural chunks. These methods are presented in the following section.

III. IDENTIFICATION OF PROCEDURAL CHUNKS

The chunks were identified on the basis of a hypothesis stated by Chase and Simon [4], which states that longer time interval during the reconstruction of a meaningful unit of material (*i.e.*, the material about which we have some relevant knowledge) reveals the recall of a new structure/chunk from the long-term memory. In our experiments, the students did not deal with *reconstructions* of chess positions (as in Chase and Simon [4], and Bratko *et al.* [5]) or particular move sequences (as in Krivec *et al.* [3]), but were actually *playing* against the computer.

The relative time of particular person was considered instead of an absolute 2-second limit used by Chase and Simon. We defined a *longer time interval* in the following way. Times of each participant were normalized using two different methods: (1) we calculated the percentage of time used for a certain move with regard to the time spent for a whole game, and (2) by converting them into *z* values. The quantity *z* represents the distance between the raw score and the population mean in units of the standard deviation. The value of *z* is negative when the raw score is below the mean, and positive when above.

All relevant symmetries were taken into account when processing individual moves in the identification of procedural chunks. For example, the move Bh7 (the bishop moves to h7) in the sequence 1.Nf7+ Kg8 2.Bg6 Kf8 3.Bh7 (see Fig. 1) is equivalent to the move Ba2 (the bishop moves to a2) when the enemy king is in the opposite “wrong” corner of the board and thus the sequence is actually 1.Nc2+ Kb1 2.Bb3 Kc1 3.Ba2.

For all moves in each game, an average value and standard deviation of normalized time medians was calculated. All the moves that exceeded the boundary of the average value plus one standard deviation were considered as a “long time interval” and as such candidates for the beginning of a

new procedural chunk. If such a candidate appeared in the majority of the games, it was considered as the beginning of a procedural chunk.

Validity of this method of chunk identification was statistically verified as follows. We randomly generated input data, having the same number of chunks as in the original data. After this, we calculated the co-occurrence of the chunks beginning. We repeated this 100 times. Then we calculated 95-percentile of the sum of co-occurred chunk beginning. We compared the possibility that the original results (*i.e.*, the beginning of the chunks) are the result of a chance. That is, if the co-occurrences of the beginning of the chunks in the results of the real play represented more than 95% co-occurrences in randomly generated results, it was considered that it is highly improbable that the co-occurrences happened by chance only.

IV. RESULTS

A. Deviation from Optimal Play

In order to track the progress by the students as they were more and more exposed to the textbook instructions and example games between (but not during) their trial games against the computer, we observed the deviations of the moves they played from an optimal play. Chess tablebases served us for this purpose, providing the number of moves required to deliver checkmate from any given position assuming optimal play by both players. Although the goal of the conceptualized procedural knowledge included in the textbook instructions is not to teach students how to play “optimally,” but merely to enable them to achieve a step-by-step progress towards the ultimate goal – delivering checkmate – deviation from optimal play was chosen as a sensible measure of quality of their play.

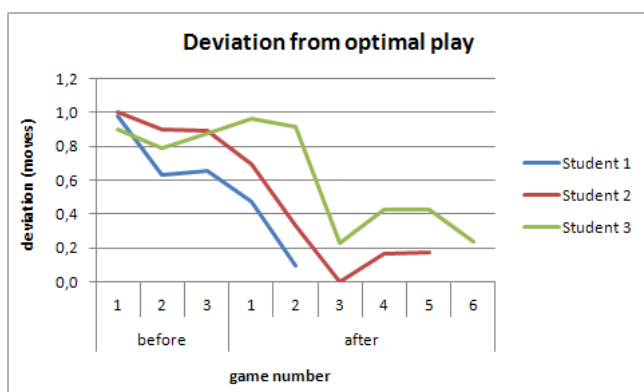


Figure 2. The average students’ deviations from optimal play in the games of both stages of the experiment, *i.e.*, before and after they were first given access to the textbook instructions and the example games.

The results of these observations are presented in Figure 2. They demonstrate the average students’ deviations from

optimal play in all their games until they successfully checkmated the optimally-defending computer for the first time (this game is included in the graph). The lower deviation from optimal play means a better performance of the player.

The deviations from optimal play for a particular move played by the player were calculated as follows:

$$DTM_{dev} = DTM_{played} - DTM_{optimal} \quad (1)$$

where “DTM” represents the distance to mate in moves (rather than *plies* or half-moves). $DTM_{optimal}$ is the value of DTM of an optimal move, and DTM_{played} is the value of DTM of the move played by the student. DTM_{dev} (deviation from optimal play) value of 0 therefore means that the student played a given move optimally, the value of 1 means that the distance to mate remained the same after the execution of the moves by the player and (optimally defending) computer, and DTM_{dev} values higher than 1 for a given move mean that on the next player’s move DTM even increased.

The results clearly suggest that the speed of achieving mastery of this difficult chess endgame is correlated with the chess-playing strength. Student 1, the strongest of the three players, not only successfully checkmated the opponent already in the second game after having studied the teaching materials – he also made less inferior moves earlier than the other two students. The other two students checkmated in games 5 and 6, respectively. Once they achieved the win the students had no problems at all achieving it again, even with the white bishop being placed on the opposite square color than in all previous games. The results also demonstrate a vast progress of all three students after they got acquainted with (sub)goals and procedures presented in the teaching materials.

It is particularly interesting that the second student played optimally(!) in his third game of the second stage of the experiment. He actually played 22 optimal moves in a row – an achievement that a chess grandmaster could be proud of. Moreover, it happened in less than an hour after he was first given access to the textbook instructions and example games. This result would be very hard or even impossible to achieve without an effective way of memorizing particular (sub)goals or concepts of procedural knowledge required in order to master this difficult endgame.

B. Procedural Chunks Identified

We identified procedural chunks separately for each of the three phases mentioned in II-A (repeated here for clarity):

Phase I:

Driving the opposing king to the edge of the board (the black king aims towards the “wrong” corner).

Phase II:

Forcing the king from the “wrong” corner to the “right” corner (where checkmate can be delivered).

Phase III:

Delivering checkmate (once a “barrier” is set up).

The students actually tended to spend more time on moves that indicate a borderline between two phases. Based on this observation, we determined the start of Phase II just before a waiting move with the bishop before blocking the way of the black king to the wrong corner (see the move 2.Bf5-g6 in Figure 1), and the start of Phase III just after the barrier is established. Tables II, III, and IV show identified procedural chunks in the games of the second stage of the experiment, *i.e.*, after the teaching materials were presented to the students, and frequencies of their occurrence in the playouts. The chunks are described by meaningful descriptions.

Table II
PROCEDURAL CHUNKS DETECTED IN PHASE I.

#	Chunk Description	Freq.
1	Finding the path for the knight to attack the corner square.	14
2	Bringing the bishop into the game.	9
3	Bringing the knight into the game.	8
4	Using the king to push the enemy king towards the edge.	6

Let us take a look how the chunks identified in Phase I (Table II) are associated with the goals (see Table I) given in the textbook instructions. Chunk #1 represents preparation for execution of Goal 6 (“Block the way to the wrong corner.”). To achieve this goal, White must first bring the knight to the square from which it attacks the wrong corner square (see Figure 1). While it may take a fraction of a second for a master to spot the path with the knight to a given square, the chess beginners involved in our experiments typically paused for a while before executing a sequence of moves that brought the knight to a desired square. Chunks #2 and #4 can be associated with Goal 8 (“Push black towards the edge.”), and the latter is also associated with Goal 5 (“Approach black from the center.”), Goal 9 (“Approach with the king.”) and Goal 11 (“Keep the kings close.”). Chunk #3 is associated with Goal 10 (“Bring the knight closer.”).

Table III
PROCEDURAL CHUNKS DETECTED IN PHASE II.

#	Chunk	Freq.
1	A waiting move with the bishop before blocking the way.	7
2	The knight keeps the enemy king on the edge.	7
3	Building a barrier with the knight and the bishop.	6
4	The king keeps the enemy king on the edge.	5

In Phase II (Table III), Chunk #1 represents a part of an execution of Goal 6 (“Block the way to the wrong corner.” – see Figure 1). Chunks #2 and #4 are associated with Goal 7 (“Push black towards the right corner.”) in which White also

needs to keep the enemy king at the edge of the chessboard – note that two chunks were learned for an execution of a single goal, which incidentally also turned out to be the most difficult of the goals to be learned (judging from the times spent for its execution). Chunk #3 represents an execution of Goal 4 (“Build a barrier and squeeze black king’s area.”).

Note that Phase II is the most difficult part of the KBNK endgame, since a precise sequence of moves must be executed and a single mistake may have a fatal consequence: the black king may escape to the opposite wrong corner before the barrier is established. The students learned this sequence of moves by remembering meaningful intermediate subgoals, as suggested by the identified procedural chunks.

Table IV
PROCEDURAL CHUNKS DETECTED IN PHASE III.

#	Chunk	Freq.
1	Squeezing the enemy king into the right corner (start).	8
2	Manoeuvring the bishop to set up the “minimal area”.	7
3	Squeezing the enemy king into the right corner (continue).	6
4	Calculating the checkmate procedure.	6
5	Approaching with the knight for delivering checkmate.	5

In Phase III, Chunks #1 and #3 are associated with Goal 4 (“Build a barrier and squeeze black king’s area.”), Chunk #2 closely resembles Goal 3 (“Restrain black to a minimal area beside the right corner.”), and Chunk #5 is associated with Goal 2 (“Prepare the knight for checkmate.”). Finally, Chunk #4 is associated with the highest goal in the hierarchy, Goal 1 (“Deliver checkmate.”).

All the described chunks were detected automatically by using the methods described in Section III. As it can be seen from the descriptions above, they cover all 11 goals presented in the textbook instructions.

Figure 3 shows the progress of the students by means of the different goals executed in their playout games. The results closely resemble the ones demonstrated in Figure 2: Student 1, the strongest of all three students in terms of chess strength, was the first to master all 11 goals given in the textbook instructions, and all three players demonstrated in their games a progress towards the final goal – successfully checkmating the opponent’s king.

In the figure, it can be seen that some goals were only partially executed. This happened on occasions where a particular goal (as presented in Table I) consisted of more than one procedural chunk (as given in Tables II, III, and IV). In the first stage of the experiment, the students were merely able to execute the most intuitive goals. One such goal is Goal 5 (“Approach black from the center.”), which is very intuitive for a human – it is useful for the white king to approach the black king from the central part of the board.



Figure 3. Number of instruction goals the students successfully executed in the playoff games against the computer.

V. CONCLUSION AND FUTURE WORK

In this paper, we studied how procedural knowledge for solving problems in a domain is learned operationally by students from “textbook instructions” (a manual). In our study, textbook instructions had the form of if-then rules that specify goals to be achieved in solving a particular problem in the domain, ordered according to the degree of ambition of the goals which roughly corresponds to the time order of subtasks.

In our experimental study, we measured the students’ progress in assimilating this procedural knowledge by observing their skill at the given task (checkmate in the KBNK endgame). Roughly, our subjects were just slightly better than complete chess beginners.

We were interested in two questions:

- 1) How useful are the goal-oriented instructions to the student as a help towards mastering the play in this domain?
- 2) What was the form of the student’s “internal representation” of the acquired knowledge? Our hypothesis was that it was a goal-based representation with a similar goal structure as in the instructions.

Our hypothesis regarding the students’ internal representation of the acquired skill was experimentally tested by means of the identification of *procedural chunks*, using a new method for chunk identification from games played. Roughly, a procedural chunk is a sequence of chess moves that all together belong to a chess concept, and are therefore memorized by a player as a whole. The chunk identification method is based on observing the times between consecutive moves in a game played. Longer time intervals between moves indicate boundaries between procedural chunks.

Our findings concerning the two questions above were as follows:

- Finding regarding question (1): The students learned the skill operationally in up to an hour’s time of studying the instructions and testing their skill in actual problem

solving (playing the endgame). To put this result in perspective, it should be remembered that even chess grandmasters often have serious difficulties in playing this endgame, occasionally failing to deliver mate at all.

- Finding regarding question (2): Automatically detected procedural chunks in the students’ games corresponded almost perfectly to the goal-oriented rules in the textbook instructions. We also measured the dynamics of acquiring these chunks during the learning time, that is the number of different chunks appearing in consecutive games played by a student.

As future work, we intend to strengthen these experimental results by scaling up the experiments in terms of the number of subjects, and by extending the experiments to other domains (other chess tasks and domains other than chess).

REFERENCES

- [1] A. de Groot, *Thought and Choice in Chess*. Mouton, The Hague, 1965.
- [2] F. Gobet, P. Lane, S. Croker, P. Cheng, G. Jones, I. Oliver, and J. Pine, “Chunking mechanisms in human learning,” *Trends in Cognitive Sciences*, vol. 5, no. 6, pp. 236–243, 2001.
- [3] J. Krivec, M. Guid, and I. Bratko, “Identification and characteristic descriptions of procedural chunks,” in *Proceedings of the 2009 Computation World: Future Computing, Service Computation, Cognitive, Adaptive, Content, Patterns*, ser. COMPUTATIONWORLD ’09. Washington, DC, USA: IEEE Computer Society, 2009, pp. 448–453.
- [4] W. Chase and H. Simon, “Perception in chess,” *Cognitive Psychology*, vol. 4, pp. 55–81, 1973.
- [5] I. Bratko, P. Tancig, and S. Tancig, “Detection of positional patterns in chess,” *International Computer Chess Association Journal*, vol. 7, no. 2, pp. 63–73, 1984.
- [6] V. Ferrari and E. Didierjean, Andre an Marmeche, “Dynamic perception in chess,” *The Quarterly Journal of Experimental Psychology*, vol. 59, no. 2, pp. 397–410, 2006.
- [7] A. Linhares and A. E. Freitas, “Questioning Chase and Simon’s (1973) “Perception in Chess”: The “experience recognition” hypothesis,” *New Ideas in Psychology*, vol. 28, no. 1, pp. 64–78, 2010.
- [8] K. Thompson, “Retrograde analysis of certain endgames,” *International Computer Chess Association Journal*, vol. 9, no. 3, pp. 131–139, 1986.
- [9] M. Guid, M. Možina, A. Sadikov, and I. Bratko, “Deriving concepts and strategies from chess tablebases,” in *ACG*, 2009, pp. 195–207.
- [10] M. Možina, M. Guid, A. Sadikov, V. Groznic, and I. Bratko, “Goal-oriented conceptualization of procedural knowledge,” in *Lecture Notes in Computer Science*, vol. 7315, 2012, p. to appear.
- [11] M. Guid, “KBNK,” <http://www.ailab.si/matej/KBNK/>, 2012.
- [12] A. Elo, *The Rating of Chessplayers, Past and Present*. Arco, 1978.

Learning Long Sequences in Binary Neural Networks

Xiaoran Jiang, Vincent Gripon, and Claude Berrou

Telecom Bretagne, Electronics department

UMR CNRS Lab-STICC

Brest, France

xiaoran.jiang@telecom-bretagne.eu, vincent.gripon@telecom-bretagne.eu, claude.berrou@telecom-bretagne.eu

Abstract—An original architecture of oriented sparse neural networks that enables the introduction of sequentiality in associative memories is proposed in this paper. This architecture can be regarded as a generalization of a non oriented binary network based on cliques recently proposed. Using a limited neuron resource, the network is able to learn very long sequences and to retrieve them from only the knowledge of any sequence of consecutive symbols.

Index Terms—oriented neural network; learning machine; associative memory; sparse coding; directed graph; sequential learning; efficiency.

I. INTRODUCTION

Sequence learning in neural networks has been an important research topic in a large number of publications, since the forward linear progression of time is a fundamental property of human cognitive behavior. Different approaches have been carried on. Among them, the most important and commonly studied are the simple recurrent networks (SRN) [1] [2] and the short term memory (STM) [3] [4], which uses the dynamics of neural networks. Other structures have been proposed, especially those based on the Hopfield network principle [5]. However, many Hopfield-like connectionist networks do not have good performance when learning sequences, as the learning of new information completely disrupts or even eliminates that previously learnt by the network. This problem is identified as “catastrophic interference” [6] or “catastrophic forgetting” (CF) [7] in some literature. There are indeed strong interferences as the learning process relies on changing the connection weight (what is called plasticity by neurobiologists). Therefore, there is no guarantee that the ability of the network to recall messages will remain still when learning new ones.

A recently proposed non-oriented kind of network based on cliques and sparse representations [8] [9] follows a different approach by comparison with Hopfield-like networks. The neurons and the connections are all binary. The connection weight is equal to zero if the connection does not exist, otherwise this weight is equal to one. Subsequent learning will never impact on the weights of the existing connections. Therefore, we explain in this paper how the architecture of these networks can be efficiently modified to allow learning sequences with less degree of interference with the previously

learned ones. However, the clique-based networks only enable the learning of fixed-length messages, and the learning and retrieving are rather synchronous than following time progression. In order to learn information arriving in separate episodes over time, one may replace the non oriented graph by an oriented one, and consider a more flexible structure than cliques.

The rest of paper is organized as follows: Section II recalls the principles of learning fixed length messages by non oriented clique-based networks, which is at the root of the works presented in this paper. In Section III, the oriented sparse neural networks based on original oriented graphs, called “chains of tournaments” are demonstrated to be good material to learn sequential information. Generalization is proposed in Section IV. Finally, a conclusion is proposed in Section V.

II. LEARNING FIXED LENGTH MESSAGES ON CLIQUES

Let \mathfrak{M}_B be a set of binary messages of fixed length B bits. For each message $m \in \mathfrak{M}_B$, we split it into c sub-messages of length $\frac{B}{c}$: $m = m^1 m^2 \dots m^c$. Each sub-message is then associated with a unique extremely sparse codeword (each sub-message is encoded by a single neuron), within a unique cluster of neurons in the network. For $1 \leq i \leq c$, m^i of length $\frac{B}{c}$ can take $2^{\frac{B}{c}}$ values, that leads to an extremely sparse code of length $2^{\frac{B}{c}}$, and the corresponding cluster of size $l = 2^{\frac{B}{c}}$. An example is represented in Figure 1, in which there are $c = 4$ clusters (filled circles, filled rectangles, rectangles and circles) of $l = 16$ neurons, that we call fanals, according to the vocabulary in [8]. In this figure, one message of 16 bits: 1110100111011010 is split into 4 sub-messages, $m^1 = 1110$, $m^2 = 1001$, $m^3 = 1101$, $m^4 = 1010$. Each sub-message is then mapped to a unique fanal in the corresponding cluster. The fundamental idea is to transform the learning of such a message into embedding a clique into the network (thick lines in Figure 1 for the message mentioned above). In graph theory, a clique in an undirected graph is a subset of its vertices such that every two vertices in the subset are connected by an edge. Any binary message in \mathfrak{M}_{16} can be learnt by this network in embedding corresponding cliques. Let (m_1, m_2, \dots, m_N) be any N -tuple of binary messages in \mathfrak{M}_B . If we denote $W(m_n)$ the connection set of the corresponding clique after learning message m_n , the connection set of the associated graph after learning (m_1, m_2, \dots, m_N) can therefore

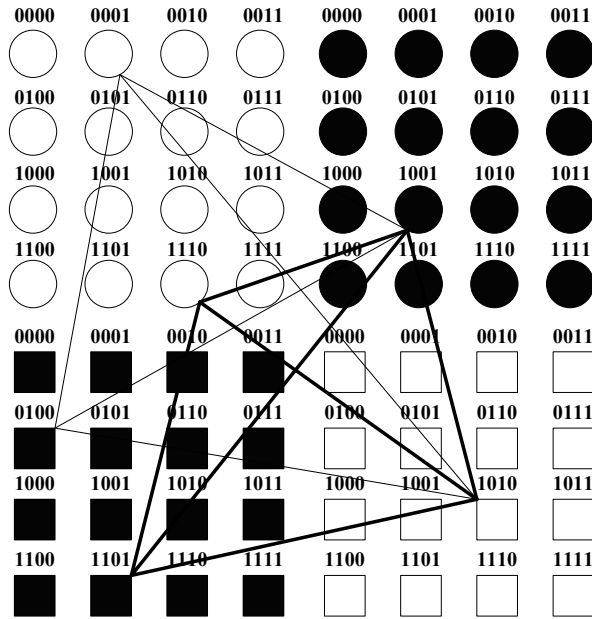


Fig. 1. Learning process illustration for non-oriented clique-based networks. The pattern to learn (with thick edges) connects fanals from four clusters composed of 16 fanals each (filled circles, filled rectangles, rectangles and circles).

be defined by the union:

$$W(m_1, m_2, \dots, m_N) = \bigcup_{n=1}^N W(m_n) \quad (1)$$

The clique offers a large degree of redundancy that one can take advantage of during the retrieval process. For instance, there are 6 edges in a clique of 4 vertices, but only two of them are sufficient to identify such a clique. If some of the sub-messages are erased, it is likely that the whole message can still be retrieved thanks to this high redundant representation.

Let us denote by v_{ij} the actual value of n_{ij} , which is the j^{th} fanal in the i^{th} cluster. $\omega_{(ij)(i'j')}$ is the connection weight between n_{ij} and $n_{i'j'}$. $\omega_{(ij)(i'j')} = 1$ if this connection exists, 0 otherwise. The message retrieving can then be expressed by an iterative process as following:

$$\forall i, j, v_{ij} \leftarrow \sum_{i'=1}^c \min \left(\sum_{j'=1}^l \omega_{(ij)(i'j')} v_{i'j'}, 1 \right) + \gamma v_{ij} \quad (2)$$

$$v_i^{max} \leftarrow \max_j (v_{ij}) \quad (3)$$

$$\forall i, \forall j, v_{ij} \leftarrow \begin{cases} 1 & \text{if } v_{ij} = v_i^{max} \text{ and } v_i^{max} \geq \sigma \\ 0 & \text{otherwise} \end{cases} \quad (4)$$

Equation (2) counts for each candidate in their corresponding cluster the number of connections to active fanals in other clusters. This equation offers an improvement with respect to

that in [8] via the min function, which guarantees that the maximum contribution of a cluster can not exceed one. γ is the memory effect, which we generally set to 1. Equation (3) picks up the maximum fanal value in each cluster. If the input pattern contains the set of fanals corresponding to a learnt message, as these correct fanals connect to at least one active fanal per cluster, they will always have the maximum score after (2), and thus will be selected by (4), which expresses the “winner-take-all” rule. σ is a threshold, which deserves to be well chosen according to different applications. At a particular step of the process, there can be several fanals having the maximum score, which we call ambiguities, in a given cluster. Further iterations are helpful to continuously minimize the number of ambiguities, and hopefully to converge to a stable solution.

The number of messages that these clique-based sparse neural networks are able to learn and recall outperforms the previously state-of-the-art neural networks. For instance, for the same amount of used memory of 1.8×10^6 bits, the clique-based network model with $c = 8$ and $l = 256$ is 250 times superior to Hopfield Neural Networks (HNN) in terms of diversity (the number of messages that the network is able to learn and to retrieve) [8]. The diversity follows a quadratic law of the number of neurons per cluster, while that of HNN follows a sublinear law of the total number of neurons.

III. LEARNING LONG SEQUENTIAL MESSAGES ON CHAIN OF TOURNAMENTS

The clique-based networks offer good performance in learning fixed length atemporal messages. The way to map a sub-message to a particular fanal in the corresponding cluster via a very sparse code makes the length of the sub-message strictly equal to $\log_2(l)$, with l the number of fanals per cluster. All the clusters are synchronously involved in the learning and the retrieving process. An order of sub-messages is naturally predefined by the bijection between clusters and sub-messages. For instance, in Figure 1, this predefined ordering is : circle, filled circle, filled rectangle and rectangle. This ordering is not reflected in the decoding equations (2) - (4).

However, sequentiality and temporality is omnipresent in human cognitive behavior. Non oriented graphs and more particularly the cliques are not suitable to learn and retrieve sequential messages. An architecture with unidirectional links seems the right way to go, since for example it is much more difficult to sing a song in a reversed order. The information dependencies should also be limited in a certain neighborhood of time. For instance, in order to continue playing, a pianist only needs to remember a short sequence of several notes that he has just played, instead of what he played one hour ago. Inspired by clique-based networks, the main contribution of this paper is to propose an oriented graph regularly defined, which we call a “chain of tournaments” that is able to learn very long sequences using a limited number of neurons, and then to retrieve the next element of a sequence uniquely from the knowledge of part of the previous ones.

In graph theory, a tournament is a directed graph obtained by assigning a direction to each edge in a non oriented

complete sub-graph. A tournament offers less redundancy than a clique, since the number of connections is divided by two (one can consider an edge in non oriented graphs as two arrows in opposite direction). The progression of time is then reflected in the succession of tournaments. An example of “chain of tournaments” is illustrated in Figure 2. Clusters are represented by circles, and an arrow represents not a single connection between two fanals, but a set of possible connections between two clusters. One can consider such an arrow as a vectorial connection. The connections are authorized between the cluster i and j , only if $|j - i| \leq r$. r is the incident degree, which is the number of incoming vectorial connections of any cluster.

Let us take as an example the longest word in French “anticonstitutionnellement”, which contains 25 letters. If one learns this word using the non-oriented clique-based network introduced in Section II, the network should be composed of 25 clusters of 43 fanals (cardinality of the French alphabet with accented letters). In fact, there are several ways to divide this word into sub-words, all of them leading to a network of an unreasonably large size. (If we divide it into c sub-words of length $\frac{25}{c}$, each cluster should contain $43^{\frac{25}{c}}$ neurons and the total number of neurons would be $c \times 43^{\frac{25}{c}}$. So, the best choice is $c = 25$.) But if one considers this word as a sequence of letters, it can be learnt by the “chain of tournaments” illustrated in Figure 2. The associated connectivity graph after learning this word is partially illustrated by Figure 3. The connections are successively established as the sequence is going on. Any sub-sequence of 4 letters is considered as an entity forming a tournament. For instance, the learning of the sub-sequence “anti” is equivalent to embedding 6 new arrows into the graph: $a \rightarrow n$, $a \rightarrow t$, $a \rightarrow i$, $n \rightarrow t$, $n \rightarrow i$ and $t \rightarrow i$. Only three of them are sufficient to define this sub-

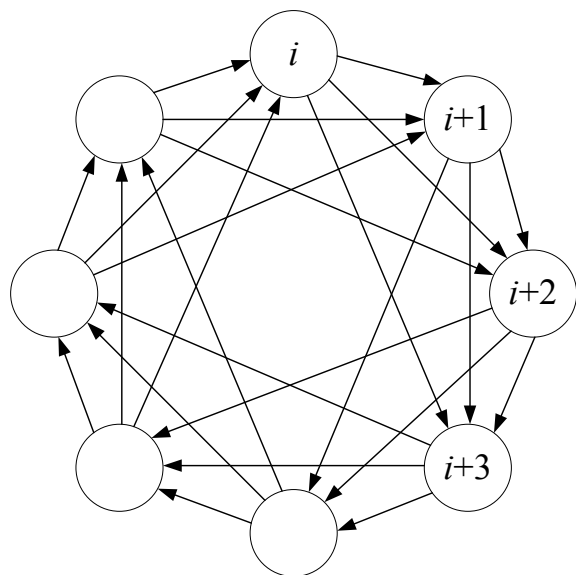


Fig. 2. Structure of the chain of tournaments with 8 clusters and incident degree $r = 3$.

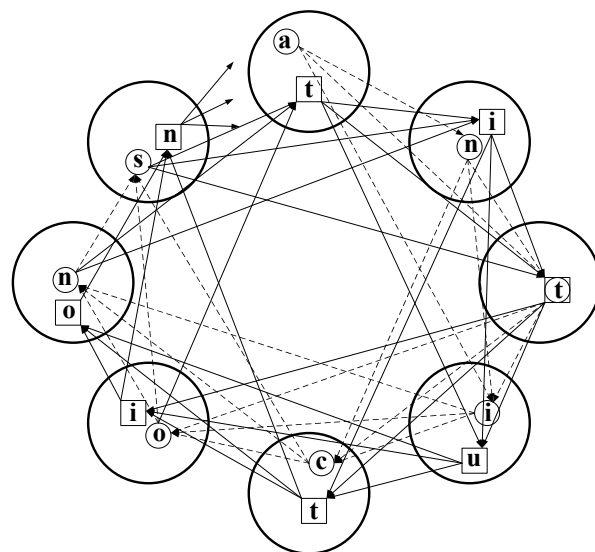


Fig. 3. The partial connectivity graph after learning the longest French word “anticonstitutionnellement” in the chain of tournaments of 8 clusters with incident degree $r = 3$. For the sake of clarity, only the beginning of the sequence and corresponding connections are represented. The fanals corresponding to the first passage are represented by small circles, while those corresponding to the second passage are represented by squares. All the fanals are exactly of the same nature despite the different representations.

sequence ($a \rightarrow n$, $n \rightarrow t$ and $t \rightarrow i$), and the rest of them serves as redundancy, which one can take advantage of during the decoding process. The learning of the next sub-sequence “ntic” adds another three arrows ($n \rightarrow c$, $t \rightarrow c$ and $i \rightarrow c$) to complete a new tournament. The loop structure of this graph enables the reuse of neuron resources. A cluster, and even a neuron, can be used at several times. In Figure 3, when the cluster on the top is solicited for the second time, connections to a new fanal corresponding to the letter “t” are established, without erasing any other existing connections.

The network is then able to retrieve the whole word from a very limited knowledge of the first three letters “a-n-t”. The three fanals corresponding to the sub-sequence “a-n-t” are activated at the beginning. The decision of the fourth letter is made by selecting the fanal in the next cluster with the maximum number of connections to “a-n-t”. The correct fanal “i” will be selected with a score of three. Then, the retrieval process continues decoding the next letter from the knowledge of three previous letters “n-t-i”, and so on. Obviously, if this sequence contains a repetitive sub-sequence of length larger than 3, this illustrated network is potentially not able to make a correct decision. Fortunately, this is not the case for the word “anticonstitutionnellement”. Anyway, it would be possible to add random signatures to complex sequences in order to solve this problem.

Formally, after learning S sequences of length L , the network (chain of tournaments composed of c clusters of l fanals each with parameter r) is defined by:

$$\forall(i, i') \in [1; c]^2, \forall(j, j') \in [1; l]^2,$$

$$\omega_{(i,j)(i',j')} = \begin{cases} 1, & \text{if } 1 \leq (i' - i) \bmod c \leq r \\ & \text{and } \exists s \leq S, \exists k \leq \frac{L}{c}, \begin{cases} d_{i+(k-1)c}^s = j \\ d_{i'+(k-1)c}^s = j' \end{cases} \\ 0, & \text{otherwise} \end{cases} \quad (5)$$

\mathbf{d} is the matrix of learnt sequences, where $d_{i+(k-1)c}^s$ refers to the fanal index in the cluster i corresponding to the k^{th} passage on this cluster by the s^{th} sequence.

After learning S sequences, the density of the network, which is defined as the ratio between the number of established connections and that of all potential ones, can be expressed as:

$$d = 1 - \left(1 - \frac{1}{l^2}\right)^{S \frac{L}{c}} \quad (6)$$

To start the retrieval process, the network should be provided with any r consecutive symbols, in particular the first r symbols if we want to retrieve the sequence from the beginning. It is important to note that if the provided part is in the middle of the sequence, one has to know the emplacement of the corresponding clusters to begin with. Formally, the decoding can be expressed as follows:

$$\text{for } r+1 \leq p \leq L : \begin{cases} i \leftarrow p \bmod c + 1 \\ \forall j, v_{ij} \leftarrow \\ \sum_{1 \leq \delta(i') \leq r} \min \left(\sum_{j'=1}^l \omega_{(i,j)(i',j')} v_{i'j'}, 1 \right) \\ \text{where } \delta(i') = (i' - i) \bmod c \\ v_i^{\max} \leftarrow \max (v_{ij}) \\ \forall j, v_{ij} \leftarrow \begin{cases} j \\ 0 \text{ otherwise} \end{cases} \end{cases} \quad (7)$$

The sequence retrieval error rate (SRER) is a measure of the network performance, which is here defined as the probability of getting at least one symbol error during the sequence retrieval process, given the first r consecutive symbols of a learnt sequence. After learning S sequences, SRER can be estimated by the following formula:

$$P_e = 1 - \left(1 - \left[1 - \left(1 - \frac{1}{l^2}\right)^{S \frac{L}{c}}\right]^r\right)^{(l-1)(L-r)} \quad (8)$$

By means of simulation, if one considers a chain of tournaments composed of 16 clusters of 512 fanals each with incident degree 9 learning 10000 random sequences of average length 90 (in symbols), that is to say 8.1 Mbits in total, in 98.4% of cases the network retrieves successfully the entire sequence

only being provided with the 9 first symbols (10% of the whole sequence length).

For a fixed error probability, one can deduce the diversity of the network as:

$$S_{\max} = \frac{\log \left(1 - \left[1 - (1 - P_e)^{\frac{1}{(l-1)(L-r)}}\right]^{\frac{1}{r}}\right)}{\frac{L}{c} \log \left(1 - \frac{1}{l^2}\right)} \quad (9)$$

The maximum number of bits stored by the network is expressed by:

$$C_{\max} = S_{\max} k c \log_2(l) \quad (10)$$

where $k = \frac{L}{c}$, the number of re-use of each cluster. The quantity of memory used by the network is:

$$Q = r c l^2 \quad (11)$$

This leads to the expression of the network efficiency, which is the ratio $\frac{C_{\max}}{Q}$:

$$\eta = \frac{S_{\max} k \log_2(l)}{r l^2} \quad (12)$$

Note that the efficiency is not directly dependant on the number of clusters c , but on k , the number of re-use of each cluster.

The previous equations lead to Table 1 that gives theoretical values for several different configurations of the network. With a sufficient incident degree r , the network efficiency reaches around 20%.

TABLE I
MAXIMUM NUMBER OF SEQUENCES (DIVERSITY) S_{\max} THAT A CHAIN OF TOURNAMENTS IS ABLE TO LEARN AND RETRIEVE WITH AN ERROR PROBABILITY SMALLER THAN 0.01, FOR DIFFERENT VALUES OF c , l , r AND L . THE VALUES OF CORRESPONDING EFFICIENCY η ARE ALSO MENTIONED.

c	l	r	L	S_{\max}	η
8	512	2	16	155	0.5%
8	512	3	16	1513	3.4%
8	512	3	32	578	2.6%
8	512	2	64	225	2%
20	512	10	100	12741	21.9%
50	512	20	1000	1823	22.2%

The propagation of errors is especially harmful in successive decoding process. One can investigate the proportion of non propagative errors which do not cause a second error in following consecutive r decoding steps. In Figure 4, the chain of tournaments of 16 clusters of 512 fanals with $r = 9$ is able to learn and retrieve 15000 sequences of 90 symbols, that is to say 810 bits, while maintaining a satisfying proportion (more than 90%) of non propagative errors. Logically, a chain of tournaments with $r = c - 1$ offers the best performance possible.

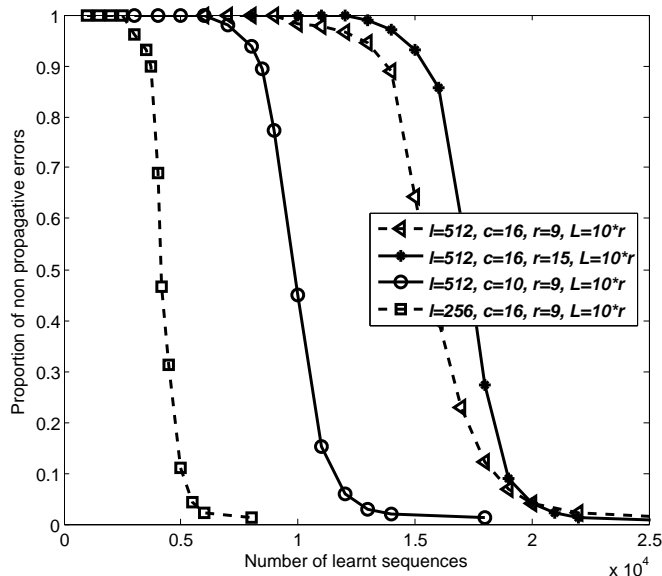


Fig. 4. Proportion of non propagative errors in function of the number of the sequences learnt by chains of tournaments. The first input symbols are of 10% length of the whole sequences.

IV. LEARNING VECTORIAL SEQUENCES

As a matter of fact, the structure represented in Figure 2 is a generalization of clique-based networks. It becomes a clique by setting $r = c - 1$ (two oriented connections being equivalent to a non oriented one). It is still possible to generalize furthermore this topology:

- 1) A chain of tournaments is not necessarily a closed loop;
- 2) A given element of the sequence at time τ , s^τ , is not necessarily a single symbol, but a set of parallel symbols that corresponds to a set of fanals in different clusters. The sequence then becomes vectorial. We call these sets of parallel symbols as “vectors” or “patterns”.

An illustration of this generalization is given in Figure 5. The network is composed of 100 clusters, represented by squares in the grid. Four patterns with different sizes are represented: filled circles (size 4), grey rectangles (size 3), grey circles (size 2) and filled rectangles (size 5). There are no connections within a pattern. Two patterns that are linked are associated through an oriented complete bipartite graph. The succession of patterns is then carried by a chain of tournaments with parameter r . In Figure 5, we have $r = 2$, since the first pattern (filled circles) is connected to the second (grey rectangles) and to the third (grey circles), but not to the fourth (filled rectangles). This concept is similar to that in [10], although the latter only considers connections between two consecutive patterns, and the way of the organization in clusters is different.

During the decoding process, the network is provided with r successive patterns. A priori, the locality of the next pattern is unknown. As a consequence, at each step of the decoding, one has to process a global “winner-take-all” rule instead of

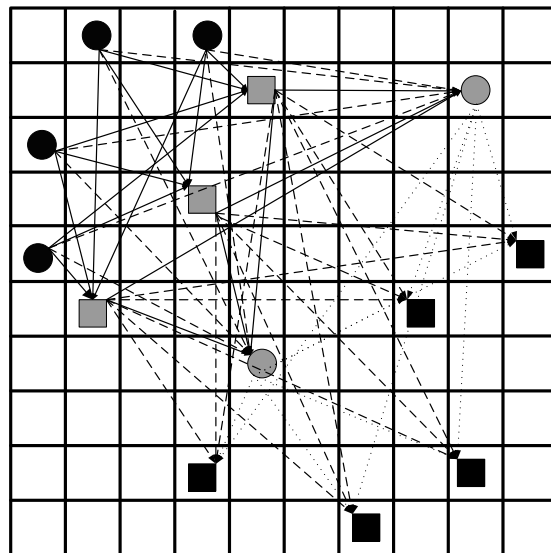


Fig. 5. Learning vectorial sequences in a network composed of 100 clusters by the generalized chain of tournaments. Clusters are represented by squares in the grid. Four patterns with different sizes are represented: filled circles, grey rectangles, grey circles and filled rectangles. The incident degree is $r = 2$.

a local selection expressed in (3) or (7). In other words, one has to go through the whole network to select all the fanals with the maximum score, which is normally the product of the incident degree and the size of patterns, instead of doing this selection within selected clusters.

By means of simulation, our network learns a set of long vectorial sequences composed of randomly generated patterns, and it shows outstanding performance in retrieving them. For example, with the incident degree $r = 1$, the network composed of only 6400 neurons (100 clusters \times 64 fanals/cluster) is able to learn a sequence of 40000 random patterns of size 20 each, that is to say about 10 Mbits, with a SRER = 10% despite a relatively high network density $d = 0.32$. Nevertheless, this network is more at ease to learn sequences of big patterns (for instance, size 20) rather than those of small patterns (for instance, size 3), which suffers more from the problem of error propagation and diaphony. Since the patterns are randomly generated, one has few chance to get too many similar patterns. Anyway, in a similar way as mentioned in Section III, our model is also able to learn sequences of correlated patterns as well as those of non correlated ones, although the provided input patterns should not be strongly correlated with the rest of the sequence. The cost is to add random signatures in order to decorrelate the source, and to correspondingly double the number of clusters and neurons.

V. CONCLUSION AND OPENING

While the clique-based non oriented networks enable the learning of fixed length atemporal messages, the model proposed in this paper is able to learn very long sequences, the length of which is not limited by the size of the network, but

only by its binary resource. As described in Section IV, the network made of 6400 neurons is able to learn a vectorial sequence composed of 40000 patterns of 20 parallel symbols, which corresponds to about 10 Mbits of information. This property could give them the ability to encode the flows with voluminous information, such as multimedia streams.

This model remains simple to be implemented, since all the connections and the neurons are binary. Oriented graphs are biologically plausible, as synapses (neuronal inputs) and axons (neuronal outputs) are not interchangeable.

Generally, time is embodied in a temporal message in two ways: temporal order and time duration. By now, the time involved in our model is discrete. It would be thus interesting to introduce the notion of duration in associative memories, which will have utilities to applications like natural language processing considering phoneme sequences. The learning of abstract structure [11] [12], which might lead to a hierarchical architecture, is another interesting possibility that remains open to further investigation.

REFERENCES

- [1] J. L. Elman, "Finding structure in time", *Cognitive Science*, vol. 14, pp. 179-211, 1990.
- [2] A. Cleeremans, D. Servan-Schreiber, and J. L. McClelland, "Finite state automata and simple recurrent networks", *Neural Computation*, vol. 1, pp. 372-381, 1989.
- [3] D. Wang and M. A. Arbib, "Complex temporal sequence learning based on short-term memory", *Proceedings of the IEEE*, vol. 78, no. 9, September 1990.
- [4] D. Wang and B. Yuwono, "Incremental learning of complex temporal patterns", *IEEE Transactions on Neural Networks*, vol. 7, pp. 1465-1481, 1996.
- [5] J. J. Hopfield, "Neural networks and physical systems with emergent collective computational properties", *Proceedings of the National Academy of Sciences, Biophysics*, vol. 79, pp. 2554-2558, USA, 1982.
- [6] M. McCloskey and N. J. Cohen, "Catastrophic interference in connectionist networks: The sequential learning problem", *The Psychology of Learning and Motivation*, vol. 23, Academic Press, pp. 109-164, New York, 1989.
- [7] R. M. French, "Catastrophic forgetting in connectionist networks: causes, consequences and solutions", *Trends in Cognitive Science*, vol. 3(4), pp. 128-135, 1999.
- [8] V. Gripon and C. Berrou, "Sparse neural networks with large learning diversity", *IEEE Transactions on Neural Networks*, vol. 22, no. 7, July 2011.
- [9] V. Gripon and C. Berrou, "A Simple and efficient way to store many messages using neural cliques", *IEEE Symposium Series on Computational Intelligence*, Paris, April 2011.
- [10] G. J. Rinkus, "TEMECOR: An associative, spatio-temporal pattern memory for complex state sequences", *Proceedings of the World Congress on Neural Networks*, Washington, D.C., pp. 1.442-1.448, 1995.
- [11] G. F. Marcus, S. Vijayan, S. Bandi Rao, and P. M. Vishton, "Rule learning by seven-month-old infants", *Science*, vol. 283, no. 5398, pp. 77-80, January 1999.
- [12] T. Lelekov and P. F. Dominey, "Human brain potentials reveal similar processing of non-linguistic abstract structure and linguistic syntactic structure", *Neurophysiologie Clinique*, vol. 32, pp. 72-84, 2002.

Extending the World to Sense and Behave: A Supportive System Focusing on the Body Coordination for Neurocognitive Rehabilitation

Hiroaki Wagatsuma, Marie
Fukudome

Department of Brain Science and
Engineering, Graduate School of Life
Science and Systems Engineering
Kyushu Institute of Technology
Kitakyushu, JAPAN
{waga, fukudome-
marie}@brain.kyutech.ac.jp

Kaori Tachibana

Department of Physical Therapy,
School of Health Sciences
Ibaraki Prefectural University of
Health Sciences
Inashiki-Gun, JAPAN
tachibana@ipu.ac.jp

Kazuhiro Sakamoto

Research Institute of Electrical
Communication
Tohoku University
Sendai, JAPAN
sakamoto@riec.tohoku.ac.jp

Abstract—We focus on the difficulty in people with cerebral palsy to perform motor skills in a coordinated and purposeful way and designed a robotic training support system for children with cerebral palsy, which enhance their motivation to do the training. The first target is to regenerate a balance between right and left motions in a rhythmic task. In the paddling task with both hands for rolling a long bar systematically, we found a pace-making dynamics with recovering an preferable motion to individuals and realize that it is the key to build extensive rhythm-based tools for improvements of cerebral palsy symptoms to capture the sense of the world and increase an active range of motion.

Keywords—physical therapy (PT); robotic therapy; epigenetic robotics; neurocognitive rehabilitation.

I. INTRODUCTION

Cerebral palsy (CP) is the most frequent physical disability, or disorder, that mainly onsets in childhood. Over the past four decades, the number of patient has reported constant at 2 to 3 per 1,000 live births in industrialized countries, with low fetal mortality [1] [2]. Treatment of CP is a lifelong process that requires the collaboration of medical professionals including physiotherapists, the children, and their families. This is a sort of permanent disorder, but not unchanging in the viewpoint of neuro-developmental aspect.

The patients have problems in muscle tone, movement, and motor skills, especially in the ability to move body parts in a coordinated and purposeful way. Some patients also exhibit disability in other health issues, such as vision, hearing, and speech and learning problems, implying concerns about a relation to the impairment of intellectual development. Physical therapy treatments of medical professionals largely contribute to reconstruction in motor skills, and the procedure is well investigated and adequately equipped to care for patients with brain damage. In adult cases, patients are convinced by the experience of the physiotherapists and intend to do unpleasant trainings for recovery. However, children's expectations of the physical therapy even with well-equipped procedure often do not coincide with reality, and unwillingness often results.

Recently, brain plasticity enhanced by the presence of awareness, attention and concentration is focused in studies for recovery of the brain function [3] and clinical treatments of rehabilitation, so-called cognitive- or neuro-cognitive rehabilitation [4]. The combination of physical therapy procedures and retention of cognitive process in thinking and awareness starts anticipating for development of effective strategies that will open a new door in treatments of children's care, toward CP patients and its developmental difficulty [5].

In the present study, we are devoted to developing a robotic training support device (Fig. 1), which holds automated parts to enhance, support and burden a user's motion. The device is capable of recording their motions and performances as a training history to help visualize their developmental processes. As the framework, requirements for such devices are 1) modifiable structure, 2) adjustable kits and 3) rearrangement of parts in a structure, and 4) switching tasks and 5) changing challenging levels to the task difficulty as functions. In the viewpoint of the task design, we focus on a sense of cognitive space during the motor training. Ultimate goal is to provide a training method to encourage subjects to capture an appropriate cognitive space, and we start to investigate an effective method to regenerate a balance between right and left motions.

We hypothesized that a clue to the regeneration problem is to enhance an internal rhythm when subjects perform periodic movements, such as pedaling with legs and paddling with hands. Finally the concept of right-and-left coordination should be extended to an arbitral configuration, or a flexible sense of position in space, which are necessary for skills of musical instruments, like multiple percussions.

In the present paper, we describe an important relationship between cognitive and operational space in the viewpoint of neurocognitive rehabilitation in chapter II, our framework of a training support system for CP in chapter III, results of the pilot experiment to investigate an musculoskeletal pace-making dynamics during the paddling task in chapter IV, and the conclusion in chapter V.

II. COGNITIVE AND OPERATIONAL SPACE

Cognitive motor control refers to processes that blend cognitive and motor functions in a seamless, interwoven fashion [6]. Through such experiences, the functions evolve in space and time at various levels of difficulty and complexity. Training programs in physical therapy mainly focus on improvements of motor abilities, which may be distinct from the target of occupational therapy, but programs for children with CP are inescapable to include cognitive trainings, for example a task to require not only pointing a letter in text but also reading the letter and understanding what it describes (Fig. 2).

In a memory task, we observed a child with CP who can retrieve greater than seven random numbers presented by the therapist in a voice, suggesting an above-average IQ over children with the same age, but decreases its performance if random positions are presented in a table. Another child with CP who has taken an adequate physical therapy for movements in the paralysis side still demonstrates asymmetric operational areas between right and left hands (Fig. 4). One possible hypothesis is that cognitive and operational spaces link together and cognitive tasks to be aware of things in the paralysis side can be used as a complementary approach to the physiotherapy treatment for children with CP. We focus on the coordination between cognitive sense of space and behavioral structure in motion and designed a prototype of the robotic training support system to enhance the link between cognitive and operational spaces.

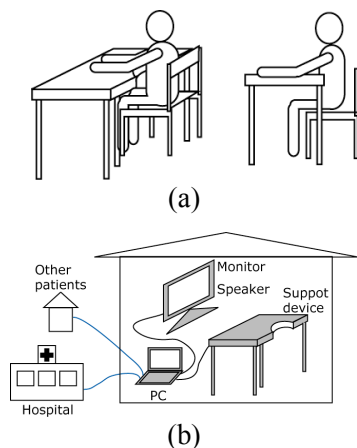


Figure 1. A prototype of the robotic training support device for execution of various handling tasks and monitoring the behavior. (a) Sensors spread over the flat table to detect hands' motion. Children with CP sit at the table because they mostly deficit self-standing ability in an early stage of rehabilitation and the device is devoted to examining how their cognitive developments proceed through memory tasks of visual stimulus and tracing hand movements in this case. (b) Portable PC is implemented in the device for task presentation, recording of behavioral data and communicating with physiotherapists in the hospital and other children with CP to play an interactive training game together.

III. FRAMEWORK DESIGN

We designed a training device for children with CP, which enhance their motivation to do the training through rhythmic game-like tapping devices. Palm-sized buttons can be used for designing such devices, by putting buttons with on the table and the buttons respond a touch by sound and light like musical instruments. Possible arrangements are given according to the subjects' deficits and we can consider various configurations (Fig. 3) to examine changes cognitive and operational areas between both hands (Fig. 2). However, our purpose does not design a musical instrument in a passive manner, but design an active device to be able to synchronize the internal rhythm that appears when individual subjects perform a rhythmic task at their own paces.

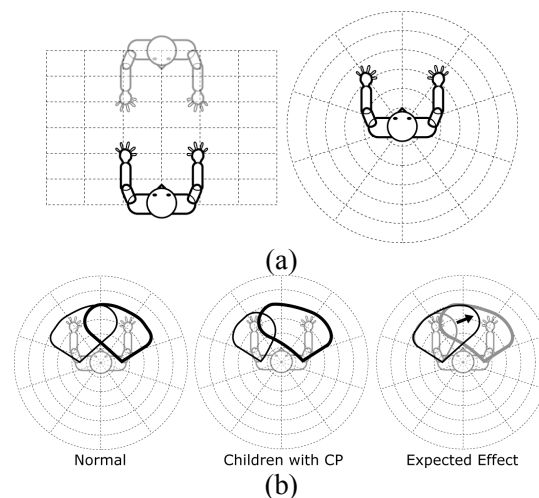


Figure 2. A concept of cognitive motor space. (a) (left) Allocentric coordinate or objective space to enable two persons to share the same space. (right) Egocentric coordinate or subjective space for handling by oneself. Cognitive development is considered to extend from egocentric to allocentric coordinates. (b) Cognitive and operational space in stages of rehabilitation. (left) In normal subjects, reachable spaces of right and left hands are consistent with spaces of easy-to-operate. (center) Patients with deficits in the right hemisphere of the brain are not good at handling things in the left side, known as hemispatial neglects [7]. (right) An ideal process of regenerate a balance between right and left motions after appropriate rehabilitations.

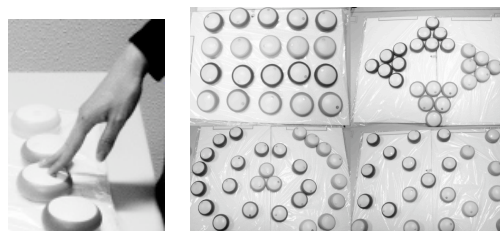


Figure 3. Palm-sized buttons are implemented in the table device. The button lightens the surface when touched and/or controlled by the PC according to the automated task program in an active manner (left), and are aligned in various ways such as grid-like, square, circle, and a spokewise structure (right). This helps to provide a tapping task in accordance with music.

IV. A PILOT EXPERIMENT

Firstly, we investigated a pace-making dynamics in motor trainings according to the concept of neurocognitive rehabilitation (Fig. 4a) and designed a padding task of hand motions [8] with two options: 1) with/without circular guides in both sides for navigating cyclic motions (position guidance) and 2) with/without balls in both sides for enhancing forces in cyclic motions (acceleration guidance). We built the equipment for the task and the real-time recording system of motion information through accelerometers (Fig. 5) by using the Nintendo Wii remote controller [9] [10] with the real-time Bluetooth wireless communication to an external PC (Fig. 6).

As the first step, six normal subjects were trained in the paddling task without guides and without balls, which consists of continuous five sessions (#1-#5) of a minute with interval breaks of five minutes. In the observation of paddling motions of a subject, we found a certain period of cyclic motions at a constant pace and a cracking between periods (Fig. 7). Interestingly, our experimental data exhibits a recovering dynamics to connect constant periods, with semi-conscious deorbit process (black lines in Fig. 7, 8) and conscious or quasi-conscious back-on-track process (blue lines in Fig. 7, 8) in Session #1. Due to the tendency to enlarge the constant period, the number of cracking decreases which is also observed in the frequency component analysis (Fig. 9). This tendency was observed in other subjects except in performances at the slow pace of cycling. This fact suggests that this phenomenon requires a certain workload for individual subjects, and this indicates the existence of a comfortable pace-making in the paddling task as the result of a synergy among the subject's internal rhythm, constraints of the support device and effect of training, such as habituation and learning.

V. CONCLUDING REMARKS

We introduced a concept of relationship between cognitive and operational space in the viewpoint of neurocognitive rehabilitation concepts, and demonstrate a pilot experiment to investigate an integral pace-making dynamics during a paddling task. We hypothesized that a clue to the regeneration problem is to enhance an internal rhythm when subjects perform periodic movements, such as paddling motions with hands. In further analysis and developments of the device and task design, we attempt to apply this result to the framework in an arbitral configuration, which enable the device to supply complex rhythmic and coordinating motions accompanied with memory skills in a cognitive space. For extending to the table-shaped device with palm-sized buttons aligned in a various structure, the device may require to detect the integral pace that is generated from such a synergy among the subject's internal rhythm, task constraints and learning effects and to synchronize it as a tempo of the music. It is expected to enhance the coordination between cognitive and behavioral sense, which may be observed as changes operational areas of both hands. This rhythm-based cognitive motor training

coupled with the supportive autonomous system opens new doors for a self-sustained interactive rehabilitation.

ACKNOWLEDGMENT

This work is partially supported by JSPS KAKENHI (22300081).

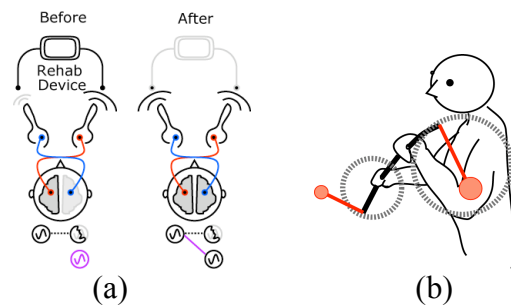


Figure 4. A possible rehabilitations process for reorganization through rhythmic motions. (a) An expected process of rehabilitations through the device, which is inspired from [11][12]. (b) Our proposed paddling tasks with the 180cm bar, which allows a certain flexion according to the cyclic motion like a fishing pole. The task has two options: with/without circular guides in both sides for navigating cyclic motions (position guidance) and with/without balls in both sides for enhancing forces in cyclic motions (acceleration guidance).

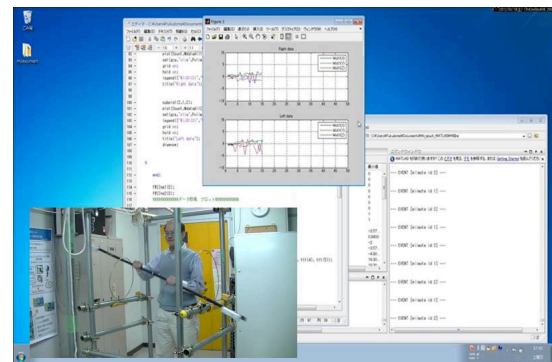


Figure 5. A demonstration of the paddling task. The left-bottom panel denotes a snapshot of the paddling motion in the equipment. The top plot exhibits a real-time observation of values from three dimensional acceleration meters (Fig. 6), which attached on both ends of the bar. The recording system was designed by MATLAB.

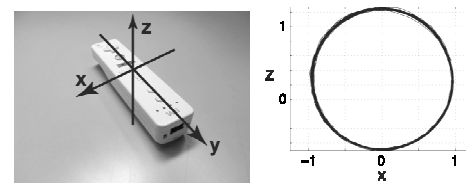


Figure 6. A Wii remote controller to connect to the PC via the wireless Bluetooth communication. This includes acceleration sensors with three orthogonal axes. (right) X-Z accelerometer values in machine rotations with a constant power.) (Figures from [10])

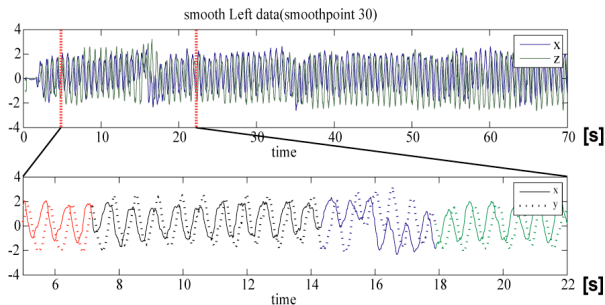


Figure 7. A temporal evolution of accelerometer values in the paddling task. (a) Experimental data of a subject in the first session #1, for 70s. (b) A highlight of a recovering process connecting two constant periods, which consists of a stable period (red), deorbit period (black), back-on-track quick process (blue) and recovered stable period (green).

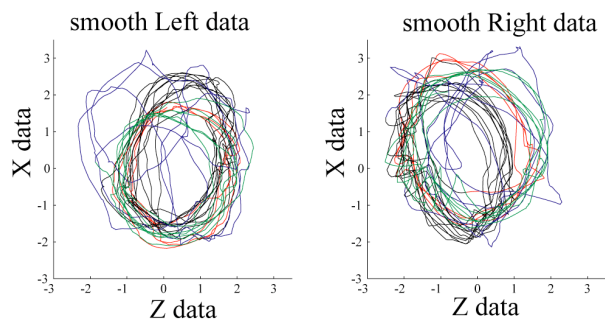


Figure 8. Replotting the recovering process of Fig. 7 in the X-Z accelerometer coordinates. This visualizes an attractor dynamics to differ the stable orbit and the deorbit processes, and to make sense two stable periods (red and green) are consistent. Line colors are the same in Fig. 7.

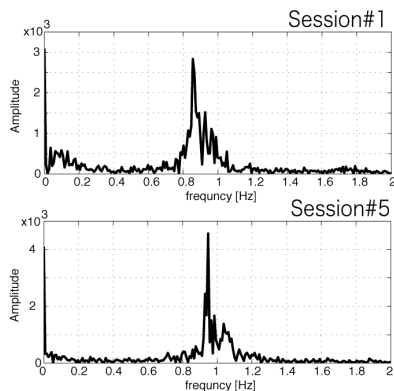


Figure 9. FFT analyses among different sessions #1 and #5, which is obtained from the same subject in Fig. 7 and Fig. 8. Peak positions are similar in two sessions, while the frequency distribution is getting sharper with a single peak, suggesting the increasing of stableness of the paddling motions at a constant speed.

REFERENCES

- [1] G. E. Molnar, "Rehabilitation in cerebral palsy," In *Rehabilitation Medicine-Adding Life to Years*, West J Med, vol.154, pp. 569-572, 1991.
- [2] K. Mattern-Baxter, "Locomotor Treadmill Training for Children With Cerebral Palsy," *Orthopaedic Nursing*, vol.29(3), pp. 169-173, 2010.
- [3] V. S. Ramachandran and S. Blakeslee, "Phantoms in the Brain: Probing the Mysteries of the Human Mind," New York: William Morrow, 1998.
- [4] K. D. Cicerone, C. Dahlberg, J. F. Malec, D. M. Langenbahn, Y. Felicetti, S. Kneipp, W. Ellmo, K. Kalmar, J. T. Giacino, J. P. Harley, L. Laatsch, P. A. Morse, and J. Catanese, "Evidence-based cognitive rehabilitation: updated review of the literature from 1998 through 2002," *Arch Phys Med Rehabil*, vol.86(8), pp. 1681-1692, August 2005.
- [5] "Robotic therapy holds promise for cerebral palsy - Devices can help children with brain injuries learn to grasp and manipulate objects," MIT news, <http://web.mit.edu/newsoffice/2009/robototherapy-0519.html>
- [6] A. P. Georgopoulos, "Cognitive motor control: spatial and temporal aspects," *Curr Opin Neurobiol*, vol.12(6), pp. 678-683, December 2002.
- [7] P. Malhotra, E. Coulthard, and M. Husain, "Hemispatial neglect, balance and eye-movement control," *Curr Opin Neurol*, vol.19(1), pp. 14-20, 2006.
- [8] M. Fukudome and H. Wagatsuma, "A supportive system focusing on the body coordination for neurocognitive rehabilitation," *Proceedings of the 21st Annual Conference of the Japanese Neural Networks Society (JNNS 2011)*, pp. 216-217, 2011.
- [9] S. Brosnan, "The potential of Wii- rehabilitation for persons recovering from acute stroke," *Physical Disabilities Special Interest Section Quarterly*, vol.32(1), pp. 1-3, 2009
- [10] G. Goldberg, H. Rubinsky, E. Irvin, E. Linneman, J. Knapke, and M. Ryan, "Doing WiiHab: Experience with the Wii video game system in acquired brain injury rehabilitation," *Journal of Head Trauma Rehabilitation*, vol.23(5), pp. 350, 2008.
- [11] H. Haken, J. A. S. Kelso, and H. Bunz "A Theoretical Model of Phase Transitions in Human Hand Movements," *Biological Cybernetics*, vol.51, pp. 347-356, 1985.
- [12] B. A. Kay, J. A. S. Kelso, E. L. Saltzman, and G. S. Schöner, "The Space-time Behavior of Single and Bimanual Movements: Data and Model," *Journal of Experimental Psychology: Human Perception and Performance* vol.13, pp. 178-192, 1987.